CONSTRUCTION OF CAPACITY SPECTRUMS OF INELASTIC UNBRACED STEEL FRAMES WITH SEMI RIGID CONNECTIONS
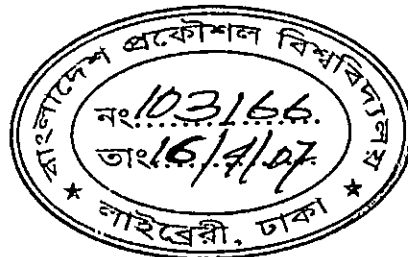
BY

PARTHA PRATIM DAS

A thesis submitted to the Department of Civil Engineering,
Bangladesh University of Engineering and Technology, Dhaka
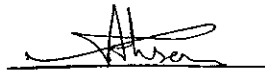in partial fulfilment of the degree of

MASTER OF SCIENCE IN CIVIL ENGINEERING

April, 2007

The thesis titled **"Construction of Capacity Spectrums of Inelastic Unbraced Steel Frames with Semi Rigid Connections"** submitted by **Partha Pratim Das, Roll: 040304316 F, Session: April 2003,** has been accepted as satisfactory in partial fulfilment of requirement for the degree of **Master of Science in Civil Engineering** (Civil & Structural).

BOARD OF EXAMINERS

Dr. Raquib Ahsan
Associate Professor
Department of Civil Engineering
BUET, Dhaka.

Chairman
(Supervisor)

Dr. Md. Mazharul Hoque
Professor and Head
Department of Civil Engineering
BUET, Dhaka.

Member

Dr. Md. Zakaria Ahmed
Professor
Department of Civil Engineering
BUET, Dhaka.

Member
(internal)

Dr. Md. Mozammel Hoque
Assistant Professor
Department of Civil Engineering
DUET, Gazipur.

Member
(external)

DECLARATION

Except for the content where specific reference has been made to the work of others the work embodied in this thesis is the result of investigation carried out by the author. No part of this thesis has been submitted or is being concurrently submitted in candidature for any degree at any other institution.

পার্থ প্রতিম দাস

Author

To my sister,

Urmi Rani Das

ACKNOWLEDGEMENT

ABSTRACT

The influence of semi-rigid connection behaviour on the response of the overall structures has long been recognized. However, it has been common practice to treat connections in steel structures as either perfectly rigid or pinned. Due to lack of commercial packages to include semirigid connection effects directly in analysis and design seems to be the main reason behind this. The need for including the effects of connection semirigidity in the analysis of building systems is particularly important for use in limit state design methods and in evaluating the seismic risk for existing structures.

The Capacity Spectrum Method (CSM), by means of a graphical procedure, compares the capacity of the structure with the demands of earthquake ground motion on the structure. The capacity of the structure is represented by a nonlinear force-displacement curve, sometimes referred to as a pushover curve. The base shear forces and roof displacements are converted to equivalent spectral accelerations and spectral displacements, respectively, by means of coefficients that represent effective modal masses and modal participation factors. These spectral values define the capacity spectrum. The demands of the earthquake ground motion are represented by response spectra. A graphical construction that includes both capacity and demand spectra, results in an intersection of the two curves that estimates the performance of the structure to the earthquake.

An approach is presented which includes connection semirigidity in the analysis for evaluating the seismic performance of steel framed structures using the capacity spectrum method. The capacity spectrum is structural property which relates the fundamental period of vibration to the level of deformation. The spectrum is obtained using an inelastic analysis which in this case includes nonlinear connection response and plastification of beam-column elements. The capacity spectrum is used together with elastic response spectra to approximation the inelastic response of the structure using Procedure-A of ATC-40 for given design earthquake.

This dissertation is limited to developing global force deformation characteristics of a ten story and a six story steel frame structure with several types of nonlinear semirigid connections. The seismic performance of such frame structures is investigated. From the present study it is found that rigid structure may fail to withstand the limit state of maximum considered earthquakes (MCE). For semirigid frames, where particular frame is assumed to posses same type of semirigid connection at all joints, it can be notified that they experience almost no plastic deformation at members at their performance point though the shear capacity is lower and the demand displacement is higher than those of rigid structures. Different combinations of rigid and semirigid connections on frames may be used for better performance.

In this study normalized response spectra for 5% damping ratio, BNBC, 1993 is used as earthquake ground motion. Provision for connection flexibility should be made in building code according to the performance of the structure.

CONTENTS

LIST OF FIGURES

LIST OF TABLES

LIST OF NOTATIONS

A	Area of the cross-section
ΔA	Area of the sub-element of the cross-section
$A(0)$	0% Integration Point
$A(30)$	30% Integration Point
$A(50)$	50% Integration Point
$A(-30)$	-30% Integration Point
$A(-50)$	-50% Integration Point
A_c	Area of exterior column at building base
B	Base width of frame
C_A, C_V	Seismic Coefficient
C_{j1}, C_{j2}	Connection stiffness at ends 1 and 2 of a beam element
E	Young's modulus of elasticity of steel
E_{eff}	Effective modulus elasticity
F	Force
F_t	Concentrated lateral force at roof
h	height of storey
H	Overall height of a frame
I	Importance Factor
I_b, I_c	Second moment of area of a beam and a column section respectively
k_b	Rotational stiffness of a beam
k_c	Rotational stiffness of a column
k_e	effective length factor
k_j	Linear rotational stiffness of a connection
k_0	Initial rotational stiffness of a connection
k_1, k_2, k_3	Rotational stiffness in a tri-linearised representation of the connection
L_b	Length of a beam
L_c	Length of a column
$\overline{m}$	ratio of connection moment and the full plastic moment of beam
M	Moment
M_B	Base moment
M_{eff}	Effective moment

M_p	Plastic moment capacity of a beam
M_u	Ultimate moment capacity of a connection
$M\text{-}\phi$	Moment-rotation characteristic
n	Shape parameter of the three parameter power model
N_c	Number of columns
N_1 to N_6	Shape functions for the semi-rigid element
$\overline{N}_1$ to $\overline{N}_2$	Shape functions for the rigid element
q	Intensity of uniformly distributed load
R	Response modification coefficient
R_{ki}	Initial connection stiffness
S	Site coefficient for soil characteristics
Sa	Spectral acceleration
Sd	Spectral displacement
Sv	Spectral velocity
T	Time period
u, v	Displacement components in a general point
v_0	Initial displacement at the free end of member
V	Base shear
V_c	Column wind shear
V_g	Girder wind shear
w	Intensity of uniformly distributed load
W	Total building weight
Z	Seismic zone factor

Greek Symbols

Δ	Top lateral drift of a frame
$\Delta_{semi\text{-}rigid}$	Sway of a semi-rigid frame
Δ_{rigid}	Sway of a rigid frame
Δ_{roof}	Roof displacement
σ	Stress
σ_y	Yield stress
ε	Strain at a cross section
α	Modal mass coefficient

ϕ	Rotation of connection
ϕ_{im}	Amplitude of mode m at level i.
$\lambda_{cr\ rigid}$	elastic critical load with all joints taken as rigid
$\lambda_{cr\ semi\text{-}rigid}$	elastic critical load considering initial stiffness of semi-rigid joints
θ_j	Rotation of connection
θ_{jl}	Rotation of connection at the beam end 1
θ_{jab}	Rotation of connection at end 'b' due to mode shape 'a'
γ_1 and γ_2	Two non-dimensional parameters
μ	Fixity factor

Matrices and Vectors

$[B]$	Strain displacement matrix
$[D]$	Elasticity matrix
$[K_E]$	Elastic stiffness matrix based on small deflection theory
$[K_G]$	Geometrical stiffness matrix which depends on the level of axial force of the element
$[K_L]$	Large displacement stiffness matrix which depends on the displaced shape of the element
$[K_T]$	Tangential stiffness matrix
$[N]$	Shape function matrix
$\{P_0\}$	Imaginary set of forces simulating initial deflections
$\{\delta\}$	Displacement vector
$\{\delta^*\}$	Initial nodal displacement vector

Abbreviations

2D	Two Dimensional
3D	Three Dimensional
AISC	American Institute of Steel Construction
ADRS	Acceleration Displacement Response Spectra
ATC	Applied Technology Council
AWS	American Welding Society
EPA	Effective Peak Acceleration
FE	Finite Element

FEMA	Federal Emergency Management Agency
GXY	Shear Modulus
BNBC	Bangladesh National Building Code
CJP	Complete Joint Penetration
CS	Capacity Spectrum
CSM	Capacity Spectrum Method
EC3	Eurocode 3
FR	Fully restrained
FEM	Fixed end moment
KEYOPT	Key Options
LRFD	Load and Resistance Factor Design
MCE	Maximum Considered Earthquake
NSP	Nonlinear Static Procedure
OD	Outer Diameter
PF	Modal Participation Factor
PBSD	Performance-Based Seismic Design
PSA	Peak Spectral Acceleration
PSV	Peak Spectral Velocity
PSD	Peak Spectral Displacement
PR	Partially restrained
SAC	SAC Joint Venture; a partnership of the Structural Engineers Association of California, the Applied Technology Council, and California Universities for Research in Earthquake Engineering.
SHEARZ	Shear Deflection Constant
SMRF	Special Moment Resisting Frame
TKWALL	Wall Thickness
UT	Ultrasonic Testing
cm	Centi metre
FT	Feet
KN	Kilo Newton
m	Metre
mm	Milli metre
rad	Radian

CHAPTER 1

Introduction
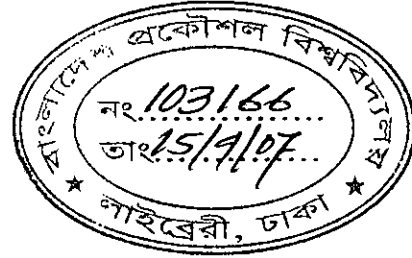
1.1   General

Steel skeletal structures have long been widely used in different countries because of their relative economy and ease of construction. In Bangladesh, however, the use of steel as a framing material for buildings has been rare because of the availability of reinforced concrete at an economical cost. But recently the trend of using steel as a framing material, mainly for industrial use, is on the rise in Bangladesh. The reason behind this trend lies in the fact that, when adequate initial fund is available, steel structures can be constructed in relatively very short period of time and with sufficient ease. Thus with early occupation and shorter pay back period, such construction proves to be economical in the long run. Importantly, steel construction has an added advantage from the point of view of seismic resistant design. Steel contributes ductility to frame and steel frame is normally 25 to 35 percent lighter than a concrete frame.

Currently, seismic design is usually based on an elastic analysis where some approximation is used to account for the inelastic response of the structure. The loading used in the elastic analyses may be based on equivalent static forces obtained from design codes such as Uniform Building Code, or they may be obtained from a modal analysis using a design spectrum. The advantage of these methods is that they are relatively straight forward, and are convenient for design. The disadvantage, however, is that elastic design methods offer little information regarding the inelastic response of the structure. Hence, the success of such methods lies largely in the reliability obtained through a track record of reasonable performance for standard building configurations with moderate ductility. As such, elastic design methods are not well suited for structures of irregular configuration or for evaluating the damage susceptibility of existing buildings to various levels of seismic forces.

Sophisticated nonlinear time history analysis methods are available which represent the best available technology for simulating the response of structures subjected to strong earthquake loadings. However, a major drawback of such methods is the time and expense required to perform the analysis and interpret the results for design. Therefore, while advanced dynamic analyses are useful for investigations under a specific set of circumstances, they are currently still considered too cumbersome for most routine applications.

The capacity spectrum method incorporates the inelastic response of the structure in the analysis, but is based on a quasistatic approach which is amenable to current engineering practice. This method was first presented by Freeman (1978, 1989) for the design and evaluation of reinforced concrete structures. The essence of this method entails calculation of the capacity spectrum (CS) which relates the natural period of vibration of the structure to the level of induced response. In the capacity spectrum method, the capacity spectrum is used together with elastic response spectra to obtain an approximation of the actual response.

The Nonlinear Static Procedure or Pushover analysis has been developed over the past twenty years and has become the preferred analysis procedure for design and seismic performance evaluation purposes as the procedure is relatively simple and considers postelastic behaviour. However, the procedure involves certain approximations and simplifications that some amount of variation is always expected to exist in seismic demand prediction of nonlinear static analysis. As traditional pushover analysis is widely used for design and seismic performance evaluation purposes, its limitations, weaknesses and the accuracy of its predictions in routine application should be identified by studying the factors affecting the pushover predictions. In other words, the applicability of nonlinear static analysis in predicting seismic demands should be investigated for low, mid and high-rise structures by identifying certain issues such as modelling nonlinear member behaviour with nonlinear semi-rigid connection, computational scheme of the procedure, variations in the predictions of various lateral load patterns utilized in traditional pushover analysis, efficiency of invariant lateral load patterns in representing higher mode effects and accurate estimation of target displacement at which seismic demand prediction of pushover procedure is performed.

At the design stage, column-beam connections of steel structures are assumed as fully rigid or as hinges, and the design is completed with these assumptions. On the other hand, in practice, steel column-beam connections show neither fully rigid nor fully hinge behaviour, and the characteristic behaviour of the connections lies between these two special cases. A great deal of research has been conducted to represent the behaviour of such connections and different models have also been proposed. The most reliable ones show that the connection moment-rotation relationship is, in general, non-linear. Performing realistic calculation of forces and knowing the behaviour of structures close to reality will decrease life and goods losses to the minimum level in a probable of earthquake to be encountered in the future. It has been already mentioned that the capacity spectrum is a structural property which relates the fundamental period of vibration to the level of deformation. The spectrum is obtained using an inelastic analysis which in this case includes nonlinear connection response and plastification of beam-column elements.

1.2 Objectives of the Study

A major challenge to performance-based seismic design and engineering of buildings is to develop simple, yet effective, methods for designing, analyzing and checking the design of structures so that they reliably meet the selected performance objectives. Needed are analysis procedures that are capable of predicting the demands – forces and deformations – imposed by earthquakes on structures more realistically than has been done in building codes. The main objectives of the study can be outlined as follows:

1. To develop the relationship between base shear and roof (Nth floor) displacement commonly known as the "pushover curve" which includes nonlinear connection response and plastification of beam-column elements.

2. To convert the pushover curve to a capacity spectrum where the initial semi-rigidity of the connection will be considered for the fundamental vibration mode.

3. To investigate the effects of different semirigid connection types on the performance of the frame.

1.3 Outline of Methodology

In this study first of all a finite element program of 2D inelastic unbraced framed structures with nonlinear beam-column connection is developed by which the user may model and analyze the structures with the help of ANSYS. ANSYS is a general purpose Finite Element Software. The developed program is verified against some theoretical or test results.

At the design stage, column-beam connections of steel structures are assumed as fully rigid, and the design is completed with these assumptions. Then for the selected geometry and loading, two dimensional plan frames, a ten story and a six story, are analyzed and evaluated for rigid and different types of non linear semi-rigid connections. In the next step, the relationship between base shear and roof displacement is developed for nonlinear beam-column steel frames with rigid and different types of nonlinear semirigid connections. Furthermore, modal analysis is performed for each of the above mentioned frames to get the essential parameters for constructing capacity spectrum. The global force deformation curve (Base Shear Vs Roof Displacement) is converted into Acceleration Displacement Response Spectra (ADRS) format (Spectral Acceleration Vs Spectral Displacement), which is an integral part of Capacity Spectrum Method; a performance based seismic analysis technique. Finally, the performance of 2D steel frames is investigated for rigid and different types of semi-rigid connections. The capacity spectrum is used together with elastic response spectra (BNBC, 1993) to approximation the inelastic response of the structure using Procedure-A of ATC-40 for given design earthquake.

1.4 Scope of the Study

The extent of this study is limited to developing of global force deformation characteristics of a ten story and a six story steel frame structure with several types of nonlinear semirigid connections and investigating the seismic performance of such frame structures. Connection semirigidity is dependent on beam-column connection detailing. There are various types of detailing. In this study, top and seat angle connection is considered. Three Parameter Power Model is used to get the non linear

4

moment-rotation behaviour of the connection (Kishi and Chen, 1990). Frames are assumed to consist of ideal members having no residual stress or initial imperfection. The global imperfections of frames are also ignored. Inclination of members is not considered in this study. Only major axis bending of members is considered. The other potential limitation of this study is that, P-Δ (second-order) effects are not considered in the analysis. Nonlinear Static Analysis Procedure is used to determine the displacement demand imposed on a building expected to deform inelastically with help of the ATC-40, FEMA-273 and FEMA-350.

1.5   Organization and Contents

The thesis work conducted for the achievement of the stated objectives is presented in this dissertation in several chapters organised in a way so that the steps involved in the study may properly delineate the methodology. This document is organized into seven chapters with some appendices and a list of reference. This discourse addresses the more general and conceptual aspects of the methodology as well as the more technical and analytical aspects of the methodology. A brief description of the contents of each chapter follows:

Chapter 1, **Introduction**, provides a statement of the purpose and scope of this thesis, followed by a brief description of the content of each of the chapters and a summary of supporting appendices.

Chapter 2, **Literature Review**, presents a review of the related research work in the field of steel-moment frames and analysis procedures.

In chapter 3, **Numerical Model**, the basic formulation of the finite element model is illustrated and verification of the finite element model is discussed in short.

Chapter 4, **Modelling and Nonlinear Static Analysis**, presents a comprehensive account of Nonlinear Static Analysis by furnishing the details of modeling and analysis assumptions, the procedure for construction of capacity (pushover) curve and its subsequent conversion into capacity spectrum. Several examples of capacity spectrum for different types of nonlinear semi-rigid connections are included as well.

Chapter 5, **Seismic Performance of Structures**, presents analytical procedures for evaluating the performance of the frames for different types of connectivity. Demand response spectrum conversion in ADRS (Acceleration-Displacement Response Spectra, Mahaney et al., 1993) format is studied.

Chapter 6, **Conclusions and Recommendations**, a brief narrative associated with the development of this thesis about the limitations of the analytical procedures, the potential benefits of this established systems, recommendations and future direction are reviewed.

Appendix A, labelled as **The Three Parameter Power Model**, incorporates a short account of the three parameter power model that is used in this study to describe the nonlinear moment-rotation curve of semi-rigid connections. This also includes an example of connection modelling.

Appendix B, entitled **Computation of Integration Points**, incorporates the definition of integration points and mathematical formulae required for the derivation of true areas and input areas of the 2D elastic-plastic Beam23 in conjunction with an example calculation.

Appendix C, called **Basic of structural Dynamics**, provides background information on basic principles of structural dynamics in connection with the study. In addition, explanation and uses of modal analysis quantities are reviewed.

Appendix D, labelled **Computer Program**, offers the code written in ANSYS language for modelling the frames, the Nonlinear Static Analysis, extraction of the results and the macro files that comprise the tri linearization points of different semi-rigid connection types.

Appendix E, labelled **Calculation of Performance Point**, presents a step by step calculation of performance point using Procedure-A of ATC-40 for rigid steel moment frame structure.

CHAPTER 2

Literature Review

2.1   General

For many years, the basic intent of the building code seismic provisions has been to provide buildings with an ability to withstand intense ground shaking without collapse, but potentially with some significant structural damage. In order to accomplish this, one of the basic principles inherent in modern code provisions is to encourage the use of building configurations, structural systems, materials and details that are capable of ductile behavior. A structure is said to behave in a ductile manner if it is capable of withstanding large inelastic deformations without significant degradation in strength, and without the development of instability and collapse. The design forces specified by building codes for particular structural systems are related to the amount of ductility the system is deemed to possess. Generally, structural systems with more ductility are designed for lower forces than less ductile systems, as ductile systems are deemed capable of resisting demands that are significantly greater than their elastic strength limit.

2.2   Behaviour of Steel Moment Frames

Starting in the 1960s, engineers began to regard welded steel moment-frame buildings as being among the most ductile systems contained in the building code. Many engineers believed that steel moment-frame buildings were essentially invulnerable to earthquake-induced structural damage and thought that should such damage occur, it would be limited to ductile yielding of members and connections. Earthquake-induced collapse was not believed possible. Partly as a result of this belief, many large industrial, commercial and institutional structures employing steel moment-frame systems were constructed, particularly in the western United States.

The Northridge earthquake of January 17, 1994 challenged this paradigm. Following that earthquake, a number of steel moment-frame buildings were found to have

experienced brittle fractures of beam-to-column connections. The damaged buildings had heights ranging from one story to 26 stories, and a range of ages spanning from buildings as old as 30 years to structures being erected at the time of the earthquake. The damaged buildings were spread over a large geographical area, including sites that experienced only moderate levels of ground shaking. Although relatively few buildings were located on sites that experienced the strongest ground shaking, damage to buildings on these sites was extensive. Discovery of these unanticipated brittle fractures of framing connections, often with little associated architectural damage, was alarming to engineers and the building industry. The discovery also caused some concern that similar, but undiscovered, damage may have occurred in other buildings affected by past earthquakes. Later investigations confirmed such damage in a limited number of buildings affected by the 1992 Landers, 1992 Big Bear and 1989 Loma Prieta earthquakes.

In general, steel moment-frame buildings damaged by the Northridge earthquake met the basic intent of the building codes. That is, they experienced limited structural damage, but did not collapse. However, the structures did not behave as anticipated and significant economic losses occurred as a result of the connection damage, in some cases, in buildings that had experienced ground shaking less severe than the design level. These losses included direct costs associated with the investigation and repair of this damage as well as indirect losses relating to the temporary, and in a few cases, long-term, loss of use of space within damaged buildings.

Steel moment-frame buildings are designed to resist earthquake ground shaking based on the assumption that they are capable of extensive yielding and plastic deformation, without loss of strength. The intended plastic deformation consists of plastic rotations developing within the beams, at their connections to the columns, and is theoretically capable of resulting in benign dissipation of the earthquake energy delivered to the building. Damage is expected to consist of moderate yielding and localized buckling of the steel elements, not brittle fractures. Based on this presumed behavior, building codes permit steel moment-frame buildings to be designed with a fraction of the strength that would be required to respond to design level earthquake ground shaking in an elastic manner. Steel moment-frame buildings are anticipated to develop their ductility through the development of yielding in beam-column assemblies at the

beam-column connections. This yielding may take the form of plastic hinging in the beams (or, less desirably, in the columns), plastic shear deformation in the column panel zones, or through a combination of these mechanisms. It was believed that the typical connection employed in steel moment-frame construction, shown in Figure 2.1, was capable of developing large plastic rotations, on the order of 0.02 radians or larger, without significant strength degradation.
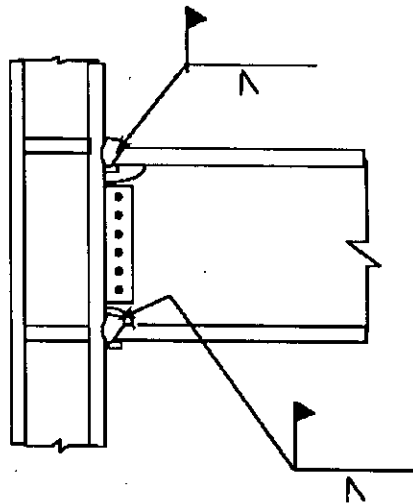
Figure 2.1 Typical Welded Moment-Resisting Connection Prior to 1994

Observation of damage sustained by buildings in the 1994 Northridge earthquake indicated that, contrary to the intended behavior, in many cases, brittle fractures initiated within the connections at very low levels of plastic demand, and in some cases, while the structures remained essentially elastic. Typically, but not always, fractures initiated at the complete joint penetration (CJP) weld between the beam bottom flange and column flange (Fig 2.2). Once initiated, these fractures progressed
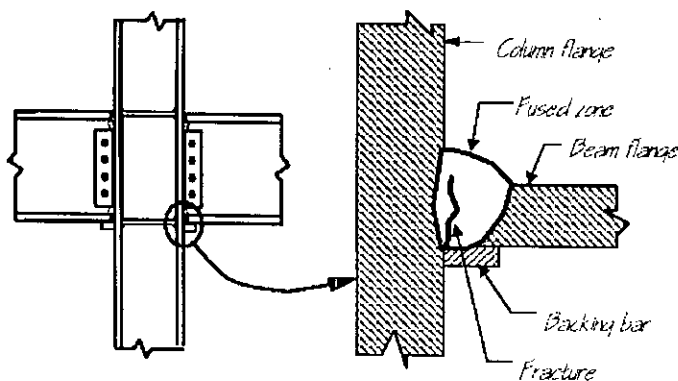
Figure 2.2 Common Zone of Fracture Initiation in Beam –Column Connection

along a number of different paths, depending on the individual joint conditions.

In some cases, the fractures progressed completely through the thickness of the weld, and when fire protective finishes were removed, the fractures were evident as a crack through exposed faces of the weld, or the metal just behind the weld (Figure 2.3a). Other fracture patterns also developed. In some cases, the fracture developed into a crack of the column flange material behind the CJP weld (Figure 2.3b). In these cases, a portion of the column flange remained bonded to the beam flange, but pulled free from the remainder of the column. This fracture pattern has sometimes been termed a "divot" or "nugget" failure.

A number of fractures progressed completely through the column flange, along a near horizontal plane that aligns approximately with the beam lower flange (Figure 2.4a). In some cases, these fractures extended into the column web and progressed across the panel zone (Figure 2.4b). Investigators have reported some instances where columns fractured entirely across the section.

a. Fracture in Weld Zone
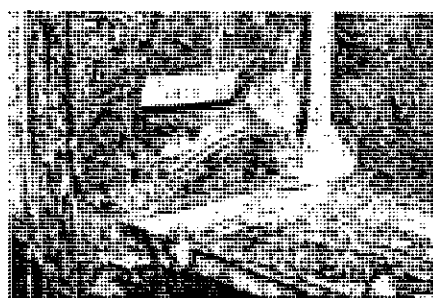
b. Column Flange "Divot" Fracture

Figure 2.3 Fractures of Beam-to-Column Joints (FEMA-350)
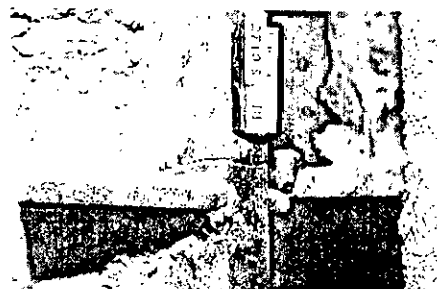
a. Fractures through Column Flange
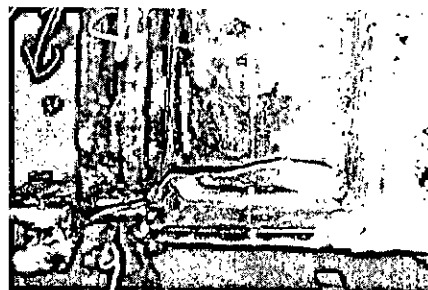
b. Fracture Progresses into Column Web

Figure 2.4 Column Fractures (FEMA-350)

10

Once such fractures have occurred, the beam-column connection has experienced a significant loss of flexural rigidity and strength to resist those loads that tend to open the crack. Residual flexural strength and rigidity must be developed through a couple consisting of forces transmitted through the remaining top flange connection and the web bolts. However, in providing this residual strength and stiffness, the bolted web connections can themselves be subject to failures. These include fracturing of the welds of the shear plate to the column, fracturing of supplemental welds to the beam web or fracturing through the weak section of shear plate aligning with the bolt holes (Figure 2.5).

Despite the obvious local strength impairment resulting from these fractures, many damaged buildings did not display overt signs of structural damage, such as permanent drifts or damage to architectural elements, making reliable postearthquake damage evaluations difficult. In order to determine if a building has sustained connection damage it is necessary to remove architectural finishes and fireproofing, and perform detailed inspections of the connections. Even if no damage is found, this is a costly process. Repair of damaged connections is even more costly. At least one steel moment-frame building sustained so much damage that it was deemed more practical to demolish the building than to repair it.
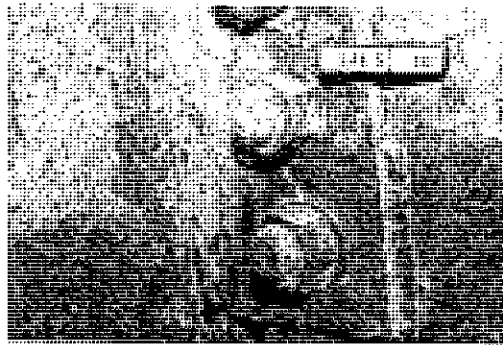
Figure 2.5 Vertical Fracture through Beam Shear Plate Connection (FEMA-350)

Initially, the steel construction industry took the lead in investigating the causes of this unanticipated damage and in developing design recommendations. The American Institute of Steel Construction (AISC) convened a special task committee in March, 1994 to collect and disseminate available information on the extent of the problem (AISC, 1994a). In addition, together with a private party engaged in the construction of a major steel building at the time of the earthquake, AISC participated in

sponsoring a limited series of tests of alternative connection details at the University of Texas at Austin (AISC, 1994b). The American Welding Society (AWS) also convened a special task group to investigate the extent to which the damage was related to welding practice, and to determine if changes to the welding code were appropriate (AWS, 1995).

In September, 1994, the SAC Joint Venture, AISC, the American Iron and Steel Institute and National Institute of Standards and Technology jointly convened an international workshop (SAC, 1994) in Los Angeles to coordinate the efforts of the various participants and to lay the foundation for systematic investigation and resolution of the problem. Following this workshop, FEMA entered into a cooperative agreement with the SAC Joint Venture to perform problemfocused studies of the seismic performance of steel moment-frame buildings and to develop recommendations for professional practice (Phase I of SAC Steel Project). Specifically, these recommendations were intended to address the following: the inspection of earthquake-affected buildings to determine if they had sustained significant damage; the repair of damaged buildings; the upgrade of existing buildings to improve their probable future performance; and the design of new structures to provide reliable seismic performance.

During the first half of 1995, an intensive program of research was conducted to explore more definitively the pertinent issues. This research included literature surveys, data collection on affected structures, statistical evaluation of the collected data, analytical studies of damaged and undamaged buildings, and laboratory testing of a series of full-scale beam-column assemblies representing typical pre-Northridge design and construction practice as well as various repair, upgrade and alternative design details. The findings of these tasks formed the basis for the development of FEMA-267 – Interim Guidelines: Evaluation, Repair, Modification, and Design of Welded Steel Moment Frame Structures, which was published in August, 1995. FEMA-267 provided the first definitive, albeit interim, recommendations for practice, following the discovery of connection damage in the 1994 Northridge earthquake.

In September 1995 the SAC Joint Venture entered into a contractual agreement with FEMA to conduct Phase II of the SAC Steel Project. Under Phase II, SAC continued its extensive problem-focused study of the performance of moment resisting steel

frames and connections of various configurations, with the ultimate goal of develop seismic design criteria for steel construction. This work has included: extensive analyses of buildings; detailed finite element and fracture mechanics investigations of various connections to identify the effects of connection configuration, material strength, and toughness and weld joint quality on connection behavior; as well as more than 120 full-scale tests of connection assemblies. As a result of these studies, and independent research conducted by others, it is now known that the typical moment-resisting connection detail employed in steel moment-frame construction prior to the 1994 Northridge earthquake, and depicted in Figure 2.1, had a number of features that rendered it inherently susceptible to brittle fracture. These included the following:

• The most severe stresses in the connection assembly occur where the beam joins to the column. Unfortunately, this is also the weakest location in the assembly. At this location, bending moments and shear forces in the beam must be transferred to the column through the combined action of the welded joints between the beam flanges and column flanges and the shear tab. The combined section properties of these elements, for example the cross sectional area and section modulus, are typically less than those of the connected beam. As a result, stresses are locally intensified at this location.

• The joint between the bottom beam flange and the column flange is typically made as a downhand field weld, often by a welder sitting on top of the beam top flange, in a so-called "wildcat" position. To make the weld from this position each pass must be interrupted at the beam web, with either a start or stop of the weld at this location. This welding technique often results in poor quality welding at this critical location, with slag inclusions, lack of fusion and other defects. These defects can serve as crack initiators, when the connection is subjected to severe stress and strain demands.

• The basic configuration of the connection makes it difficult to detect hidden defects at the root of the welded beam-flange-to-column-flange joints. The backing bar, which was typically left in place following weld completion, restricts visual observation of the weld root. Therefore, the primary method of detecting defects in these joints is through the use of ultrasonic testing (UT). However, the geometry of the connection also makes it very difficult for UT to detect flaws reliably at the

13

bottom beam flange weld root, particularly at the center of the joint, at the beam web. As a result, many of these welded joints have undetected significant defects that can serve as crack initiators.

• Although typical design models for this connection assume that nearly all beam flexural stresses are transmitted by the flanges and all beam shear forces by the web, in reality, due to boundary conditions imposed by column deformations, the beam flanges at the connection carry a significant amount of the beam shear. This results in significant flexural stresses on the beam flange at the face of the column, and also induces large secondary stresses in the welded joint. Some of the earliest investigations of these stress concentration effects in the welded joint were conducted by Richard, et al. (1995). The stress concentrations resulting from this effect resulted in severe strength demands at the root of the complete joint penetration welds between the beam flanges and column flanges, a region that often includes significant discontinuities and slag inclusions, which are ready crack initiators.

• In order that the welding of the beam flanges to the column flanges be continuous across the thickness of the beam web, this detail incorporates weld access holes in the beam web, at the beam flanges. Depending on their geometry, severe strain concentrations can occur in the beam flange at the toe of these weld access holes. These strain concentrations can result in low-cycle fatigue and the initiation of ductile tearing of the beam flanges after only a few cycles of moderate plastic deformation. Under large plastic flexural demands, these ductile tears can quickly become unstable and propagate across the beam flange.

• Steel material at the center of the beam-flange-to-column-flange joint is restrained from movement, particularly in connections of heavy sections with thick column flanges. This condition of restraint inhibits the development of yielding at this location, resulting in locally high stresses on the welded joint, which exacerbates the tendency to initiate fractures at defects in the welded joints.

• Design practice in the period 1985-1994 encouraged design of these connections with relatively weak panel zones. In connections with excessively weak panel zones, inelastic behavior of the assembly is dominated by shear deformation of the panel zone. This panel zone shear deformation results in a local kinking of the column flanges adjacent to the beamflange-to-column-flange joint, and further

increases the stress and strain demands in this sensitive region. In addition to the above, additional conditions contributed significantly to the vulnerability of connections constructed prior to 1994.

- In the mid-1960s, the construction industry moved to the use of the semi-automatic, selfshielded, flux-cored arc welding process (FCAW-S) for making the joints of these connections. The welding consumables that building erectors most commonly used inherently produced welds with very low toughness. The toughness of this material could be further compromised by excessive deposition rates, which unfortunately were commonly employed by welders. As a result, brittle fractures could initiate in welds with large defects, at stresses approximating the yield strength of the beam steel, precluding the development of ductile behavior.

- Early steel moment frames tended to be highly redundant and nearly every beam-column joint was constructed to behave as part of the lateral-force-resisting system. As a result, member sizes in these early frames were small and much of the early acceptance testing of this typical detail was conducted with specimens constructed of small framing members. As the cost of construction labor increased, the industry found that it was more economical to construct steel moment-frame buildings by moment-connecting a relatively small percentage of the beams and columns and by using larger members for these few moment-connected elements. The amount of strain demand placed on the connection elements of a steel moment frame is related to the span-to-depth ratio of the member. Therefore, as member sizes increased, strain demands on the welded connections also increased, making the connections more susceptible to brittle behavior.

- In the 1960s and 1970s, when much of the initial research on steel moment-frame construction was performed, beams were commonly fabricated using A36 material. In the 1980s, many steel mills adopted more modern production processes, including the use of scrap-based production. Steels produced by these more modern processes tended to include micro-alloying elements that increased the strength of the materials so that despite the common specification of A36 material for beams, many beams actually had yield strengths that approximated or exceeded that required for grade 50 material. As a result of this increase in base metal yield strength, the weld metal in the beam-flange-to-column-flange joints became under-matched, potentially contributing to its vulnerability.

15

At this time, it is clear that in order to obtain reliable ductile behavior of steel moment-frame construction a number of changes to past practices in design, materials, fabrication, erection and quality assurance are necessary. The recommended criteria contained in this document, and the companion publications, are based on an extensive program of research into materials, welding technology, inspection methods, frame system behavior, and laboratory and analytical investigations of different connection details. The recommended criteria presented herein are believed to be capable of addressing the vulnerabilities identified above and providing for frames capable of more reliable performance in response to earthquake ground shaking.

2.3 Joint Behaviour and Representation in Steel frames

An extensive review of literature would be carried out to determine a suitable model of connection moment-rotation relationship that would yield appropriate results for nonlinear static analysis. For seismic design purposes, fully welded connections are traditionally used in moment resisting frames. More economical types of bolted connections were not utilized mainly due to their relative flexibility as compared to fully welded forms, to large deformations under the same forces. Whereas this treatment applies for static conditions, the response under dynamic loading may be substantially different. Due to the period of elongation of the frame as well as the higher energy dissipation in the connection, semi rigid frames may attract lower loads and possess higher damping. Consequently, the displacements associated with bolted frames may be lower than that experienced in their welded counterparts. Whereas extensive experimental, analytical and design studies have been undertaken on the static behaviour of bolted semi rigid connections [e.g., Kishi et al. (1990); Bjorhovde et al. (1998)], relatively less attention was given to their seismic performance. Recent studies Nader and Astaneh 1991; Takanashi et al. 1998) have highlighted the feasibility of using semi rigidly connected frames for seismic resistance even in areas of high peak ground parameters. These investigations, among others [e.g., Bernuzzi et al (1996); Leon (1990)], have opened the door for further detailed assessment of the seismic behaviour of semi rigid frames. Many semi rigid frames are currently designed with some guidance given in North American (Load 1993) and European

16

codes (Eurocode 3 1993) for static design. It is therefore necessary to develop techniques for assessing their inherent earthquake resistance to enable full utilization of seismic design.

The significance of examining the behaviour of semi rigid frames under earthquake loads was given an added urgency by the reported failures in welded connections during the Northridge earthquake of 1994, followed by further evidence from the Hyogo-ken Nanbu (Kobe) earthquake of 1995. These repeated observations of failure lend further weight to the effort dedicated to the utilization of other forms of connection.

The prediction of joint rotational behaviour is a preliminary step in the analysis of semi-rigid frames. Numerous investigations into the behaviour of beam-to-column connections have been reported during past few decades. The flexural behaviour of a connection is best represented by the relationship between M, the moment transmitted through the connection, and ϕ, the relative rotation of the two members fastened by the connection. At the University of Illinois, Wilson and Moore, 1917 performed the first experiment to assess the rigidity of steel frame connections. Since then, experimental investigation into connection behaviour has been continued. Prior to 1950, most connection tests were focused on riveted joints (Young and Dunbar, 1928; Batho and Lash, 1936). After 1950, high strength bolted connections were used extensively in steel construction. A large number of tests have been made and reported. Jones et al., 1980 reviewed and collected a total of 323 tests from 29 separate studies. Nethercot, 1985 examined and evaluated more than 800 individual tests from open literature. Goverdhan, 1984 collected a total of 230 experimental moment-rotation curves and digitised them to form the database of connection behaviour. Kishi and Chen, 1986 extended Goverdhan's collection to a total of 303 tests and created a computerised data bank system together with a modified exponential curve-fitting program. Abdalla and Chen, 1995 expanded the database by adding additional 46 experimental test data pertaining to steel beam-to-column connections.

To realise a rational design method for flexibly jointed frames, availability of moment-rotation relations or M-ϕ curves of practical connections is a prerequisite. Since it is not convenient to use the experimental results in the analysis or design of a

frame, it is important to model the connection M-ϕ behaviour mathematically so that a reasonable estimate of the rotational stiffness of the connection at any level of moment can be made. Based on observed experimental results a number of such analytical models for predicting moment-rotation behaviour of semi-rigid connections have been developed by several researchers. In an attempt to analytically model a connection behaviour, the most notable developments include the Frye-Moriss polynomial model (Frye and Moriss, 1975) and the Kishi-Chen three-parameter power model (Kishi and Chen, 1990). These models are satisfactory for some particular type of connections, for others the researchers are still dependent on experimentally available M-ϕ data. Several techniques exist for representing experimental connection behaviour for its use in numerical frame analysis programs. Jones et al, 1981 used a cubic B-spline fitting through experimental M-ϕ data and demonstrated that Cubic B-spline fitting are superior to polynomial or exponential type of fitting. Attempts were made to use further simplified representation of experimentally obtained connection behaviour. It has been shown that structural responses predicted by using Cubic B-spline fitting are in close agreement with those predicted by a simple tri-linear approximation of moment-rotation curves (Ahmed, 1992).

To perform static analysis on flexibly connected frames, Ahmed, 1992 developed a Finite Element program where the connection flexibility was incorporated by modifying the shape of a conventional beam column element (Rifai, 1987). Ahsan, 1997 used this method to develop a methodology for determination of static lateral drift of sway frames. To perform dynamic analysis on flexibly connected frames, Ahsan et al, 2005 also developed a Finite Element program. Suarez et al, 1996 proposed a method for the modal analysis of frames with flexible connections having linear moment-rotation relationship.

2.4 Methods of Analysis of Semi-Rigid Frames

Attempts to include semi-rigid joint action in the analysis include a wide range of work; from modification of traditional methods of analysis of rigid frames to the formulation of classical finite element models. A brief review of this work is made in the following sections.

2.4.1 Modification of the Conventional Methods

As long ago as 1942, the slope deflection equations were used to represent members with semi-rigid joints at ends by modifying the coefficients of the usual rigid case (Johnston and Mount, 1942). The procedure is otherwise the same as the conventional slope deflection method. The modified moment distribution method also follows the same procedure as the conventional one, with the only difference being that different distribution and carry over factors are used with semi-fixed end moments. The other basic methods like the Method of Three Moments and the deformeter Methods have also been modified to take account of the semi-rigid nature of the beam-column connections.

In all of these modifications a linear connection stiffness was assumed, which is taken as the initial slope of the connection M-ϕ curve. This simplification, however, remains a formidable shortcoming because of the fact that, in most cases, non-linearity in connection behaviour starts even at a small load application. These methods have not become popular because of this limitation coupled with the complexities in their use.

2.4.2 Computer Analysis of Semi-Rigidly Connected Plane Frames

The application of computers has made it possible to represent the joint behaviour in a more refined and accurate manner. Most approaches to the analysis of semi-rigid frames have been developed with one or other of the two basic philosophies :

i) By introducing one or more discrete spring elements (Goverdhan, 1984; Lui, 1985) to simulate the joint response (Fig. 2.6). Each of these springs can be assigned a predetermined force-displacement relation representing the axial, shear and flexural behaviour of the joint. Any type of constitutive law can, in principle,
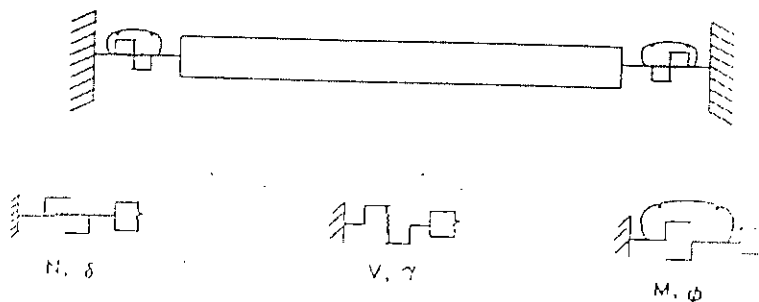
Figure 2.6 The Beam-Joint Model for Various Force Components
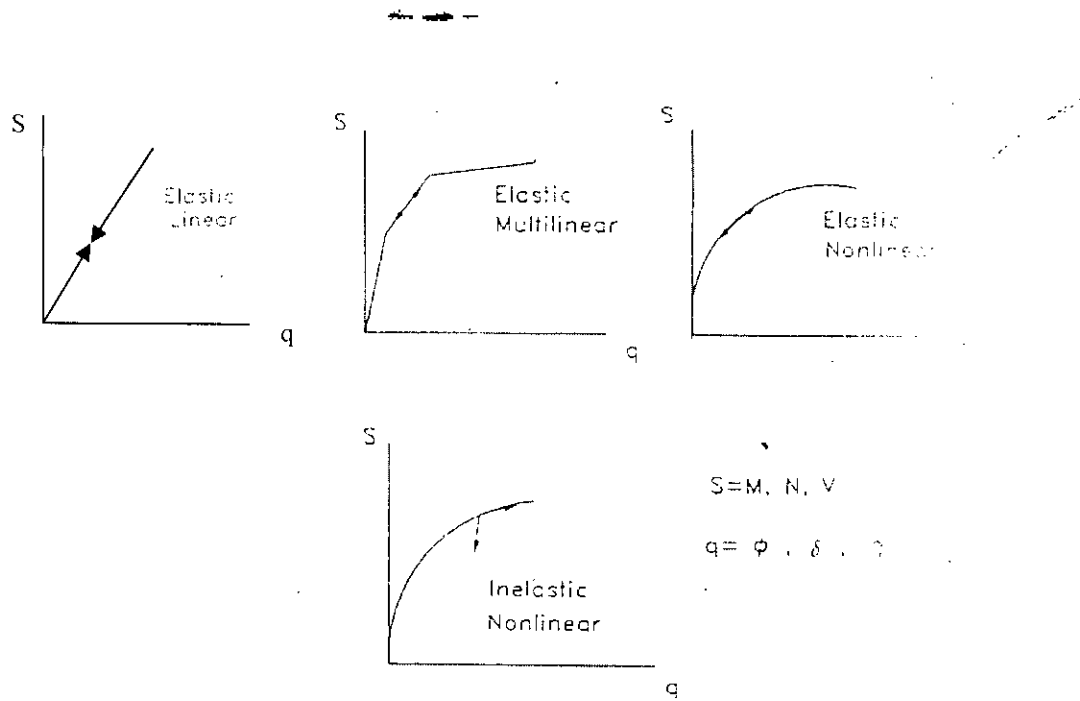
Figure 2.7 Various Representations of The Joint Behaviour

be assumed : linear elastic, non-linear elastic or inelastic (Fig. 2.7). However, research studies have shown that, for rectilinear frames, flexural behaviour of the joint is the most significant one.

ii)   By directly modifying the member stiffness relationships to account for the partial rotational restraining effect of the connections (Nethercot, 1974; Allen and Bulson, 1980; Wang, 1983; Lee, 1987).

The former approach has the disadvantage that the total number of degrees of freedom required to model the deformed configuration of the structure increases significantly. Despite wide-spread availability of microcomputers, these approaches are more suitable for an academic setting than day-to-day design office practice. The main features of some of the important developments in the recent years are discussed here.

Ackroyd, 1979 developed a computer program for the analysis of flexibly connected steel frames. Based on a secant stiffness formulation, this development accounts for both material and geometric non-linearity including loading and unloading capabilities of non-linear connection M-ϕ behaviour.

Cosenza, De Luca and Failla, 1984 also developed a computer program which utilises the stiffness method of analysis and includes second order effects. Semi-rigid joints

20

were modelled as extra elements consisting of short rigid segments and springs with axial, shear and rotational stiffness (Fig. 2.8). Many alternative approaches for representing the connection M-ϕ relationship have been considered. The behaviour of multi-story flexibly connected frames has been studied using this program and it was concluded that the use of stiffer connections increases the critical load for the frame.
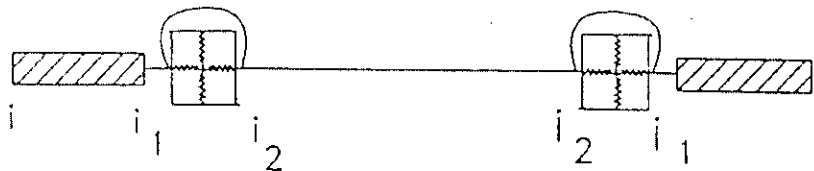
Figure 2.8 Semi-Rigid Beam-Joint Element by Cosenza et al, 1984.

Anderson and Lok, 1985 developed a method of analysis to incorporate the influence of connection flexibility into the analysis of plane frames. Second order effects were considered in this elastic analysis procedure. In the analysis the rotations at any connections except real pins are initially assumed to be zero. Using conventional rigid frame analysis, the displacement and rotations are calculated and hence the member end reactions are obtained using slope deflection equations. Connection M-ϕ characteristics are then used to assess connection rotations and these are used to amend the applied load vector. Using this new vector of applied loads, a new vector of displacements and thus new member end reactions are obtained. The procedure is repeated until the convergence is achieved. The stiffness matrix at each iteration is kept unchanged and thus a saving in computer time is achieved.

Chen and Lui, 1985 employed the stiffness method in which the element matrices were derived on the basis that an element with two semi-rigid joints at its ends is treated as a sub-structure. The sub-structure consists of three sub-elements : two joint elements and one beam-column element (Fig. 2.9). Stability functions derived by Lui, 1985 were used to account for the presence of axial forces in the beam-column
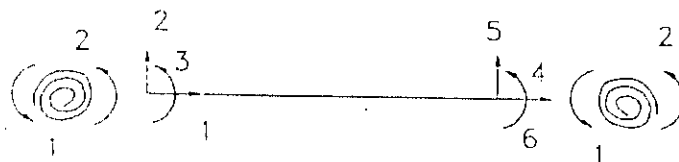
Figure 2.9 Semi-Rigid Beam-Joint Element by Chen and Lui, 1985.

21

elements and an incremental iterative type of analysis was used. The M-ϕ data for the connections were represented by an exponential function.

Poggi and Zandonini, 1985 reported the development of a program by modifying the program developed by Corradi and Poggi, 1985 to include the effect of semi-rigid joints. In this program M-ϕ data for the connection was modelled by a series of straight lines. It is based on small deflection theory - which obviously affects its performance for the analysis of flexibly connected sway frames, where the occurrence of large displacements is commonly encountered. This analysis program includes neither material nor geometrical imperfections and is capable of handling column bending about the major axis only.

Lee, 1987 developed a large-displacement inelastic formulation based on the secant stiffness approach for the limit load analysis of planar frames with partially restrained connections. It has been claimed that, as opposed to the tangent stiffness approach, the use of a secant stiffness approach allows the use of an increment size large enough to limit the required number of iteration cycles for convergence. The analytical approach is based on the slope-deflection method in which the equilibrium equations are written with respect to the deformed shape of the structure (Galambos, 1968) and involves the use of stability functions to reflect the effect of member axial forces exactly.

Jones, 1980 developed a computer program to trace the load deflection behaviour of an isolated column with semi-rigid joints up to its failure load. This finite element program includes both geometric and material non-linearity. The column was assumed to be connected to infinitely rigid beams through semi-rigid joints (i.e. beam stiffness were not included). A non-linear M-ϕ relationship was utilised. Jones was the first to use the B-spline technique to model the connection M-ϕ relationship. He concluded that use of even the most flexible connections may improve the buckling load of the column considerably.

Following Jones' work, Rifai, 1987 developed a program to analyse a beam-column subassemblage (Fig. 2.10). This finite element formulation again considers both geometric and material non-linearity; the influence of residual stresses and geometric imperfections is included. This program can only handle subassemblages of the fixed shape shown in Fig. 2.10. He concluded that the stiffness of the beam and the

22

performance of the joint stiffness both influence the restraint for the column. The accuracy of the program was verified by experimental work undertaken by Davison, 1987.
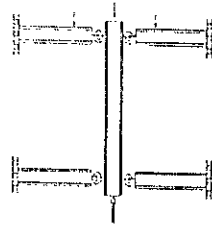
Figure 2.10 Limited Column-Subassemblage Considered by Rifai 1987.

Anderson et al, 1991 extended a computer program originally developed by Majid and Anderson, 1968 and based on the matrix-displacement method of analysis to include the effect of semi-rigid connections which are treated as elastic hinges. The non-linear M-ϕ curve is idealised as piece-wise linear relations and successive estimates are made of the secant stiffness of each connection as the iteration proceeds.

Ahmed, 1992 modified the finite element program developed by Rifai, 1987 to facilitate a behavioural study of flexibly connected steel frames. This program included material non-linearity, geometric non-linearity and full connection non-linearity. Initial member imperfections and cyclic loading-unloading behaviour of connections were also considered in this program. The prediction of this program was then validated against available analytical and experimental results. Ahmed used this program for limited parametric study and he proposed a simplified design method for non-sway semi-rigid steel frames.

The methods of analysis mentioned here are only a few selected from a much higher number of available techniques which vary in their level of refinement and in their capacity to simulate full physical behaviour accurately.

2.5 The Performance Based Seismic Design

A performance objective specifies the desired seismic performance of the building. Seismic performance is described by designating the maximum allowable damage state (performance level) for an identified seismic hazard (earthquake ground motion). A performance objective may include consideration of damage states for several

levels of ground motion and would then be termed a dual or multiple level performance objectives.

The purpose of Performance-Based Seismic Design (PBSD) is to give a realistic assessment of how a structure will perform when subjected to either particular or generalized earthquake ground motion. While the code design provides a pseudo-capacity to resist a prescribed lateral force; this force level is substantially less than that to which a building may be subjected during a postulated major earthquake. It is assumed that the structure will be able to withstand the major earthquake ground motion by components yielding into the inelastic range, absorbing energy, and acting in a ductile manner as well as by a multitude of other actions and effects not explicitly considered in code applications (Freeman, 1992). Although the code requires special ductile detailing, it does not provide a means to determine how the structure will actually perform under severe earthquake conditions. This is the role of PBSD (Freeman et al., 2004).

The Capacity Spectrum Method (CSM) is a procedure that can be applied to PBSD. The CSM was first introduced in the 1970s as a rapid evaluation procedure in a pilot project for assessing seismic vulnerability of buildings at the Puget Sound Naval Shipyard (Freeman et al., 1975). In the 1980s, it was used as a procedure to find a correlation between earthquake ground motion and building performance (ATC, 1982). The method was also developed into a design verification procedure for the Tri-services (Army, Navy, and Air Force) "Seismic Design Guidelines for Essential Buildings" manual (Freeman et al., 1984; Army, 1986). The procedure compares the capacity of the structure (in the form of a pushover curve) with the demands on the structure (in the form of a response spectrum). The graphical intersection of the two curves approximates the response of the structure. In order to account for non-linear inelastic behavior of the structural system, effective viscous damping values are applied to the linear-elastic response spectrum similar to an inelastic response spectrum. In the mid 1990s, the Tri-services manual was updated (WJE, 1996). By converting the base shears and roof displacements from a non-linear pushover to equivalent spectral accelerations and displacements and superimposing an earthquake demand curve, the non-linear pushover becomes a capacity spectrum. The earthquake demand curve is represented by response spectra, plotted with different levels of

"effective" or "surrogate" viscous damping (e.g. 5%, 10%, 15%, 20% and sometimes 30% to approximate the reduction in structural response due to the increasing levels of damage). By determining the point, where this capacity spectrum "breaks through" the earthquake demand, engineers can develop an estimate of the spectral acceleration, displacement, and damage that may occur for specific structure responding to a given earthquake.

In recent years, there has been substantial research and discussion on the merits of inelastic response spectra and equivalent (surrogate) damped spectra and on the appropriateness of using damped spectra to represent inelastic response (e.g., Chopra and Goel, 1999; Fajfar, 1998; Judi et al., 2002). Although the conclusions of these researchers are not wholly consistent with each other, it has been claimed by some (Chopra and Goel, 1999) that use of damped spectra may lead to less conservative results as compared to inelastic spectra. The comparisons, in general, are based on the ATC 40 Type A damped spectra. A number of changes have been proposed to the capacity spectrum method that increase the complexity and computational effort associated with this method, usually requiring iteration to find the "exact" point where the capacity spectrum intersects the "correct" level of damping. Freeman (Freeman et al, 2004) believes that iteration is unnecessarily complex and clumsy for the intended use of this procedure; rather, he views the capacity spectrum method as a tool for estimating and visualizing the likely behavior of the structure under a given earthquake in a simple graphical manner. By formatting the results in the acceleration-displacement response- spectrum format (Mahaney et al., 1993) in lieu of the traditional spectral acceleration (Sa) versus period (T) format, the graphical and intuitive nature of the capacity spectrum method become even more apparent.

2.5.1 Performance Definition in accordance with FEMA

The performance evaluation procedures contained in FEMA-350 (Recommended Seismic Design Criteria for New Steel Moment-Frame Buildings) permit estimation of a level of confidence that a structure will be able to achieve a desired performance objective. Each performance objective consists of the specification of a structural performance level and a corresponding hazard level, for which that performance level is to be achieved. For example, a design may be determined to provide a 95% level of confidence that the structure will provide Collapse Prevention or better performance

25

for earthquake hazards with a 2% probability of exceedance in 50 years, or a 50% level of confidence that the structure will provide Immediate Occupancy or better performance, for earthquake hazards with a 50% probability of exceedance in 50 years.

2.5.2 Hazard Level

FEMA-302 defines two specific levels of hazard for consideration in design and specifies methods for developing response spectra for each of these levels. The two levels are:

1. Maximum Considered Earthquake (MCE) ground shaking. This is the most severe level of ground shaking that is deemed appropriate for consideration in the design process forbuilding structures, though not necessarily the most severe level of ground shaking that could ever be experienced at a site. In most regions, this ground shaking has a 2% probability of exceedance in 50 years, or roughly a 2,500 year mean recurrence interval.

2. Design Earthquake (DE) ground shaking. It is defined as a spectrum that is 2/3 of the shaking intensity calculated for the MCE spectrum, at each period.

2.5.3 Performance Levels

A performance level describes a limiting damage condition which may be considered satisfactory for a given building and a given ground motion. The limiting condition is described by the physical damage within the building, the threat to life safety of building's occupants created by the damage, and the post-earthquake serviceability of the building. Building performance is a combination of the performance of both structural and nonstructural components. Table 2-1 describes the overall levels of structural and nonstructural damage that may be expected of buildings meeting two performance levels, termed Collapse Prevention and Immediate Occupancy. These performance descriptions are not precise and variation among buildings must be expected, within the same Performance Level.

26

Table 2-1 Building Performance Levels

	Building Performance Levels	
	Collapse Prevention Level	**Immediate Occupancy Level**
Overall Damage	**Severe**	**Light**
General	Little residual stiffness and strength, but gravity loads are supported. Large permanent drifts. Some exits may be blocked. Exterior cladding may be extensively damaged and some local failures may occur. Building is near collapse.	Structure substantially retains original strength and stiffness. Minor cracking of facades, partitions, ceilings, and structural elements. Elevators can be restarted. Fire protection operable.
Nonstructural components	Extensive damage.	Equipment and contents are generally secure, but may not operate due to mechanical failure or lack of utilities.

CHAPTER 3

Numerical Model

3.1   Introduction

The success of the finite element method in solving various physical problems has resulted in its widespread use in structural problems. Although the analysis of structures by the finite element method has become fairly common due to the abundance of computers in the design offices, the major drawback lies in the simplifying assumptions that are almost certainly have to be made in any such computer model. Such assumptions normally include idealised behaviour which is the basis of most of the available formulations. One of the important idealisations commonly made in the analysis of structural frames relates to the behaviour of the connections which are usually taken either as perfectly hinged or rigidly fixed, However, as mentioned earlier, the realistic behaviour of the connection is semi-rigid and its inclusion in the analysis and design is advantageous in the sense of reliability and economy of construction. .

The effect of semi-rigid connections on member stiffness can be accounted for in two ways. One is to represent the connection stiffness by introducing discrete elements at the ends of the member in the form of springs with flexural, shear and axial stiffness; the other is to modify directly the member stiffness relationships to account for the partial rotational restraining effect of the connections. In the present study, a finite element program of 2D inelastic unbraced framed structures with nonlinear beam-column connection is developed by which the user may model and analyze the structures with the help of ANSYS. This program incorporates the semirigid connection behaviour by introducing discrete elements at the ends of the member in the form of springs with flexural, shear and axial stiffness .To validate the developed program the program is verified against some theoretical or test results.

3.2   Finite Element Formulation

For representing the beams and columns, 2-D Plastic Beam element called 'BEAM23' is used. For the simulation of semi-rigid action of the connections, a rotational spring element has been used. This element has the advantage of considering the non-linear moment-rotation behaviour of connections. This element is termed as 'COMBIN39' (non-linear spring). For the frame modelling, the Nonlinear Static Analysis, the modal analysis and the macro files that comprise the tri linearization points of different semi-rigid connection types, codes written in ANSYS language are given in Appendix-D.

3.2.1   Beam and Column (Element BEAM23)

BEAM23 is a uniaxial element with tension-compression and bending capabilities. The element has three degrees of freedom at each node: translations in the nodal X and Y direction and rotation about the nodal Z-axis. The element has plastic, creep, and swelling capabilities.

Input Data

The geometry, node locations, and the coordinate system for this element are shown in BEAM23 (Figure 3.1). Any one of four cross-sections may be selected with the appropriate value of KEYOPT(6). The element is defined by two nodes, the cross-sectional area, moment of inertia, the height for rectangular beams, the outer diameter (OD), and the wall thickness (TKWALL), for thin-walled pipes, the outer diameter for solid circular bars, and the isotropic material properties.

The general cross-section option allows inputting a section height and a five-location area distribution. If the section is symmetric, only the first three of the five areas need be input since the fourth area defaults to the second and the fifth area defaults to the first. The areas input should be a weighted distribution at the -50% integration point A(-50), the -30% integration point A(-30), the 0% integration point
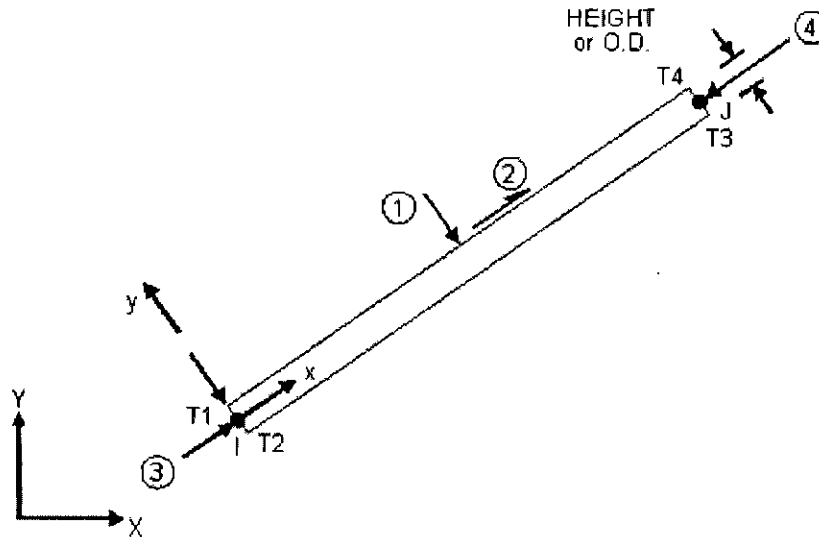
Figure 3.1 BEAM23 2-D Plastic Beam

A(0), the 30% integration point A(30), and the 50% integration point A(50). Each area A(i) is as shown in Characteristics. The height is defined as the distance between the $\pm$ 50% integration points, and is not necessarily the distance between the outermost fibers of the section. Determination of the input areas is accomplished as follows. Estimate one of the input areas by the formula A(i) = L(i) x HEIGHT, where L(i) is the width of the section at integration point i. Substitute this area along with the section moment of inertia, I_{zz}, and total area, A, into the above equations and solve them simultaneously for the remaining two input areas. A(0) is usually the easiest to estimate; for instance, as a first guess A(0) for an I-beam would be the web thickness times the height. A trial and error procedure (by modifying the estimated input area) may be needed if the calculated input areas are inconsistent, such as a negative area.

The input areas, A(i), are related to the true areas, $A_t(i)$, corresponding to each integration point, by:

$A_t(-50) = 0.0625\ A(-50)$, $A_t(50) = 0.0625\ A(50)$,

$A_t(-30) = 0.28935\ A(-30)$, $A_t(30) = 0.28935\ A(30)$,

$A_t(0) = 0.29630\ A(0)$

Shear deflection may be controlled with the KEYOPT(2) value. The shear deflection constant (SHEARZ) is input only for the general cross-section. The shear modulus (GXY) is used only with shear deflection.

Pressures may be input as surface loads on the element faces as shown by the circled numbers on BEAM23. Positive normal pressures act into the element. Lateral pressures are input as a force per unit length. End "pressures" are input as a force. KEYOPT(10) allows tapered lateral pressures to be offset from the nodes. Temperatures and fluences may be input as element body loads at the four "corner" locations shown in BEAM23. The first corner temperature T1 defaults to TUNIF. If all other temperatures are unspecified, they default to T1. If only T1 and T2 are input, T3 defaults to T2 and T4 defaults to T1. For any other input pattern, unspecified temperatures default to TUNIF. Similar defaults occurs for fluence except that zero is used instead of TUNIF.

A summary of the element input is given in Input Summary. Element Input gives a general description of element input.

a) Printout Locations

b) Weighting Functions for General Section (KEYOPT (6) = 4)
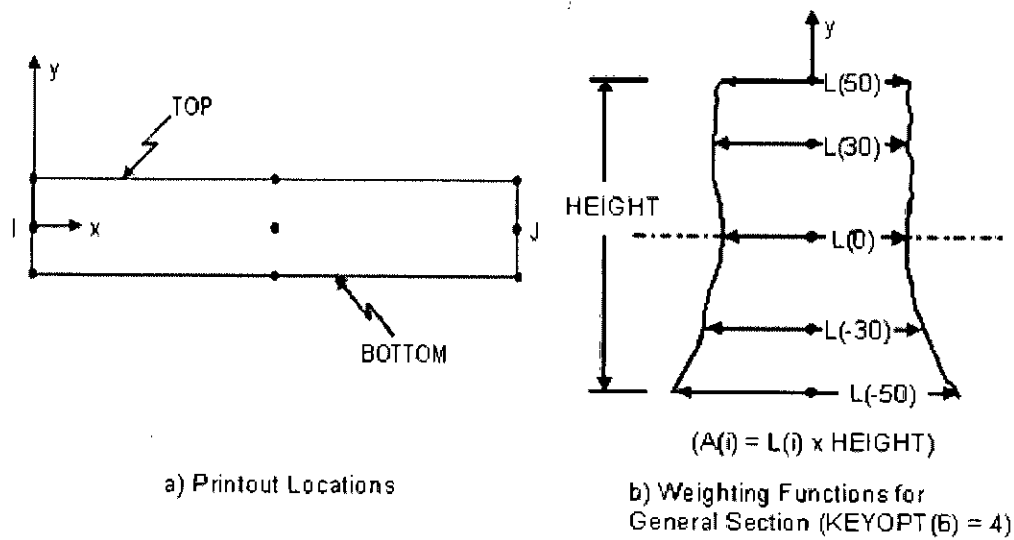
Figure 3.2 BEAM23 Characteristics

BEAM23 Input Summary

Element Name	BEAM23
Nodes	I, J
Degrees of Freedom	UX, UY, ROTZ
Real Constants	AREA, IZZ, HEIGHT if KEYOPT (6) = 0, or
	OUTER DIAMETER, WALL THICKNESS if KEYOPT (6) = 1, or
	OUTER DIAMETER if KEYOPT (6) = 2, or
	HEIGHT, A (-50), A (-30), A (0), A (30), A (50), and SHEARZ if KEYOPT (6) = 4
Material Properties	EX, ALPX, DENS, GXY, DAMP
Surface Loads	Pressures - face 1 (I-J) (-Y normal direction), face 2 (I-J) (+X tangential direction), face 3 (I) (+X axial direction), face 4 (J) (-X axial direction) (use negative value for loading in opposite direction)
Body Loads	Temperatures - T1, T2, T3, T4
	Fluences - FL1, FL2, FL3, FL4
Special Features	Plasticity, Creep, Swelling, Stress stiffening, Large deflection, Large strain, Birth and death.
KEYOPT(2)	0 - No shear deflection

	1 -	Include shear deflection (also input SHEARZ if KEYOPT(6)=4)
KEYOPT(4)	0 -	No printout of member forces and moments
	1 -	Print out member forces and moments in the element coordinate system
KEYOPT(6)	0 -	Rectangular section
	1 -	Thin walled pipe
	2 -	Round solid bar
	4 -	General section

For sample calculation of integration point of this element see Appendix- B.

3.2.2 Beam - Column Connection (Element COMBIN39)

COMBIN39 is a unidirectional element with nonlinear generalized force-deflection capability that can be used in any analysis. The element has longitudinal or torsional capability in one, two, or three-dimensional applications. The longitudinal option is a uniaxial tension-compression element with up to three degrees of freedom at each node: translations in the nodal X, Y, and Z directions. No bending or torsion is considered. The torsional option is a purely rotational element with three degrees of freedom at each node: rotations about the nodal X, Y, and Z-axes. No bending or axial loads are considered. The element has large displacement capability for which there can be two or three degrees of freedom at each node.
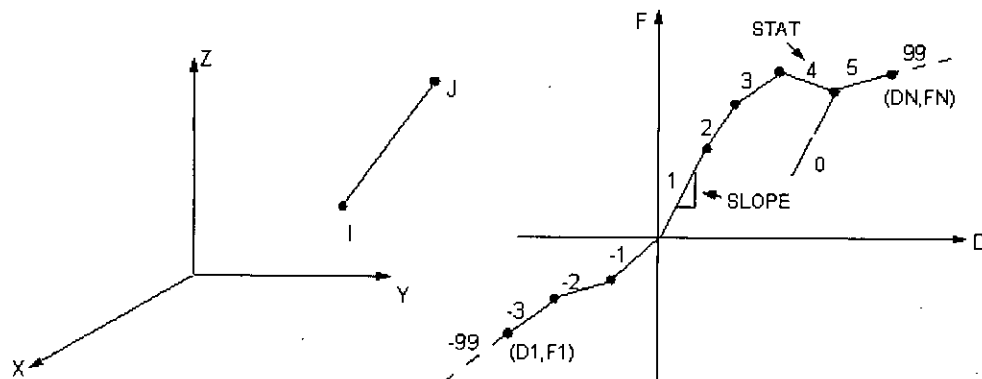
Figure 3.3 COMBIN39 Nonlinear Spring

33

Input Data:

The geometry, node locations, and the coordinate system for this element are shown in COMBIN39. Two node points and a generalized force-deflection curve define the element. The points on this curve (D1, F1, etc.) represent force (or moment) versus relative translation (or rotation) for structural analyses, and heat (or flow) rate versus temperature (or pressure) difference for a thermal analysis. The loading curve should be defined on a full 360° basis for an axisymmetric analysis.

The force-deflection curve should be input such that deflections are increasing from the third (compression) to the first (tension) quadrants. Adjacent deflections should not be nearer than 1E-7 times total input deflection range. The last input deflection must be positive. Segments tending towards vertical should be avoided. If the force-deflection curve is exceeded, the last defined slope is maintained, and the status remains equal to the last segment number.

COMBIN39 Input Summary

Element Name	COMBIN39
Nodes	I, J
Degrees of Freedom	UX, UY, UZ, ROTX, ROTY, ROTZ, PRES, or TEMP. Make 1-D choices with KEYOPT(3). Make limited 2- or 3-D choices with KEYOPT(4).
Real Constants	D1, F1, D2, F2, D3, F3, D4, F4, ...D20, F20
Material Properties	None
Surface Loads	None
Body Loads	None
Special Features	Nonlinear, Stress stiffening, Large displacement
KEYOPT(1)	0 - Unload along same loading curve
	1 - Unload along line parallel to slope at origin of loading curve
KEYOPT(2)	0 - Compressive loading follows defined compressive curve (or reflected tensile curve if not defined)
	1 - Element offers no resistance to compressive loading
	2 - Loading initially follows tensile curve then follows compressive curve after buckling (zero or negative stiffness)
KEYOPT(3)	(KEYOPT(4) overrides KEYOPT(3))
	0, 1 - UX (Displacement along nodal X axes)

	2 -	UY (Displacement along nodal Y axes)
	3 -	UZ (Displacement along nodal Z axes)
	4 -	ROTX (Rotation about nodal X axes)
	5 -	ROTY (Rotation about nodal Y axes)
	6 -	ROTZ (Rotation about nodal Z axes)
	7 -	PRES
	8 -	TEMP
KEYOPT(4)	0 -	Use any KEYOPT(3) option
	1 -	3-D longitudinal element (UX, UY and UZ)
	2 -	3-D torsional element (ROTX, ROTY and ROTZ)
	3 -	2-D longitudinal element. (UX and UY) Element must lie in an X-Y plane
KEYOPT(6)	0 -	Basic element printout
	1 -	Also print force-deflection table for each element (only at first iteration of problem)

In this study moment versus rotation of this element has taken from Tri-linearised moment-rotation relationship of different type of connections. For sample calculation see Appendix- A.

3.3 Verification of the Computer Program

To carry out finite element analysis in order to predict the behaviour of any structure, it is essential to verify the developed program against some theoretical or test results to ensure that the developed model is acting in the way it was supposed to be. The verification of the frame models having rigid, pin, semi-rigid beam-to-column connection in static and modal analysis which are more relevant to the present study are discussed in the following section.

3.3.1 Single-Storey Single Bay Rigid Frame

Single-storey single-bay rigid frame is the basic form of sway frames that has immense importance from analysis point of view. The construction of semi-rigid frames differs from that of rigid frames in that connection behaviour must be taken into consideration in the analysis and design procedure.

3.3.1.1 Description of the Problem

To verify the numerical results, a stepwise approach was followed. The single-storey single bay frame as shown in Figure 3.4 was analyzed and compared with the theoretically obtained results (Ahmad, S., Chapter 4).

Storey height and width of the bay are 30ft and 50ft respectively. The frame was assumed to made of steel (E $^\wedge$ 30x10^3 ksi). The moment of inertia of the column is 7000 in^4 while the same for the beam is 14000 in^4. The frame is subjected to a horizontal wind load of 500 Lb/ft along AB. The key results for this case were moments at support A and at connection C, and the lateral sway of the frame.
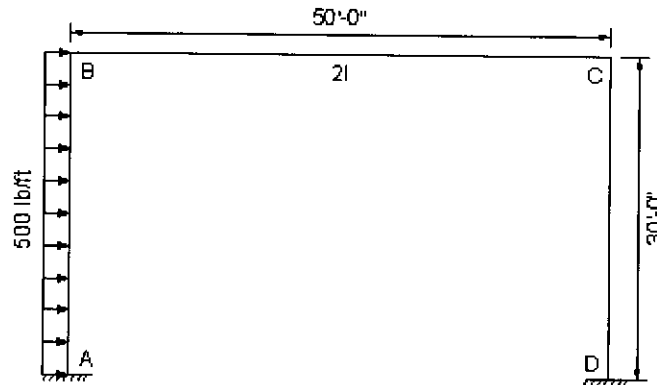
Figure 3.4 One Storey Single Bay Rigid Frame Subjected to Uniform Wind Load

3.3.1.2 Finite Element Modelling of the Frame

Each column was divided into five elements and the beam was divided into ten elements in the finite element model. The beam and columns were modelled by '2D Elastic Beam' elements. For FE analysis the beam and column sections were assumed to be square and hence the corresponding cross sectional areas were determined from the respective moment of inertia values.

3.3.1.3 Comparison of Results

Table 4-1 shows the comparison of FE and theoretical results obtained by moment distribution method (Wang, C. K., Chapter 8). In this table a negative value of moment refers to an anti-clockwise rotation. From Table 4-1 it is observed that the

values of moment at point A and lateral drift of point B are the same for both the methods of calculation. But the magnitude of moment at point C differs insignificantly. This difference is due to rounding of values during hand computation.

Table 3-1 Comparison of FE Analysis and Theoretical Results for Frame Shown in Figure 3.4

Considered parameter	FE results	Theoretical results	% variation
M_{AB} (kip-inch)	-104.2	-104.2	0
M_{CD} (kip-inch)	-39.9	-40	-0.25
Lateral drift	0.0864	0.0864	0

The results in Table 3-1 show the accuracy of the FE model developed and its method of analysis. But since it represents the simplest form of frames, FE models for multi-storeyed frames having multiple bays are to be verified in the same manner. The following section extends the verification to two-storied single bay rigid frame.

3.3.2 Two-Storey Single Bay Rigid Frame

As the storey height of structural frames increases it is usually subjected to greater lateral drift and in fact this lateral drift is the limiting design criterion for sway frames rather than ultimate strength of the members.

3.3.2.1 Description of the Problem

The second problem treats a frame (Figure 3.5) which is simultaneously subjected to concentrated horizontal loads along with concentrated and uniformly distributed vertical loads. Different moment of inertia for almost all the beams and columns has made the problem a critical one. Moments at different sections were determined to check the accuracy of the finite element model.

37
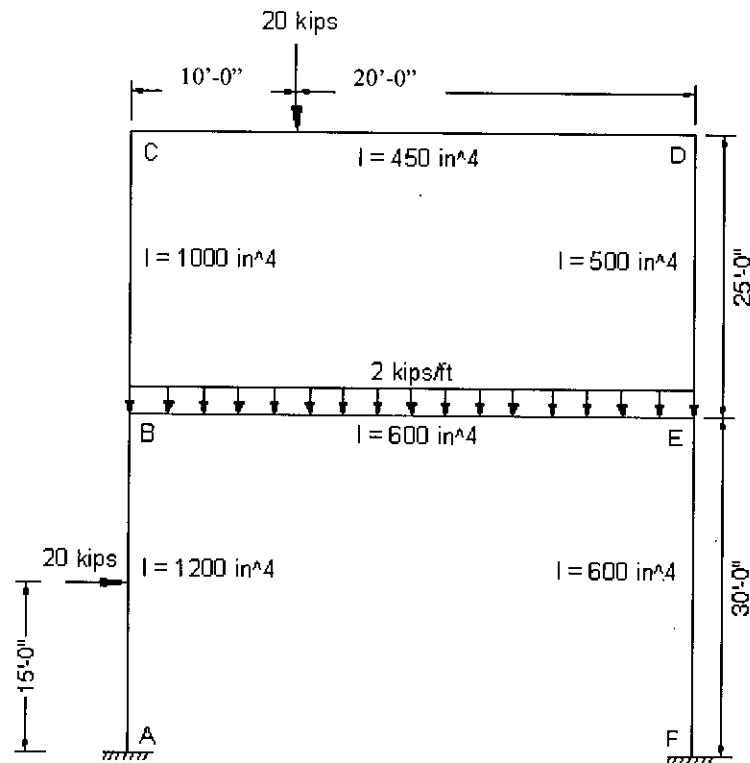
Figure 3.5 Two Storey Single Bay Rigid Frame Subjected to Both Lateral and Vertical Loads.

3.3.2.2 Finite Element Modelling of the Frame

Column AB was divided into seven elements while the other columns BC, DE and EF were divided into five elements each, and, on the other hand, the beams were divided into six elements in the FE model. The beams and columns of the frame were modelled by '2D Elastic Beam' elements and for different values of moment of inertia; five different real constant sets were being employed. As mentioned in the previous example, all beam and column sections were assumed to have square cross sections and the corresponding cross sectional areas were determined from the respective inertia values.

3.3.2.3 Comparison of results

Table 3-2 shows the comparison of finite element analysis and theoretical results obtained by moment distribution method (Wang, C. K., Chapter 8). In this case moments at different locations of the frame were compared. From quantities presented in Table 3-2 it is observed that the magnitude of moments at some locations i.e. M_{DE},

38

M_{ED}, M_{EF} differs by a small percentage from the calculated results. This difference is due to the propagation of round off error resulting in moment distribution method during hand calculation.

Table 3-2 Comparison of FE Analysis and Theoretical Results for Frame Shown in Figure 3.5

Moment (kip-ft)	FE results	Theoretical results	% variation
M_{AB}	-34.4	-34.4	0
M_{BA}	90	90	0
M_{BC}	125.7	125.7	0
M_{BE}	-215.7	-215.7	0
M_{CB}	127	127	0
M_{DE}	5.3	5.1	3.92
M_{ED}	-8.1	-7.7	5.19
M_{EB}	56.3	55.9	0.72
M_{EF}	-48.2	-48.2	0
M_{FE}	-7.6	-8.1	-6.17

3.3.3 Two-Storey Single Bay Frame Analyzed by Lui and Chen

This frame was analyzed Lui and Chen, 1988 with a view to verifying their proposed method and corresponding computer program for sway frame analysis. In order to make a more realistic approach the connections of the frame were modelled by non-linear curves for semi-rigid action analysis.

3.3.3.1 Description of the Frame

The frame analyzed in this section is a two-storey frame as shown in Figure 3.6. The beams were W14 x 48 sections and the columns were W12 x 96 sections. The beams and columns were selected of the aforementioned size as those sections were used in actual tests. The beams were modelled by two elements while the columns by one element. In this example, small lateral forces were applied to the frame to induce sway. The magnitudes of the lateral forces were 0.001P for the top storey and 0.002P for the bottom storey.
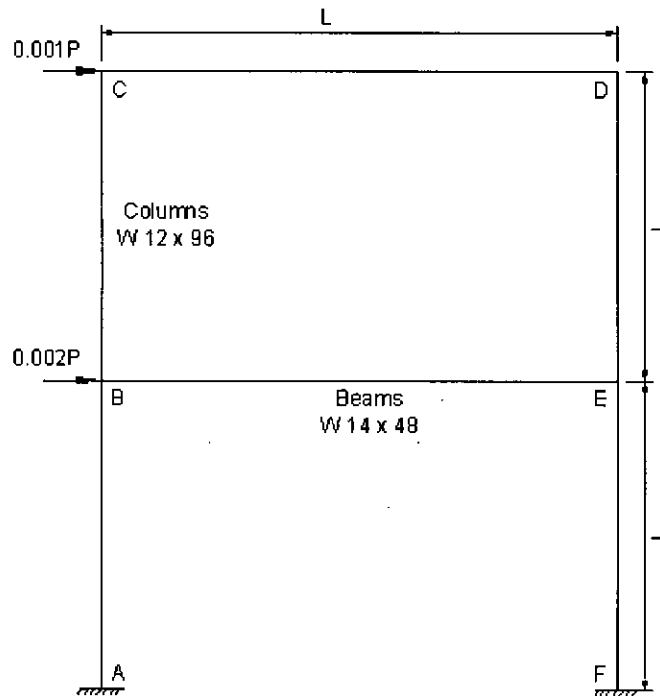
Figure 3.6 Two Storey Frame as Analyzed by Lui and Chen, 1988

3.3.3.2 Rigid Action Analysis

Lui and Chen, 1988 analyzed the aforementioned frame for both rigid and semi-rigid actions of the beam-to-column connections. For the simulation of rigid action a direct connection between beam and column was made and no other connecting elements were being used. To verify the accuracy of the obtained results from the developed finite element model, a graphical comparison is stated in Figure 3.7. From this figure it is observed that the FE model gives satisfactory results for rigidly connected frames.
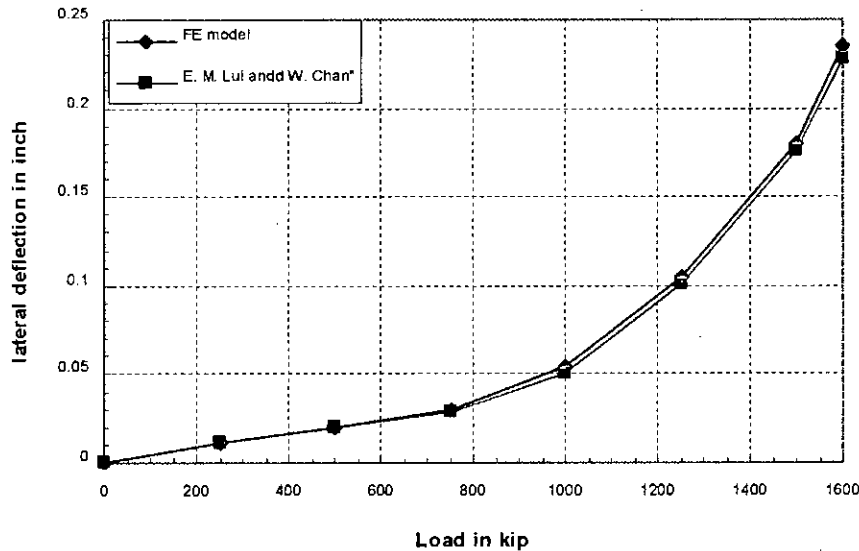
Figure 3.7 Comparison of Elastic Load Deflection Curves for Rigidly Connected Unbraced Frames having Fixed Support.

3.3.3.3 Semi-Rigid Action Analysis

The aforementioned frame used for verification of the FE model was rigidly connected. But in actual practice the existence of rigid connection is very rare. The connections of steel frames actually show semi-rigid behaviour. For the simulation of semi-rigid action of the connections a rotational spring element has been used. This element has the advantage of considering the non-linear moment-rotation behaviour of connections. This element is termed as 'Combin-39' (non-linear spring). At every beam-to-column connection a spring element of zero length and having a predefined moment-rotation characteristics has been introduced for the simulation of semi-rigid action. Lui and Chen, 1988 made their study for four types of semi-rigid connections. But for verification an extended end plate connection was considered. This connection was tested and the obtained moment-rotation behaviour of the connection is shown in Figure 3.8.After completion of the analysis of P-Δ effect, a graphical comparison of results has been shown in Figure 3.9. From this figure it is observed that the results obtained using numerical method are very close to those
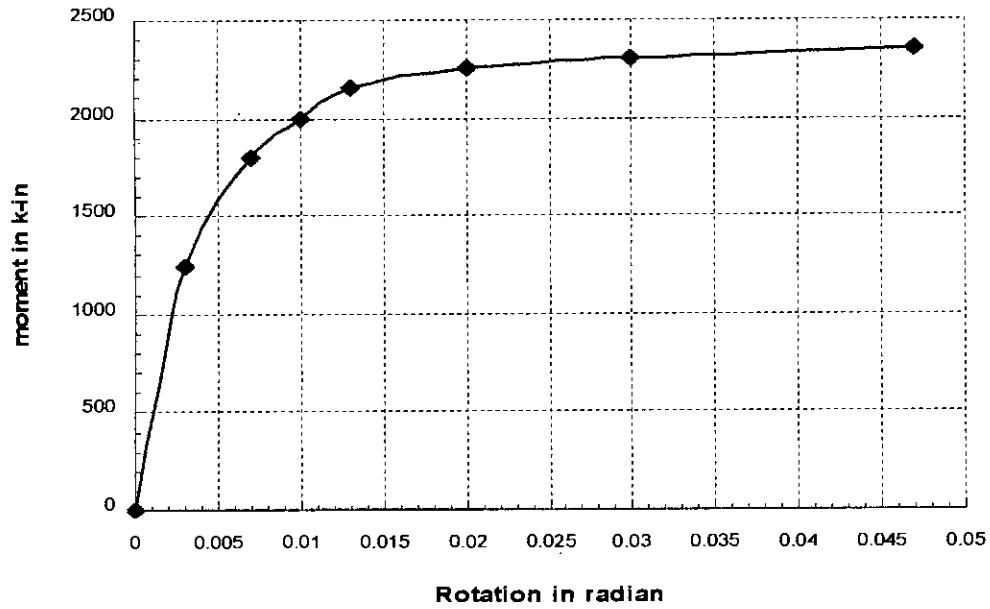
Figure 3.8 Moment-Rotation Relations of Extended End Plate Connection
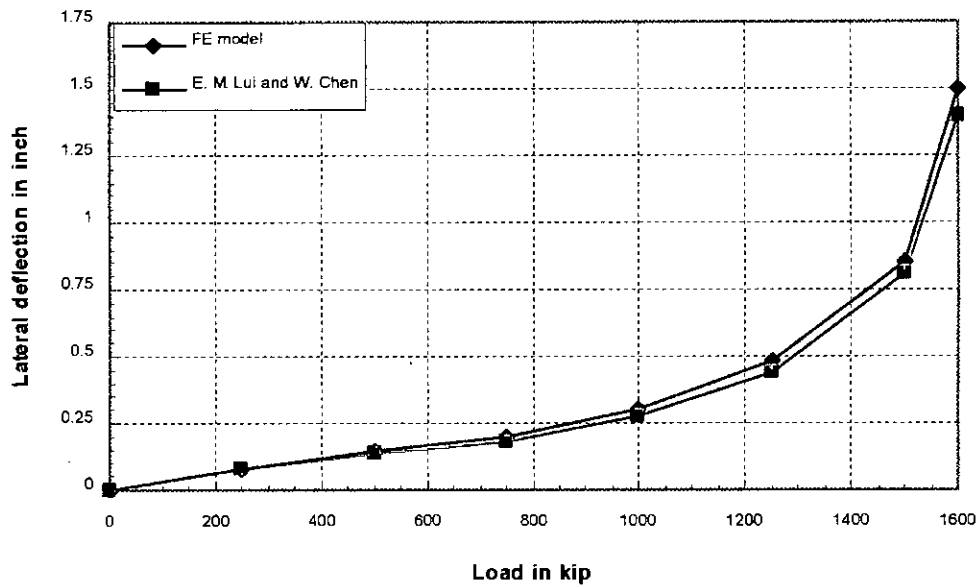
Figure 3.9 Comparison of Elastic Load Deflection Curves for Semi-Rigidly Connected Unbraced Frames having Fixed Support

obtained by Lui and Chen, 1988. So it can be concluded that FE models for semi-rigid frames give satisfactory results so that farther analysis regarding the behavioural study of the semi-rigid steel frames can be made using numerical simulation.

3.3.4 Comparison for Sway Frames

Ahmed B., 1996 analyzed a number of sway frames subjected to a horizontal load at the top. The frames selected for analyses included universal sections of beams and columns and different connection stiffness.

3.3.4.1 Description of the Frames

Connections having stiffness of 0 (pin connection), 6000 kN-m/rad, 30000 kN-m/rad and infinite (rigid connection) have been used. The universal section 203 X 203 UC 46 has been used to represent beam and columns. The storey height and width of each storey was 4.953m. In all the cases the applied load was a horizontal one acting at the top of the frame. Different sets of analyses were performed using frames ranging from single storey to four stories and number of bay was varied from one to two.

3.3.4.2 Comparison of Results

The results obtained from FE analysis using the developed FE model have been compared with those obtained by Ahmed and the results are given in Figures 3.10 to 3.12. The type of frame (number of stories and number of bay) has been
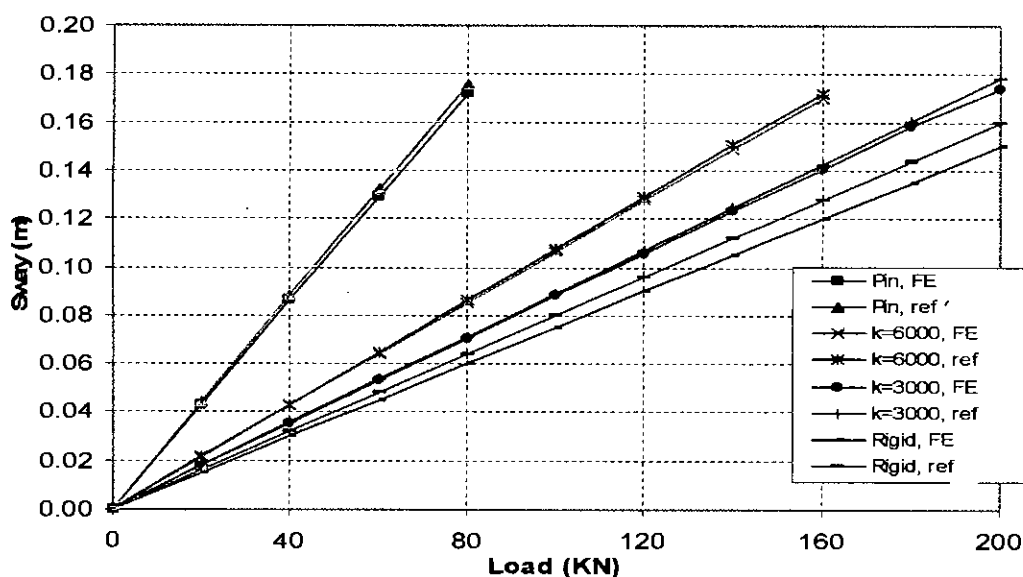
Figure 3.10 Comparison of Sway Values Calculated for One Storey Single Bay Frame
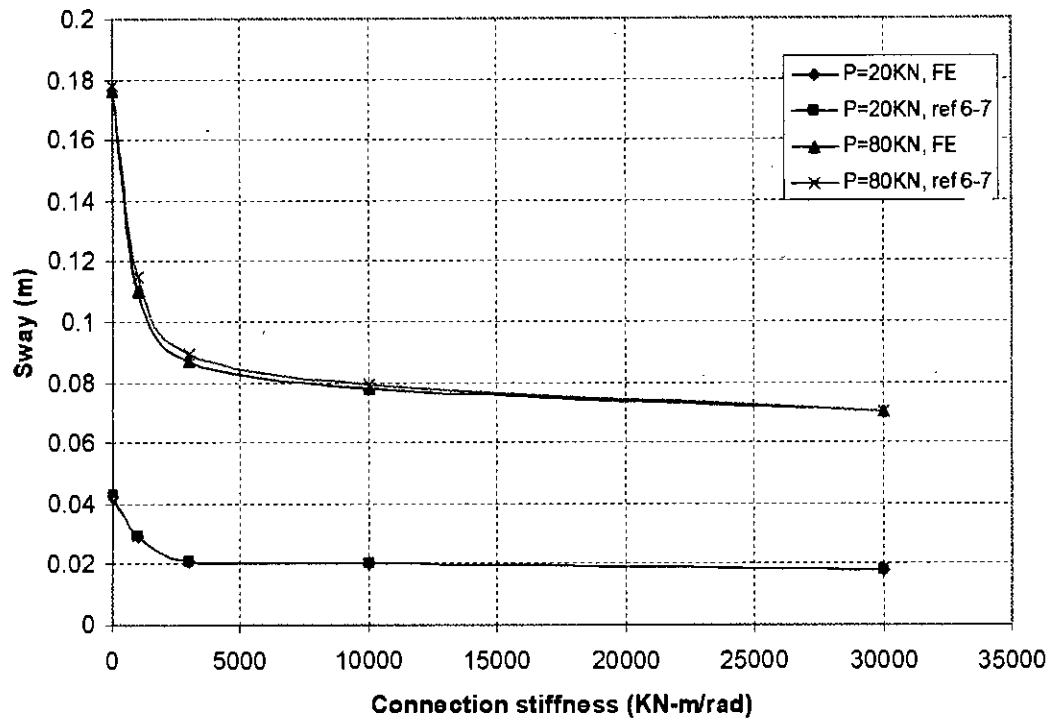
Figure 3.11 Comparison of Sway with Connection Stiffness
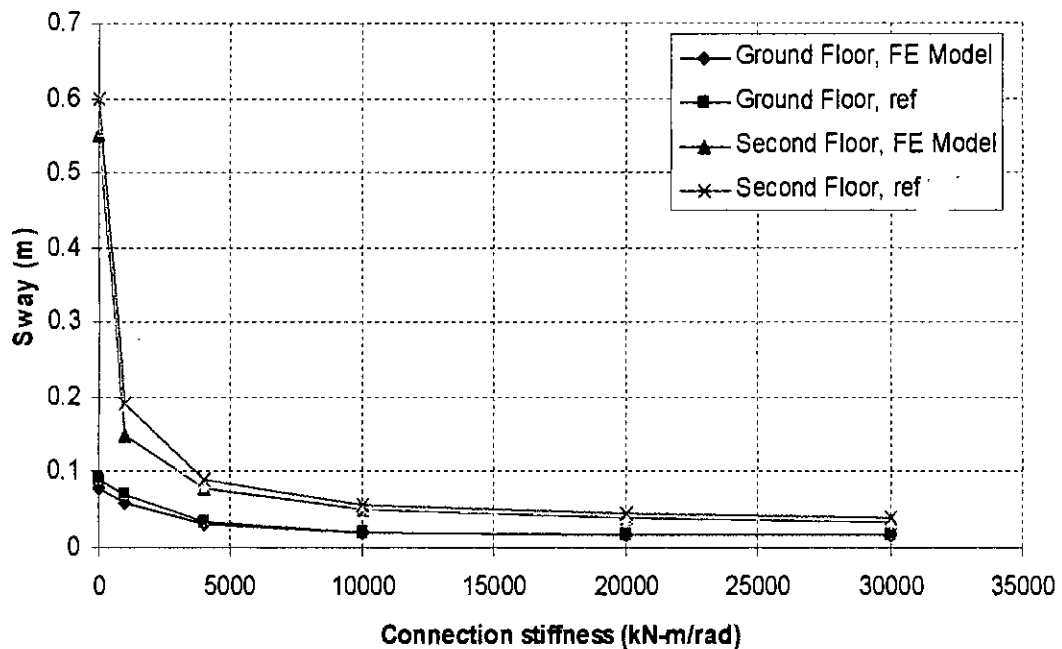
Figure 3.12 Comparison of Sway for a Three Storey Single Bay Frame

mentioned in all the figures. The results of the aforementioned Figures give an assurance about the accuracy of the developed models.

3.3.5 Ten-story Double Bay Frame Analyzed by Suarez et. al.

This frame was analyzed Suarez et. al. (1996) with a view to verifying their proposed method and corresponding computer program for sway frame analysis. The changes in the element matrices introduced by the eccentricity and flexibility of mass and stiffness on the connections are explicitly defined in closed form. Numerical results showing the effects of flexibility and eccentricity on the dynamic characteristics as well as on the seismic response of a building frame are presented. The elements of the correction matrix were functions of two non-dimensional parameters, which the authors referred to as "fixity factors".

3.3.5.1 Description of the frame

One of the transverse planar frameworks from a 10 story unbraced steel building is used to illustrate the effect of the connection flexibility on the dynamic properties and seismic response. The structure is shown in Fig. 3.13, along with its geometry and member properties. The model has 33 nodes and a total of 90 degrees of freedom. In addition to the distributed mass of the members, additional lumped masses of 2400 slugs are added to each node to include the floor mass. Only the beam-to-columns connections are considered to be flexible and identical, since this would be usually the case for this type of structural systems.

The following two-nondimensional parameters $\gamma_1 and \gamma_2$ have been introduced.

$$\gamma_i = \frac{EI}{L}\frac{1}{k_i}; i = 1, 2$$

Fixity factors:

$$\mu_i = \frac{1}{1+3\gamma_i}; i = 1, 2$$
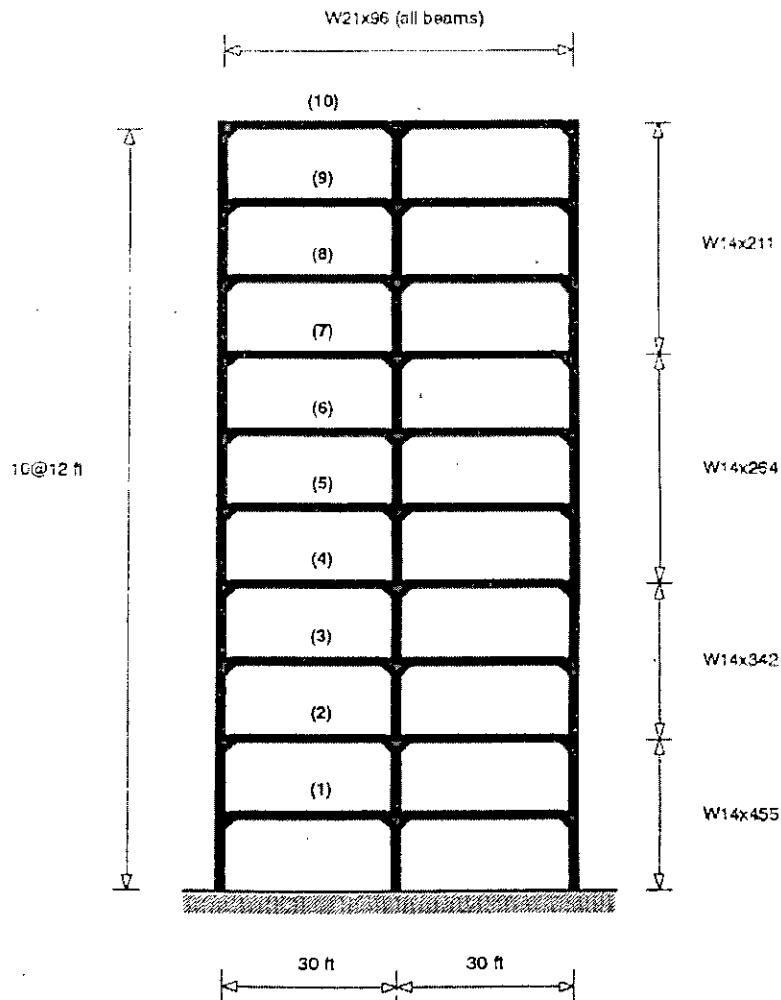
Figure 3.13 Ten-Story Steel Frame Considered for Numerical Study

3.3.5.2 Comparison of Results

The results obtained from FE analysis using the developed FE model have been compared with those obtained by Suarez et al. (1996) and the results are given in Figure 3.14. The natural frequencies are normalized by dividing their values by the frequencies obtained for the structure with rigid connections. The results of the aforementioned figure give an assurance about the accuracy of the developed models.

46
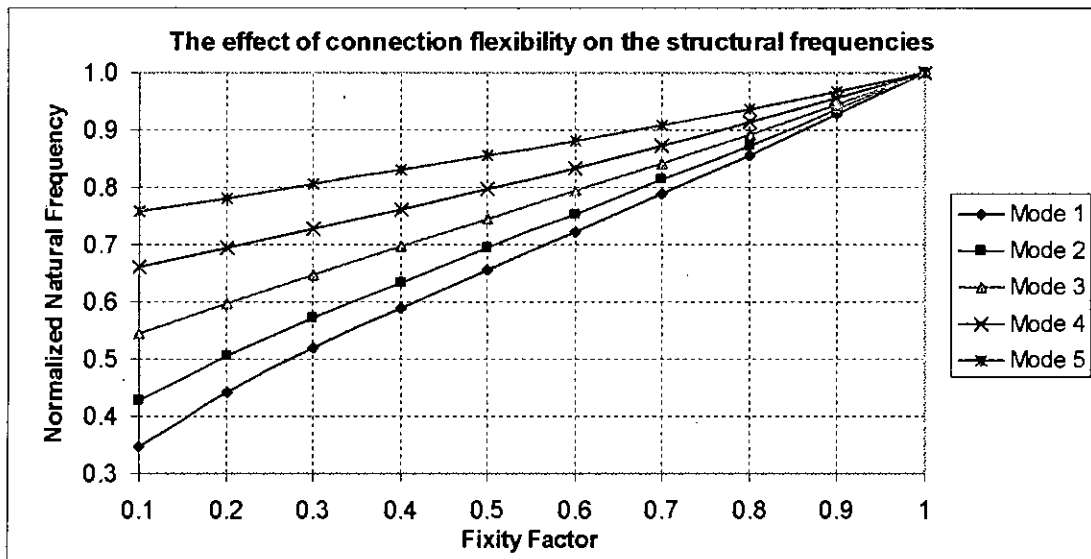
Figure 3.14 Comparison of the Effect of Connection Flexibility on the Structural Frequencies

3.3.5.3 The Study of the Natural Frequencies

Suarez et al (1996) studied the seismic performance for 10-story two bay frame with flexible connection. In this section 10-story with 4-bay frame is considered to study the dynamic characteristics of the frame. Each story has a height of 12 feet while the size of each bay as well as frame spacing is 30 ft. In addition to the distributed mass of the members, additional lumped masses of 2400 slugs are added to each node to include the floor mass. Only the beam-to-columns connections are considered to be flexible and identical. The results obtained from FE analysis using the developed FE model has been presented in Figure 3.15. The natural frequencies are normalized by dividing their values by the frequencies obtained for the structure with rigid connections. Observing the figure one can see that flexibility of the connections does have a relatively more pronounced effect on the lower frequencies. This observation has relevance for seismic analysis, as the seismic response of structures is generally dominated by the lower modes. Moreover, since the response is also strongly influenced by the frequency content of the earthquake motion, a proper consideration of the flexibility of the joints is necessary to obtain the correct values of the natural frequencies because resonance effect in the response may be otherwise unappreciated.

The effect of connection flexibility on the structural frequencies
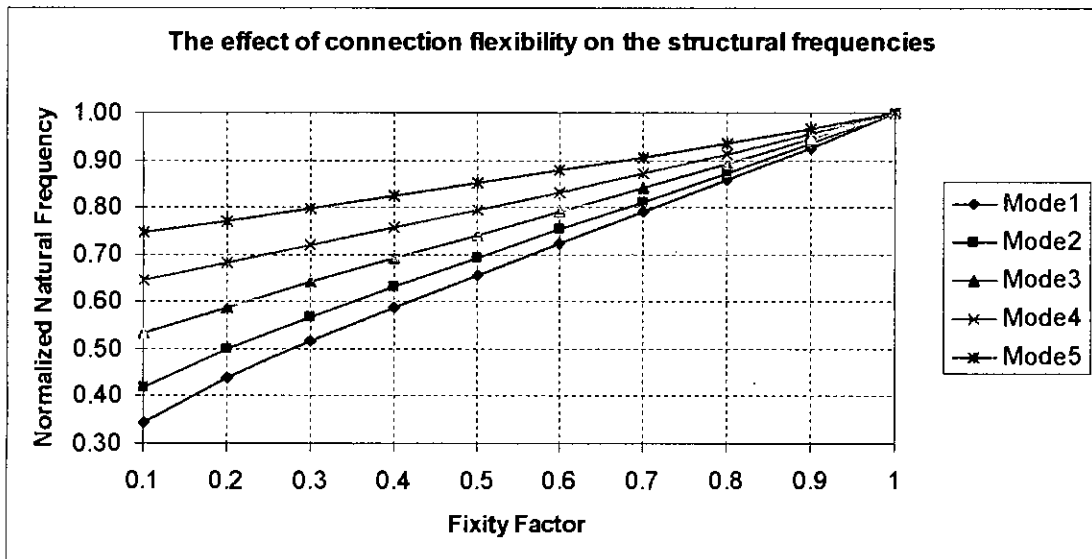
Figure 3.15 The Effect of Connection Flexibility on the Structural Frequencies for 10-Story 4-Bay

3.4 Conclusions

In this chapter various types of frames having both rigid and semi-rigid connections have been analyzed and results were compared with the predetermined results. From both the tabular and graphical comparisons it has been observed that the developed finite element models give satisfactory results in all the cases - from rigid to semi-rigidly connected frames, from single storey to multi-storied frames and even for frames having single bay to multi-bay under static loads. Dynamic characteristics of the building have been also verified. Finally it can be concluded that the developed program is dependable.

CHAPTER 4

Modelling and Nonlinear Static Analysis

4.1 Introduction

As a building responds to earthquake ground motion, it experiences lateral displacements and in turn, deformations of its individual elements. At low levels of response, the element deformation will be within their elastic (linear) range and no damage will occur. At higher levels of response, element deformations will exceed their linear elastic capacities and the building will experience damage. In order to evaluate the performance of a steel moment-frame building it is necessary to construct a mathematical model of the structure that represents its strength and deformation characteristics, and to conduct an analysis to predict the values of various design parameters when it is subjected to design ground motion.

Standard code procedures include both static and dynamic analysis methods. The code static lateral force procedure is commonly used by the engineering professionals to design buildings. In this methodology, the building code prescribes a formula that determines lateral forces. These forces are applied in a prescribed manner to determine the adequacy of the structural system. If some of the components of the designed structural system are not adequate, the design is revised and the modified design is reanalyzed. This process is repeated until all the provisions of the building code are satisfied. The procedure relies on principles of statistics and the structural components are evaluated for serviceability in the elastic range of strength and deformation. Additional requirements are prescribed to supply ductile and energy dissipating characteristics to the structural system to enable it to survive excursions into the inelastic range of lateral displacements during major earthquakes. Although this procedure is commonly called a static lateral force procedure, it does include some implicit elements of dynamics. These include the use of the fundamental period of vibration (T) to determine the amplification (C-factor) of ground motion

acceleration (Z-factor) and the use of vertical distribution of force equations to approximate modal response. Because of these features, the methodology is sometimes referred to as the equivalent lateral force procedure.

In some cases, a building requires an explicit dynamic lateral force procedure, which may be either a response spectrum analysis or an elastic time history analysis. While these procedures add aspects of dynamics to the design procedure, resulting forces are generally scaled to match the lateral force used in the static procedure. Also, components are still evaluated for serviceability in the elastic range of strength and deformation.

Although an elastic analysis gives a good indication of the elastic capacity of structures and indicates where first yielding will occur, it cannot predict failure mechanisms and account for redistribution of forces during progressive yielding. Inelastic analysis procedures help demonstrate how buildings really work by identifying modes of failure and the potential for progressive collapse. The use of inelastic procedures for design and evaluation is an attempt to help engineers better understands how structures will behave when subjected to major earthquakes, where it is assumed that the elastic capacity of the structure will be exceeded. This resolves some of the uncertainties associated with code and elastic procedures. The most basic inelastic analysis method is the complete nonlinear time history analysis, which at this time is considered overly complex and impractical for general use. Available simplified nonlinear analysis methods, referred to as nonlinear static analysis procedures, include the capacity spectrum method (CSM) that uses the intersection of the capacity (pushover) curve and a reduced response spectrum to estimate maximum displacement.

In this chapter, to get member sizes of the frames, a ten story and a six story, at first the ten story steel frame structure will be designed by the equivalent lateral force method (BNBC, 1993). Then the inelastic analysis is performed to get the inelastic capacity of the structure. Graphical representation of base shear versus roof displacement commonly known as pushover curve will be developed for the selected frame for different types of connectivity such as fully rigid, fully semirigid and combined rigid and semirigid. Then capacity spectrum will be developed by converting pushover curve. To get the dynamic characteristics of the structures modal

analysis has been performed. In conversion of pushover curve to capacity spectrum the initial semirigidity will be considered for the fundamental vibration mode where semirigid connection is used in the selected frame.

4.2 Selection of Frames

Ten storied four-bay and six storied four-bay steel frame structures have been selected in this study to get the effects of the connection flexibility on the seismic performance of the structures. Ten storied steel frame (Natural frequency, $^{N}/_{10}$ from empirical equation, is 1 Hz where N = no. of story) is selected based on the assumption of the predominant frequency of soil which is normally 1 Hz. In Bangladesh most of the high rise buildings are six storied. Bay width is 30-ft each and story height is 12-ft each for both ten storied and six storied steel frames. For section properties of beams and columns, the ten storied frame is designed by equivalent static force method described in Section 4.2.1. The members and joint characteristics of the six storied. frame are just similar to the bottom six stories of the ten storied frame.

4.2.1 Seismic Design of the Ten Story Steel Frame

The ten storied four-bay steel frame is designed for combination of dead loads (1745 lb/ft), live loads (740 lb/ft) and earthquake load. The seismic forces in a structure depend on a number of factors, including the size and other characteristics of the earthquake, the distance from the fault, the site geology, and the type of lateral-load-resisting system. The importance of the structure may also be of concern in the design. The earthquake load is based on the equivalent lateral forces specified in the Bangladesh National Building Code (BNBC, 1993).

Parameters Given

Seismic Zone Factor, Z = 0.25 Zone 3

Importance Factor, I = 1.0 Standard Occupancy Structures

Site Coefficient, S = 1.5 Soft to Medium Clay and Sand

(Soil Type S3)

Period using Method A

$$T= C_t*(h_n)^{3/4}$$

Total Building Height, hn = 36.6m

$Ct =$ 0.083   For Steel Moment Resisting frame

$T =$ 1.24 sec

$C=$ 1.63

Seismic Force

Basic Structural System = Moment Resisting Frame

Lateral Load Resisting System = Special Moment Resisting Frame

(SMRF)

$R =$ 12;   C/R = 0.14>0.075   OK

Total Building Weight, W = 13992 KN

Base Shear, V = 474.8 KN   3.39% of total structure Weight.

Ft = 41.06 KN   8.65% of Base Shear   OK

Use, Ft = 41.06 KN   in calculations below

Floor Name	Floor Height Above (m)	Elevation above ground (m)	Floor Weights (KN)	wihi KN-m	wxhx S(wihi)	Seismic Force Fe (KN)	Seismic Shear Ve (KN)	Seismic Moment Me KN-m
10	3.66	36.59	1272	46536.6	0.1818	119.9	119.9	0
9	3.66	32.93	1272	41882.9	0.1636	71.0	190.9	439
8	3.66	29.27	1272	37229.3	0.1455	63.1	254.0	698
7	3.66	25.61	1272	32575.6	0.1273	55.2	309.2	929
6	3.66	21.95	1272	27922	0.1091	47.3	356.5	1131
5	3.66	18.29	1272	23268.3	0.0909	39.4	395.9	1304
4	3.66	14.63	1272	18614.6	0.0727	31.5	427.5	1449
3	3.66	10.98	1272	13961	0.0545	23.7	451.1	1564
2	3.66	7.32	1272	9307.32	0.0364	15.8	466.9	1651
1	3.66	3.66	1272	4653.66	0.0182	7.9	474.8	1708
Base	3.66	0.00	1272	0	0.0000	0.0	474.8	1737
							OK	
			13992	255951				

The AISC specification is used to determine the design forces and to select member sizes from a property table. For a proper design the stress ratio will be just less than one; however, this is not always possible, due to the finite number of steel sections which are available. Members which have a stress ratio greater than one are modified, and the stress check is repeated. In this manner the results in members which meet the design criteria and are economical. The designed ten storied steel frame and the corresponding final stress ratios are summarized in Figure-4.1 and Figure-4.2.
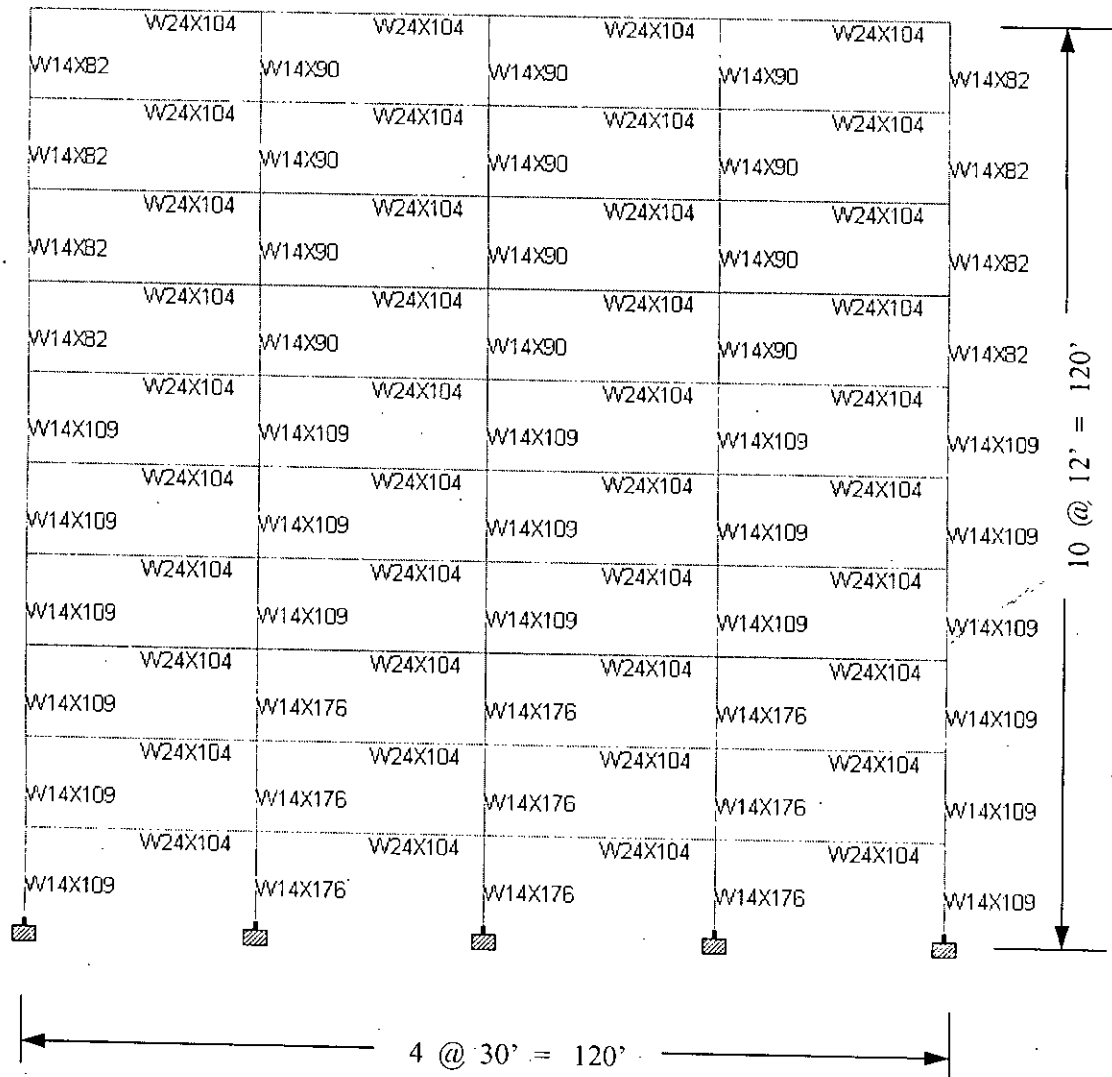
Figure 4.1 Designed Sections of Ten Story Frame

53

Col 1	Beam	Col 2	Beam	Col 3	Beam	Col 4	Beam	Col 5
	0.618		0.624		0.624		0.618	
.544		.264		.269		.257		.544
	0.577		0.644		0.615		0.572	
.586		.438		.424		.438		.567
	0.659		0.706		0.679		0.654	
.662		.595		.586		.594		.66
	0.73		0.759		0.736		0.72	
.765		.749		.739		.748		.764
	0.797		0.813		0.79		0.797	
.615		.741		.736		.741		.614
	0.845		0.845		0.83		0.846	
.675		.859		.854		.858		.673
	0.895		0.868		0.859		0.881	
.752		.976		.961		.975		.75
	0.96		0.915		0.909		0.941	
.754		.689		.676		.688		.753
	0.965		0.939		0.943		0.957	
.841		.757		.738		.756		.84
	0.931		0.894		0.893		0.929	
.887		.864		.852		.862		.884

10 @ 12' = 120'

4 @ 30' = 120'

Figure 4.2 Stress Ratio of Ten Story Frame

4.3 Material Properties

An elastic-perfectly-plastic material behavior is assumed in the analysis. The reason for considering plastic behavior of material is that for very flexible connections tall frames undergo excessive drift which induce second order effects causing material to exceed its elastic limit even at the level of working load. The yield stress is taken as 250 N/sq. mm (36ksi) and the modulus of elasticity is assumed to be 210 KN/ sq. mm (30X103ksi).

54

4.4　Connection Details

Since the main objective of the present study is to examine the influence of different type semi-rigid connections on the capacity spectrum of medium rise buildings, a wide spectrum of M-ϕ relationship covering the whole range between rigid and pinned behaviour has been considered. To this end, different details of top- and seat-angle connection (with / without double web-angle) have been varied to obtain a wide variation of rigidity of such connection. The details of the connections studied are shown in Table 4-1. Since the actual test results of these connections, used with the beam and column sections mentioned earlier, are not available, a mathematical model has to be used to obtain the moment-rotation relationships.

For this purpose the three-parameter power model (Kishi and Chen, 1990) has been used to obtain the non-linear M-ϕ relationship of the semi-rigid connections. Sample calculations for joint type 'A' are given in Appendix-A. Once the non-linear M-ϕ relationships are obtained, their stiffness have to be represented in a tri-linearised form for use in the analysis program. The salient features of these two aspects of connection modelling are described next.

4.4.1 The Three-Parameter Power Model

This relationship was first proposed by Richard and Abbott, 1975. The model has three parameters: initial connection stiffness R_{ki} ; ultimate moment capacity M_u ; and shape parameter n. It has the following simple nondimensional form:

$$m = \frac{\theta}{(1+\theta^n)^{1/n}}$$

(Equation 4-1)

in which m and θ are defined as $m = M / M_u$, $\theta = \theta_r / \theta_0$; where M and θ_r are moment and relative connection rotation respectively and $\theta_0 = M_u / R_{ki}$. General shapes of moment-rotation curves of equation 4-1 are shown in figure 4.3(a). The two parameters of R_{ki} and M_u can be obtained by using simple structural mechanics and the third parameter n is obtained by curve fitting with the test data (Kishi et al, 1991). In the present study the three parameters have been determined using the nomographs provided by Kishi et al, 1993. The M-ϕ curves, for the connections tabulated in table 4-1, are presented in figure 4.3(b).
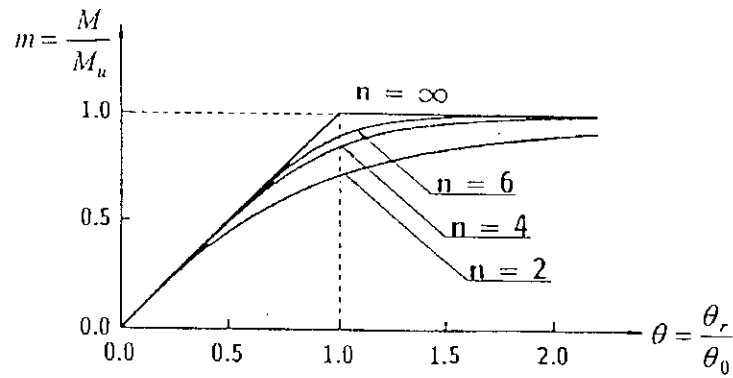
Figure 4.3 (a) General Curves of Non Dimensional Three-Parameter Power
Model
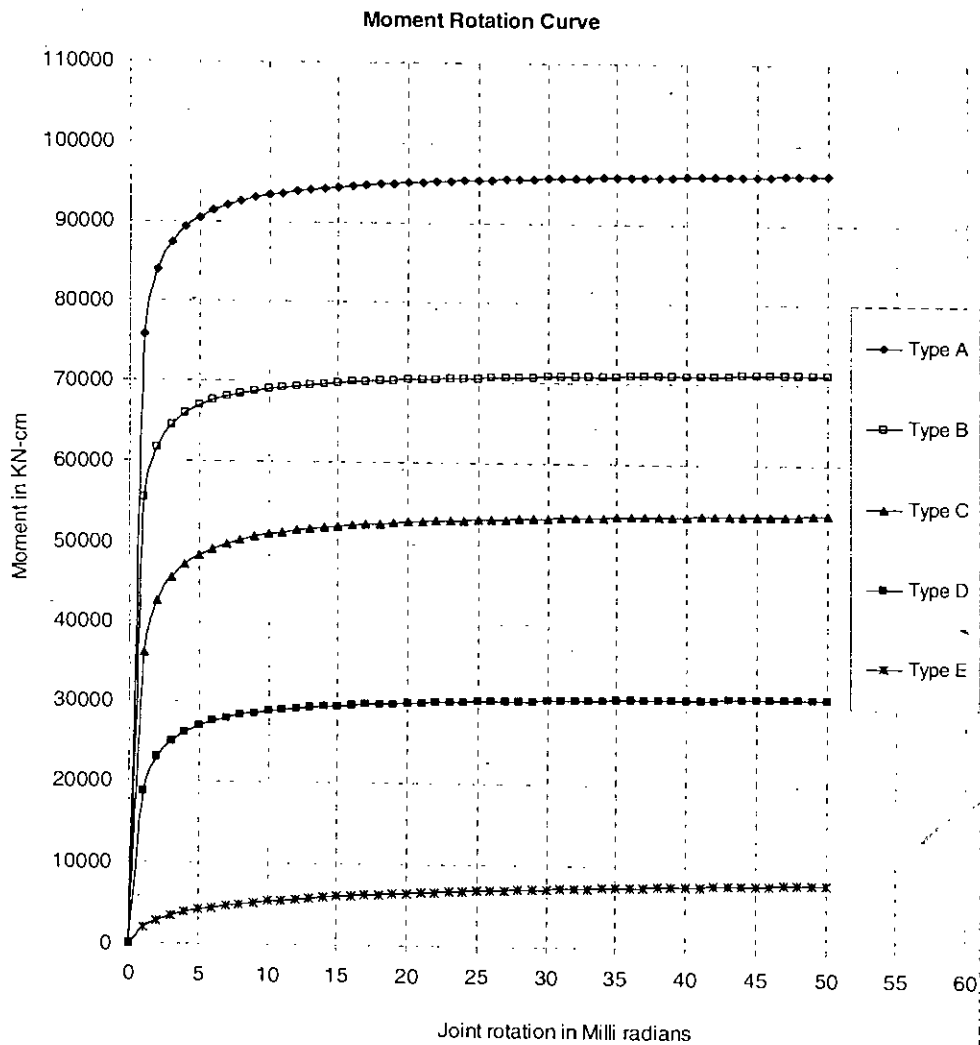
Figure 4.3 (b) Curves of the Connection under Study Derived by Three
Parameter Power Model

Table 4-1 Description of Joint Types Studied.

Joint Type	Joint Category	Top and Seat Angles		Web Angles		Beam Depth (inch)
		Designation	Length (inch)	Designation	Length (inch)	
A	Top & Seat Angle Joint with Double Web-Angle	L6x6x1	10	L4x4x7/8	10	24
B		L6x6x7/8	10	L4x4x3/4	10	24
C		L6x6x3/4	10	L4x4x1/2	10	24
D		L6x6x1/2	10	L4x4x1/2	10	24
E	Top & Seat Angle Joint without Double Web-Angle	L6x6x1/2	10	-	-	24

Common Details of the connections:

Yield stress of steel, σ_y = 36 ksi

Nominal size of the bolts, D = $^7/_8$ inch

Nominal size of the nuts, W = 1 ½ inch

Distance between heel of web angle to centre of closest to fastener closest to the web of the beam, g_w = 1 ¾ inch

Distance between heel of top or seat angle to the centre of fastener closest to flange of beam, g_t = 3 inch
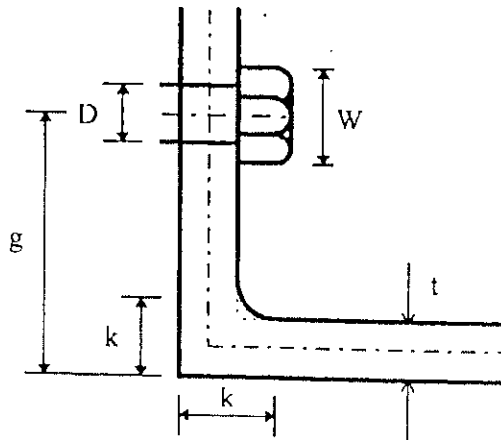
Figure 4.4 Main Parameters for an Angle

4.4.2 Tri-linearisation of the Non-linear M-φ curves

The finite element program (Ahmed I., 1992) used for the analysis of semi-rigid frames uses, as input, the connection moment-rotation relationship in tri-linearised form The non-linear M-ϕ curves generated by the three-parameter power model has been tri-linearised to provide input data for the analysis by the program. The tri-linearised representation of the non-linear curves is shown in figure 4.5. The M-ϕ curves has been tri-linearised in such a manner that the first two linear parts superpose the curve as closely as possible and the last linear portion is plotted as best fit.
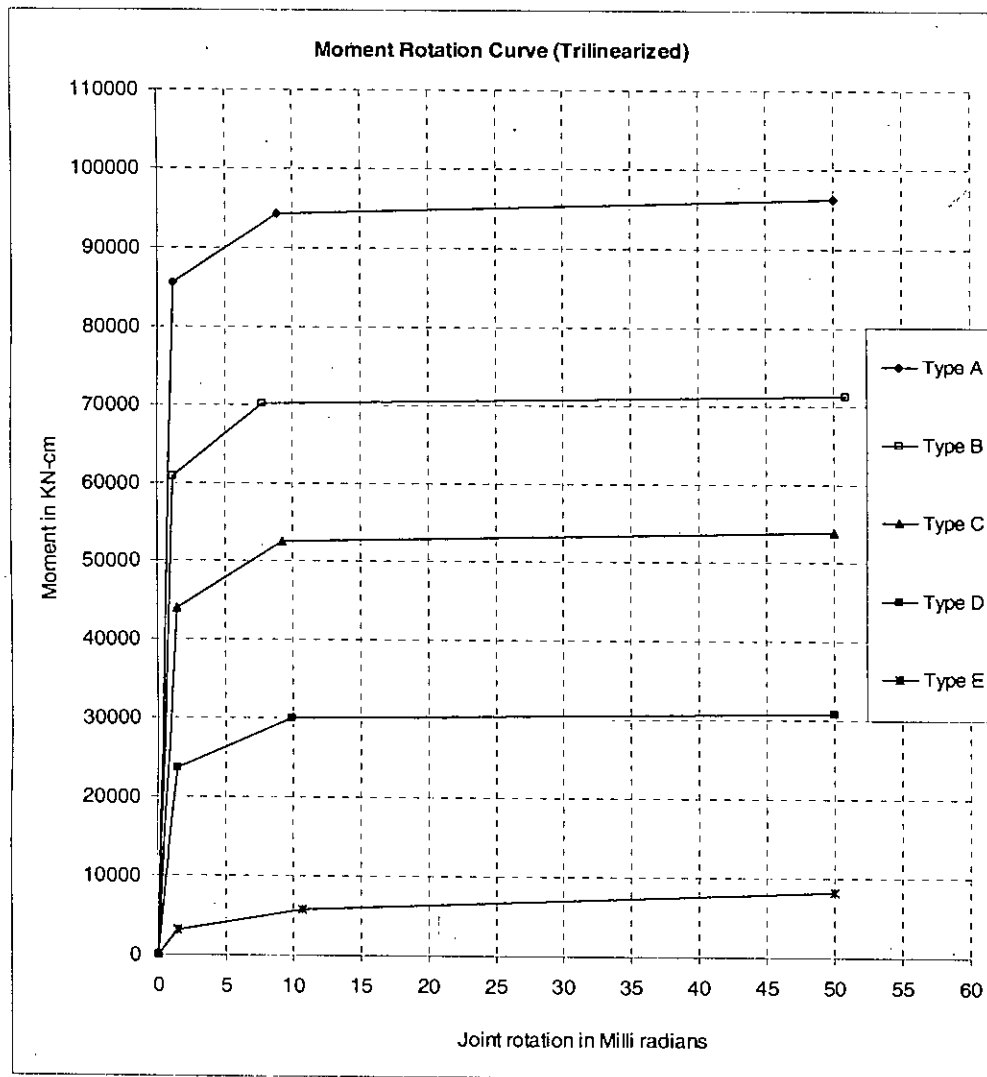
Figure 4.5 Tri-Linearised Moment-Rotation Relationship of Different Type of Connections

4.5 Construction of the Pushover Curve

The central focus of simplified nonlinear procedure is the generation of the "Pushover Curve" or Capacity curve. Structure capacity is represented by a pushover curve. As the name implies, it is the process of pushing horizontally, with a prescribed loading pattern, incrementally, until the structure reaches a limit state. The most convenient way to plot the force-displacement curve is by tracking the base shear and the roof displacement, that is, to represent the lateral displacement as a function of force applied to the structure. If a building had infinite linear elastic capacity, this capacity curve would be a straight line with slope equal to the global stiffness of the structure. Since real buildings do not have infinite linear elastic capacities, the capacity curve can be assumed to be consisting of a series of straight line segments with decreasing slope, representing the progressive degradation in structural stiffness that occurs as the building is subjected to increased lateral displacement, yielding and damage. The slope of a straight line drawn from the origin of the plot for this curve to a point on the curve at any lateral displacement, "d", represents the secant or "effective stiffness" of the structure when pushed laterally to that displacement. It should be noted that, this process is independent of the method used to calculate the "demand" or "performance point". The construction of capacity curve like any general structural analysis has three distinct steps:

- Building of the model
- Apply loads (Gravity loads and Lateral loads)
- Review the results (and plotting of the curve)

4.5.1 Building of the Model

In general, a steel moment-frame building should be modelled and analyzed as a three-dimensional assembly of elements and components. However, two-dimensional models shall provide adequate response information for regular, symmetric structures and structures with flexible diaphragms. The analytical model should accurately account for the stiffness of frame elements and connections. Only the beams and columns forming the lateral-force-resisting system need be modelled. In general, foundations should be modelled as unyielding. In this study two-dimensional ten storied four-bay and six storied four-bay steel frame structures are

considered as model. Models of frames incorporating partially restrained i.e. semi rigid connections is explicitly accounted for the stiffness of the connection.

4.5.2 Application of Loads

The next step comprises of application of lateral forces or displacement to the nonlinear mathematical model of the building until the displacement in the control node exceeds a target displacement where the structures reaches a limit state. The lateral force is incrementally adjusted and monotonically increased. The relation between base shear force and lateral displacement of the control node shall be established for control node displacement. The centre of mass at the roof of the building is considered as the control node. Gravity loads are applied to appropriate elements and components of the mathematical model during the Nonlinear Static Procedure (NSP).

The pushover procedure has been presented in various forms for use in a variety of methodologies. There are several levels of sophistication that may be used for the pushover analysis. Some examples are given below:

1. Simply apply a single concentrated horizontal force or displacement at the control node.

2. Apply lateral forces to each story in proportion to the standard code procedure without the concentrated force F_t at the top. (i.e. $F_x = [w_x h_x / \sum w_x h_x]/V$)

3. Apply lateral forces to the building in profiles that approximately bound the likely distribution of inertia forces in a earthquake.

4. apply lateral forces in proportion to the product of story masses and first mode shape of the elastic model of the structure (i.e. $F_x = [w_x \phi_x / \sum w_x \phi_x]/V$).

5. Same as methodology 4 until first yielding. For each increment beyond yielding, adjust the forces to be consistent with the changing deflected shape.

6. Similar to the methodology 4 and 5 above, but include the effects of the higher modes of vibration in determining yielding in individual structural elements while plotting the capacity curve for the building in terms of first mode forces and displacements. The higher mode effects may be determined by doing higher mode pushover analysis.

In this study, methodology 1 that means displacement is applied at the roof of the structure, that is, at the control node at an increment of 0.2 ft per each iteration, and

increased until the roof displacement reaches 10 ft, thus requiring 50 iterations in total. 100% of computed dead loads and permanent live loads and 25% of transient live loads are applied to the model as gravity load.

4.5.3 Results and Plotting of the Curve

Upon the completion of the building of the model and application of loads, as the final step, the mathematical model of the structure is analyzed and solved for each control node displacement increment, and the base shear (V) and the roof displacement (Δ_{roof}) is recorded. Data is continuously recorded until the structure reaches an ultimate limit; distortions considerably beyond the desired performance level; an element or group of elements, a connection or a group of connections reach a lateral deformation level at which significant strength degradation begins or at which loss of gravity load carrying capacity occurs. Then the Base Shear (Sum of horizontal reaction at the supports) Vs Roof displacement (Applied control node displacement) for different types of connections is plotted which is known as the pushover curve (For the ten storied frame see Figure 4.6 to Figure 4.8 and for the six storied frame see Figure 4.22). Definition of connection types (for both ten storied and six storied frames) and frame types (for ten storied frame) are as follows:

Joint Type 'Rigid' $\approx$ All beam-column connections of the frame are 'Rigid'.

Joint Type 'A' $\approx$ All beam-column connections of the frame are type 'A' (Table 4-1).

Joint Type 'B' $\approx$ All beam-column connections of the frame are type 'B' (Table 4-1).

Joint Type 'C' $\approx$ All beam-column connections of the frame are type 'C' (Table 4-1).

Joint Type 'D' $\approx$ All beam-column connections of the frame are type 'D' (Table 4-1).

Joint Type 'E' $\approx$ All beam-column connections of the frame are type 'E' (Table 4-1).

Frame Type 'R20_SR80' $\approx$ 20% beam-column connections (1st floor to 2nd floor) of the frame are 'Rigid' and rest of the connections are type 'A'.

Frame Type 'R40_SR60' $\approx$ 40% beam-column connections (1st floor to 4th floor) of the frame are 'Rigid' and rest of the connections are type 'A'.

Frame Type 'R50_SR50' $\approx$ 50% beam-column connections (1st floor to 5th floor) of the frame are 'Rigid' and rest of the connections are type 'A'.

Frame Type 'R60_SR40' $\approx$ 60% beam-column connections (1st floor to 6th floor) of the frame are 'Rigid' and rest of the connections are type 'A'.

Frame Type 'R80_SR20' $\approx$ 80% beam-column connections (1st floor to 8th floor) of the frame are 'Rigid' and rest of the connections are type 'A'.
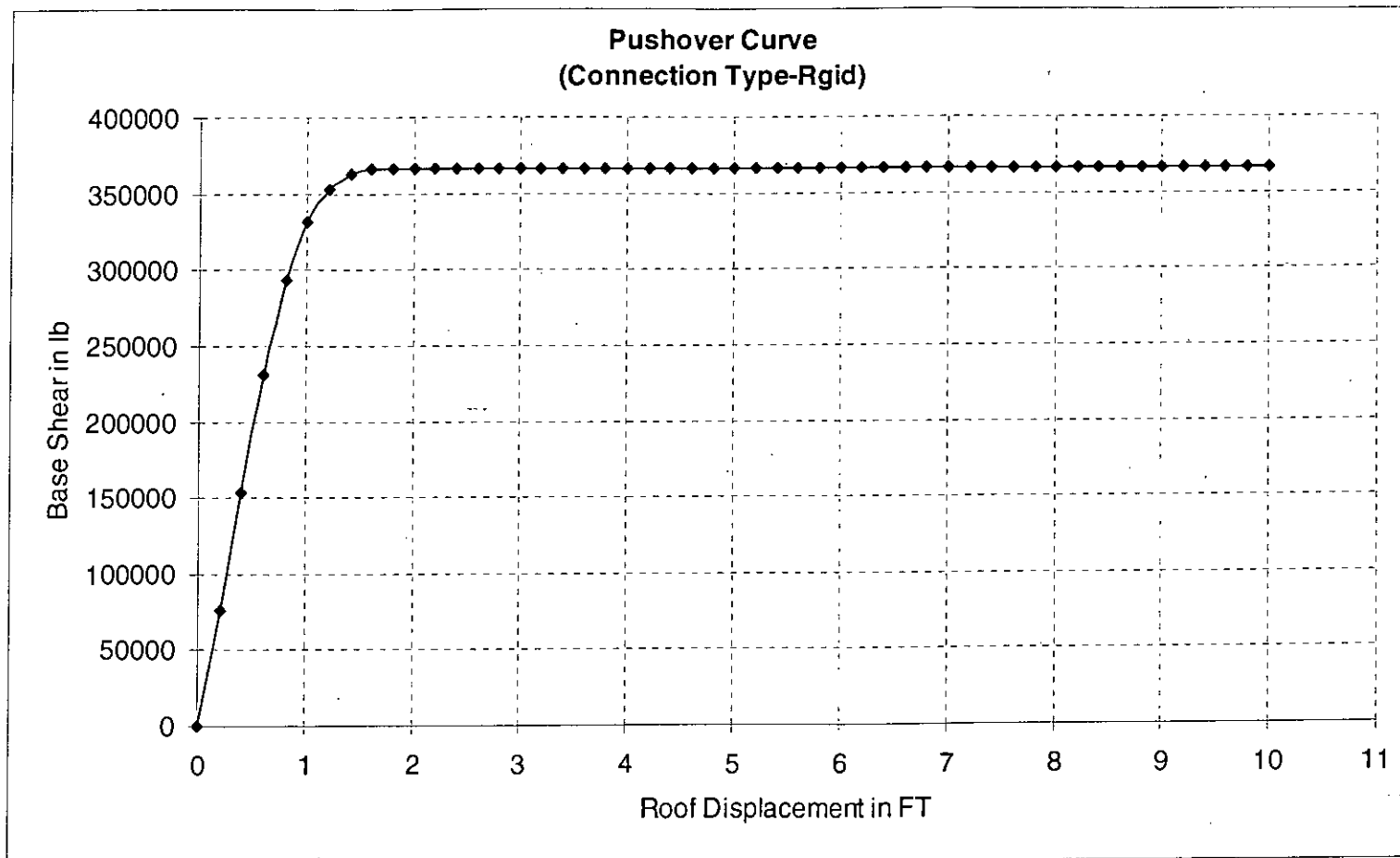
Figure 4.6 Pushover Curve of Ten Story Steel Frame (For Joint Type 'Rigid')
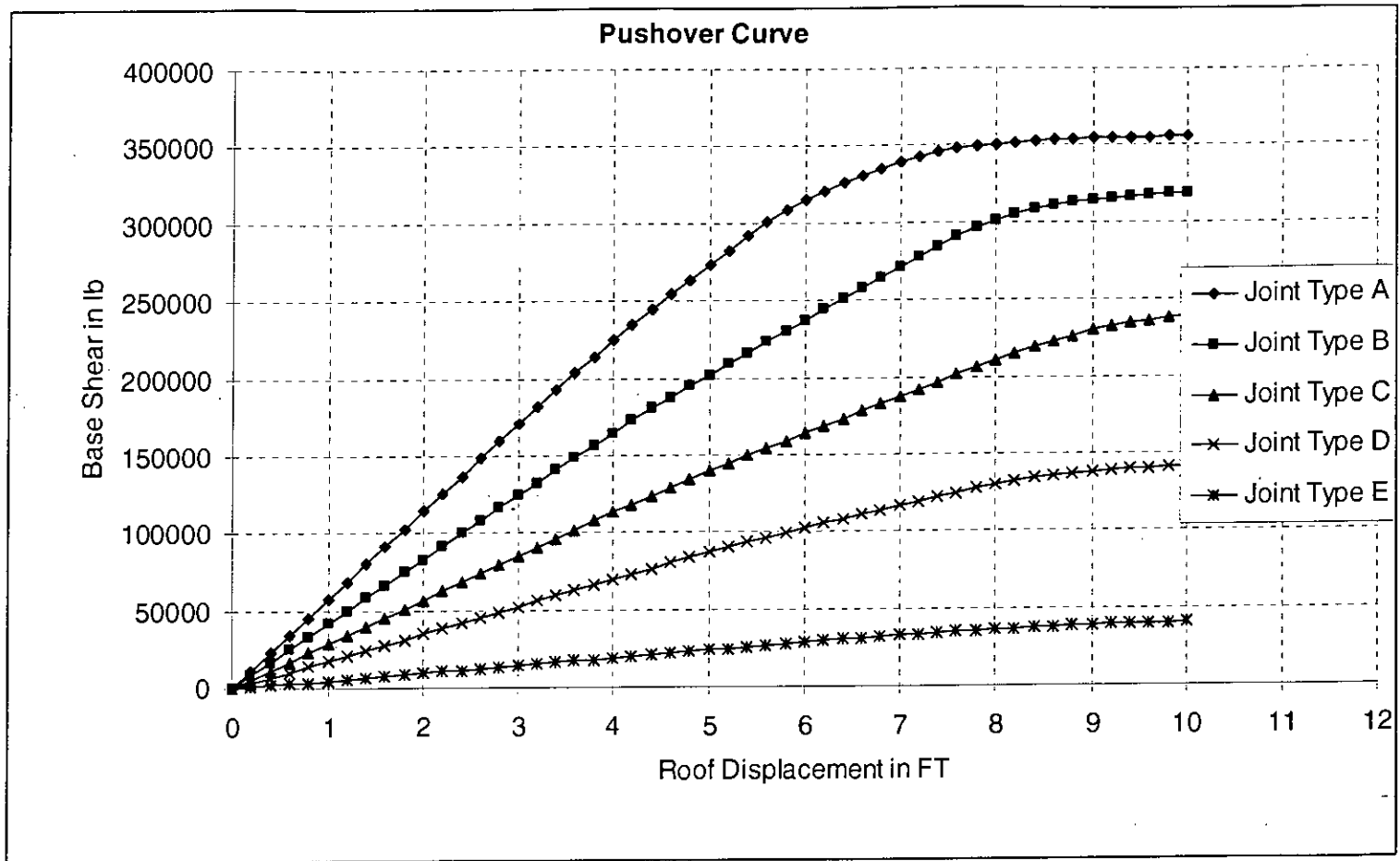
Figure 4.7 Pushover Curves of Ten Story Steel Frame for Different Types of Nonlinear Semi-rigid Connection
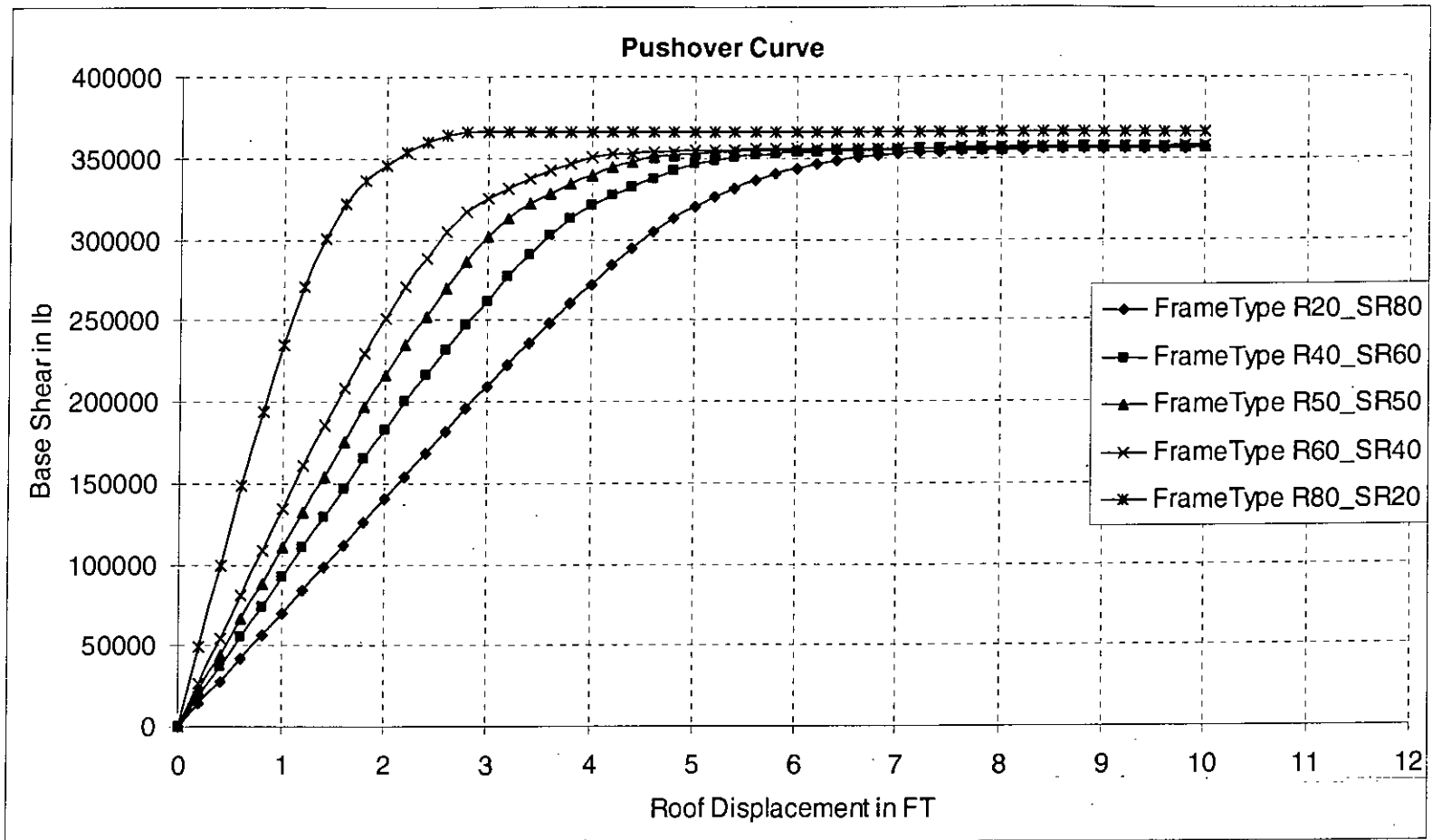
Figure 4.8 Pushover Curves of Ten Story Steel Frame for Different Types of Combination of 'Rigid' and 'Semirigid' Connection

4.6 Conversion of the Pushover Curve to the Capacity Spectrum

To use the capacity spectrum method it is necessary to convert the capacity curve, which is in terms of base shear and roof displacement to what is called a capacity spectrum, which is a representation of the capacity curve in Acceleration-Displacement Response Spectra or ADRS format (i. e. S_a vs S_d). More precisely, application of the capacity spectrum technique requires that both the demand response spectra and structural capacity (or pushover) curve be plotted in the spectral acceleration vs. spectral displacement domain. In order to develop the capacity spectrum from the capacity (or pushover) curve, it is necessary to do a point by point conversion to first mode spectral coordinates. The required equations to make the transformation are:

$$PF_1 = [\frac{\sum_{i=1}^{N}(w_i\phi_{i1}/g)}{\sum_{i=1}^{N}(w_i\phi_{i1}^2/g)}]$$ (Equation 4-2)

$$\alpha_1 = \frac{[\sum_{i=1}^{N}(w_i\phi_{i1})/g]^2}{[\sum_{i=1}^{N}(w_i/g)]\sum_{i=1}^{N}(w_i\phi_{i1}^2/g)}$$ (Equation 4-3)

$$S_a = \frac{V/W}{\alpha_1}$$ (Equation 4-4)

$$S_d = \frac{\Delta_{roof}}{PF_1 \times \phi_{roof1}}$$ (Equation 4-5)

where,

PF_1 = Modal participation factor for the first natural mode.

α_1 = Modal mass coefficient for the first natural mode.

w_i/g = Mass assigned to level i.

ϕ_{i1} = Amplitude of mode 1 at level i.

N= Level N, the level which is uppermost in the main portion of the structure.

V= Base Shear

W= Building dead weight plus likely live loads.

Δ_{roof}= Roof displacement.

S_a= Spectral acceleration

S_d= Spectral displacement.
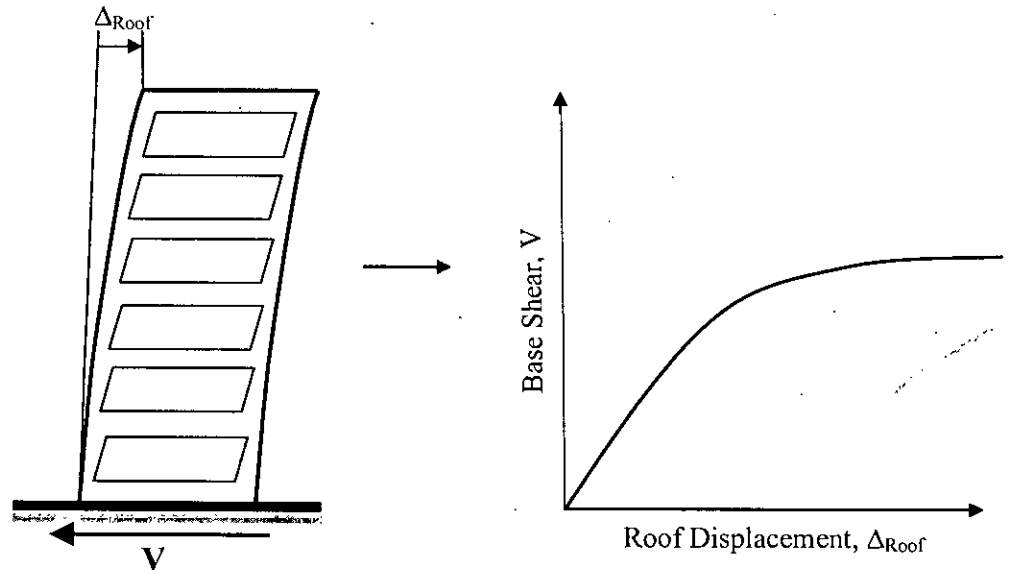
(a)
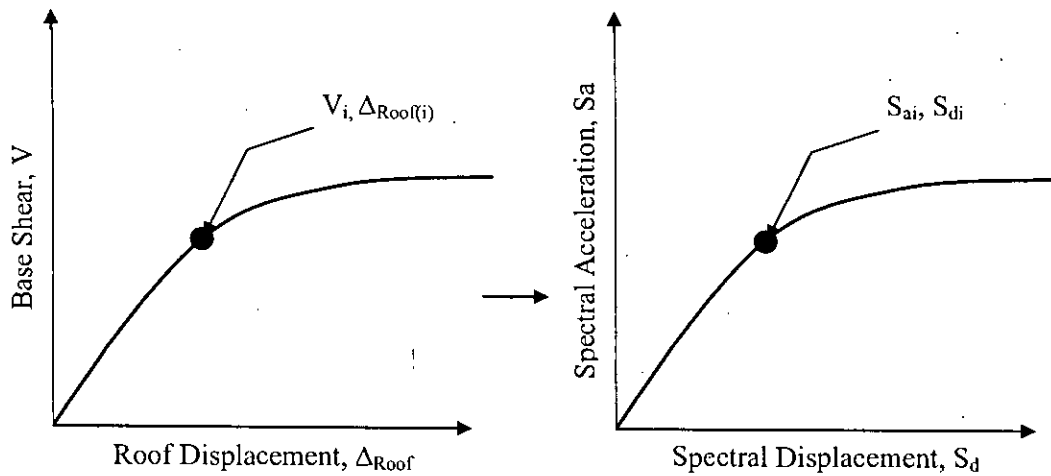
(b)

Figure 4.9: Step by step procedure to obtain capacity spectrum (a) Development of capacity (Pushover) curve by pushover analysis (b) Point to point conversion of capacity curve into capacity spectrum
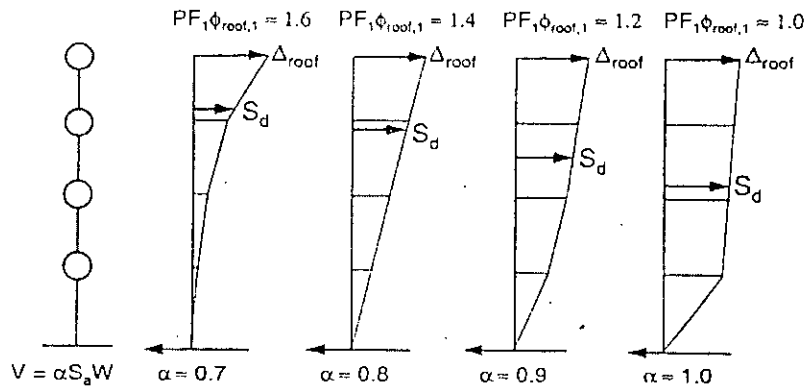
Figure 4.10 Example Modal Participation Factors and Modal Mass Coefficients

It is helpful to have some physical understanding of the relationship between the participation factor, the modal mass coefficient, and building displacement. As shown in Figure 4.10, the participation factor and modal mass coefficient vary according to the relative interstory displacement over the height of the building. For example, for a linear distribution of interstory displacement over the height of the building, $\alpha \approx 0.8$ and $PF_1\phi_{roof,1} \approx 1.4$. When the capacity curve is plotted in S_a vs. S_d coordinates, radial lines drawn from the origin of the plot through the curve at various spectral displacements have a slope, where   is the radial frequency of the effective (or secant) first mode response of the structure if pushed by an earthquake to that spectral displacement. Using the relationship $T' = 2\pi / \omega'$, it is possible to calculate, for each of these radial lines, the effective period of the structure if it is pushed to given spectral displacements.

The general process for converting the capacity curve to the capacity spectrum, that is, converting the capacity curve into the ADRS format, is to first calculate the modal participation factor PF_1 and the modal mass coefficient α_1 using equations 4-2 and 4-3. Then any point V_i, Δ_{roof} on the capacity curve is converted to the corresponding

67

point S_{ai}, S_{di} on the capacity spectrum using the following equations 4-6 and 4-7 (See Figure 4.9(b)):

$$S_{ai} = \frac{V_i / W}{\alpha_1}$$ (Equation 4-6)

$$S_{di} = \frac{\Delta_{roof}}{PF_1 \times \phi_{roof1}}$$ (Equation 4-7)

Modal analysis is required to get the structural dynamic characteristics of the building. Basic principles of structural dynamics and the equations used in modal analysis are given in Appendix C. The information needed to convert the pushover curve to the capacity spectrum is the modal participation factor and the modal mass coefficient for the first natural mode. Dynamic characteristics of the frame for different types of beam-column connections are given on Table 4-2 to Table 4-12 for the ten storied four-bay 2D steel frame structure and on Table 4-13 to Table 4-18 for the six storied four-bay 2D steel frame structure. Tables represent the periods, participation factors, effective mass coefficients and mode shapes for the first five modes of vibration parallel to the transverse axis of the building. The mode shapes can be normalized so that the roof values would be equal to 1.0. The period ratios (T/Tm), the first mode period divided by the higher mode period, indicate common mode shape characteristics.

Pushover curves, Figure 4.6 to Figure 4.8 and Figure 4.22 now can be converted to capacity spectrum using conversion factors. Fundamental mode or first natural mode is considered in conversion of pushover curves to capacity spectrum. Figure 4.11 to Figure 4.21 represent capacity spectrum of the ten storied four-bay 2D steel frame structure and Figure 4.23 to Figure 4.28 represent capacity spectrum of the six storied four-bay 2D steel frame structure for different types of connectivity. Elastic displacement lines with time period are also plotted on Figure 4.11 to Fig 4.21 and Figure 4.23 to Figure 4.28.

Table 4-2 Modal Properties for the Ten Story 2D Steel Moment Frame with Joint Type 'Rigid'

Mode		1	2	3	4	5
Period		2.662	0.929	0.547	0.383	0.287
Period Ratio, T/T_m		1	2.87	4.86	6.95	9.29
Participation Factor, PF_{Rm} at Roof		1.30	-0.40	0.27	-0.13	0.13
Effective Mass Coefficient, α_m		0.7986	0.0749	0.0369	0.0086	0.0117
Mode Shape at	0	0	0	0	0	0
Story Levels, Φ_i	1	2.96E-04	-9.05E-04	1.50E-03	-1.81E-03	2.33E-03
	2	7.33E-04	-2.07E-03	2.93E-03	-2.70E-03	2.21E-03
	3	1.17E-03	-2.87E-03	2.87E-03	-1.03E-03	-1.20E-03
	4	1.66E-03	-3.16E-03	1.07E-03	2.13E-03	-3.26E-03
	5	2.11E-03	-2.77E-03	-1.37E-03	3.10E-03	1.60E-05
	6	2.51E-03	-1.78E-03	-3.05E-03	8.05E-04	3.33E-03
	7	2.88E-03	-2.42E-04	-3.02E-03	-2.77E-03	1.01E-03
	8	3.16E-03	1.36E-03	-1.13E-03	-3.22E-03	-3.14E-03
	9	3.36E-03	2.66E-03	1.46E-03	-2.14E-05	-1.68E-03
	Roof	3.46E-03	3.38E-03	3.22E-03	3.32E-03	2.94E-03
Normalized Mode	0	0	0	0	0	0
Shape at Story	1	0.086	-0.267	0.466	-0.544	0.793
Levels, Φ_{im}	2	0.212	-0.611	0.907	-0.813	0.752
	3	0.339	-0.848	0.891	-0.310	-0.408
	4	0.480	-0.935	0.333	0.641	-1.108
	5	0.610	-0.820	-0.426	0.934	0.005
	6	0.724	-0.527	-0.946	0.242	1.129
	7	0.831	-0.072	-0.938	-0.833	0.342
	8	0.913	0.402	-0.351	-0.969	-1.067
	9	0.970	0.786	0.452	-0.006	-0.570
	Roof	1	1	1	1	1

Figure 4.11 Capacity Spectrum of the Ten Story 2D Steel Frame for Joint Type 'Rigid'

Table 4-3 Modal Properties for the Ten Story 2D Steel Moment Frame with Joint Type 'A'

Mode		1	2	3	4	5
Period		6.862	2.151	1.125	0.684	0.457
Period Ratio, T/T_m		1	3.19	6.10	10.03	15.02
Participation Factor, PF_{Rm} at Roof		1.30	-0.43	0.33	-0.17	0.17
Effective Mass Coefficient, α_m		0.7647	0.0735	0.0444	0.0148	0.0191
Mode Shape at	0	0	0	0	0	0
Story Levels, Φ_i	1	1.70E-04	-5.43E-04	9.86E-04	-1.50E-03	-2.06E-03
	2	5.53E-04	-1.62E-03	2.49E-03	-2.96E-03	-2.77E-03
	3	1.03E-03	-2.64E-03	3.04E-03	-1.86E-03	4.26E-04
	4	1.55E-03	-3.19E-03	1.91E-03	1.24E-03	3.16E-03
	5	2.05E-03	-3.00E-03	-4.37E-04	3.15E-03	8.27E-04
	6	2.50E-03	-2.10E-03	-2.62E-03	1.70E-03	-2.97E-03
	7	2.89E-03	-6.42E-04	-3.26E-03	-1.78E-03	-1.85E-03
	8	3.20E-03	1.05E-03	-1.79E-03	-3.30E-03	2.52E-03
	9	3.42E-03	2.58E-03	9.64E-04	-8.90E-04	2.35E-03
	Roof	3.57E-03	3.72E-03	3.68E-03	3.35E-03	-2.86E-03
Normalized Mode	0	0	0	0	0	0
Shape at Story	1	0.048	-0.146	0.268	-0.449	0.718
Levels, Φ_{im}	2	0.155	-0.435	0.679	-0.882	0.968
	3	0.289	-0.709	0.828	-0.557	-0.149
	4	0.433	-0.856	0.520	0.372	-1.102
	5	0.573	-0.806	-0.119	0.940	-0.289
	6	0.701	-0.565	-0.713	0.506	1.039
	7	0.811	-0.172	-0.888	-0.532	0.646
	8	0.897	0.281	-0.488	-0.984	-0.881
	9	0.959	0.692	0.262	-0.266	-0.819
	Roof	1	1	1	1	1

Figure 4.12 Capacity Spectrum of the Ten Story 2D Steel Frame for Joint Type 'A'

Table 4-4 Modal Properties for the Ten Story 2D Steel Moment Frame with Joint Type 'B'

Mode		1	2	3	4	5
Period		7.932	2.427	1.233	0.728	0.477
Period Ratio, T/T_m		1	3.27	6.43	10.90	16.62
Participation Factor, PF_{Rm} at Roof		1.32	-0.45	0.34	-0.18	0.17
Effective Mass Coefficient, α_m		0.7536	0.0769	0.0472	0.0160	0.0202
Mode Shape at	0	0	0	0	0	0
Story Levels, Φ_i	1	1.54E-04	-5.02E-04	9.37E-04	-1.47E-03	-2.04E-03
	2	5.14E-04	-1.53E-03	2.43E-03	-2.96E-03	-2.83E-03
	3	9.78E-04	-2.55E-03	3.07E-03	-1.99E-03	2.98E-04
	4	1.49E-03	-3.15E-03	2.07E-03	1.07E-03	3.14E-03
	5	2.00E-03	-3.04E-03	-2.09E-04	3.13E-03	9.86E-04
	6	2.47E-03	-2.22E-03	-2.46E-03	1.89E-03	-2.89E-03
	7	2.89E-03	-8.03E-04	-3.27E-03	-1.56E-03	-2.01E-03
	8	3.22E-03	9.05E-04	-1.96E-03	-3.30E-03	2.38E-03
	9	3.46E-03	2.53E-03	7.97E-04	-1.07E-03	2.44E-03
	Roof	3.64E-03	3.83E-03	3.72E-03	3.31E-03	-2.79E-03
Normalized Mode	0	0	0	0	0	0
Shape at Story	1	0.042	-0.131	0.252	-0.444	0.730
Levels, Φ_{im}	2	0.141	-0.401	0.655	-0.896	1.016
	3	0.269	-0.668	0.825	-0.603	-0.107
	4	0.410	-0.823	0.558	0.323	-1.125
	5	0.550	-0.795	-0.056	0.945	-0.354
	6	0.680	-0.580	-0.662	0.570	1.037
	7	0.794	-0.210	-0.881	-0.471	0.721
	8	0.885	0.236	-0.527	-0.996	-0.851
	9	0.952	0.660	0.214	-0.323	-0.875
	Roof	1	1	1	1	1

Figure 4.13 Capacity Spectrum of the Ten Story 2D Steel Frame for Joint Type 'B'

Table 4-5 Modal Properties for the Ten Story 2D Steel Moment Frame with Joint Type 'C'

Mode		1	2	3	4	5
Period		9.403	2.786	1.357	0.773	0.497
Period Ratio, T/T_m		1	3.38	6.93	12.17	18.92
Participation Factor, PF_{Rm} at Roof		1.34	-0.48	0.36	-0.18	0.17
Effective Mass Coefficient, α_m		0.7384	0.0828	0.0510	0.0173	0.0213
Mode Shape at Story Levels, Φ_i	0	0	0	0	0	0
	1	1.36E-04	-4.59E-04	8.91E-04	1.44E-03	-2.02E-03
	2	4.68E-04	-1.44E-03	2.38E-03	2.97E-03	-2.89E-03
	3	9.10E-04	-2.45E-03	3.10E-03	2.12E-03	1.74E-04
	4	1.41E-03	-3.10E-03	2.25E-03	-8.89E-04	3.12E-03
	5	1.93E-03	-3.08E-03	5.43E-05	-3.10E-03	1.14E-03
	6	2.42E-03	-2.36E-03	-2.26E-03	-2.08E-03	-2.81E-03
	7	2.87E-03	-1.02E-03	-3.26E-03	1.32E-03	-2.16E-03
	8	3.23E-03	7.06E-04	-2.14E-03	3.28E-03	2.22E-03
	9	3.52E-03	2.44E-03	5.90E-04	1.25E-03	2.52E-03
	Roof	3.74E-03	3.95E-03	3.73E-03	-3.24E-03	-2.70E-03
Normalized Mode Shape at Story Levels, Φ_{im}	0	0	0	0	0	0
	1	0.036	-0.116	0.239	-0.443	0.748
	2	0.125	-0.364	0.638	-0.916	1.070
	3	0.243	-0.621	0.833	-0.655	-0.064
	4	0.378	-0.785	0.605	0.274	-1.154
	5	0.517	-0.781	0.015	0.955	-0.423
	6	0.649	-0.599	-0.607	0.641	1.039
	7	0.767	-0.257	-0.876	-0.407	0.800
	8	0.865	0.179	-0.574	-1.010	-0.822
	9	0.941	0.618	0.158	-0.387	-0.934
	Roof	1	1	1	1	1

Figure 4.14 Capacity Spectrum of the Ten Story 2D Steel Frame for Joint Type 'C'

Table 4-6 Modal Properties for the Ten Story 2D Steel Moment Frame with Joint Type 'D'

Mode		1	2	3	4	5
Period		11.628	3.268	1.495	0.817	0.515
Period Ratio, T/T_m		1	3.56	7.78	14.23	22.57
Participation Factor, PF_{Rm} at Roof		1.37	-0.52	0.37	-0.18	0.17
Effective Mass Coefficient, α_m		0.7161	0.0935	0.0560	0.0187	0.0223
Mode Shape at	0	0	0	0	0	0
Story Levels, Φ_i	1	1.16E-04	-4.14E-04	8.52E-04	1.41E-03	-2.01E-03
	2	4.11E-04	-1.33E-03	2.33E-03	2.98E-03	-2.95E-03
	3	8.20E-04	-2.33E-03	3.15E-03	2.24E-03	5.90E-05
	4	1.30E-03	-3.02E-03	2.45E-03	-7.12E-04	3.10E-03
	5	1.82E-03	-3.12E-03	3.46E-04	-3.06E-03	1.28E-03
	6	2.34E-03	-2.54E-03	-2.02E-03	-2.26E-03	-2.72E-03
	7	2.82E-03	-1.29E-03	-3.22E-03	1.08E-03	-2.30E-03
	8	3.24E-03	4.30E-04	-2.32E-03	3.24E-03	2.07E-03
	9	3.60E-03	2.30E-03	3.49E-04	1.43E-03	2.59E-03
	Roof	3.90E-03	4.06E-03	3.68E-03	-3.15E-03	-2.61E-03
Normalized Mode	0	0	0	0	0	0
Shape at Story	1	0.030	-0.102	0.231	-0.446	0.770
Levels, Φ_{im}	2	0.105	-0.327	0.633	-0.944	1.129
	3	0.210	-0.572	0.855	-0.712	-0.023
	4	0.334	-0.744	0.666	0.226	-1.188
	5	0.468	-0.769	0.094	0.970	-0.492
	6	0.600	-0.626	-0.550	0.717	1.043
	7	0.723	-0.318	-0.876	-0.342	0.881
	8	0.832	0.106	-0.630	-1.028	-0.793
	9	0.923	0.565	0.095	-0.453	-0.994
	Roof	1	1	1	1	1

Capcity Spectrum
(Connection Type-D)

Figure 4.15 Capacity Spectrum of the Ten Story 2D Steel Frame for Joint Type 'D'

78

Table 4-7 Modal Properties for the Ten Story 2D Steel Moment Frame with Joint Type 'E'

Mode		1	2	3	4	5
Period		20.408	4.425	1.718	0.876	0.538
Period Ratio, T/T_m		1	4.61	11.88	23.29	37.96
Participation Factor, PF_{Rm} at Roof		1.46	-0.63	0.38	-0.19	0.16
Effective Mass Coefficient, α_m		0.6494	0.1379	0.0659	0.0209	0.0236
Mode Shape at	0	0	0	0	0	0
Story Levels, Φ_i	1	7.60E-05	-3.48E-04	8.07E-04	1.37E-03	-2.00E-03
	2	2.84E-04	-1.16E-03	2.28E-03	2.98E-03	-3.01E-03
	3	5.98E-04	-2.12E-03	3.23E-03	2.40E-03	-8.34E-05
	4	1.01E-03	-2.90E-03	2.75E-03	-4.79E-04	3.07E-03
	5	1.50E-03	-3.21E-03	8.02E-04	-2.99E-03	1.46E-03
	6	2.05E-03	-2.90E-03	-1.62E-03	-2.49E-03	-2.61E-03
	7	2.63E-03	-1.88E-03	-3.10E-03	7.50E-04	-2.46E-03
	8	3.22E-03	-2.11E-04	-2.55E-03	3.17E-03	1.87E-03
	9	3.80E-03	1.85E-03	-4.30E-05	1.65E-03	2.67E-03
	Roof	4.38E-03	4.06E-03	3.48E-03	-2.99E-03	-2.48E-03
Normalized Mode	0	0	0	0	0	0
Shape at Story	1	0.017	-0.086	0.232	-0.458	0.806
Levels, Φ_{im}	2	0.065	-0.287	0.655	-0.997	1.216
	3	0.136	-0.523	0.927	-0.802	0.034
	4	0.230	-0.716	0.790	0.160	-1.239
	5	0.343	-0.792	0.230	1.000	-0.588
	6	0.467	-0.716	-0.465	0.833	1.053
	7	0.599	-0.464	-0.890	-0.251	0.994
	8	0.734	-0.052	-0.732	-1.058	-0.756
	9	0.868	0.457	-0.012	-0.552	-1.076
	Roof	1	1	1	1	1

79

Figure 4.16 Capacity Spectrum of the Ten Story 2D Steel Frame for Joint Type 'E'

Table 4-8 Modal Properties for the Ten Story 2D Steel Moment Frame with Frame Type 'R20_SR80'

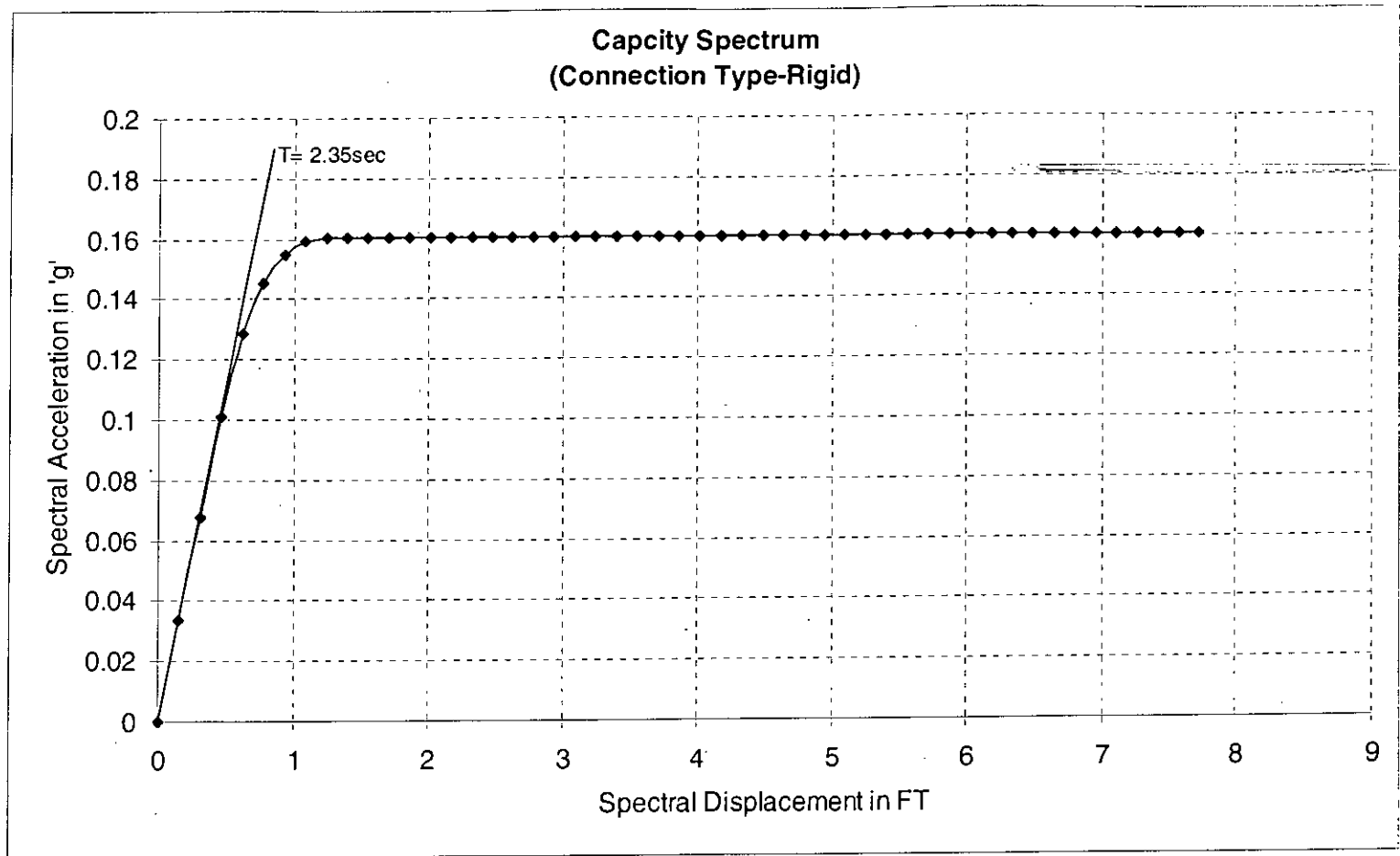| Mode		1	2	3	4	5
Period		5.654	1.757	0.948	0.621	0.433
Period Ratio, T/T_m		1	3.22	5.96	9.11	13.07
Participation Factor, PF_{Rm} at Roof		1.32	-0.50	0.45	-0.28	0.20
Effective Mass Coefficient, α_m		0.6573	0.0909	0.0891	0.0467	0.0285
Mode Shape at	0	0	0	0	0	0
Story Levels, Φ_i	1	6.15E-05	-2.79E-04	8.06E-04	1.53E-03	1.87E-03
	2	1.73E-04	-7.28E-04	1.89E-03	3.10E-03	3.02E-03
	3	4.62E-04	-1.60E-03	2.98E-03	2.92E-03	6.20E-04
	4	1.01E-03	-2.79E-03	3.17E-03	2.39E-04	-2.93E-03
	5	1.66E-03	-3.44E-03	1.37E-03	-2.60E-03	-1.57E-03
	6	2.30E-03	-3.12E-03	-1.40E-03	-2.34E-03	2.61E-03
	7	2.89E-03	-1.76E-03	-3.19E-03	9.34E-04	2.28E-03
	8	3.36E-03	2.59E-04	-2.46E-03	3.11E-03	-2.23E-03
	9	3.71E-03	2.32E-03	3.53E-04	1.19E-03	-2.49E-03
	Roof	3.94E-03	3.96E-03	3.53E-03	-3.05E-03	2.77E-03
Normalized Mode	0	0	0	0	0	0
Shape at Story	1	0.016	-0.070	0.228	-0.502	0.677
Levels, Φ_{im}	2	0.044	-0.184	0.535	-1.016	1.091
	3	0.117	-0.404	0.844	-0.958	0.224
	4	0.256	-0.706	0.897	-0.078	-1.058
	5	0.421	-0.869	0.389	0.855	-0.566
	6	0.585	-0.788	-0.397	0.768	0.943
	7	0.733	-0.446	-0.904	-0.306	0.825
	8	0.853	0.065	-0.697	-1.020	-0.805
	9	0.941	0.587	0.100	-0.389	-0.901
	Roof	1	1	1	1	1
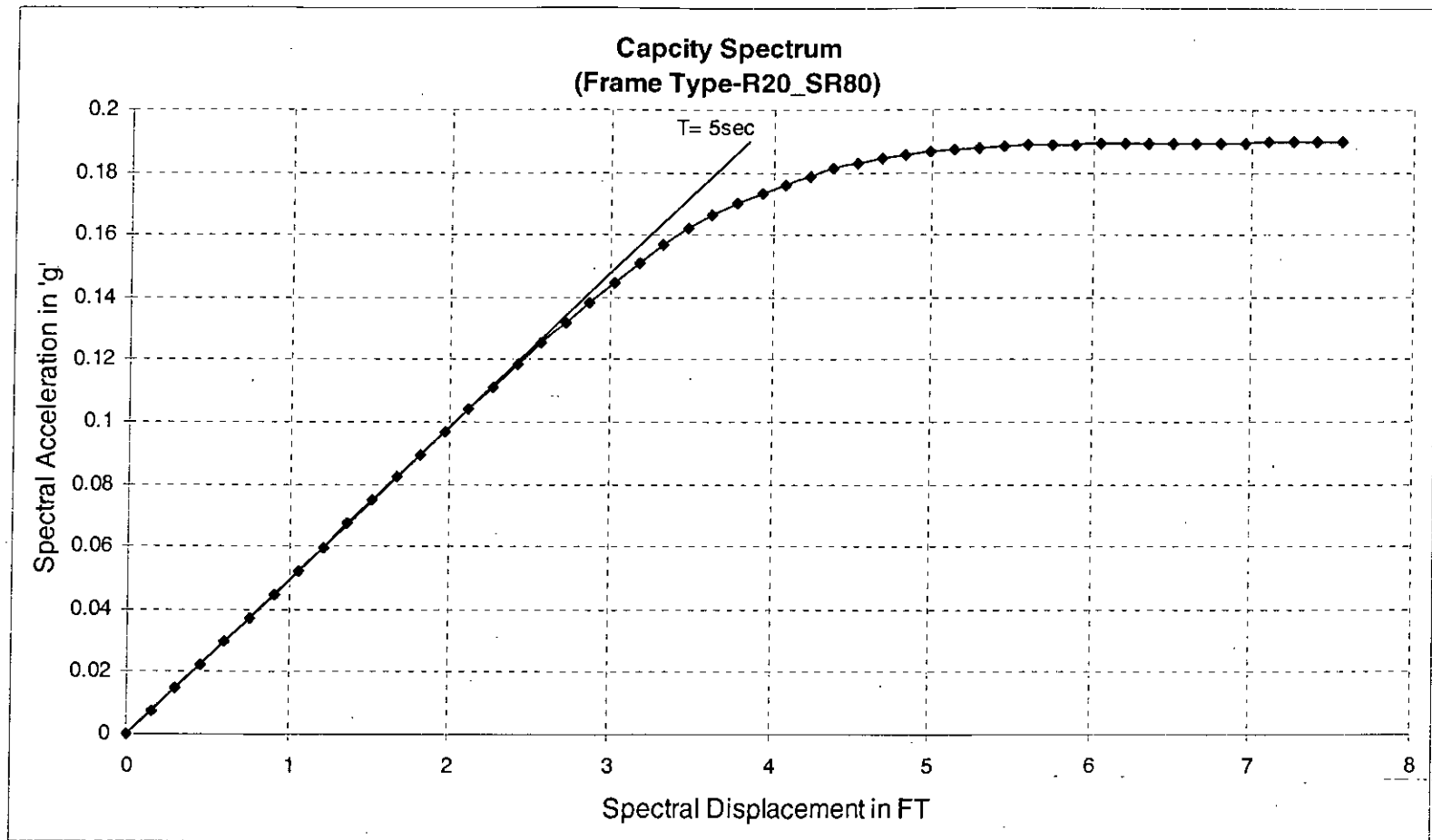
Figure 4.17 Capacity Spectrum of the Ten Story 2D Steel Frame for Frame Type 'R20_SR80'

Table 4-9 Modal Properties for the Ten Story 2D Steel Moment Frame with Frame Type 'R40_SR60'

Mode		1	2	3	4	5
Period		4.425	1.490	0.916	0.550	0.380
Period Ratio, T/T_m		1	2.97	4.83	8.05	11.65
Participation Factor, PF_{Rm} at Roof		1.38	-0.67	0.47	-0.16	0.15
Effective Mass Coefficient, α_m		0.5837	0.1880	0.0992	0.0134	0.0230
Mode Shape at	0	0	0	0	0	0
Story Levels, Φ_i	1	9.05E-05	-5.18E-04	9.08E-04	-1.20E-03	2.16E-03
	2	2.26E-04	-1.25E-03	2.07E-03	-2.33E-03	3.20E-03
	3	3.68E-04	-1.92E-03	2.86E-03	-2.30E-03	1.16E-03
	4	5.59E-04	-2.55E-03	3.05E-03	-7.83E-04	-2.54E-03
	5	1.02E-03	-3.17E-03	1.65E-03	2.16E-03	-2.87E-03
	6	1.81E-03	-3.37E-03	-1.13E-03	3.47E-03	1.13E-03
	7	2.66E-03	-2.44E-03	-3.14E-03	1.51E-04	2.81E-03
	8	3.42E-03	-4.97E-04	-2.59E-03	-3.42E-03	-1.30E-03
	9	4.00E-03	1.77E-03	2.27E-04	-1.86E-03	-2.59E-03
	Roof	4.40E-03	3.67E-03	3.52E-03	3.37E-03	2.35E-03
Normalized Mode	0	0	0	0	0	0
Shape at Story	1	0.021	-0.141	0.258	-0.356	0.918
Levels, Φ_{im}	2	0.051	-0.341	0.589	-0.693	1.359
	3	0.084	-0.523	0.814	-0.682	0.495
	4	0.127	-0.696	0.867	-0.233	-1.081
	5	0.232	-0.863	0.468	0.642	-1.219
	6	0.410	-0.918	-0.320	1.032	0.481
	7	0.605	-0.666	-0.892	0.045	1.196
	8	0.777	-0.136	-0.737	-1.016	-0.551
	9	0.910	0.482	0.064	-0.554	-1.099
	Roof	1	1	1	1	1

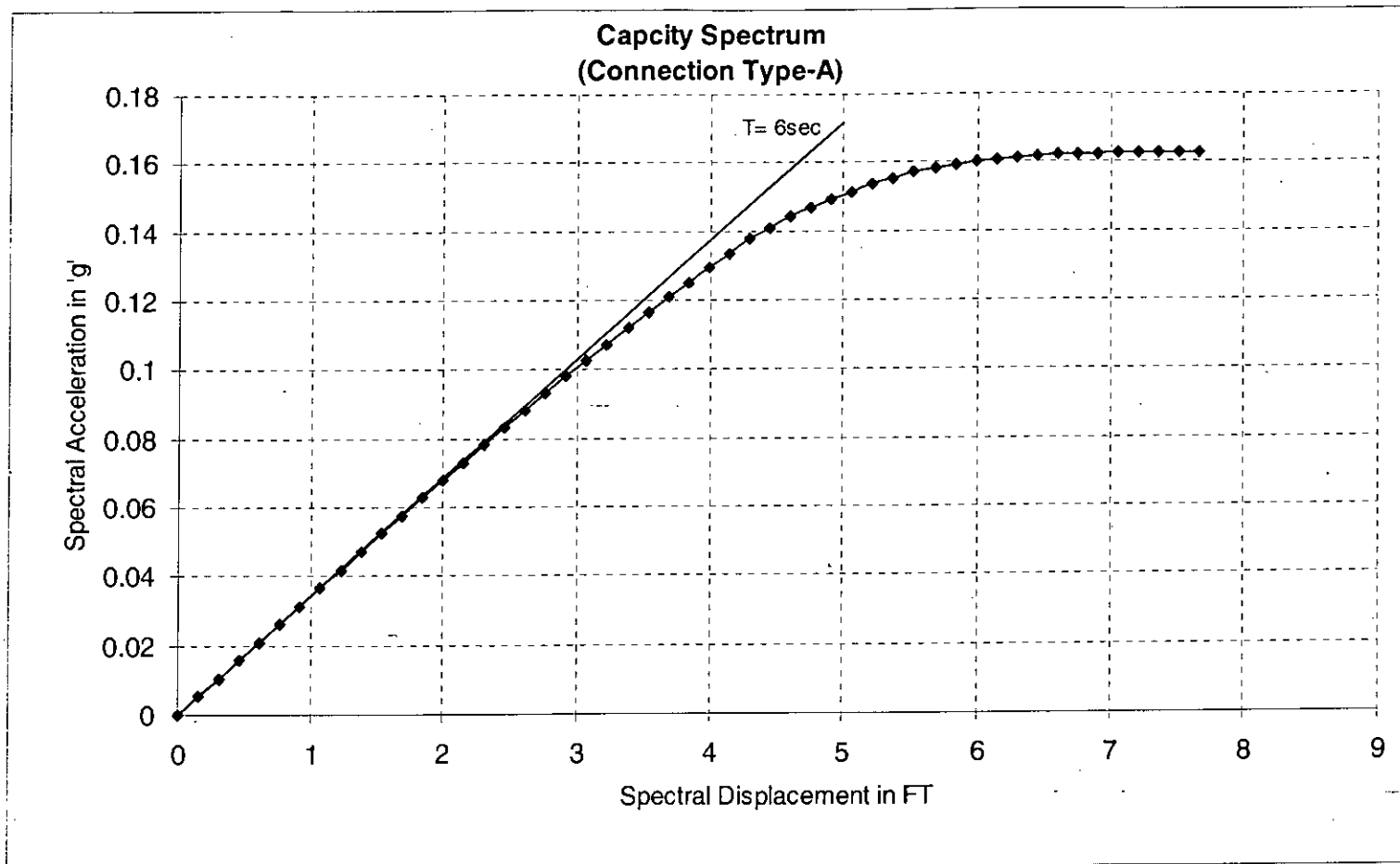**Capcity Spectrum**
(Frame Type-R40_SR60)
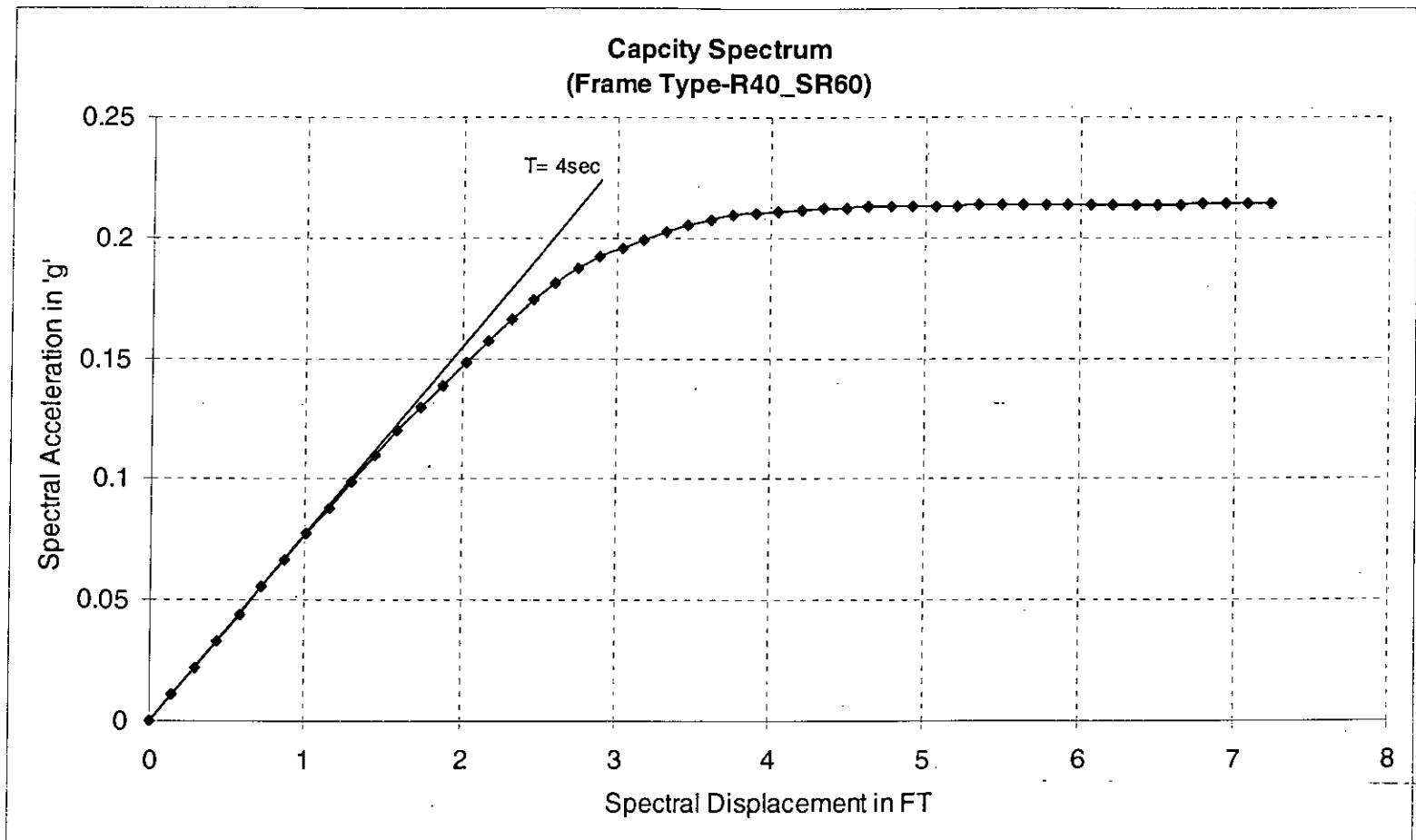
Figure 4.18 Capacity Spectrum of the Ten Story 2D Steel Frame for Frame Type 'R40_SR60'

Table 4-10 Modal Properties for the Ten Story 2D Steel Moment Frame with Frame Type 'R50_SR50'

Mode		1	2	3	4	5
Period		3.831	1.471	0.833	0.510	0.373
Period Ratio, T/T_m		1	2.60	4.60	7.52	10.27
Participation Factor, PF_{Rm} at Roof		1.45	-0.69	0.38	-0.17	0.15
Effective Mass Coefficient, α_m		0.5796	0.2346	0.0517	0.0220	0.0167
Mode Shape at Story Levels, Φ_i	0	0	0	0	0	0
	1	1.21E-04	-5.84E-04	7.88E-04	-1.67E-03	1.79E-03
	2	3.01E-04	-1.41E-03	1.76E-03	-3.12E-03	2.60E-03
	3	4.88E-04	-2.16E-03	2.35E-03	-2.77E-03	8.34E-04
	4	7.04E-04	-2.84E-03	2.39E-03	-4.53E-04	-2.26E-03
	5	9.44E-04	-3.26E-03	1.68E-03	2.19E-03	-2.80E-03
	6	1.49E-03	-3.23E-03	-6.11E-04	3.26E-03	1.20E-03
	7	2.41E-03	-2.33E-03	-3.41E-03	8.31E-04	3.42E-03
	8	3.35E-03	-5.23E-04	-3.38E-03	-2.63E-03	-1.38E-03
	9	4.11E-03	1.58E-03	-1.53E-04	-1.78E-03	-3.09E-03
	Roof	4.64E-03	3.34E-03	4.02E-03	2.69E-03	2.74E-03
Normalized Mode Shape at Story Levels, Φ_{im}	0	0	0	0	0	0
	1	0.026	-0.175	0.196	-0.619	0.654
	2	0.065	-0.421	0.439	-1.158	0.950
	3	0.105	-0.645	0.586	-1.029	0.305
	4	0.152	-0.849	0.595	-0.168	-0.827
	5	0.203	-0.976	0.419	0.815	-1.022
	6	0.320	-0.966	-0.152	1.212	0.440
	7	0.519	-0.696	-0.847	0.309	1.249
	8	0.721	-0.156	-0.841	-0.977	-0.504
	9	0.885	0.472	-0.038	-0.661	-1.130
	Roof	1	1	1	1	1

Capcity Spectrum
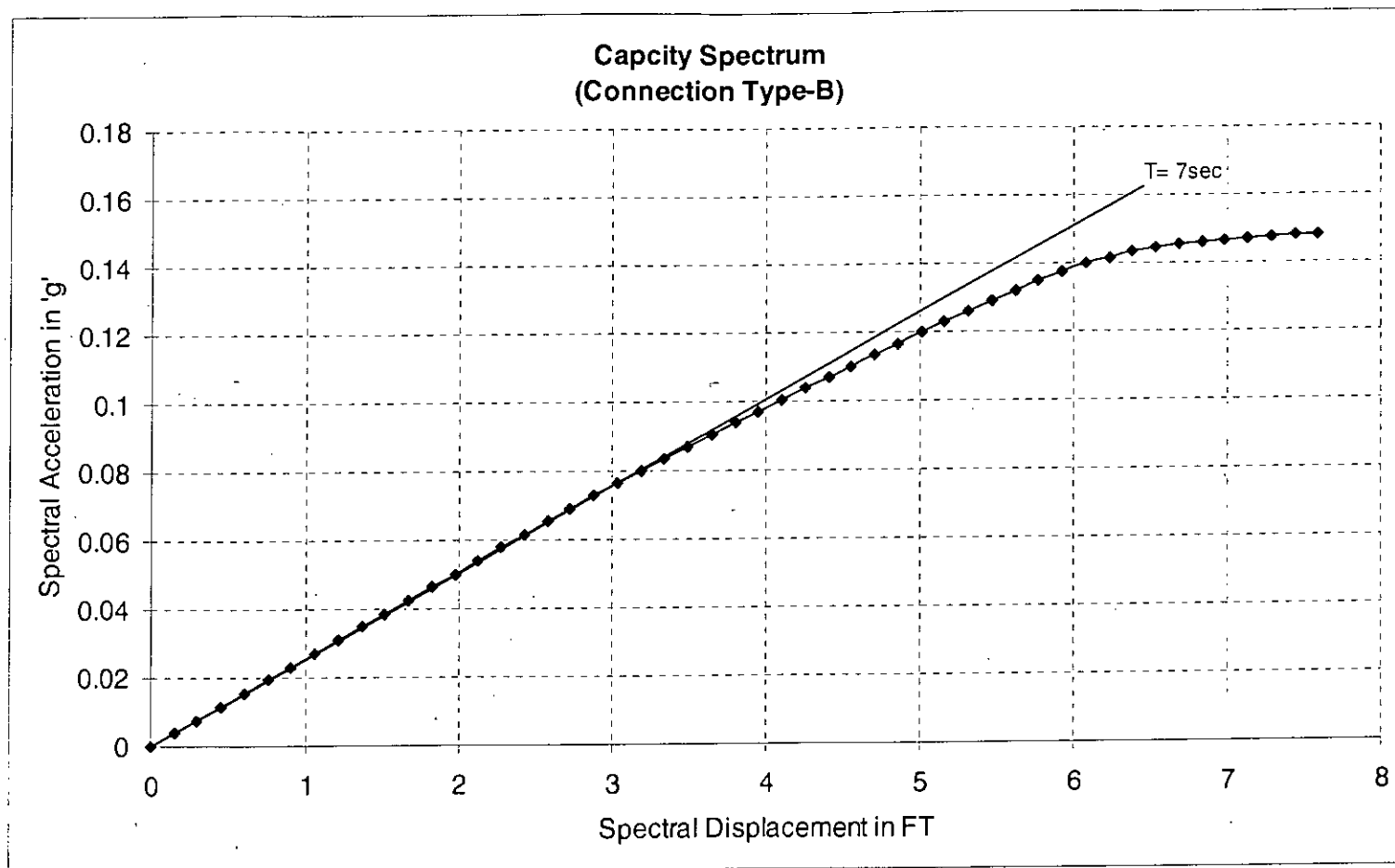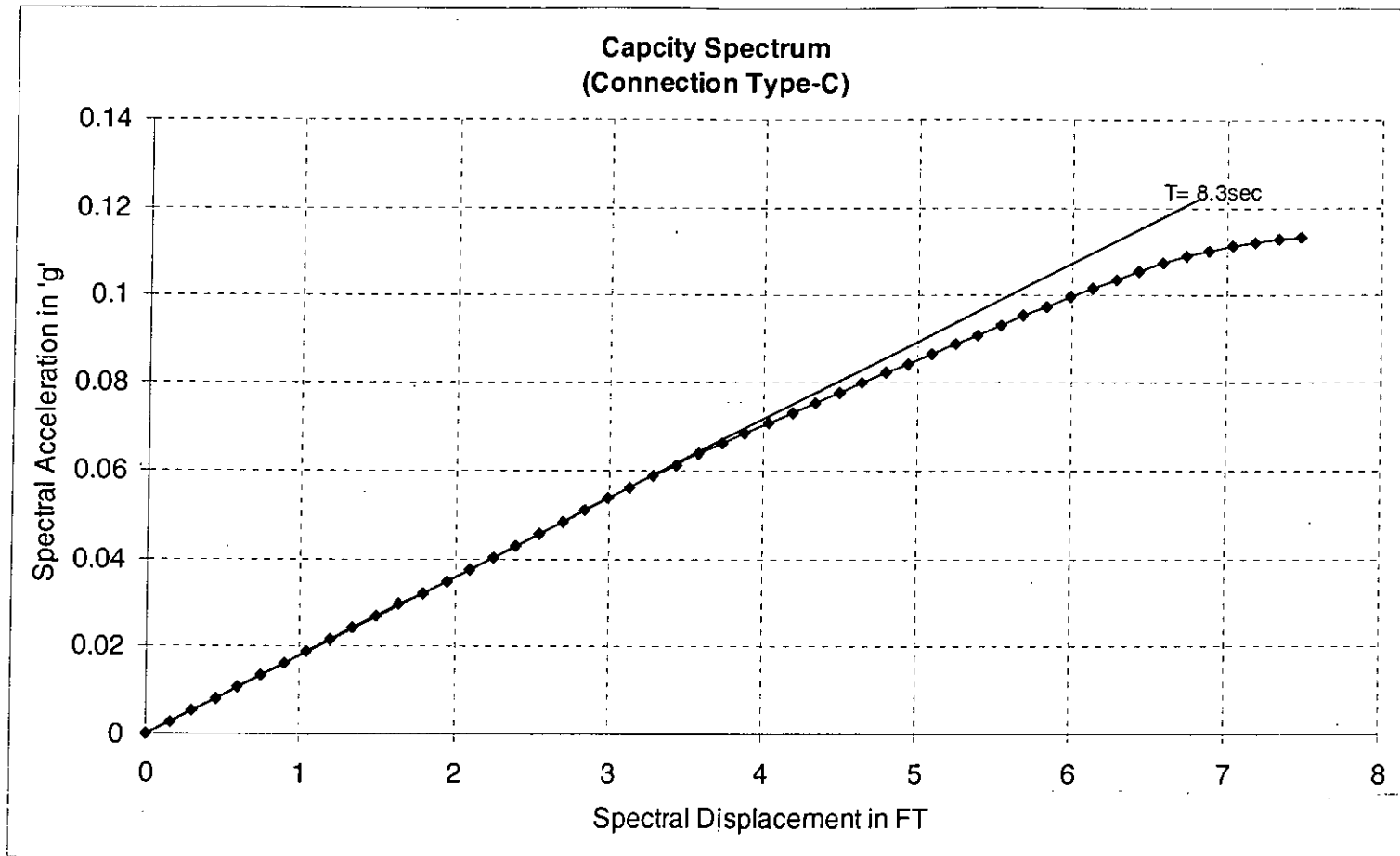**(Frame Type-R50_SR50)**

Figure 4.19 Capacity Spectrum of the Ten Story 2D Steel Frame for Frame Type 'R50_SR50'

Table 4-11 Modal Properties for the Ten Story 2D Steel Moment Frame with Frame Type 'R60_SR40'

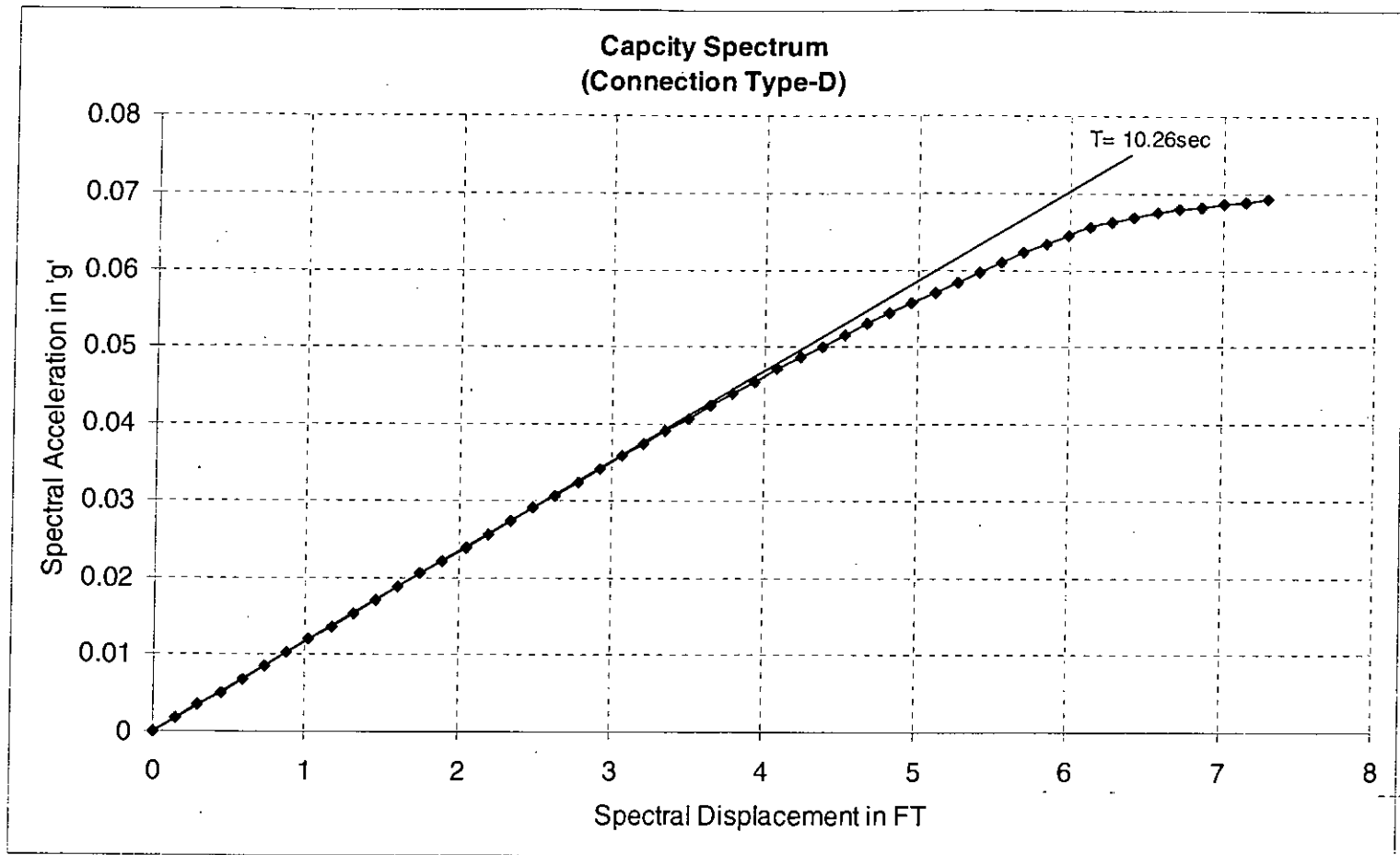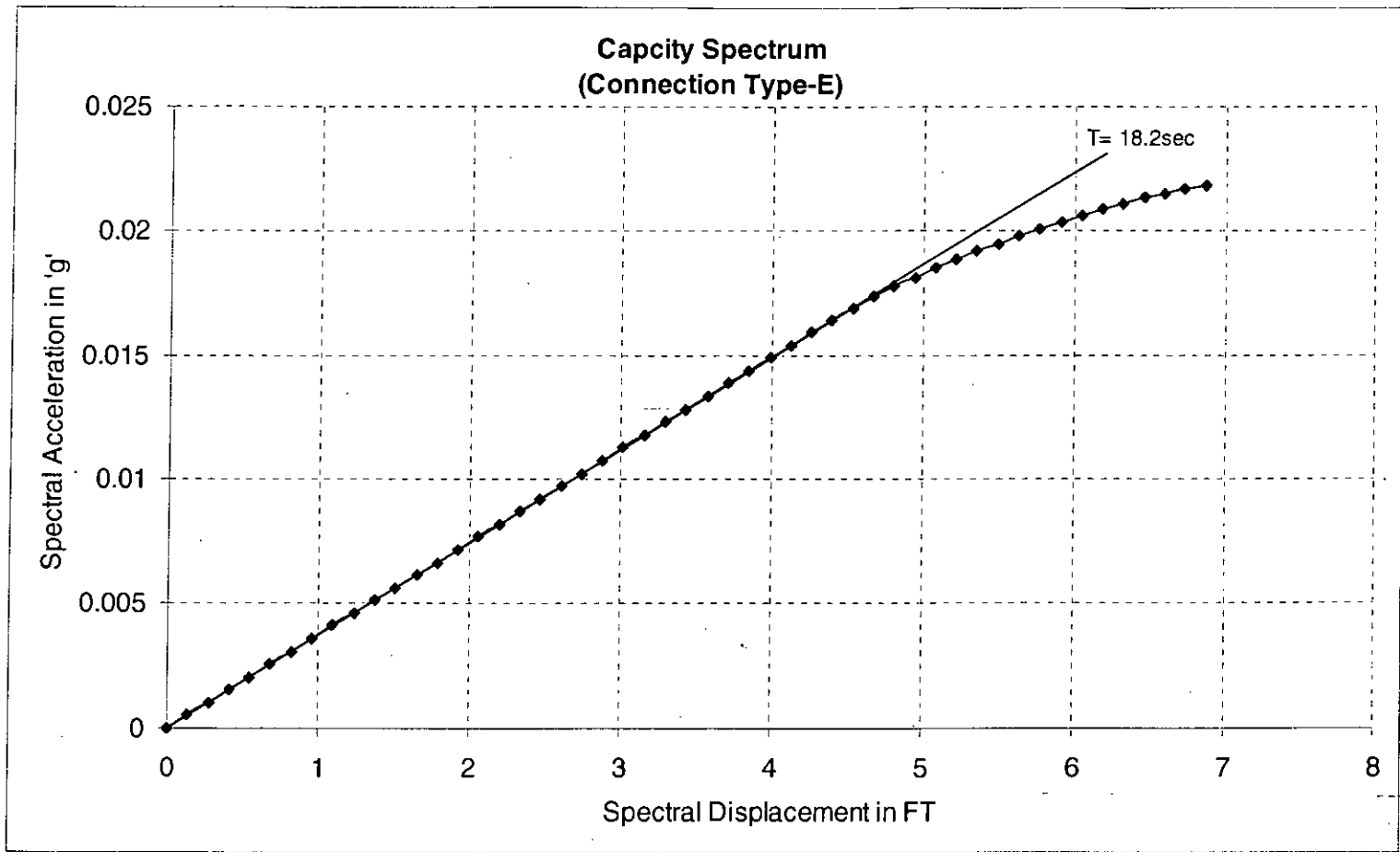| Mode		1	2	3	4	5
Period		3.332	1.464	0.724	0.509	0.340
Period Ratio, T/T_m		1	2.28	4.60	6.54	9.79
Participation Factor, PF_{Rm} at Roof		1.53	-0.69	0.34	-0.17	0.13
Effective Mass Coefficient, α_m		0.6147	0.2062	0.0449	0.0205	0.0163
Mode Shape at	0	0	0	0	0	0
Story Levels, Φ_i	1	1.65E-04	-5.59E-04	9.73E-04	-1.63E-03	2.07E-03
	2	4.11E-04	-1.35E-03	2.10E-03	-3.05E-03	2.68E-03
	3	6.63E-04	-2.06E-03	2.62E-03	-2.71E-03	2.16E-04
	4	9.50E-04	-2.71E-03	2.28E-03	-4.38E-04	-3.05E-03
	5	1.23E-03	-3.13E-03	1.14E-03	2.15E-03	-2.49E-03
	6	1.51E-03	-3.22E-03	-4.61E-04	3.27E-03	1.26E-03
	7	2.17E-03	-2.44E-03	-2.90E-03	8.44E-04	3.49E-03
	8	3.17E-03	-5.57E-04	-3.77E-03	-2.73E-03	-5.35E-04
	9	4.09E-03	1.69E-03	-7.82E-04	-1.85E-03	-2.95E-03
	Roof	4.76E-03	3.60E-03	3.85E-03	2.79E-03	2.32E-03
Normalized Mode	0	0	0	0	0	0
Shape at Story	1	0.035	-0.155	0.253	-0.584	0.894
Levels, Φ_{im}	2	0.086	-0.375	0.547	-1.092	1.156
	3	0.140	-0.574	0.681	-0.970	0.093
	4	0.200	-0.755	0.592	-0.157	-1.317
	5	0.258	-0.870	0.296	0.772	-1.075
	6	0.318	-0.896	-0.120	1.174	0.543
	7	0.456	-0.678	-0.753	0.303	1.505
	8	0.668	-0.155	-0.979	-0.978	-0.231
	9	0.860	0.470	-0.203	-0.662	-1.274
	Roof	1	1	1	1	1

Figure 4.20 Capacity Spectrum of the Ten Story 2D Steel Frame for Frame Type 'R60_SR40'

Table 4-12 Modal Properties for the Ten Story 2D Steel Moment Frame with Frame Type 'R80_SR20'

Mode		1	2	3	4	5
Period		2.728	1.116	0.680	0.445	0.313
Period Ratio, T/T_m		1	2.44	4.01	6.13	8.72
Participation Factor, PF_{Rm} at Roof		1.44	-0.54	0.33	-0.12	0.10
Effective Mass Coefficient, α_m		0.7729	0.0607	0.0520	0.0161	0.0135
Mode Shape at	0	0	0	0	0	0
Story Levels, Φ_i	1	2.78E-04	-6.03E-04	1.20E-03	-1.78E-03	-2.20E-03
	2	6.88E-04	-1.42E-03	2.54E-03	-3.05E-03	-2.49E-03
	3	1.10E-03	-2.07E-03	3.04E-03	-2.08E-03	4.86E-04
	4	1.56E-03	-2.51E-03	2.39E-03	8.91E-04	3.35E-03
	5	1.99E-03	-2.57E-03	8.03E-04	3.17E-03	1.41E-03
	6	2.37E-03	-2.24E-03	-1.11E-03	2.86E-03	-2.62E-03
	7	2.73E-03	-1.49E-03	-2.80E-03	-1.01E-04	-3.02E-03
	8	3.03E-03	-4.10E-04	-3.23E-03	-2.93E-03	1.29E-03
	9	3.44E-03	2.01E-03	-8.85E-04	-2.13E-03	3.02E-03
	Roof	3.94E-03	5.30E-03	3.42E-03	2.19E-03	-1.97E-03
Normalized Mode	0	0	0	0	0	0
Shape at Story	1	0.071	-0.114	0.351	-0.812	1.120
Levels, Φ_{im}	2	0.175	-0.267	0.744	-1.389	1.265
	3	0.280	-0.390	0.890	-0.946	-0.247
	4	0.397	-0.473	0.700	0.406	-1.703
	5	0.506	-0.484	0.235	1.447	-0.719
	6	0.601	-0.423	-0.324	1.305	1.329
	7	0.692	-0.282	-0.818	-0.046	1.536
	8	0.768	-0.077	-0.946	-1.336	-0.656
	9	0.874	0.380	-0.259	-0.971	-1.536
	Roof	1	1	1	1	1
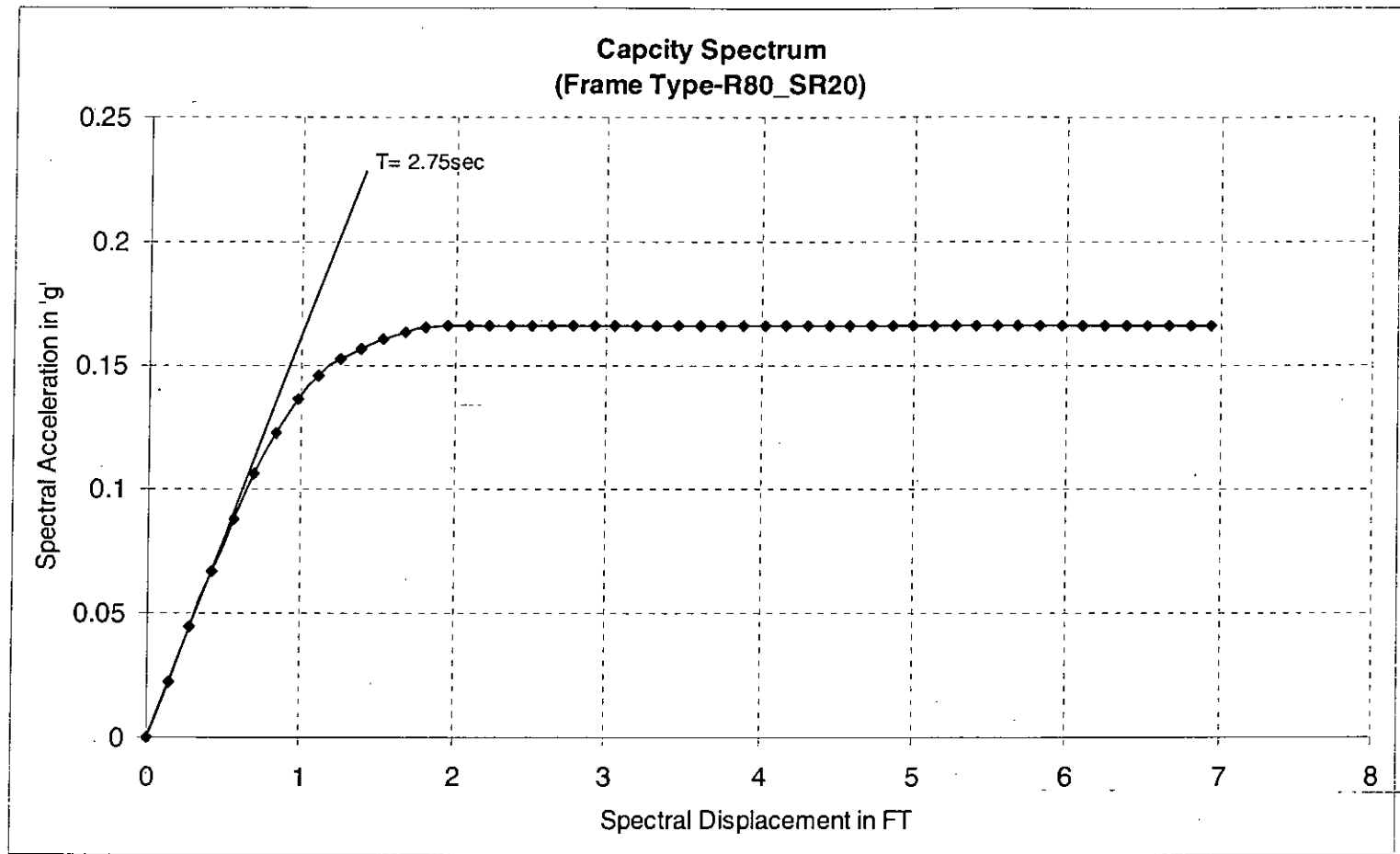
Figure 4.21 Capacity Spectrum of the Ten Story 2D Steel Frame for Frame Type 'R80_SR20'
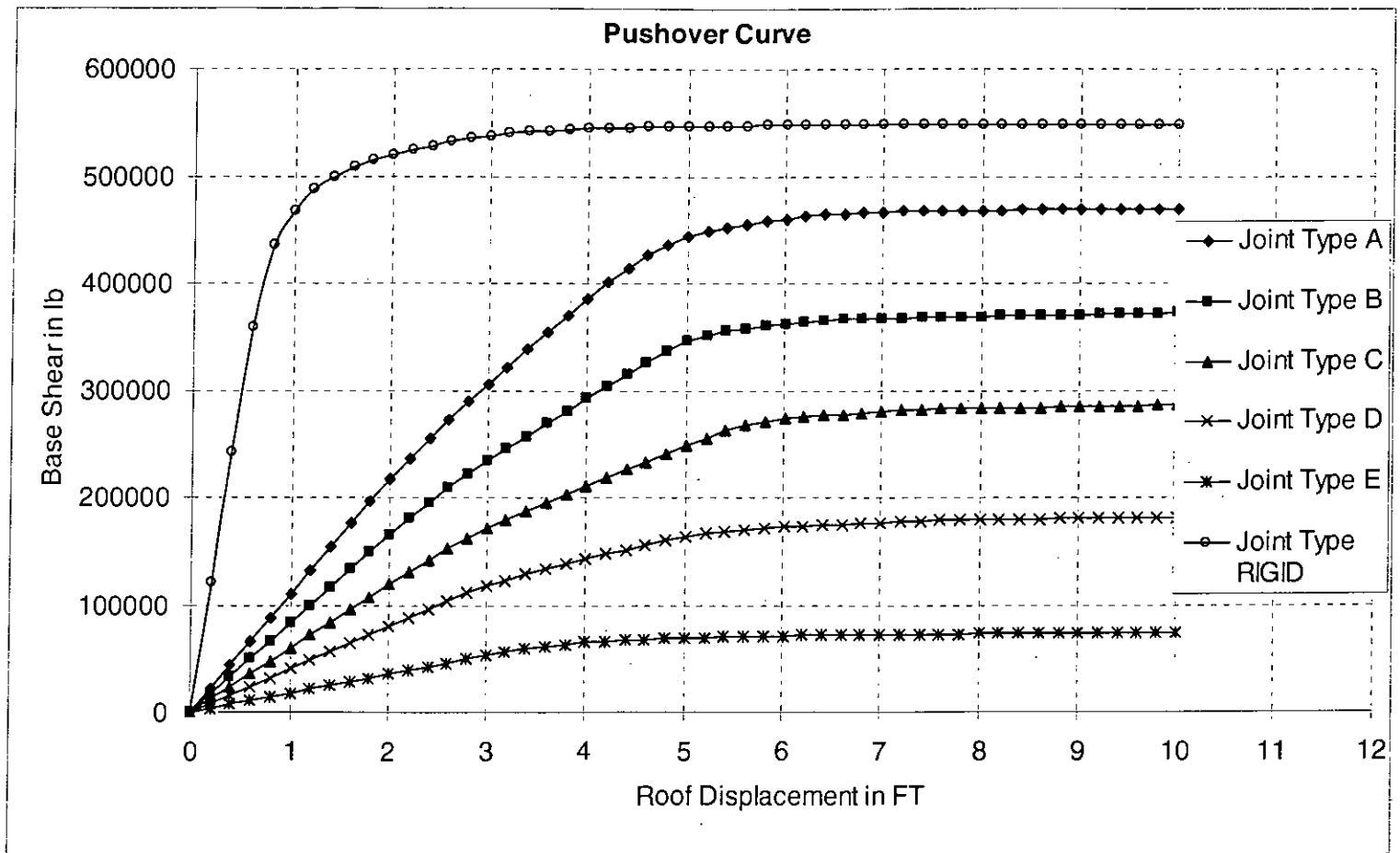
Figure 4.22 Pushover Curves of Six Story Steel Frame for Rigid and for Different Types of Nonlinear Semi-rigid Connection

Table 4-13 Modal Properties for the Six Story 2D Steel Moment Frame with Joint Type 'Rigid'

Mode		1	2	3	4	5
Period		1.905	0.597	0.322	0.222	0.174
Period Ratio, T/T_m		1	3.19	5.92	8.59	10.94
Participation Factor, PF_{Rm} at Roof		1.26	-0.34	0.30	-0.05	0.13
Effective Mass Coefficient, α_m		0.8217	0.0723	0.0541	0.0016	0.0091
Mode Shape at Story Levels, Φ_i	0	0.00E+00	0.00E+00	0.00E+00	0.00E+00	0.00E+00
	1	5.89E-04	1.97E-03	3.29E-03	-3.59E-03	-2.54E-04
	2	1.56E-03	3.83E-03	2.68E-03	6.91E-04	3.33E-04
	3	2.45E-03	3.49E-03	-1.85E-03	3.34E-03	3.68E-05
	4	3.23E-03	8.43E-04	-3.51E-03	-2.04E-03	-2.01E-04
	5	3.76E-03	-2.03E-03	-3.23E-04	-2.66E-03	3.10E-04
	Roof	3.96E-03	-3.54E-03	3.62E-03	3.56E-03	-3.83E-04
Normalized Mode Shape at Story Levels, Φ_{im}	0	0.000	0.000	0.000	0.000	0.000
	1	0.149	-0.557	0.907	-1.006	0.663
	2	0.393	-1.082	0.739	0.194	-0.870
	3	0.619	-0.986	-0.512	0.939	-0.096
	4	0.815	-0.238	-0.968	-0.571	0.525
	5	0.948	0.573	-0.089	-0.746	-0.809
	Roof	1	1	1	1	1

Capcity Spectrum
(Connection Type-Rigid)

Y-axis: Spectral Acceleration in 'g'
X-axis: Spectral Displacement in FT

T= 1.5sec

Figure 4.23 Capacity Spectrum of the Six Story 2D Steel Frame for Joint Type 'Rigid'

93

Table 4-14 Modal Properties for the Six Story 2D Steel Moment Frame with Joint Type 'A'

Mode		1	2	3	4	5
Period		4.115	1.100	0.502	0.288	0.286
Period Ratio, T/T_m		1	3.74	8.21	14.30	14.37
Participation Factor, PF_{Rm} at Roof		1.33	-0.42	0.37	-0.15	-0.08
Effective Mass Coefficient, α_m		0.7577	0.0789	0.0830	0.0352	0.0066
Mode Shape at	0	0.00E+00	0.00E+00	0.00E+00	0.00E+00	0.00E+00
Story Levels, Φ_i	1	3.71E-04	-1.36E-03	2.70E-03	-8.52E-05	-4.91E-04
	2	1.20E-03	-3.31E-03	3.68E-03	-4.87E-05	-4.47E-05
	3	2.17E-03	-3.72E-03	-4.06E-05	1.01E-04	4.87E-04
	4	3.08E-03	-1.98E-03	-3.41E-03	-1.62E-05	-8.45E-05
	5	3.84E-03	1.12E-03	-1.67E-03	-8.92E-05	-4.33E-04
	Roof	4.41E-03	4.35E-03	3.68E-03	5.68E-05	3.86E-04
Normalized Mode	0	0.000	0.000	0.000	0.000	0.000
Shape at Story	1	0.084	-0.312	0.734	-1.501	-1.273
Levels, Φ_{im}	2	0.272	-0.762	0.999	-0.859	-0.116
	3	0.492	-0.856	-0.011	1.784	1.263
	4	0.699	-0.456	-0.927	-0.286	-0.219
	5	0.869	0.259	-0.455	-1.572	-1.123
	Roof	1	1	1	1	1
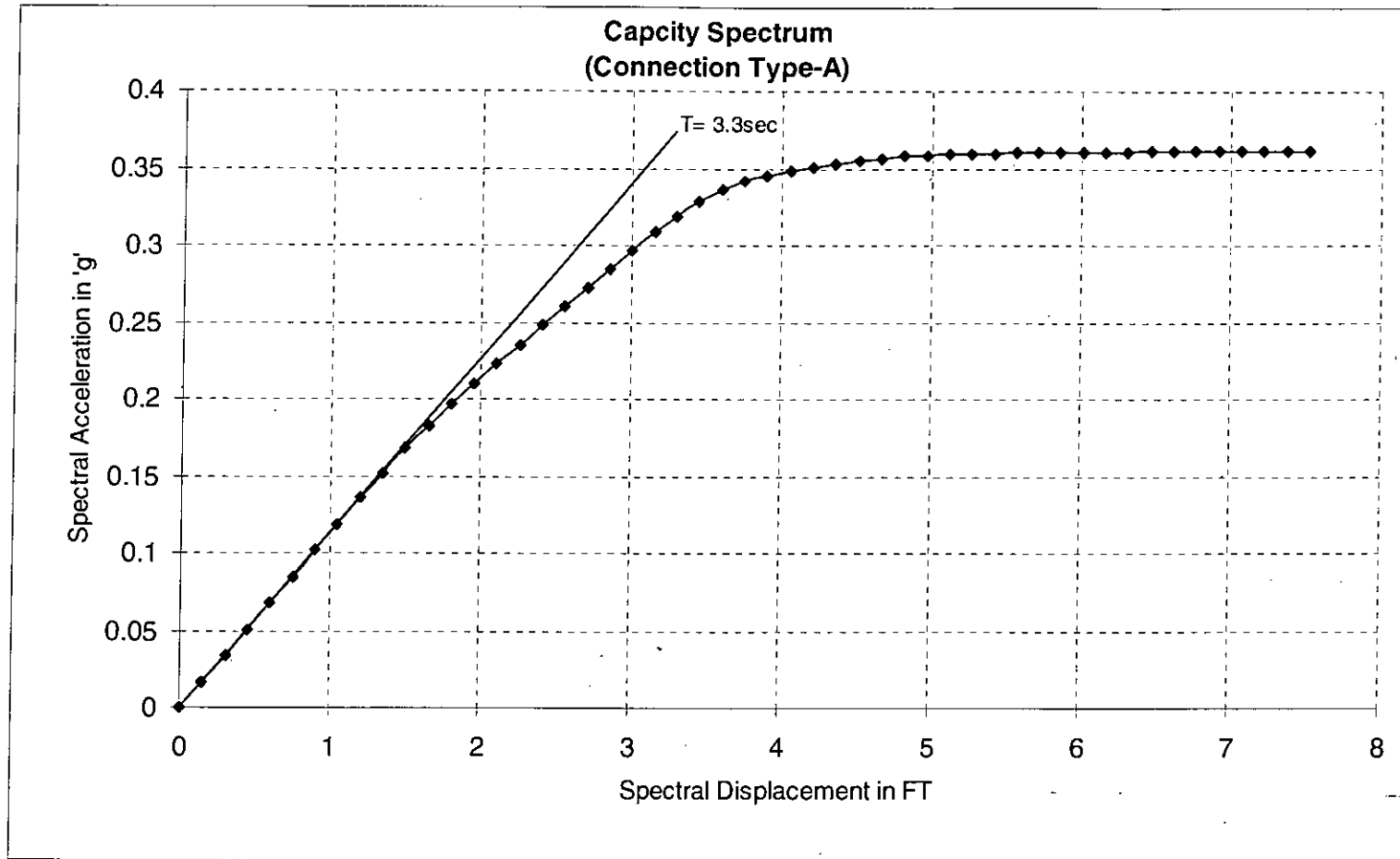
Figure 4.24 Capacity Spectrum of the Six Story 2D Steel Frame for Joint Type 'A'

95

Table 4-15 Modal Properties for the Six Story 2D Steel Moment Frame with Joint Type 'B'

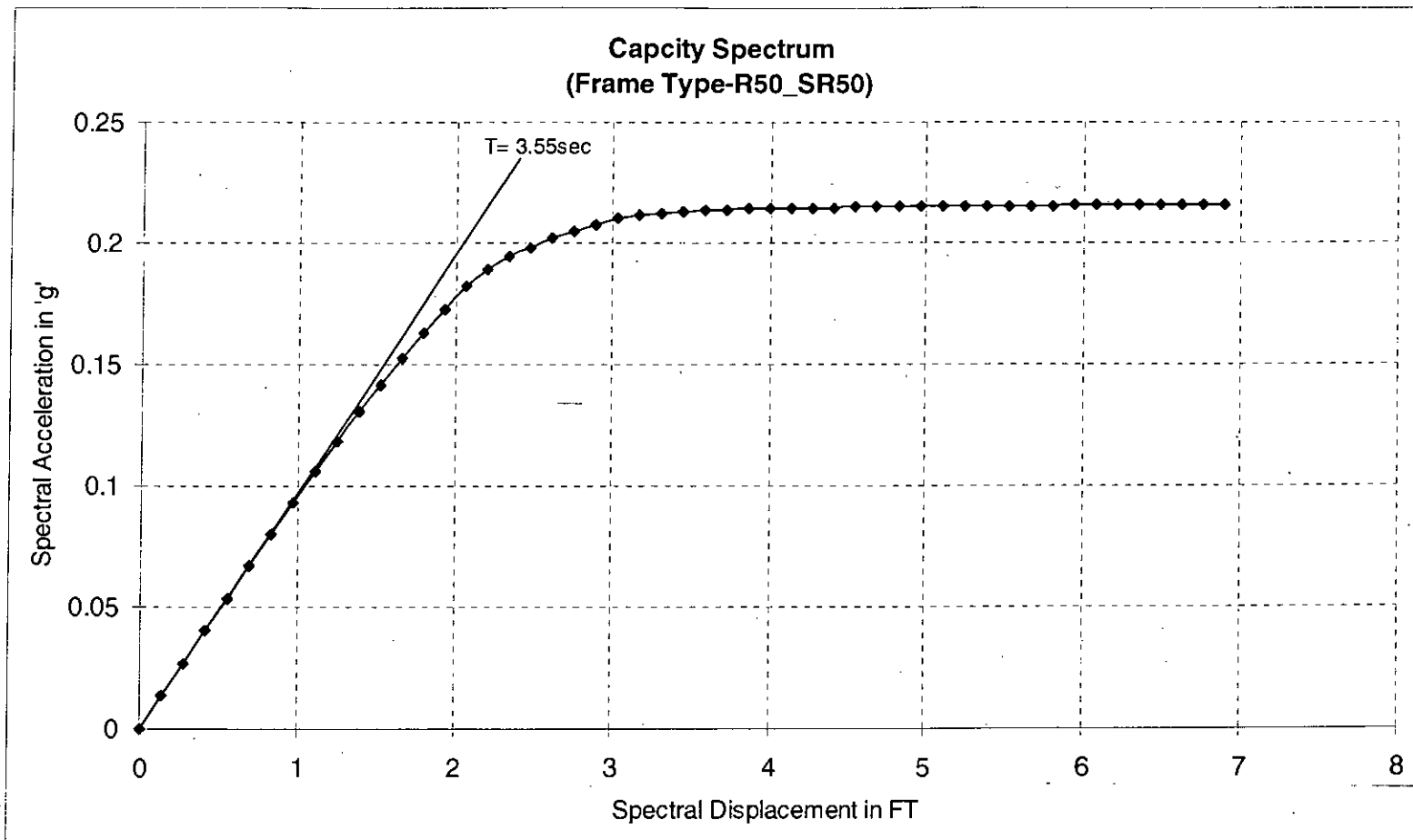| Mode		1	2	3	4	5
Period		4.647	1.193	0.522	0.301	0.298
Period Ratio, T/T_m		1	3.90	8.91	15.45	15.59
Participation Factor, PF_{Rm} at Roof		1.35	-0.44	0.37	-0.11	-0.03
Effective Mass Coefficient, α_m		0.7439	0.0847	0.0863	0.0585	0.0010
Mode Shape at Story Levels, Φ_i	0	0.00E+00	0.00E+00	0.00E+00	0.00E+00	0.00E+00
	1	3.42E-04	-1.30E-03	2.67E-03	-2.17E-05	-7.27E-05
	2	1.13E-03	-3.24E-03	3.75E-03	-1.93E-05	1.87E-05
	3	2.10E-03	-3.75E-03	1.18E-04	3.64E-05	6.17E-05
	4	3.04E-03	-2.13E-03	-3.35E-03	-7.03E-06	-1.71E-05
	5	3.85E-03	9.69E-04	-1.78E-03	-3.52E-05	-5.61E-05
	Roof	4.52E-03	4.37E-03	3.62E-03	1.14E-05	5.59E-05
Normalized Mode Shape at Story Levels, Φ_{im}	0	0.000	0.000	0.000	0.000	0.000
	1	0.076	-0.297	0.738	-1.907	-1.300
	2	0.251	-0.742	1.036	-1.701	0.333
	3	0.464	-0.858	0.032	3.204	1.103
	4	0.672	-0.488	-0.926	-0.618	-0.306
	5	0.852	0.222	-0.493	-3.099	-1.003
	Roof	1	1	1	1	1
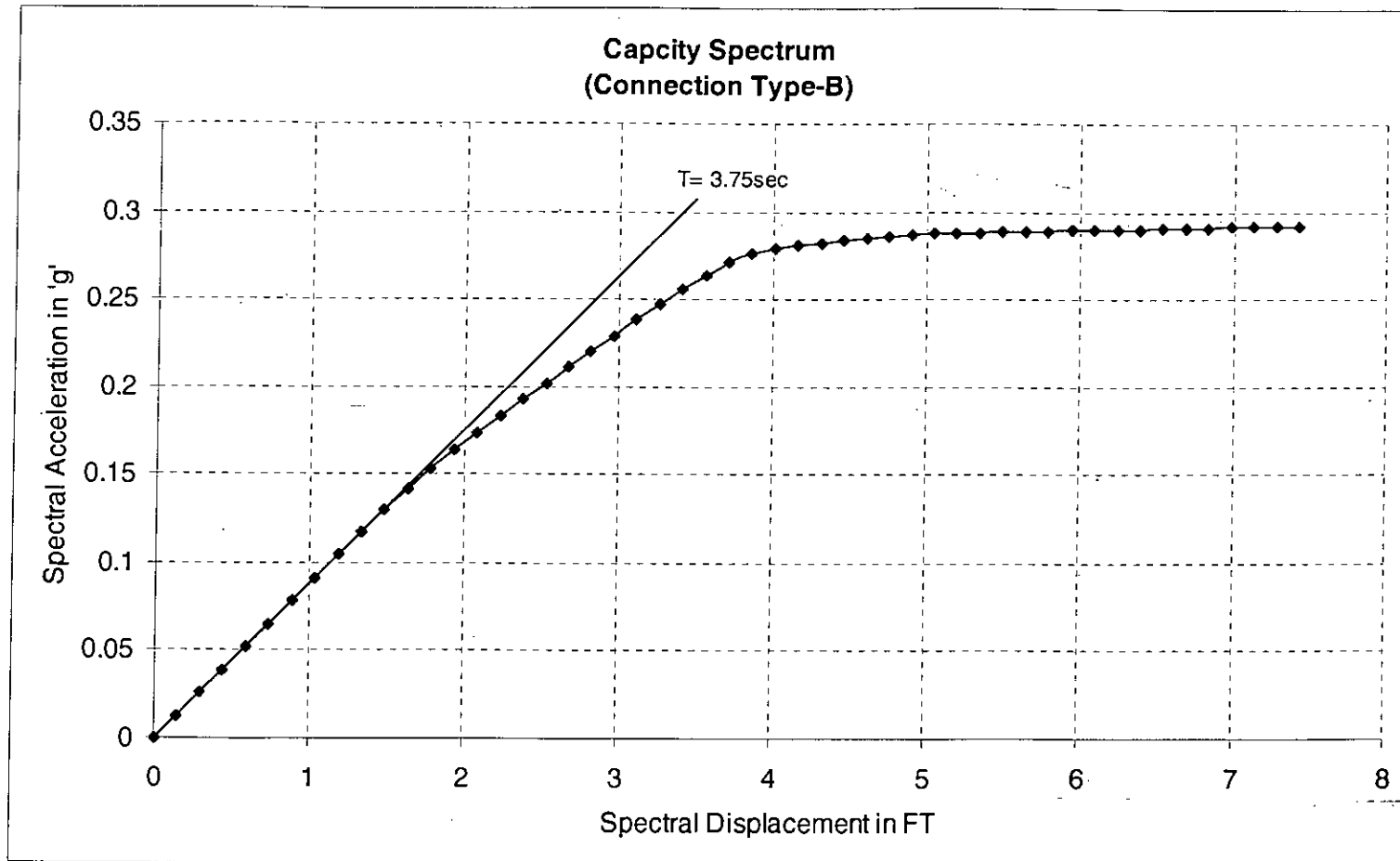
Figure 4.25 Capacity Spectrum of the Six Story 2D Steel Frame for Joint Type 'B'

Table 4-16 Modal Properties for the Six Story 2D Steel Moment Frame with Joint Type 'C'

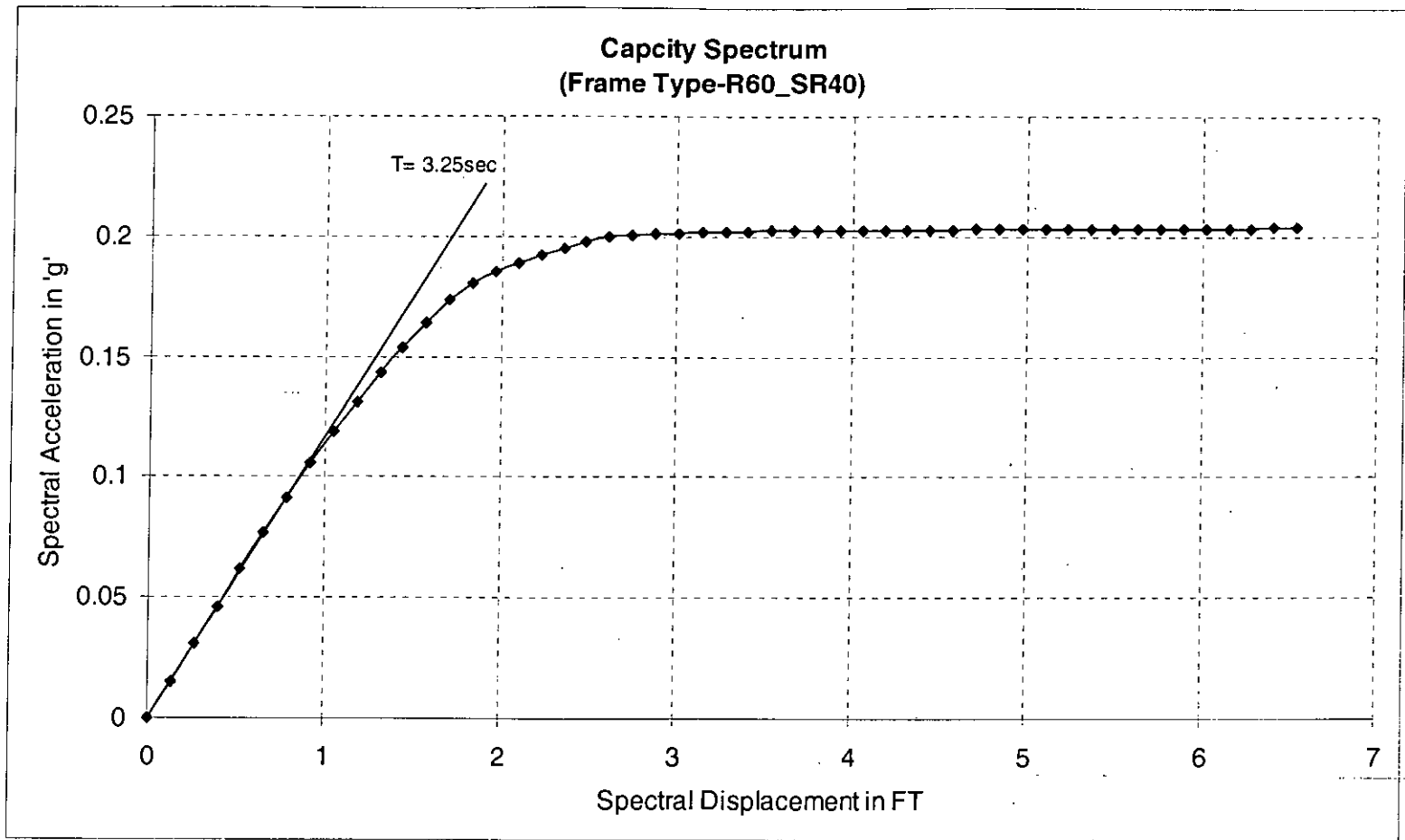| Mode		1	2	3	4	5
Period		5.370	1.296	0.541	0.314	0.310
Period Ratio, T/T_m		1	4.14	9.92	17.10	17.32
Participation Factor, PF_{Rm} at Roof		1.36	-0.46	0.37	-0.07	0.22
Effective Mass Coefficient, α_m		0.7272	0.0931	0.0896	0.0389	0.0523
Mode Shape at Story Levels, Φ_i	0	0.00E+00	0.00E+00	0.00E+00	0.00E+00	0.00E+00
	1	3.10E-04	-1.25E-03	2.65E-03	9.16E-06	-8.85E-06
	2	1.06E-03	-3.18E-03	3.82E-03	5.53E-06	1.91E-05
	3	2.00E-03	-3.78E-03	2.64E-04	-2.05E-05	-2.12E-06
	4	2.97E-03	-2.29E-03	-3.29E-03	4.79E-06	-6.83E-06
	5	3.86E-03	7.99E-04	-1.88E-03	2.15E-05	3.00E-06
	Roof	4.64E-03	4.37E-03	3.56E-03	-4.85E-06	9.33E-06
Normalized Mode Shape at Story Levels, Φ_{im}	0	0.000	0.000	0.000	0.000	0.000
	1	0.067	-0.286	0.745	-1.889	-0.948
	2	0.228	-0.729	1.073	-1.141	2.041
	3	0.432	-0.866	0.074	4.234	-0.227
	4	0.641	-0.523	-0.925	-0.988	-0.731
	5	0.832	0.183	-0.529	-4.439	0.322
	Roof	1	1	1	1	1

**Capcity Spectrum
(Connection Type-C)**
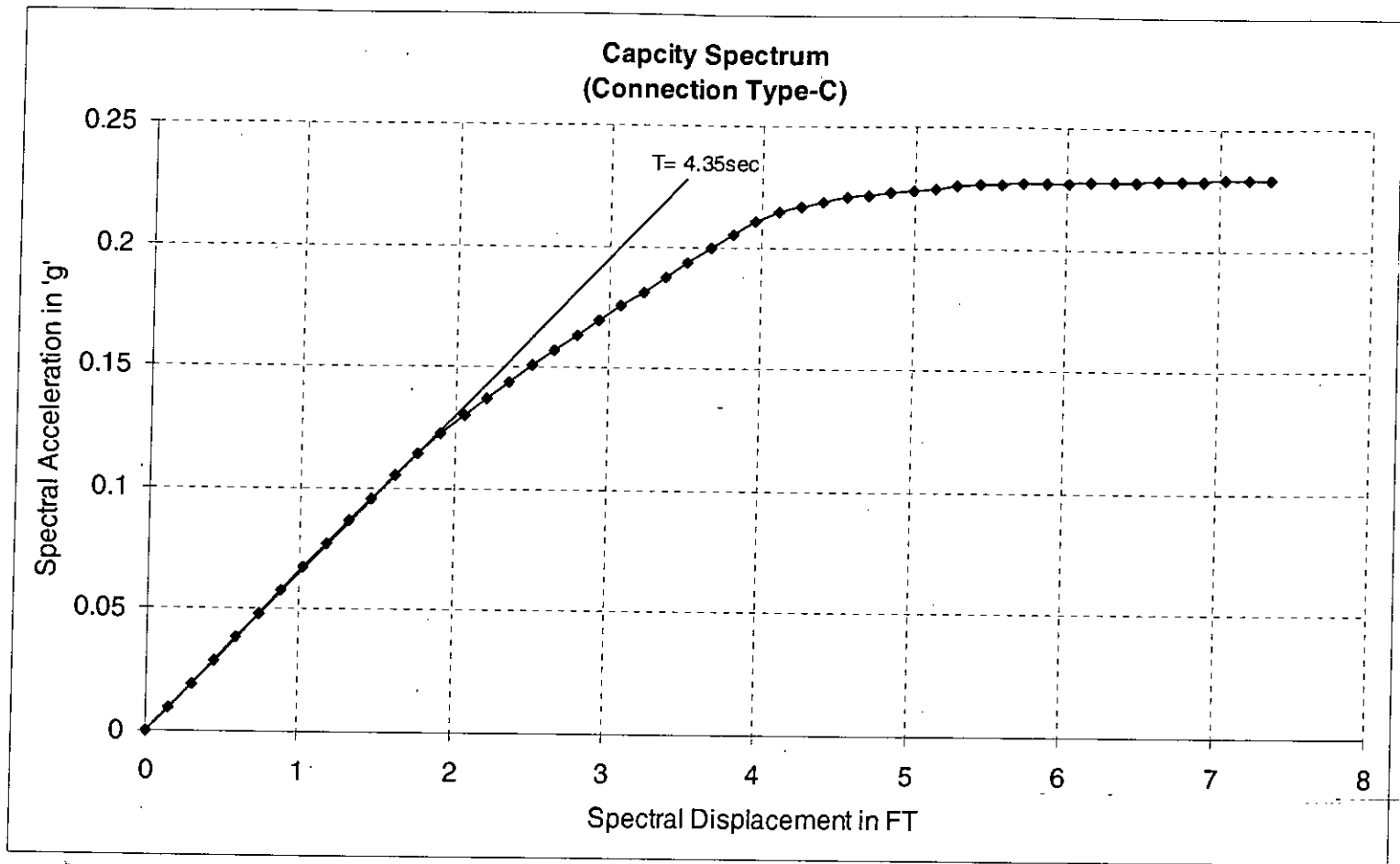
Figure 4.26 Capacity Spectrum of the Six Story 2D Steel Frame for Joint Type 'C'

Table 4-17 Modal Properties for the Six Story 2D Steel Moment Frame with Joint Type 'D'

Mode		1	2	3	4	5
Period		6.402	1.406	0.559	0.327	0.323
Period Ratio, T/T_m		1	4.55	11.46	19.61	19.85
Participation Factor, PF_{Rm} at Roof		1.38	-0.48	0.37	-0.06	0.02
Effective Mass Coefficient, α_m		0.7076	0.1043	0.0925	0.0260	0.0573
Mode Shape at Story Levels, Φ_i	0	0.00E+00	0.00E+00	0.00E+00	0.00E+00	0.00E+00
	1	2.76E-04	-1.20E-03	2.63E-03	3.97E-06	2.42E-06
	2	9.72E-04	-3.13E-03	3.88E-03	1.26E-06	8.90E-06
	3	1.90E-03	-3.82E-03	3.93E-04	-1.05E-05	-9.04E-06
	4	2.90E-03	-2.44E-03	-3.23E-03	2.69E-06	-2.76E-06
	5	3.87E-03	6.19E-04	-1.96E-03	1.15E-05	9.30E-06
	Roof	4.78E-03	4.33E-03	3.49E-03	-2.36E-06	6.63E-07
Normalized Mode Shape at Story Levels, Φ_{im}	0	0.000	0.000	0.000	0.000	0.000
	1	0.058	-0.278	0.753	-1.683	3.649
	2	0.203	-0.724	1.109	-0.533	13.424
	3	0.397	-0.883	0.113	4.446	-13.637
	4	0.606	-0.563	-0.926	-1.137	-4.156
	5	0.810	0.143	-0.562	-4.849	14.018
	Roof	1	1	1	1	1

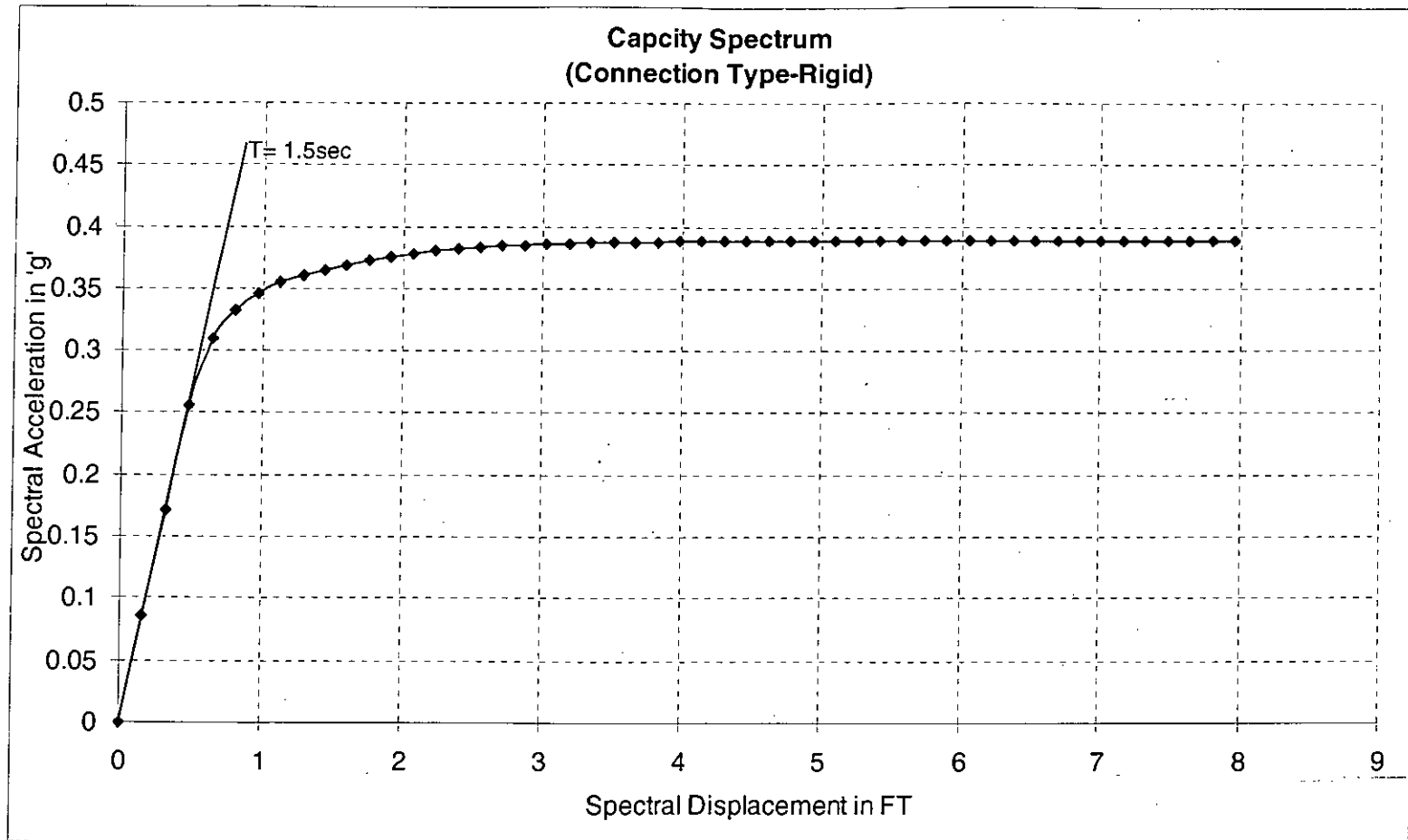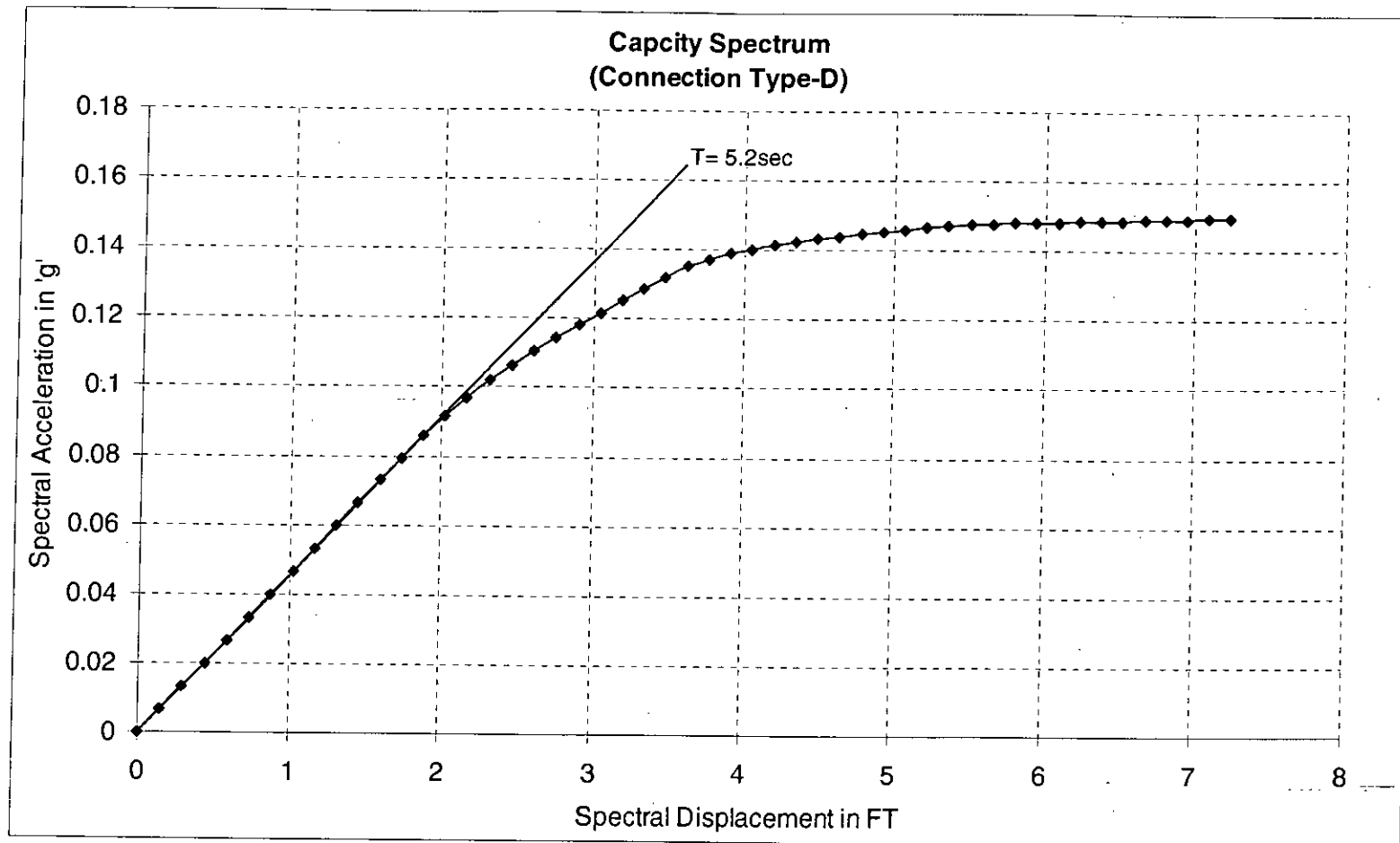**Figure 4.27 Capacity Spectrum of the Six Story 2D Steel Frame for Joint Type 'D'**

Table 4-18 Modal Properties for the Six Story 2D Steel Moment Frame with Joint Type 'E'

Mode		1	2	3	4	5
Period		9.287	1.573	0.580	0.342	0.338
Period Ratio, T/T_m		1	5.91	16.02	27.15	27.45
Participation Factor, PF_{Rm} at Roof		1.40	-0.51	0.37	-0.05	0.08
Effective Mass Coefficient, α_m		0.6748	0.1258	0.0961	0.0093	0.0678
Mode Shape at Story Levels, Φ_i	0	0.00E+00	0.00E+00	0.00E+00	0.00E+00	0.00E+00
	1	2.24E-04	-1.15E-03	2.61E-03	3.53E-07	-4.39E-07
	2	8.37E-04	-3.07E-03	3.94E-03	-9.50E-08	-1.08E-06
	3	1.72E-03	-3.88E-03	5.47E-04	-1.28E-06	1.15E-06
	4	2.77E-03	-2.65E-03	-3.16E-03	4.54E-07	4.42E-07
	5	3.88E-03	3.52E-04	-2.06E-03	1.48E-06	-1.15E-06
	Roof	5.01E-03	4.22E-03	3.41E-03	-4.13E-07	-2.47E-07
Normalized Mode Shape at Story Levels, Φ_{im}	0	0.000	0.000	0.000	0.000	0.000
	1	0.045	-0.273	0.765	-0.854	1.778
	2	0.167	-0.729	1.157	0.230	4.357
	3	0.344	-0.920	0.160	3.111	-4.673
	4	0.553	-0.630	-0.927	-1.099	-1.791
	5	0.775	0.084	-0.603	-3.584	4.659
	Roof	1	1	1	1	1
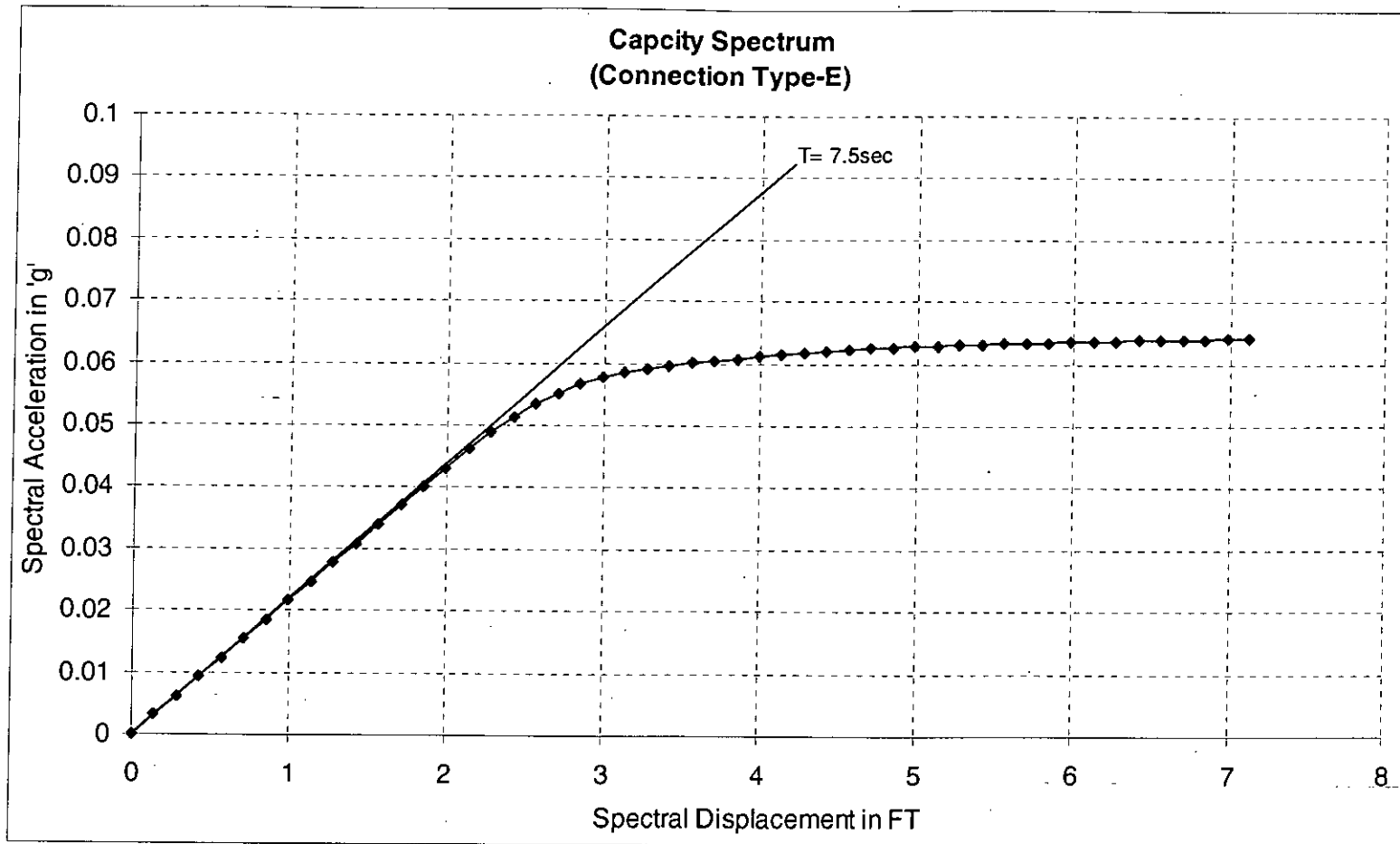
Figure 4.28 Capacity Spectrum of the Six Story 2D Steel Frame for Joint Type 'E'

CHAPTER 5

Seismic Performance of Structures

5.1 General

The structural design philosophy for most loading conditions, such as gravity loads due to everyday dead and live loads or expected wind loadings, is that the structural system, including the connections, resists the loads essentially elastically, with a safety factor to account for unexpected overloading within a certain range. The parallel philosophy for resisting earthquake-induced ground motions is in striking contrast to that for gravity or wind loading. This philosophy has evolved over the years since the inception of earthquake-resistant structural design early in the twentieth century, and is continuing to develop as engineers learn more about the performance of structures subjected to strong earthquakes. The present general philosophy for seismic design has been stated the followings:

Structures designed in conformance with these Requirements should, in general, be able to:

Resist a minor level of earthquake ground motion without damage.

Resist a moderate level of earthquake ground motion without structural damage, but possibly experience some non-structural damage.

Resist a major level of earthquake ground motion - of an intensity equal to the strongest earthquake, either experienced of forecast, for the building site – without collapse, but possibly with some structural as well as non-structural damage.

It is expected that structural damage, even in a major design level earthquake, will be limited to repairable level for most structures that meet these Requirements. In some instances, damage may not be economically repairable. The level of damage depends upon a number of factors, including the intensity and duration of ground shaking, structure configuration type of lateral force resisting system, materials used in the construction and construction workmanship.

5.2 Determination of Performance Using Capacity Spectrum Method

Two key elements of performance based design procedure are demand and capacity. Demand is a representation of the earthquake ground motion. Capacity is a representation of the structure's ability to resist the seismic demand. The performance is dependent on the manner that the capacity is able to handle the demand. In other words, the structure must have the capacity to resist the demands of the earthquake such that the performance of the structure is compatible with the objectives of the design.

The capacity spectrum method initially characterizes seismic demand using an elastic response spectrum. An elastic response spectrum, for each hazard level of interest at a site, is based on the site seismic coefficients. This spectrum is plotted in spectral ordinates (ADRS) format showing the spectral acceleration as a function of spectral displacement. This format allows the demand spectrum to be "overlaid" on the capacity spectrum for the building. The intersection of the demand and capacity spectra, if located in the linear range of the capacity, would define the accrual displacement for the structure; however this is not normally the case as most analyses include some inelastic nonlinear behaviour. To find the point where demand and capacity are equal, the engineer selects a point on the capacity spectrum as an initial estimate. Using the spectral acceleration and displacement defined by this point, the engineer then can calculate reduction factors to apply to the 5% elastic spectrum to account for the hysteretic energy dissipation, or effective damping, associated with the specific point. If the reduced demand spectrum intersects the capacity spectrum at or near the initial assumed point, then it is the solution for the unique point where capacity equals demand. If the intersection is not reasonably close to the initial point, then the engineer can assume a new point somewhere between and repeat the process initial a solution is reached. This is the performance point where the capacity of the structure matches the demand for the specific earthquake.

5.2.1 Demand Response Spectrum

Ground motion recordings indicate that ground shaking is an extremely complex waveform, containing oscillatory motion components over a broad range of

frequencies. By performing a time history analysis it is possible to determine the peak acceleration, velocity and displacement of the structure's response to a ground motion. If such analyses are performed for a series of single degree of freedom structures, each having a different period, T, and the peak response accelerations, velocities and displacements are plotted vs. the period of the structures, the resulting graphs are termed respectively acceleration, velocity and displacement response spectra.

Researcher commonly display response spectra on a 3-axis plot known as tri-partite plot (Figure 5.1) in which peak response acceleration, velocity and displacement are all plotted simultaneously against structural period. Researchers (Newmark and Hall, 1982) have found that response spectra for typical records can be enveloped by a plot with three distinct ranges: a constant peak spectral acceleration (PSA), constant peak spectral velocity (PSV) and constant peak spectral displacement (PSD).
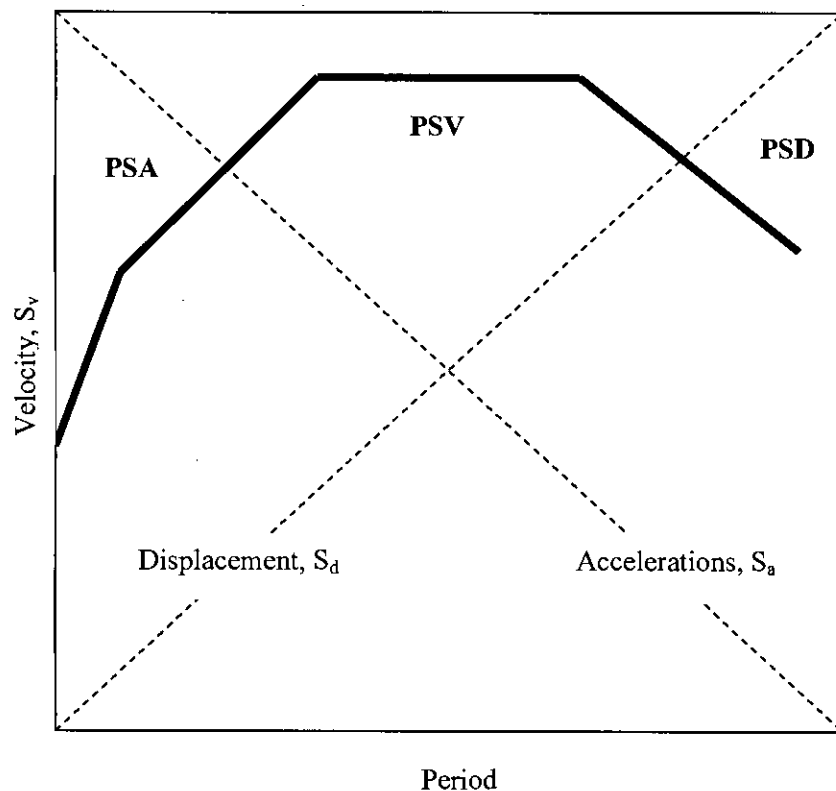
Figure 5.1 Tripartite Response Spectrum

Response spectra contained in the building code indicate the constant acceleration and velocity ranges plotted in an acceleration vs. period domain. This is convenient to the code design procedure which is based on forces (or strength) which are proportional to acceleration. In this study normalized response spectra for 5% damping ratio (Figure 5.2) is used from Bangladesh National Building Code (BNBC, 1993). In this figure notations represent as follows:

S_a = Spectral Acceleration.

g = Acceleration due to gravity.

Z = Seismic Zone Coefficient.

Soil Profile S1 = Soft to Medium Clay and Sand.

Soil Profile S2 = Deep Cohesion less or Stiff Clay Soils.

Soil Profile S3 = Rock and Stiff Soils.

For nonlinear analysis, both force and deformation are important. Therefore, spectra are plotted in an acceleration vs. displacement domain, which has been termed Acceleration-Displacement Response Spectra, ADRS (Mahaney et al., 1993). Every point on a response spectrum curve has associated with it a unique spectral acceleration, S_a, spectral velocity, S_v, spectral displacement, S_d and period T. To convert a spectrum from the standard S_a vs. T format found in the BNBC to ADRS format, it is necessary to determine the value of S_{di} for each point on the curve, S_{ai}, T_i. This can be done with the Equation 5.1:

$$S_{di} = \frac{T_i^2}{4 \times \pi^2} S_{ai} g$$

(Equation 5-1)

Demand response spectra contain a range of constant spectral acceleration and a second range of constant spectral velocity. Period in these ADRS are represented by a series of radial lines extending from the origin of the plot. Spectral acceleration and displacement at period T_i are given by:

$$S_{ai} g = \frac{2\pi}{T_i} S_v$$

(Equation 5-2)

$$S_{di} = \frac{T_i}{2\pi} S_v$$

(Equation 5-3)

Figure 5.3 represents the demand response spectrum in ADRS format for seismic zone-3 with zone coefficient Z = 0.25 for different soil profile.
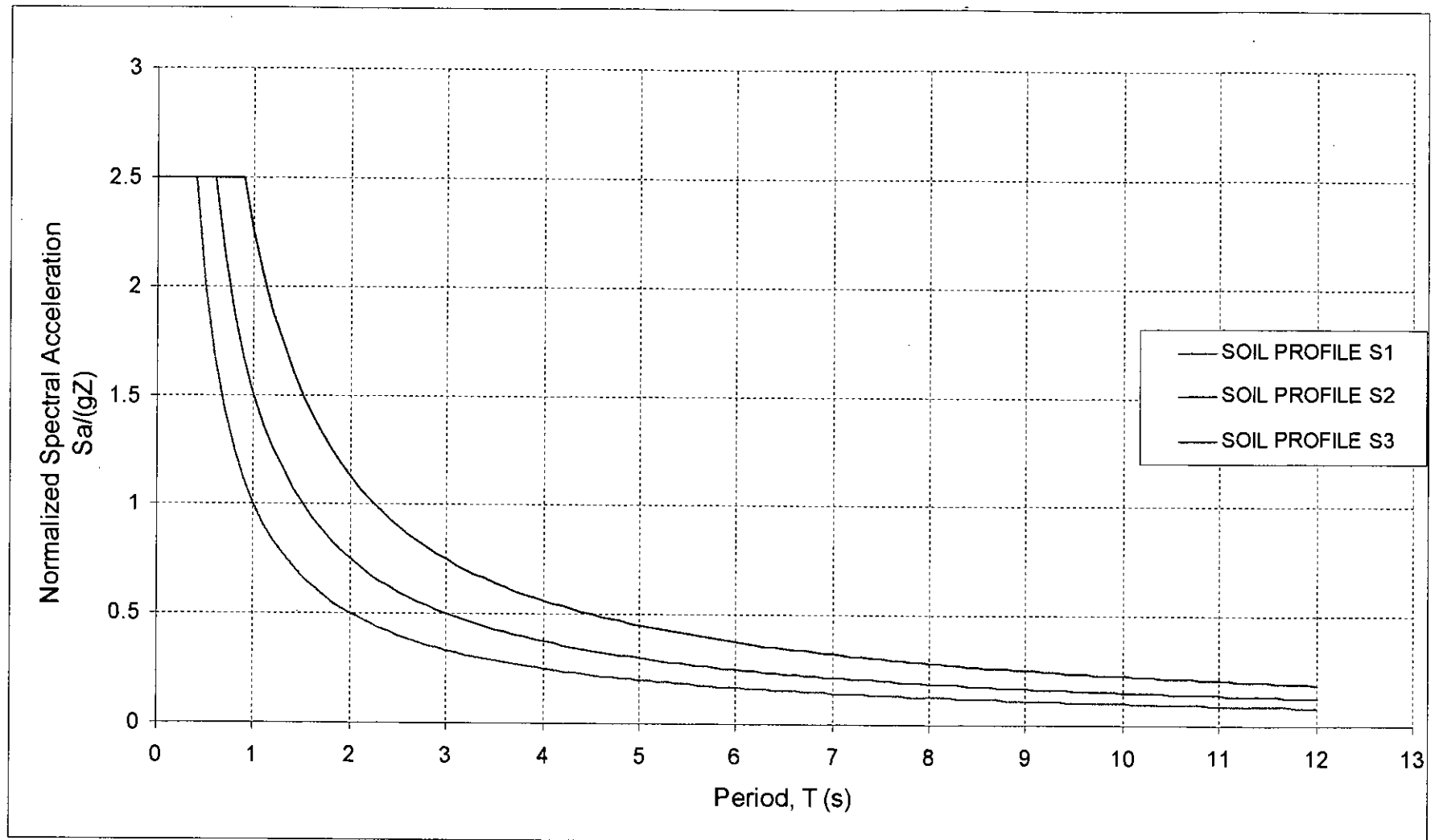
Figure 5.2 Normalized Response Spectra for 5% Damping Ratio (BNBC, 1993)
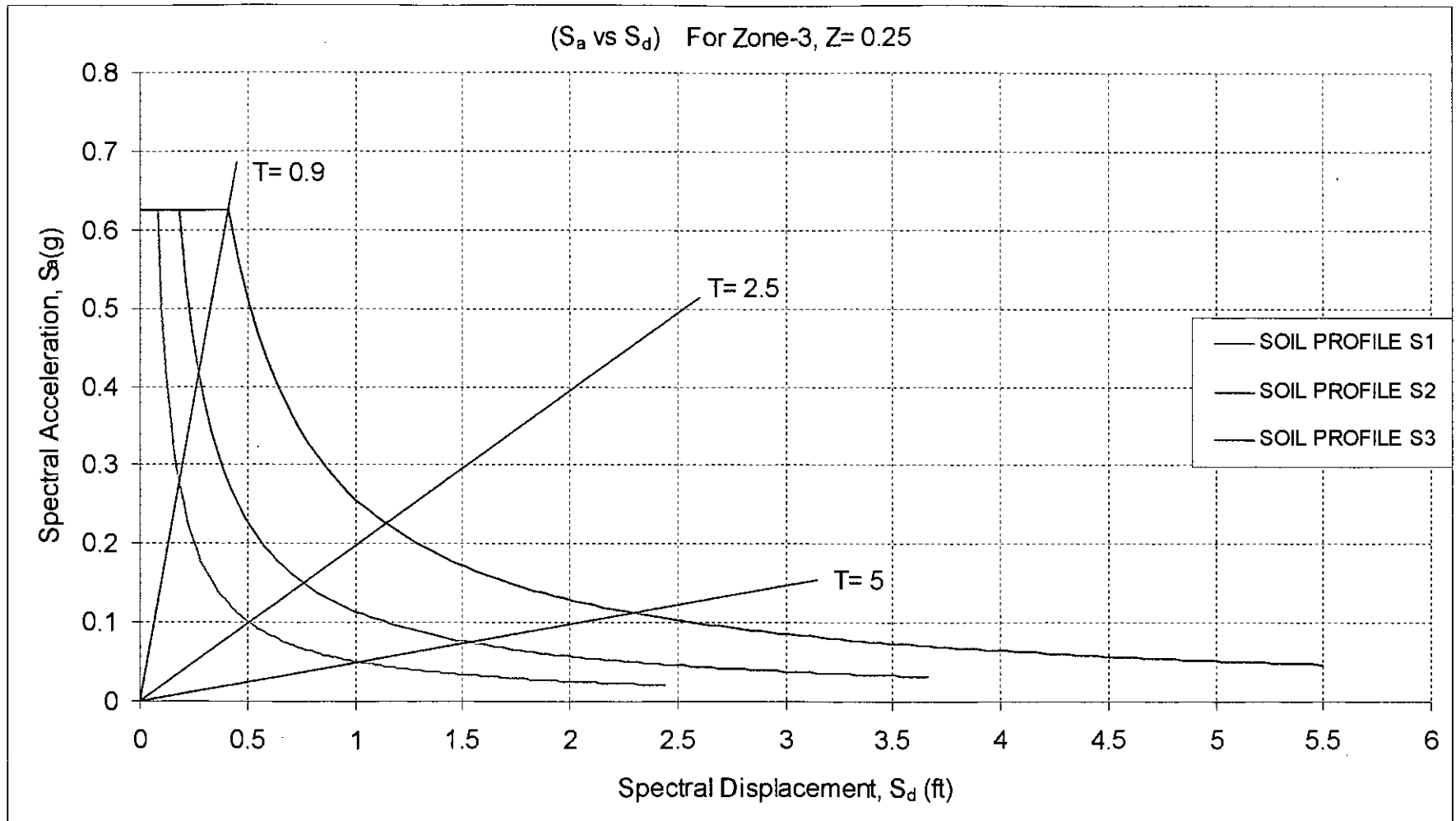
Figure 5.3 Elastic Response Spectrum in ADRS format for 5% Damping Ratio

According to ICBO, 1996 an elastic response spectrum, for each earthquake hazard level of interest at a site, is based on the seismic coefficients C_A and C_V. The seismic coefficient C_A represents the effective peak acceleration (EPA) of the ground. A factor of about 2.5 times C_A represents the average value of peak response of a 5 percent-damped short-period system in the acceleration domain. The seismic coefficient C_V represents 5 percent-damped response of a 1-second system and when divided by period defines acceleration response in the velocity domain. Figure 5.4 illustrates the construction of an elastic response spectrum.
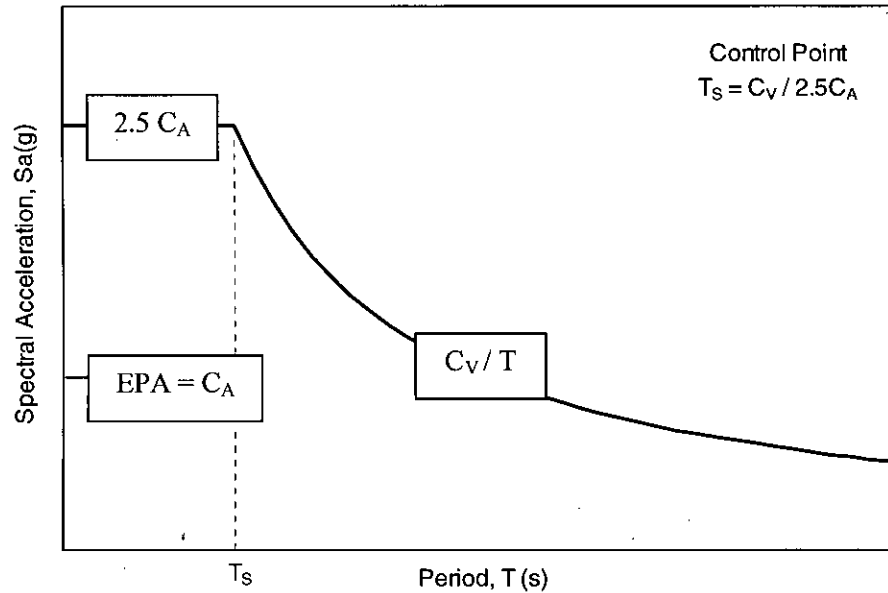
Figure 5.4 Construction of 5% Damped Elastic Response Spectrum

As the seismic coefficients C_A and C_V are not given in BNBC, 1993, these coefficients are calculated by back calculation. Table 5-1 represents the values.

Table 5-1 Seismic Coefficient, C_A and C_V for BNBC, 1993

Soil Profile Type	C_A			C_V		
	Seismic Zone			Seismic Zone		
	Z1	Z2	Z3	Z1	Z2	Z3
S1	0.075	0.150	0.250	0.075	0.150	0.250
S2	0.075	0.150	0.250	0.113	0.225	0.375
S3	0.075	0.150	0.250	0.169	0.338	0.563

5.2.2 Capacity Spectrum

Conversion of the capacity curve to the capacity spectrum is discussed in Section 4.6 of Chapter 4.

5.2.3 Calculating Demand

The location of the Performance Point must satisfy two relationships: 1) the point must lie on the capacity spectrum curve in order to represent the structure at a given displacement, and 2) the point must lie on a spectral demand curve, reduced from the elastic, 5 percent-damped design spectrum, that represents the nonlinear demand at the same structural displacement. Procedure-A of ATC-40 is used to determine the performance point. For this methodology, spectral reduction factors are given in terms of effective damping. An approximate effective damping is calculated based on the shape of the capacity curve, the estimated displacement demand, and the resulting hysteresis loop. In the general case, determination of the performance point requires a trial and error search for satisfaction of the two criterions specified above. Table 5-2 (Summary from Figure: - 5.5, 5.9, 5.13, 5.17, 5.21, 5.25, 5.27, 5.30, 5.32, 5.34, 5.36) represents Performance Point of ten storied 4-bay steel frame structure with different types of connection at seismic Zone-3 for Soil Profile Type S-3. A sample calculation of performance point using Procedure-A of ATC-40 is given in Appendix-E.

Table 5-2 Performance Point of Ten Story Steel Frame

Performance Point				
Beam-Column Connection Type	Spectral Acceleration Sa (g)	Spectral Displacement Sd (ft)	Base Shear V (kip)	Roof Displacement D (ft)
RIGID	0.152	0.865	346.67	1.12
A	0.093	2.76	203.11	3.60
B	0.08	3.2	172.18	4.21
C	0.067	3.81	141.30	5.10
D	0.054	4.78	110.44	6.55
E	-	-	-	-
R20_SR80	0.113	2.29	212.14	3.03
R40_SR60	0.13	1.735	216.72	2.40
R50_SR50	0.14	1.53	231.75	2.22
R60_SR40	0.147	1.352	258.05	2.07
R80_SR20	0.143	1.066	251.03	1.54

Table 5-3 (Summary from Figure: - 5.6, 5.10, 5.14, 5.18, 5.22, 5.26) represents Performance Point of six storied four-bay steel frame structure with different types of connection at seismic Zone-3 for Soil Profile Type S-3.

Table 5-3 Performance Point of Six Story Steel Frame

Performance Point				
Beam-Column Connection Type	Spectral Acceleration Sa (g)	Spectral Displacement Sd (ft)	Base Shear V (kip)	Roof Displacement D (ft)
RIGID	0.3	0.6	422.41	0.75
A	0.1696	1.525	220.22	2.03
B	0.1489	1.724	189.81	2.32
C	0.1279	2	159.38	2.73
D	0.1004	2.266	121.75	3.13
E	0.05712	2.922	66.05	4.10

Capacity spectrum of the ten storied steel frame for Joint Type 'Rigid' (Fig 4.11) and 5% damped Response Spectrum (Fig 5.3) at Seismic Zone-3 for Soil Profile Type- S3 are plotted on the same graph (Fig 5.5) to get the Performance Point ($S_a = 0.152g$, $S_d= 0.865ft$) of the structure using the Procedure-A of ATC-40. Performance Point calculation of this structure is given in Appendix-E. 16.0% damped response spectrum is the Demand Spectrum for this structure. Fig 5.7 represents the structural condition at performance point where base shear is V= 346.67 kip for roof displacement D= 1.12ft. Red point marked structural elements have reached beyond their elastic limit at performance point. To get the capacity curve (Fig 4.6) the structure was pushed from left to right at roof level. (As the structure is symmetrical, one can get the mirror image of columns and beams beyond their elastic limit at performance point when pushed from right to left.) Bottom end of the Column-17, 27, 37 started to yield first when the roof displacement of the structure was D= 0.8ft. No beams of this structure have reached in plastic condition. Most of the columns of the ten storied steel frame structure are fully plastic at its performance point.

Capacity spectrum of the six storied steel frame for Joint Type 'Rigid' (Fig 4.23) and 5% damped Response Spectrum (Fig 5.3) at Seismic Zone-3 for Soil Profile Type- S3 are plotted on the same graph (Fig 5.6) to get the Performance Point ($S_a = 0.3g$, $S_d=$

0.6ft) of the structure using the Procedure-A of ATC-40. 10.0% damped response spectrum is the Demand Spectrum for this structure. Fig 5.8 represents the structural condition at performance point where base shear is V= 422.41 kip for roof displacement D= 0.75ft. Red point marked structural elements have reached beyond their elastic limit at performance point. Some beams of this structure have reached in plastic condition. Like ten storied frame most of the members of six storied steel frame structure are fully plastic at its performance point.

Capacity spectrum of the ten storied steel frame for Joint Type 'A' (Fig 4.12) and 5% damped Response Spectrum (Fig 5.3) at Seismic Zone-3 for Soil Profile Type- S3 are plotted on the same graph (Fig 5.9) to get the Performance Point (S_a = 0.093g, S_d= 2.76ft) of the structure using the Procedure-A of ATC-40. 5% damped response spectrum itself is the Demand Spectrum for this structure. Fig 5.11 represents the structural condition at performance point where base shear is V= 203.11 kip for roof displacement D= 3.6ft. Red point marked structural elements have reached beyond their elastic limit at performance point. Bottom end of columns at 1st floor level have just been yield at its performance point. No beams of this structure have reached in plastic condition.

Capacity spectrum of the six storied steel frame for Joint Type 'A' (Fig 4.24) and 5% damped Response Spectrum (Fig 5.3) at Seismic Zone-3 for Soil Profile Type- S3 are plotted on the same graph (Fig 5.10) to get the Performance Point (S_a = 0.1696g, S_d= 1.525ft) of the structure using the Procedure-A of ATC-40. 5% damped response spectrum itself is the Demand Spectrum for this structure. Fig 5.12 represents the structural condition at performance point where base shear is V= 220.22 kip for roof displacement D= 2.03ft. Only five columns of the six storied steel frame have just been yield at its performance point. No beams of this structure have reached in plastic condition.

Both ten storied and six storied steel frame structures with connection type 'B' and 'C' give the similar structural condition like connection type 'A' at their performance point. But each connection type 'B' or 'C' shear capacity is lower and roof displacement is higher than the connection type 'A'. For connection type 'D' structural condition of six storied frame (Fig 5.24) is better than structural condition of ten storied frame (Fig 5.23).

Capacity spectrum of the ten storied steel for Joint Type 'E' (Fig 4.16) and 5% damped Response Spectrum (Fig 5.3) at Seismic Zone-3 for Soil Profile Type- S3 are plotted on the same graph (Fig 5.25) to get the Performance Point of the structure using the Procedure-A of ATC-40. As they do not intersect each other, there is no performance point. That means structure with connection type 'E' will fail to withstand at Seismic Zone-3 for Soil Profile Type- S3.

Capacity spectrum of the six storied steel for Joint Type 'E' (Fig 4.28) and 5% damped Response Spectrum (Fig 5.3) at Seismic Zone-3 for Soil Profile Type- S3 are plotted on the same graph (Fig 5.26) to get the Performance Point (S_a = 0.05712g, S_d= 2.922ft) of the structure using the Procedure-A of ATC-40. 11.0% damped response spectrum is the Demand Spectrum for this structure. Fig 5.28 represents the structural condition at performance point where base shear is V= 66.05 kip for roof displacement D= 4.10ft. Bottom end of columns at 1st floor level and 2nd floor level have just been yield at its performance point. No beams of this structure have reached in plastic condition.

Capacity spectrum for Frame Type 'R20_SR80' (Fig 4.17) and 5% damped Response Spectrum (Fig 5.3) at Seismic Zone-3 for Soil Profile Type- S3 are plotted on the same graph (Fig 5.27) to get the Performance Point (S_a = 0.113g, S_d= 2.29ft) of the structure using the Procedure-A of ATC-40. 5% damped response spectrum itself is the Demand Spectrum for this structure. Fig 5.29 represents the structural condition at performance point where base shear is V= 212.14 kip for roof displacement D= 3.03ft. Bottom end of the Column-14, 24, 34 started to yield first when the roof displacement of the structure was D= 2.4ft. No beams of this structure have reached in plastic condition.

Capacity spectrum for Frame Type 'R40_SR60' (Fig 4.18) and 5% damped Response Spectrum (Fig 5.3) at Seismic Zone-3 for Soil Profile Type- S3 are plotted on the same graph (Fig 5.30) to get the Performance Point (S_a = 0.13g, S_d= 1.735ft) of the structure using the Procedure-A of ATC-40. 6.5% damped response spectrum is the Demand Spectrum for this structure. Fig 5.31 represents the structural condition at performance point where base shear is V= 216.72 kip for roof displacement D= 2.4ft. Bottom end of the Column-15, 25, 35 started to yield first when the roof displacement

of the structure was D= 1.6ft. No beams of this structure have reached in plastic condition.

Capacity spectrum for Frame Type 'R50_SR50' (Fig 4.19) and 5% damped Response Spectrum (Fig 5.3) at Seismic Zone-3 for Soil Profile Type- S3 are plotted on the same graph (Fig 5.32) to get the Performance Point (S_a = 0.14g, S_d= 1.53ft) of the structure using the Procedure-A of ATC-40. 7.1% damped response spectrum is the Demand Spectrum for this structure. Fig 5.33 represents the structural condition at performance point where base shear is V= 231.75 kip for roof displacement D= 2.22ft. Bottom end of the Column-16, 26, 36 started to yield first when the roof displacement of the structure was D= 1.4ft. No beams of this structure have reached in plastic condition.

Capacity spectrum for Frame Type 'R60_SR40' (Fig 4.20) and 5% damped Response Spectrum (Fig 5.3) at Seismic Zone-3 for Soil Profile Type- S3 are plotted on the same graph (Fig 5.34) to get the Performance Point (S_a = 0.147g, S_d= 1.352ft) of the structure using the Procedure-A of ATC-40. 8.13% damped response spectrum is the Demand Spectrum for this structure. Fig 5.35 represents the structural condition at performance point where base shear is V= 258.05 kip for roof displacement D= 2.07ft. Bottom end of the Column-17, 27, 37, 47 started to yield first when the roof displacement of the structure was D= 1.2ft. No beams of this structure have reached in plastic condition.

Capacity spectrum for Frame Type 'R80_SR20' (Fig 4.21) and 5% damped Response Spectrum (Fig 5.3) at Seismic Zone-3 for Soil Profile Type- S3 are plotted on the same graph (Fig 5.36) to get the Performance Point (S_a = 0.143g, S_d= 1.066ft) of the structure using the Procedure-A of ATC-40. 8.13% damped response spectrum is the Demand Spectrum for this structure. Fig 5.37 represents the structural condition at performance point where base shear is V= 251.03 kip for roof displacement D= 1.54ft. Bottom end of the Column-19, 29, 39 started to yield first when the roof displacement of the structure was D= 0.8ft. No beams of this structure have reached in plastic condition. Most of the columns of this structure are fully plastic at its performance point.

Figure 5.5 Performance Point of Ten Story Frame for Connection Type 'Rigid'
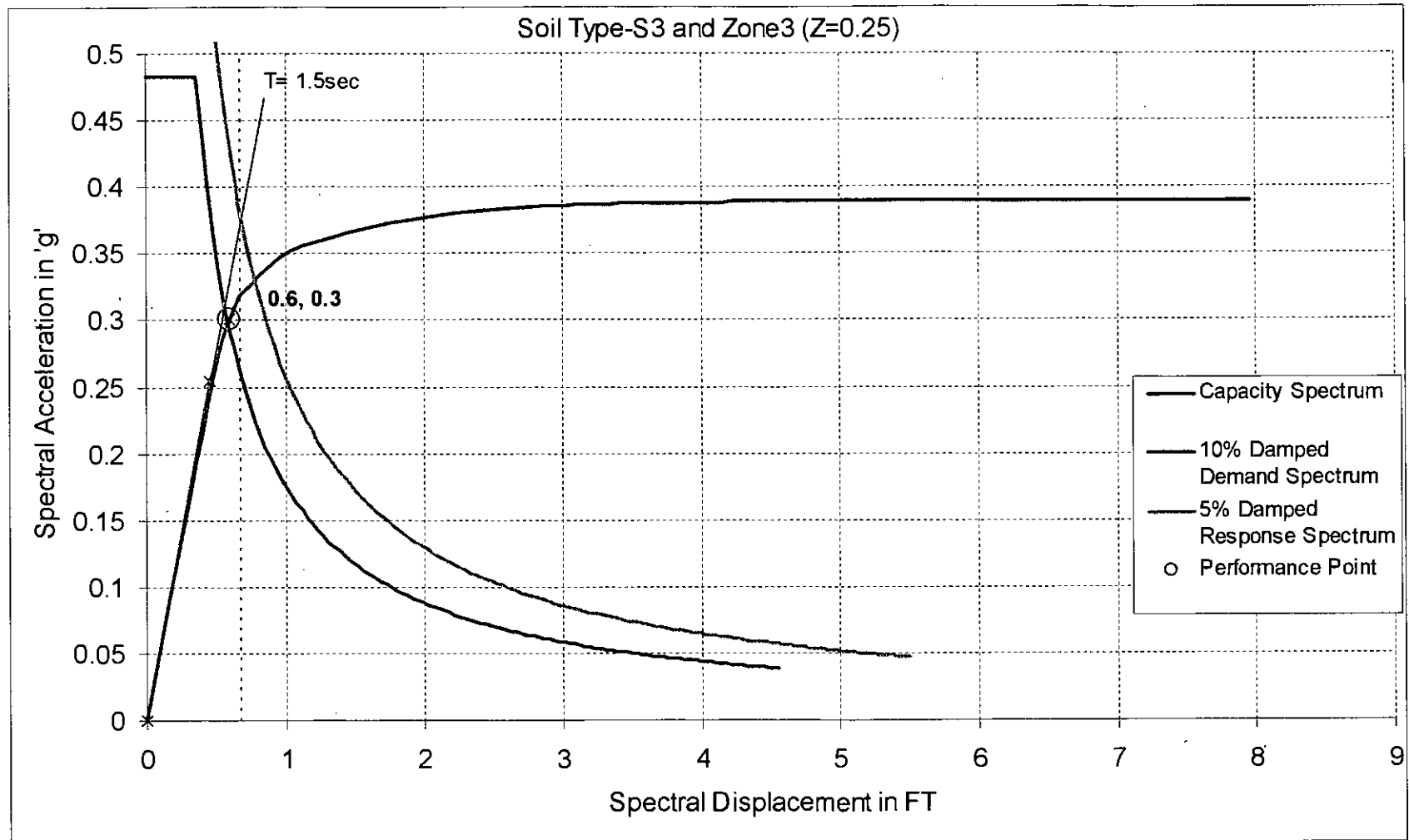
Figure 5.6 Performance Point of Six Story Frame for Connection Type 'Rigid'

117

Figure 5.7 Structural Condition of Ten Story Frame at Performance Point for
Connection Type 'Rigid'

Figure 5.8 Structural Condition of Six Story Frame at Performance Point for
Connection Type 'Rigid'

118

Figure 5.9 Performance Point of Ten Story Frame for Connection Type 'A'

Figure 5.10 Performance Point of Six Story Frame for Connection Type 'A'

ROOF

	87		88		89		90	
10		20		30		40		50

9 TH
FLOOR

	83		84		85		86	
9		19		29		39		49

8 TH
FLOOR

	79		80		81		82	
8		18		28		38		48

7 TH
FLOOR

	75		76		77		78	
7		17		27		37		47

6 TH
FLOOR

	71		72		73		74	
6		16		26		36		46

5 TH
FLOOR

	67		68		69		70	
5		15		25		35		45

4 TH
FLOOR

	63		64		65		66	
4		14		24		34		44

3 RD
FLOOR

	59		60		61		62	
3		13		23		33		43

2 ND
FLOOR

	55		56		57		58	
2		12		22		32		42

1 ST
FLOOR

	51		52		53		54	
1		11		21		31		41

Figure 5.11 Structural Condition of Ten Story Frame at Performance Point for Connection Type 'A'

ROOF

	51		52		53		54	
6		12		18		24		30

5 TH
FLOOR

	47		48		49		50	
5		11		17		23		29

4 TH
FLOOR

	43		44		45		46	
4		10		16		22		28

3 RD
FLOOR

	39		40		41		42	
3		9		15		21		27

2 ND
FLOOR

	35		36		37		38	
2		8		14		20		26

1 ST
FLOOR

	31		32		33		34	
1		7		13		19		25

Figure 5.12 Structural Condition of Six Story Frame at Performance Point for Connection Type 'A'

121
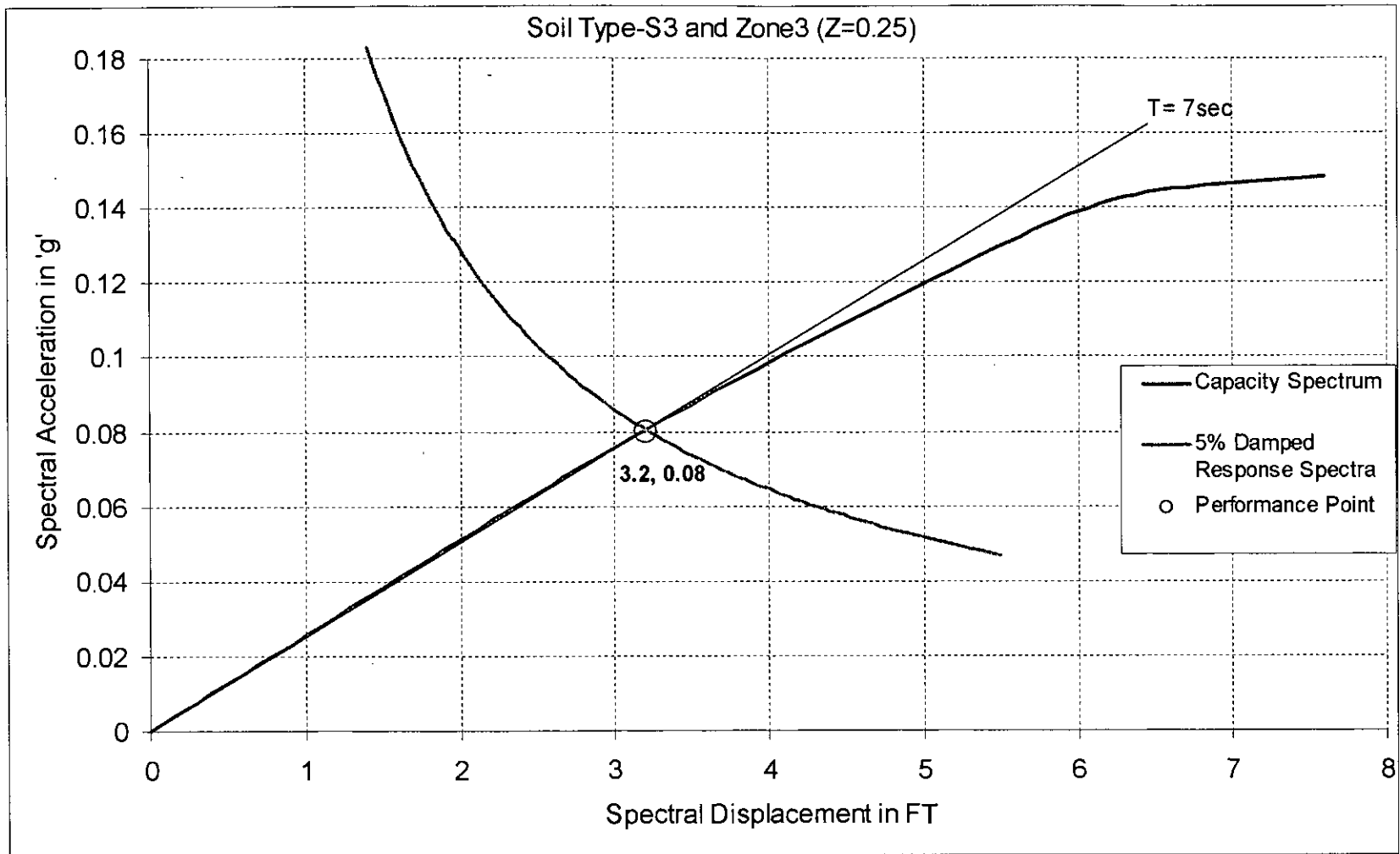
Figure 5.13 Performance Point of Ten Story Frame for Connection Type 'B'
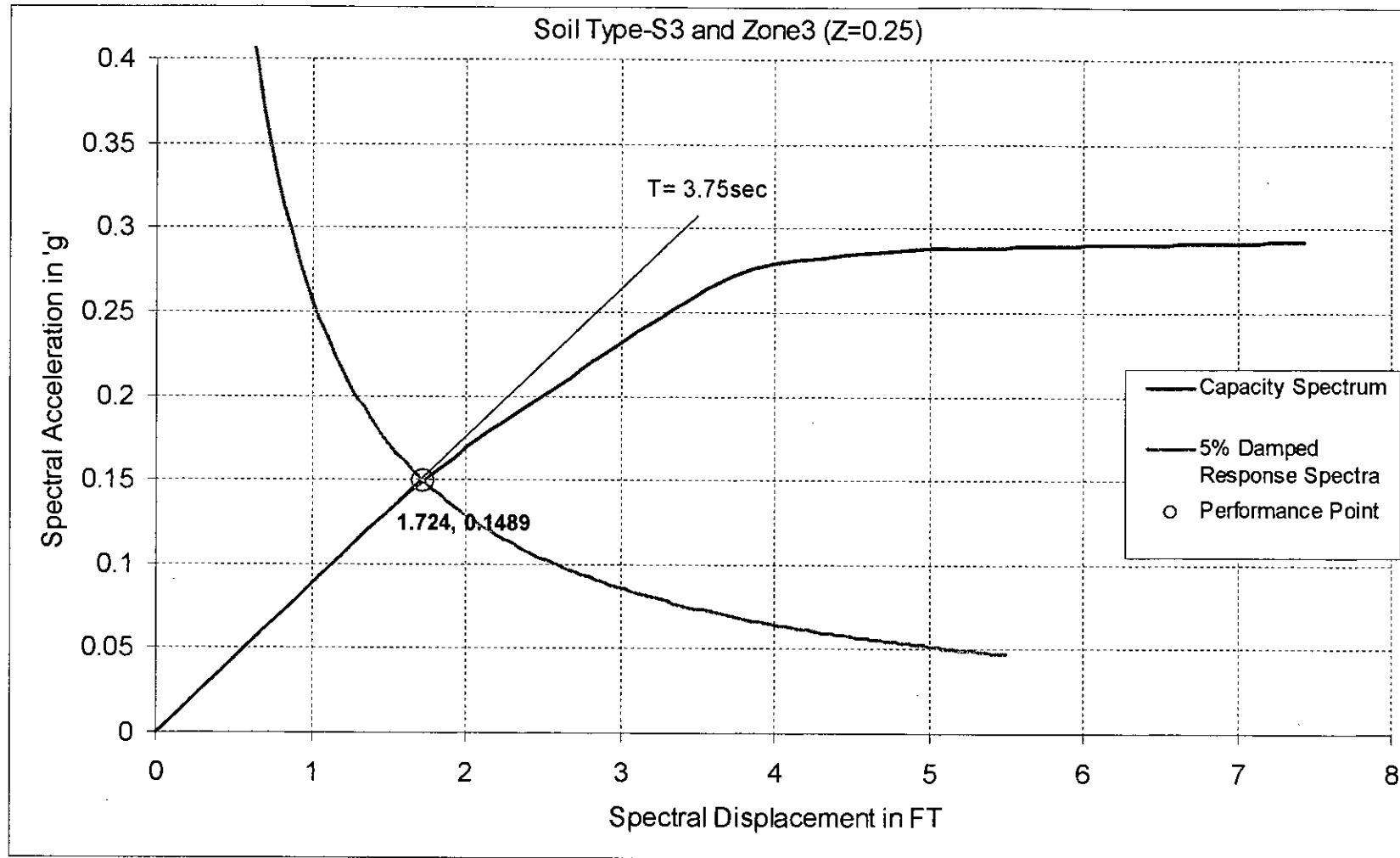
Figure 5.14 Performance Point of Six Story Frame for Connection Type 'B'

ROOF

Story	Beam	Beam	Beam	Beam	Columns (L→R)
ROOF	87	88	89	90	10, 20, 30, 40, 50
9 TH FLOOR	83	84	85	86	9, 19, 29, 39, 49
8 TH FLOOR	79	80	81	82	8, 18, 28, 38, 48
7 TH FLOOR	75	76	77	78	7, 17, 27, 37, 47
6 TH FLOOR	71	72	73	74	6, 16, 26, 36, 46
5 TH FLOOR	67	68	69	70	5, 15, 25, 35, 45
4 TH FLOOR	63	64	65	66	4, 14, 24, 34, 44
3 RD FLOOR	59	60	61	62	3, 13, 23, 33, 43
2 ND FLOOR	55	56	57	58	2, 12, 22, 32, 42
1 ST FLOOR	51	52	53	54	1, 11, 21, 31, 41

Figure 5.15 Structural Condition of Ten Story Frame at Performance Point for Connection Type 'B'

ROOF

Story	Beam	Beam	Beam	Beam	Columns (L→R)
ROOF	51	52	53	54	6, 12, 18, 24, 30
5 TH FLOOR	47	48	49	50	5, 11, 17, 23, 29
4 TH FLOOR	43	44	45	46	4, 10, 16, 22, 28
3 RD FLOOR	39	40	41	42	3, 9, 15, 21, 27
2 ND FLOOR	35	36	37	38	2, 8, 14, 20, 26
1 ST FLOOR	31	32	33	34	1, 7, 13, 19, 25

Figure 5.16 Structural Condition of Six Story Frame at Performance Point for Connection Type 'B'
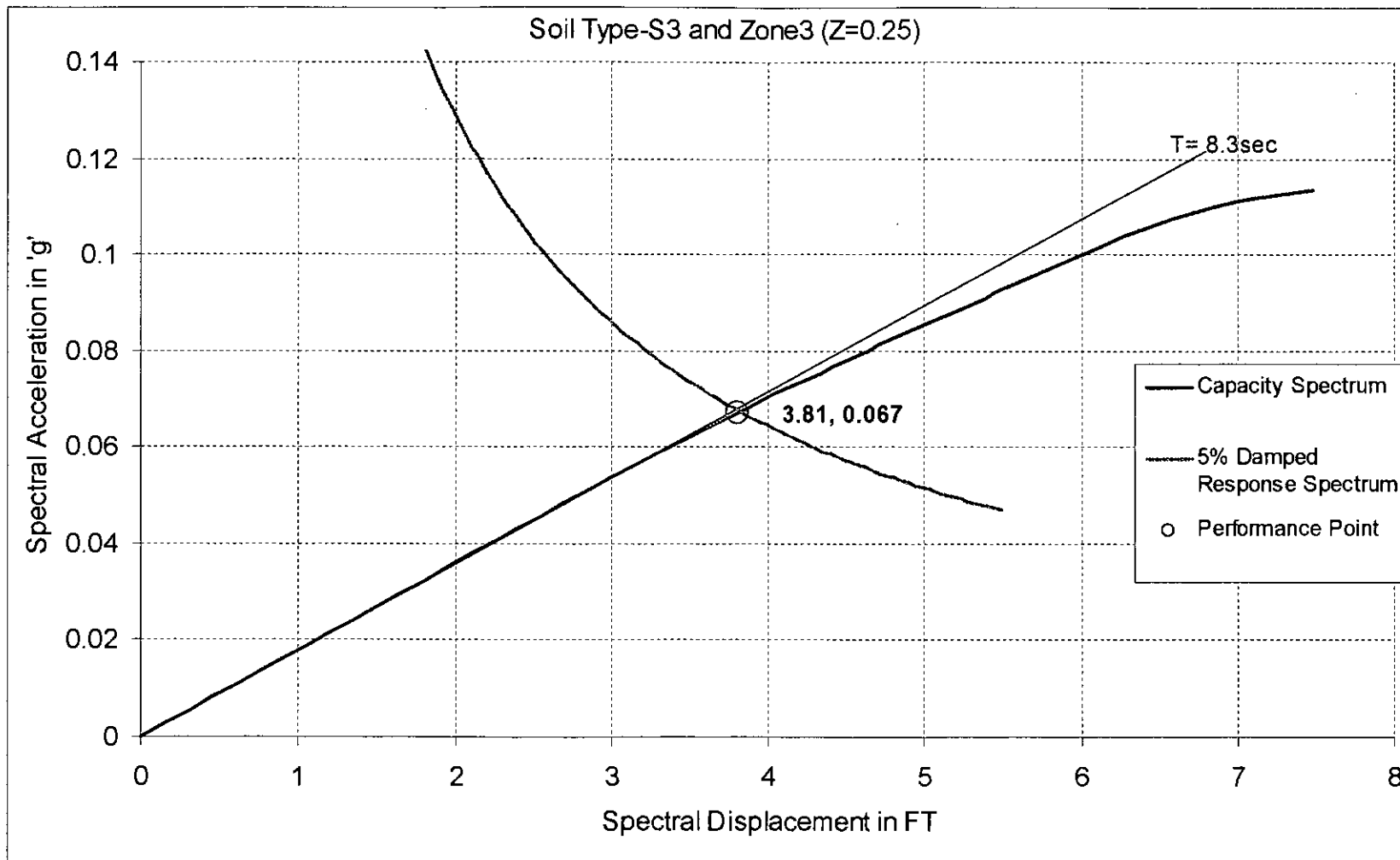
Figure 5.17 Performance Point of Ten Story Frame for Connection Type 'C'
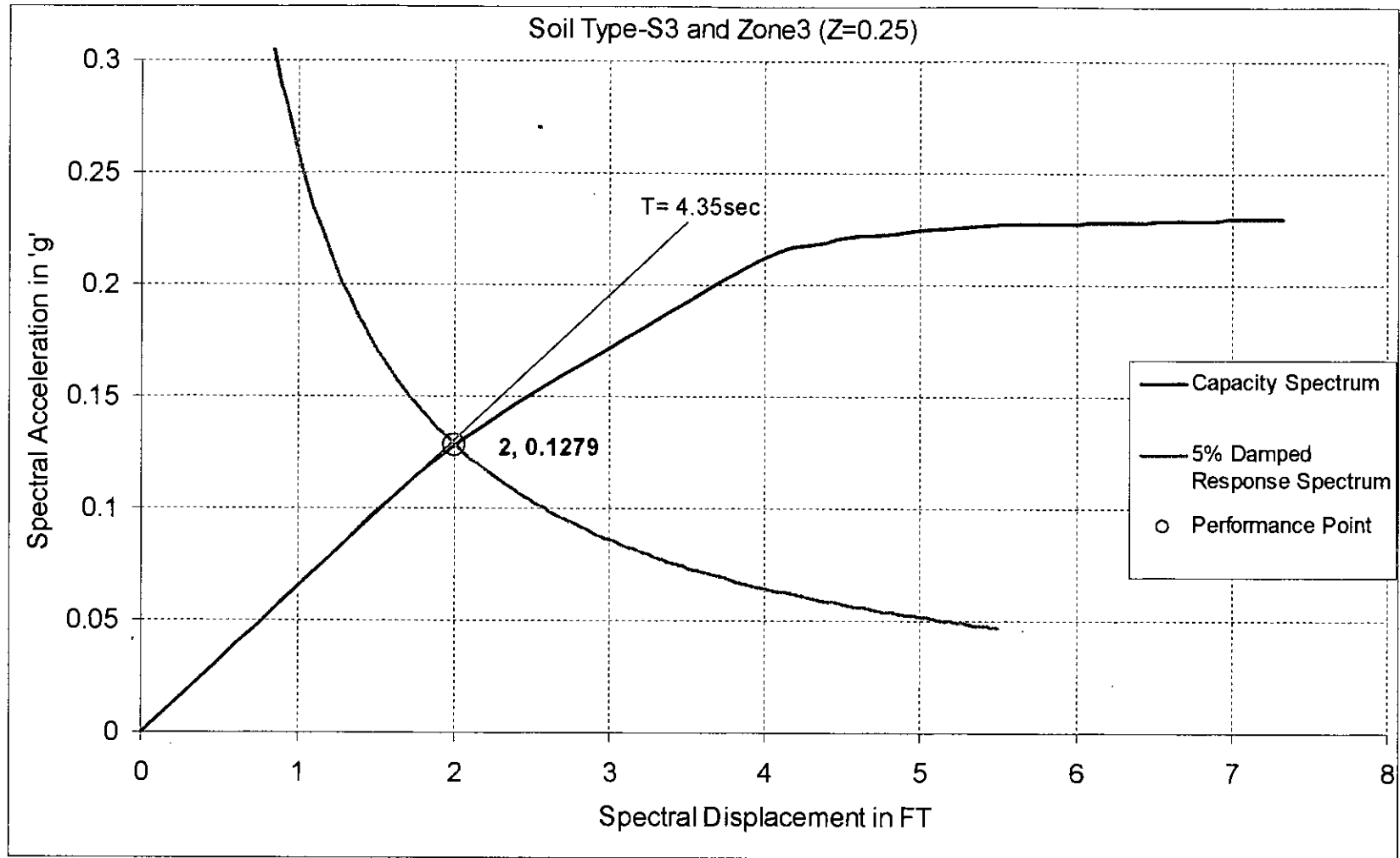
Figure 5.18 Performance Point of Six Story Frame for Connection Type 'C'

Figure 5.19 Structural Condition of Ten Story Frame at Performance Point for Connection Type 'C'

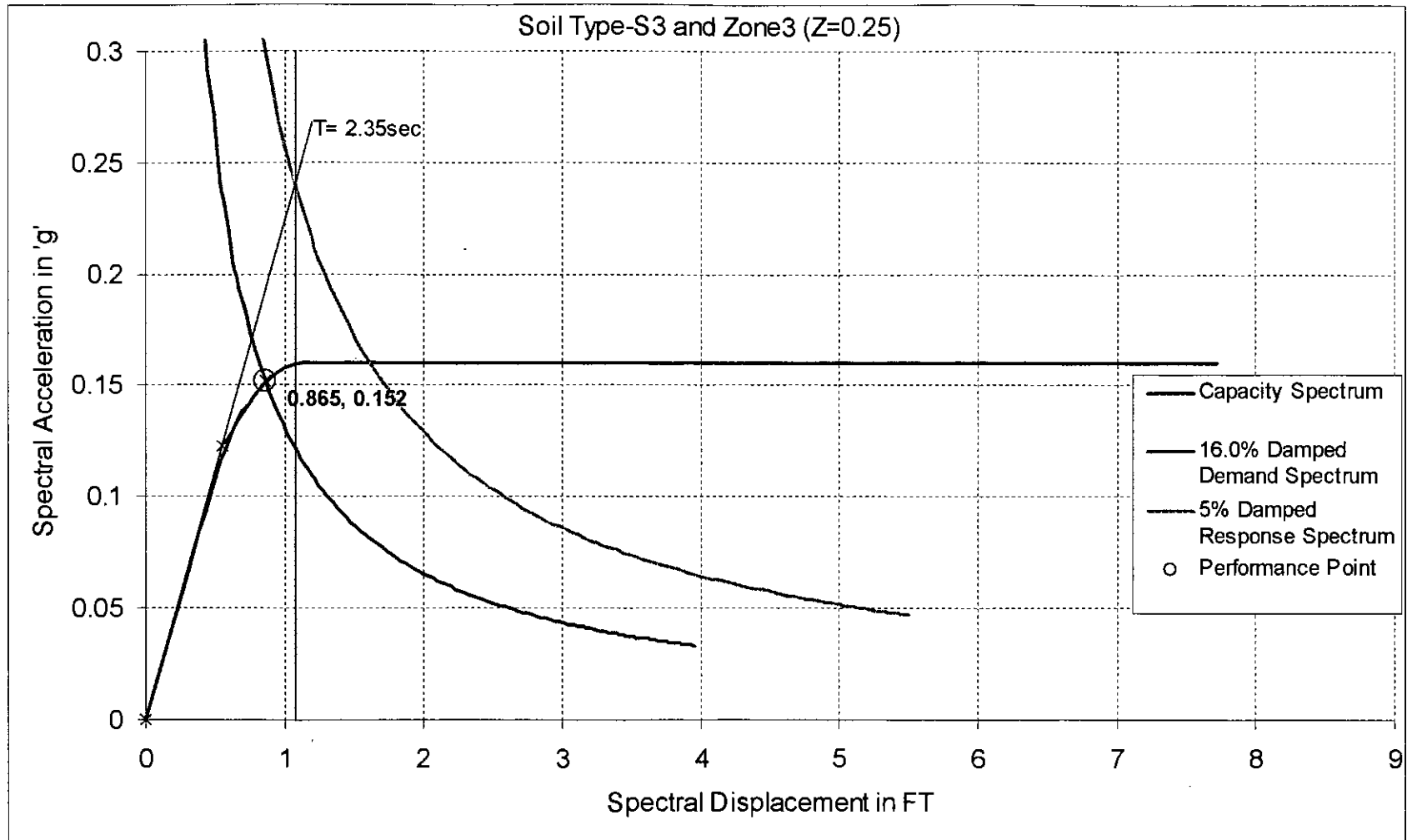**Figure 5.20 Structural Condition of Six Story Frame at Performance Point for Connection Type 'C'**

127
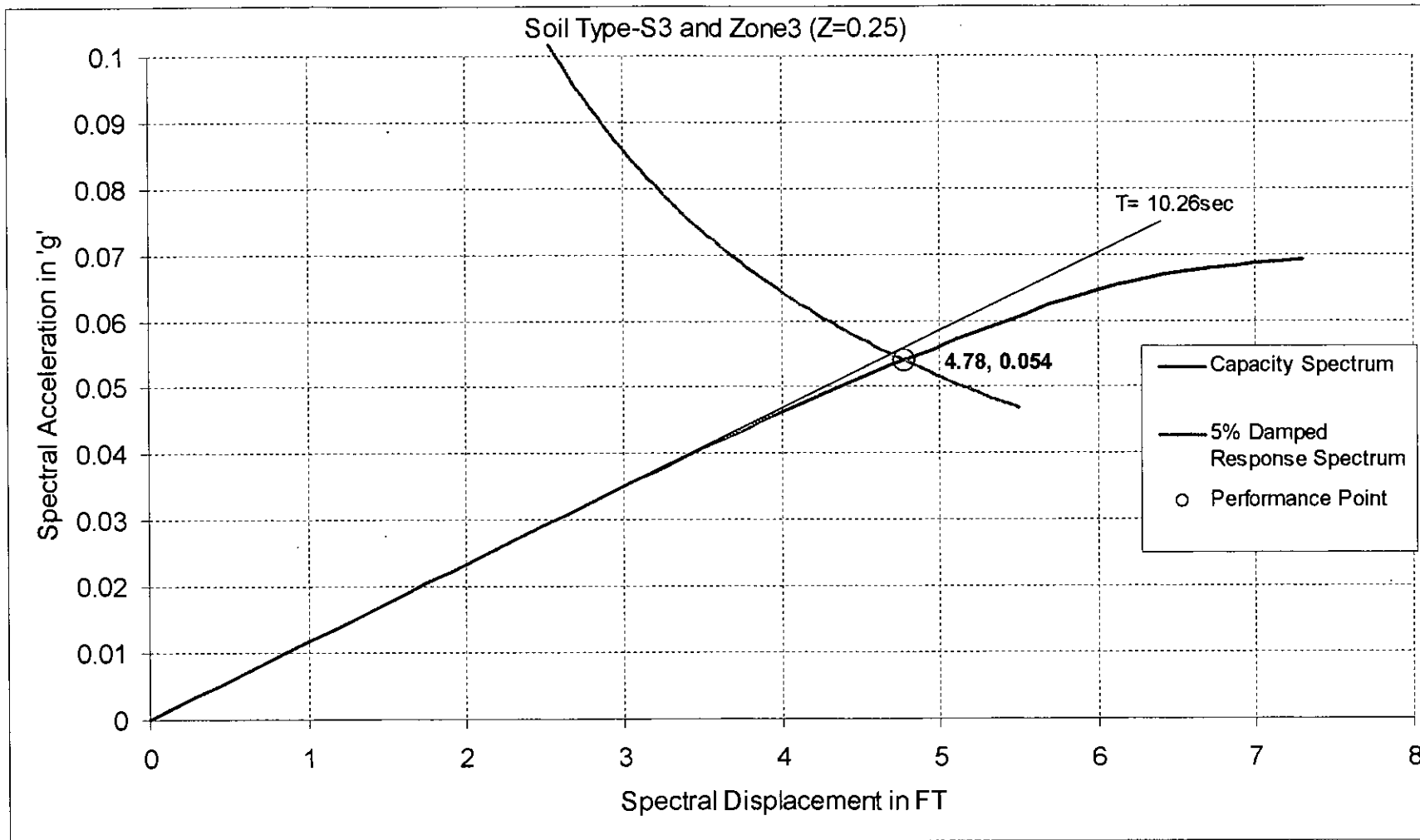
Figure 5.21 Performance Point of Ten Story Frame for Connection Type 'D'
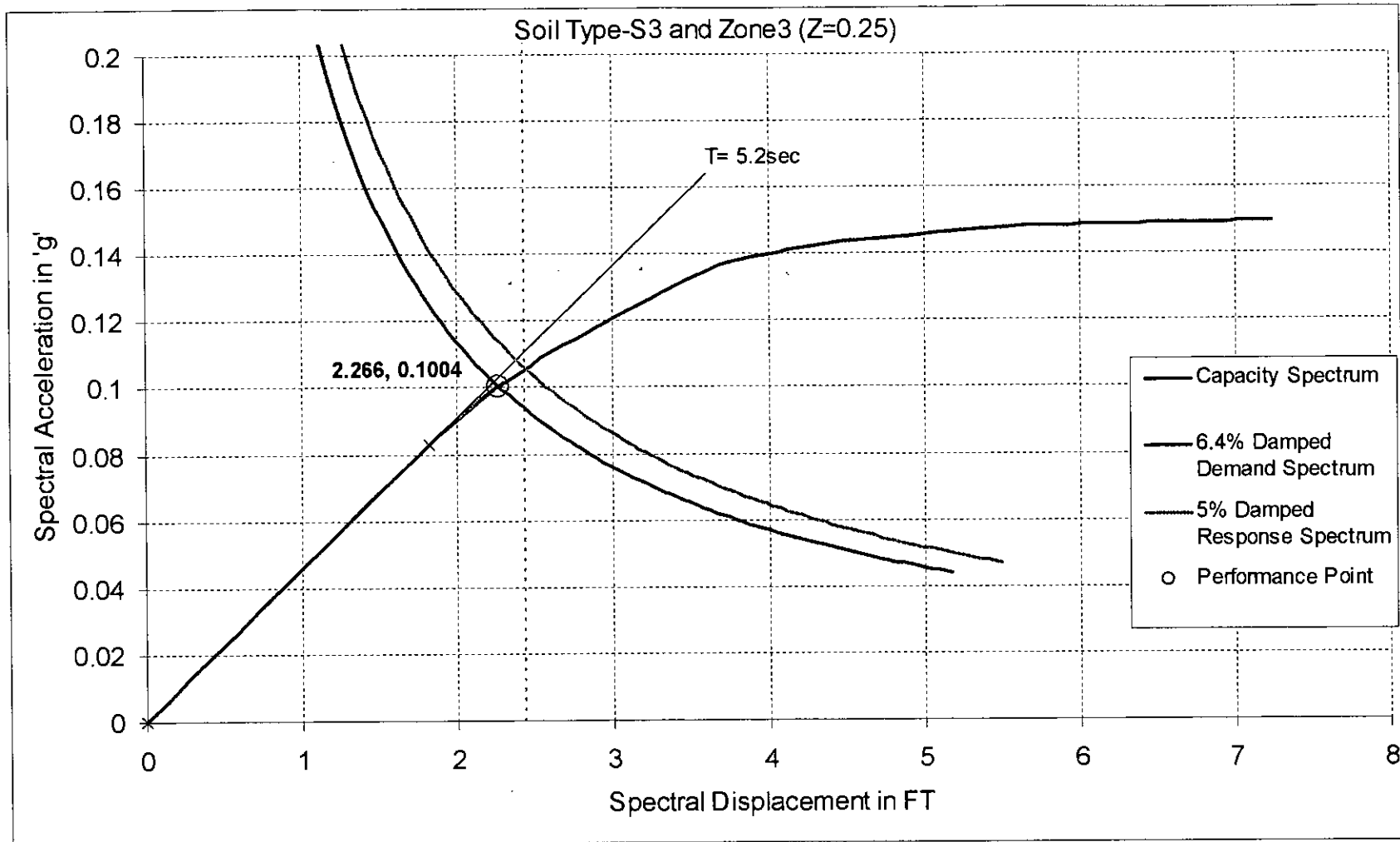
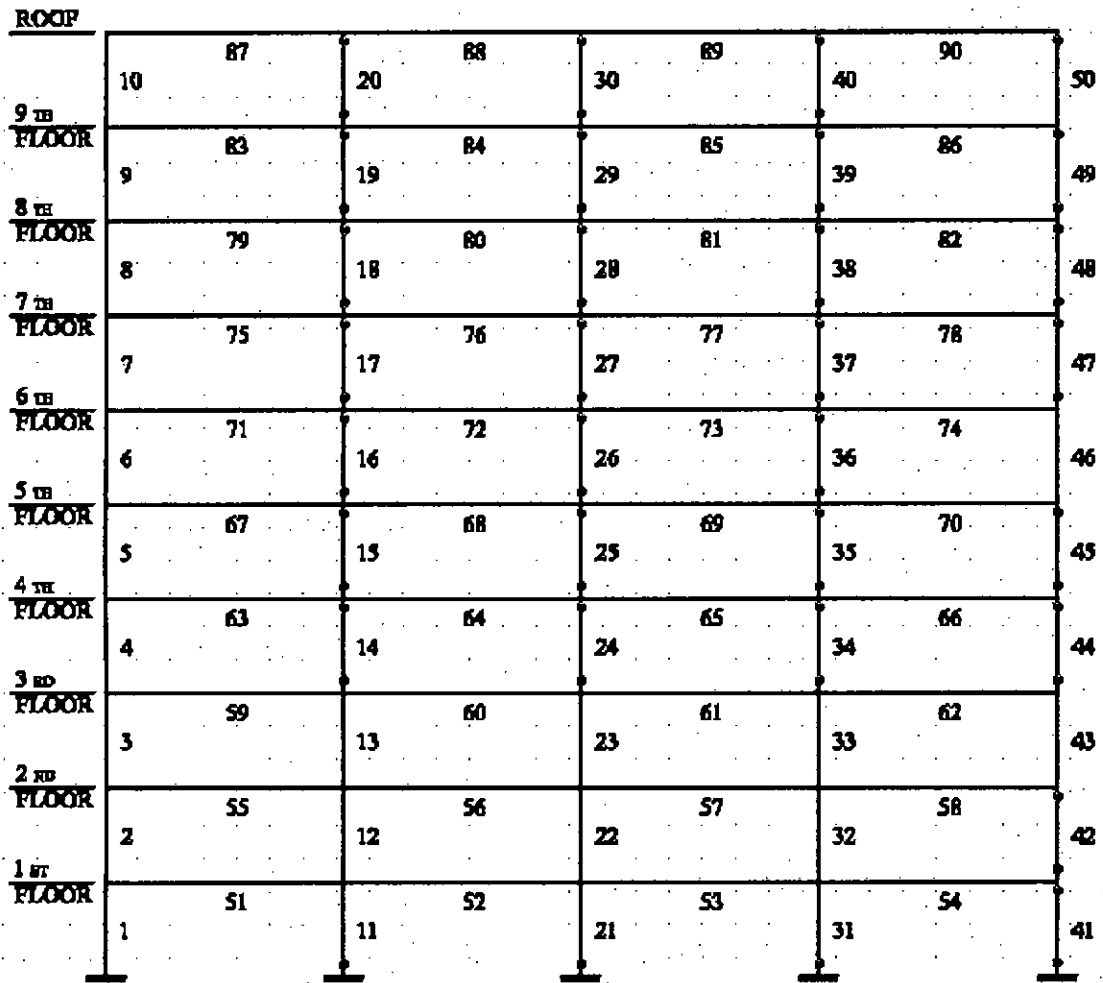**Figure 5.22 Performance Point of Six Story Frame for Connection Type 'D'**

ROOF

| | 87 | | 88 | | 89 | | 90 | |
| 10 | | 20 | | 30 | | 40 | | 50 |

9 TH
FLOOR

| | 83 | | 84 | | 85 | | 86 | |
| 9 | | 19 | | 29 | | 39 | | 49 |

8 TH
FLOOR

| | 79 | | 80 | | 81 | | 82 | |
| 8 | | 18 | | 28 | | 38 | | 48 |

7 TH
FLOOR

| | 75 | | 76 | | 77 | | 78 | |
| 7 | | 17 | | 27 | | 37 | | 47 |

6 TH
FLOOR

| | 71 | | 72 | | 73 | | 74 | |
| 6 | | 16 | | 26 | | 36 | | 46 |

5 TH
FLOOR

| | 67 | | 68 | | 69 | | 70 | |
| 5 | | 15 | | 25 | | 35 | | 45 |

4 TH
FLOOR

| | 63 | | 64 | | 65 | | 66 | |
| 4 | | 14 | | 24 | | 34 | | 44 |

3 RD
FLOOR

| | 59 | | 60 | | 61 | | 62 | |
| 3 | | 13 | | 23 | | 33 | | 43 |

2 ND
FLOOR

| | 55 | | 56 | | 57 | | 58 | |
| 2 | | 12 | | 22 | | 32 | | 42 |

1 ST
FLOOR

| | 51 | | 52 | | 53 | | 54 | |
| 1 | | 11 | | 21 | | 31 | | 41 |

Figure 5.23 Structural Condition of Ten Story Frame at Performance Point for
Connection Type 'D'

ROOF

| | 51 | | 52 | | 53 | | 54 | |
| 6 | | 12 | | 18 | | 24 | | 30 |

5 TH
FLOOR

| | 47 | | 48 | | 49 | | 50 | |
| 5 | | 11 | | 17 | | 23 | | 29 |

4 TH
FLOOR

| | 43 | | 44 | | 45 | | 46 | |
| 4 | | 10 | | 16 | | 22 | | 28 |

3 RD
FLOOR

| | 39 | | 40 | | 41 | | 42 | |
| 3 | | 9 | | 15 | | 21 | | 27 |

2 ND
FLOOR

| | 35 | | 36 | | 37 | | 38 | |
| 2 | | 8 | | 14 | | 20 | | 26 |

1 ST
FLOOR

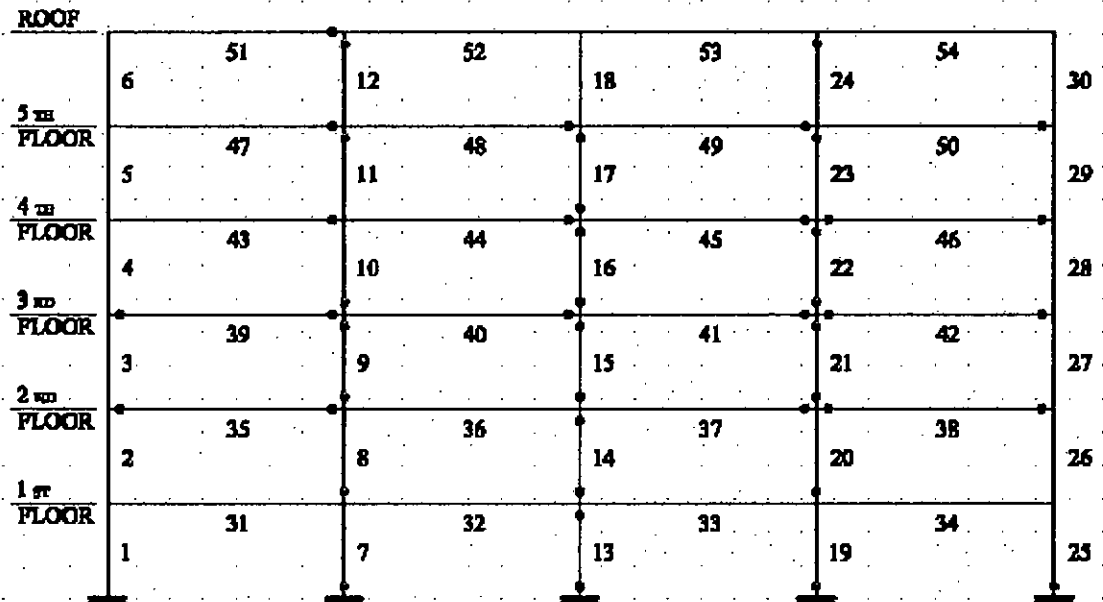| | 31 | | 32 | | 33 | | 34 | |
| 1 | | 7 | | 13 | | 19 | | 25 |

Figure 5.24 Structural Condition of Six Story Frame at Performance Point for
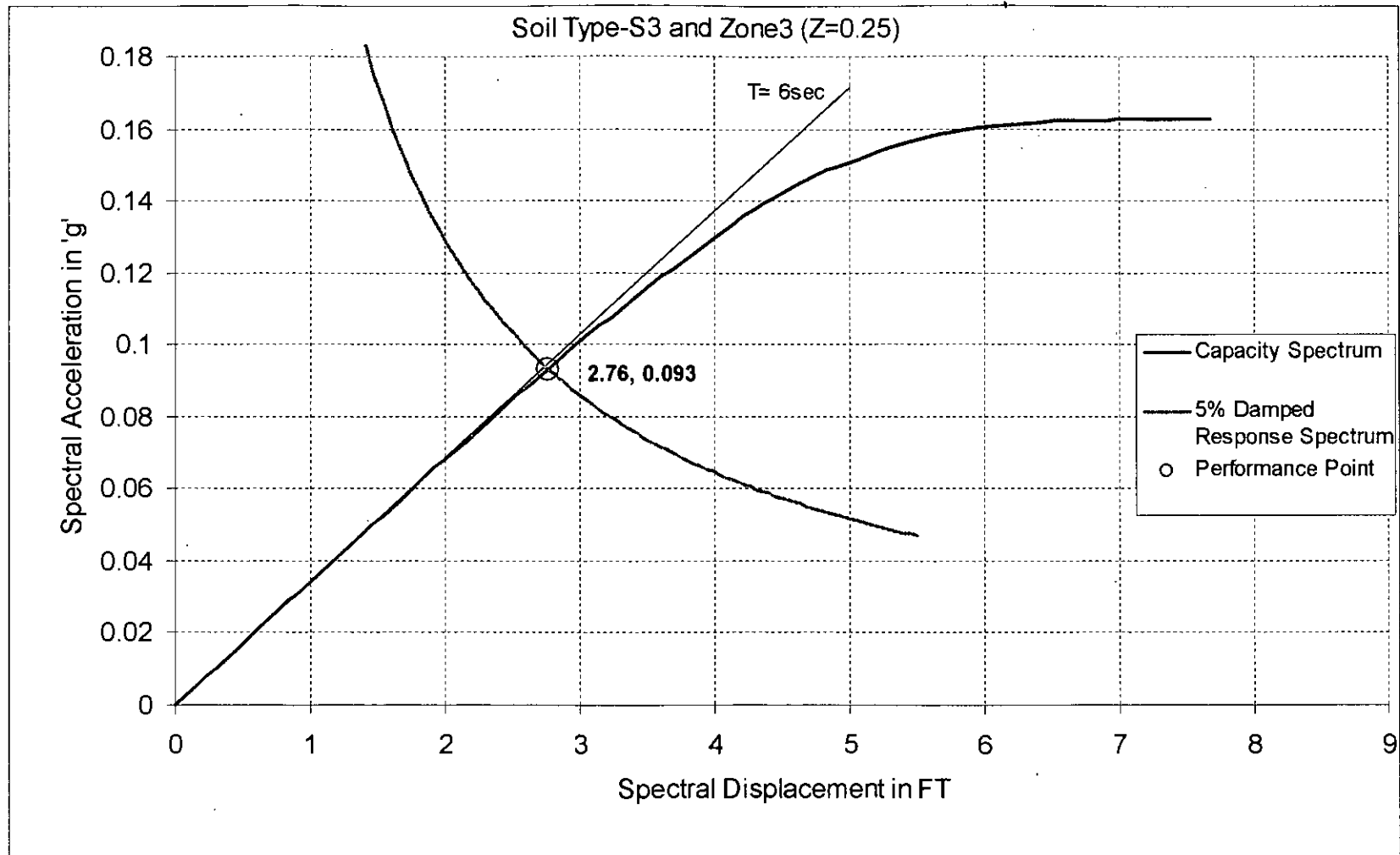Connection Type 'D'

130
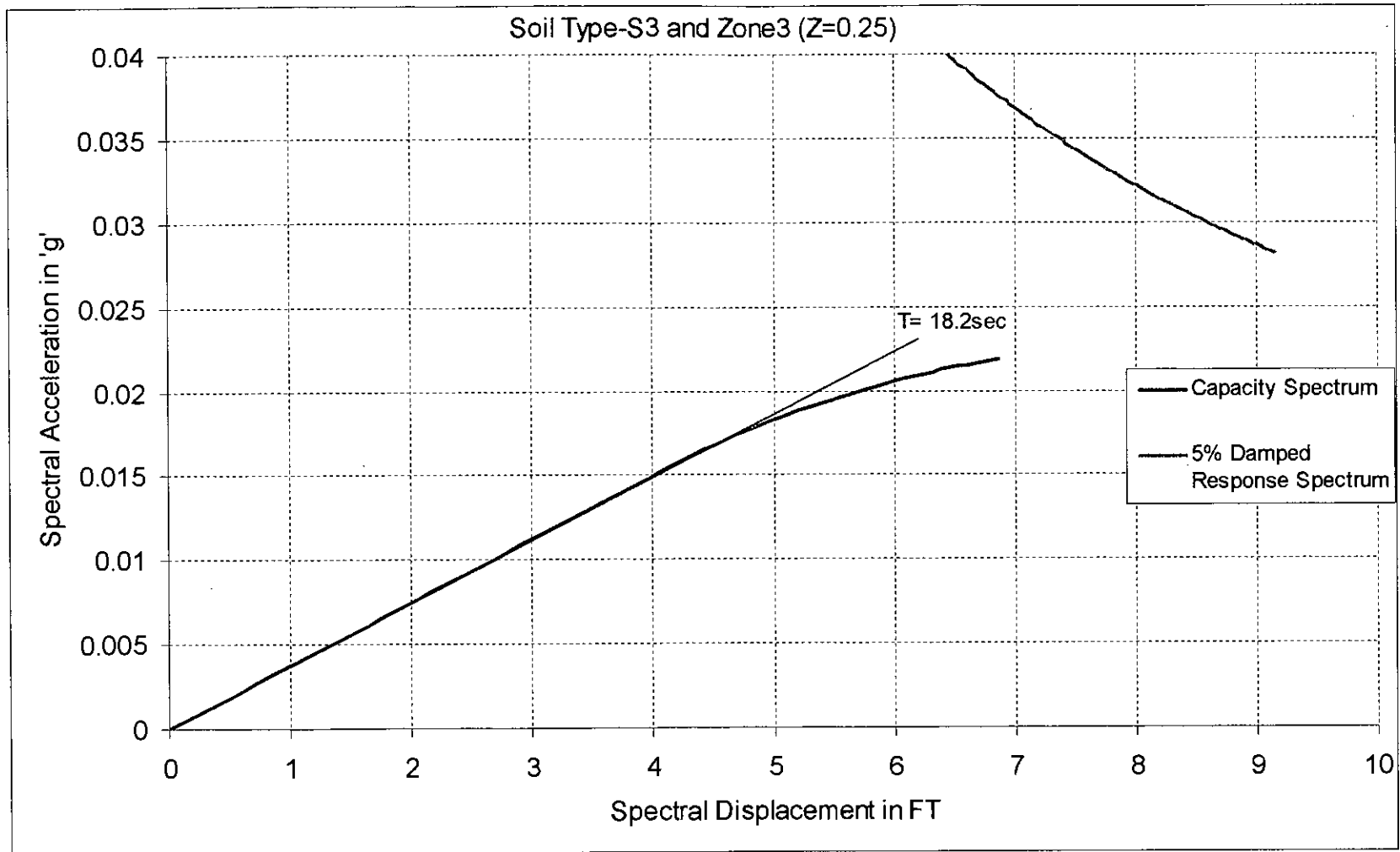
Figure 5.25 Performance Point of Ten Story Frame for Connection Type 'E'
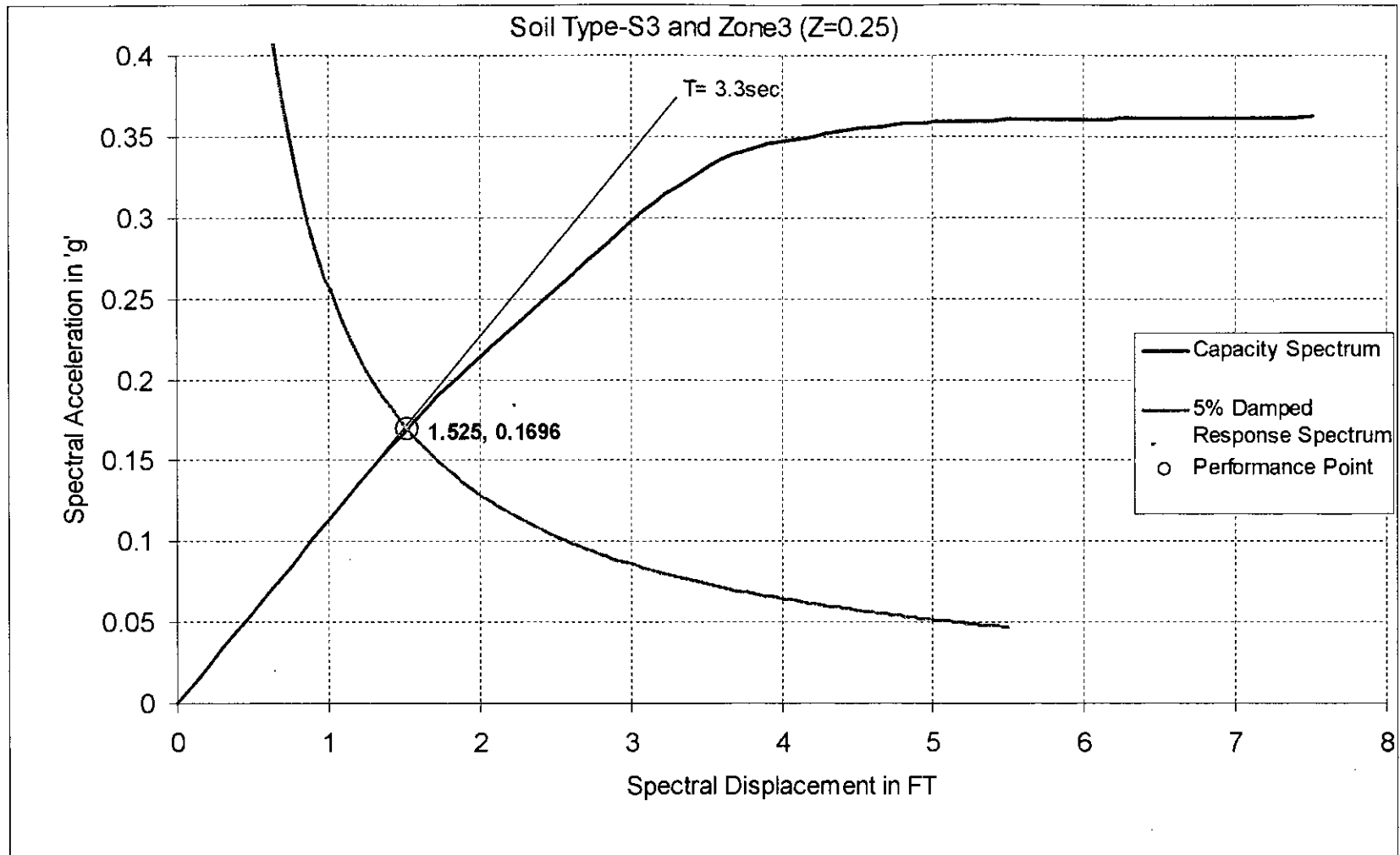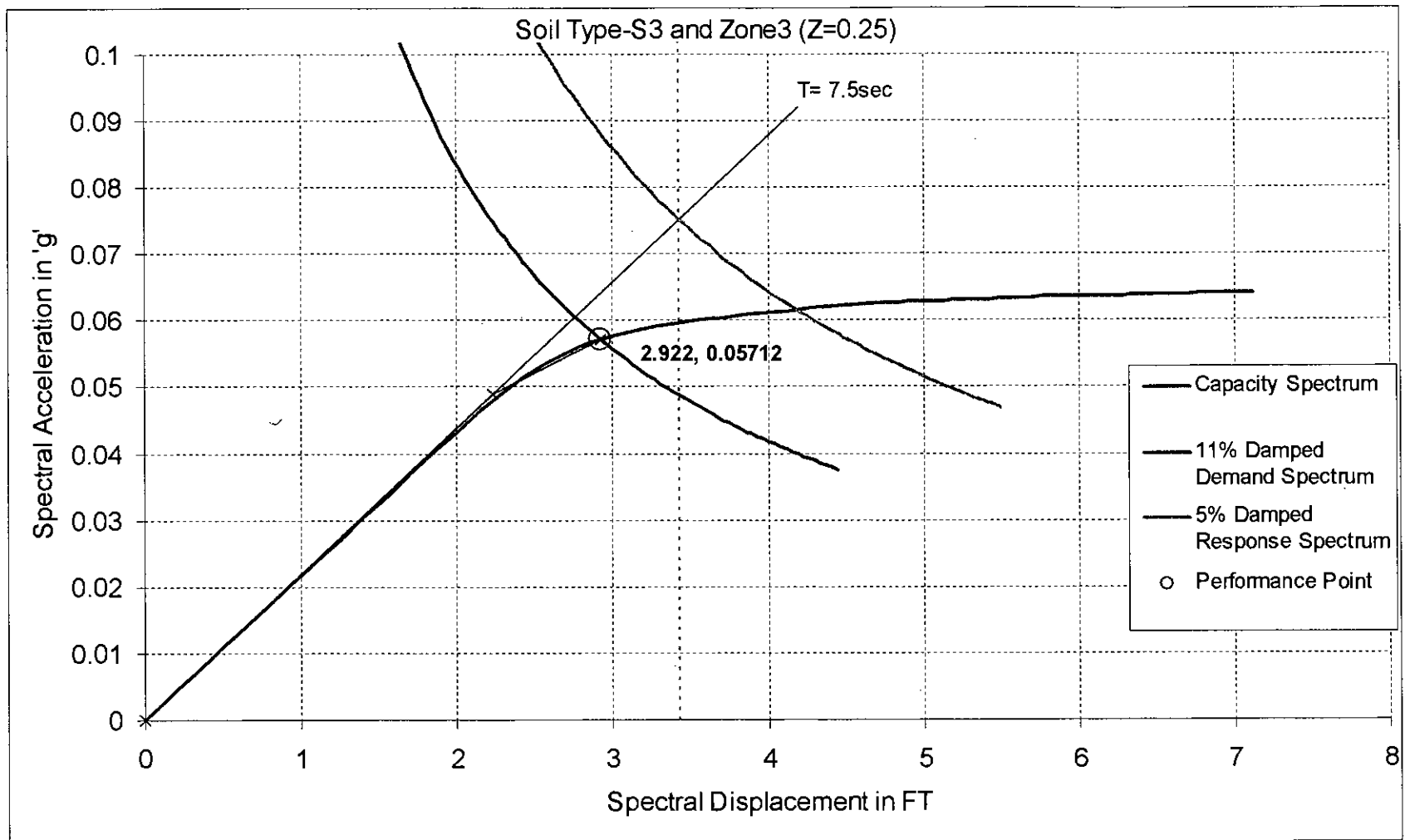
Figure 5.26 Performance Point of Six Story Frame for Connection Type 'E'

132
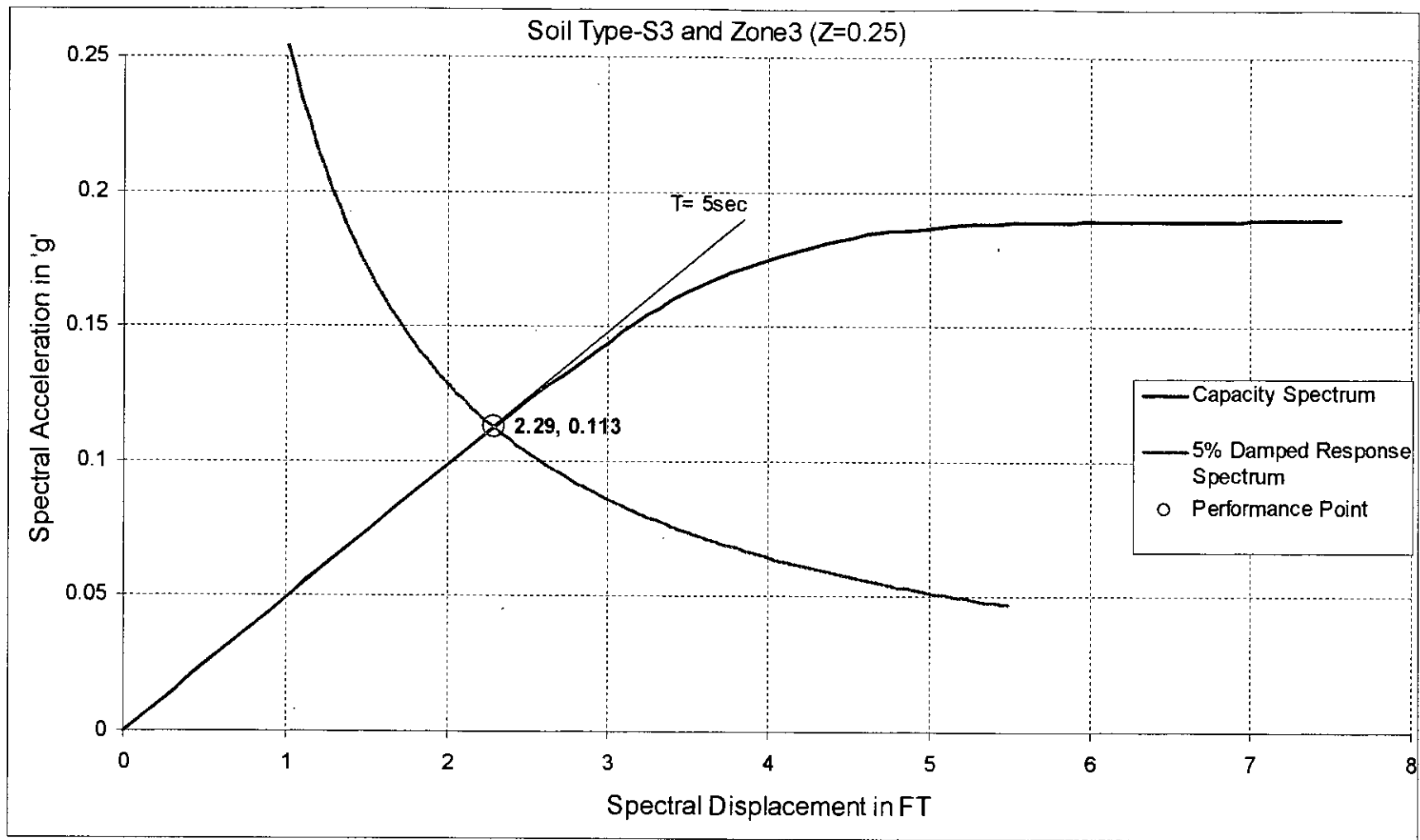
Figure 5.27 Performance Point of Ten Story Frame for Frame Type 'R20_SR80'

Figure 5.28 Structural Condition of Six Story Frame at Performance Point for Connection Type 'E'

Figure 5.29 Structural Condition of Ten Story Frame at Performance Point for Frame Type 'R20_SR80'

134
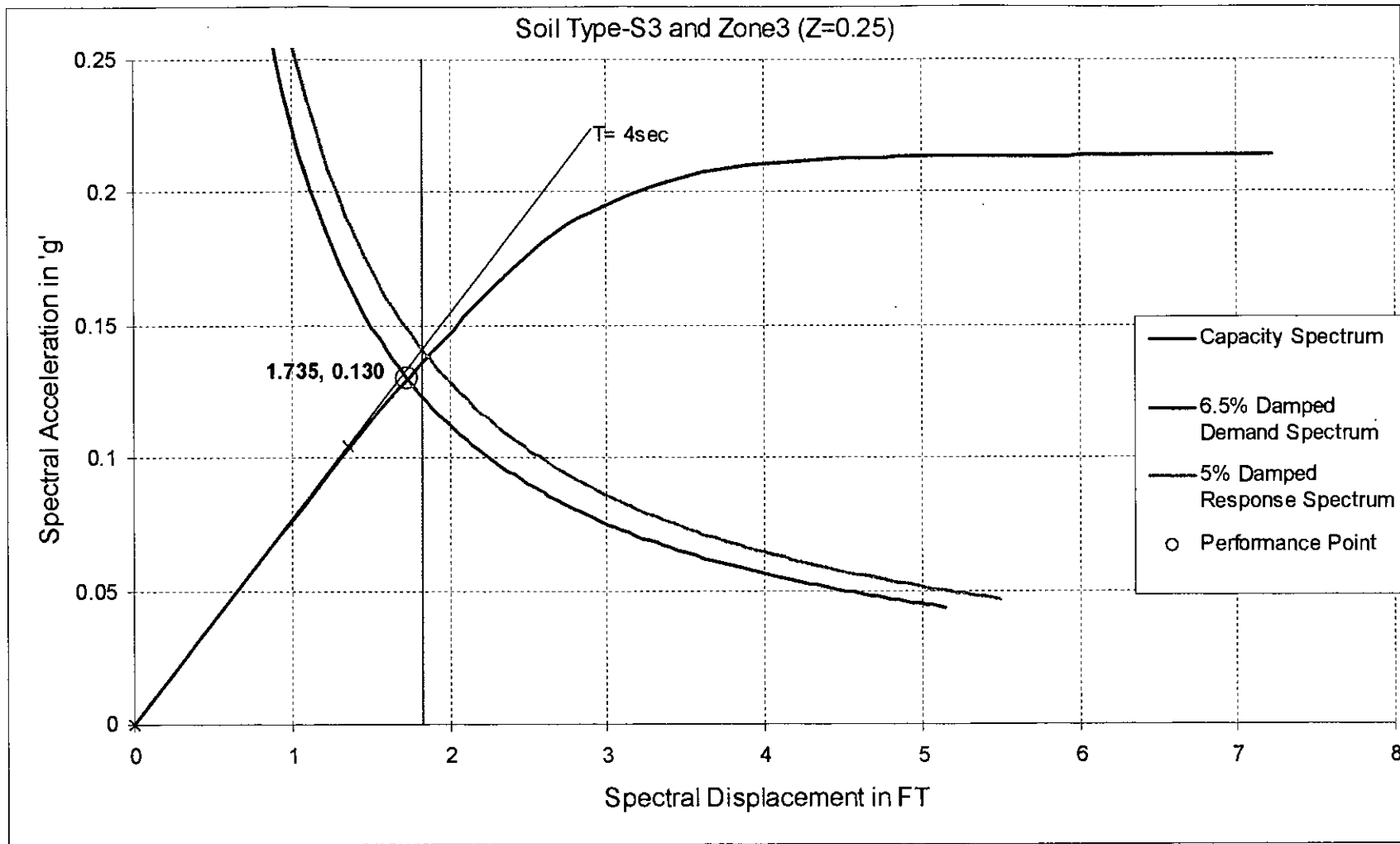
Figure 5.30 Performance Point of Ten Story Frame for Frame Type 'R40_SR60'

135

Figure 5.31 Structural Condition of Ten Story Frame at Performance Point for Frame Type 'R40_SR60'
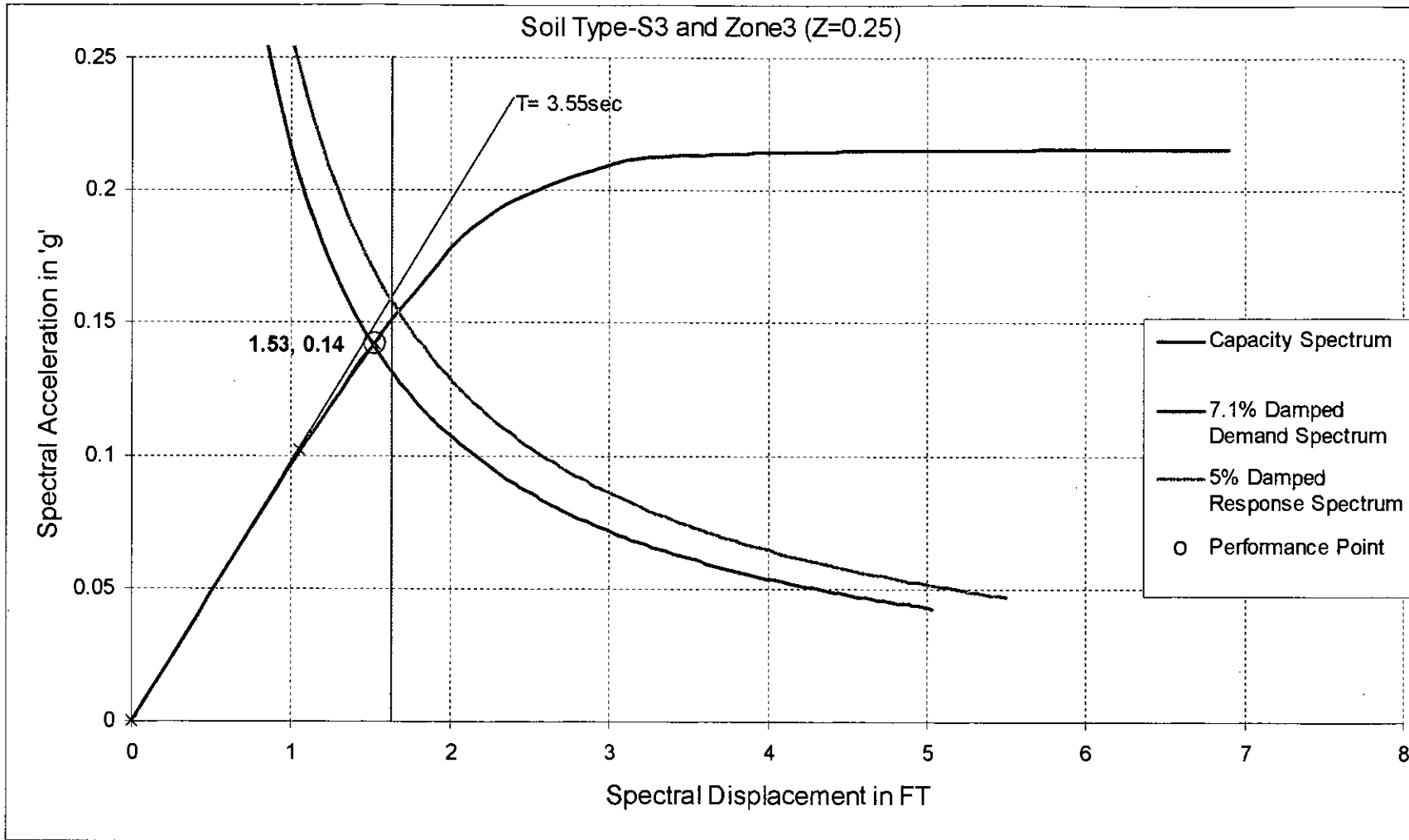
Figure 5.32 Performance Point of Ten Story Frame for Frame Type 'R50_SR50'

Figure 5.33 Structural Condition of Ten Story Frame at Performance Point for Frame Type 'R50_SR50'
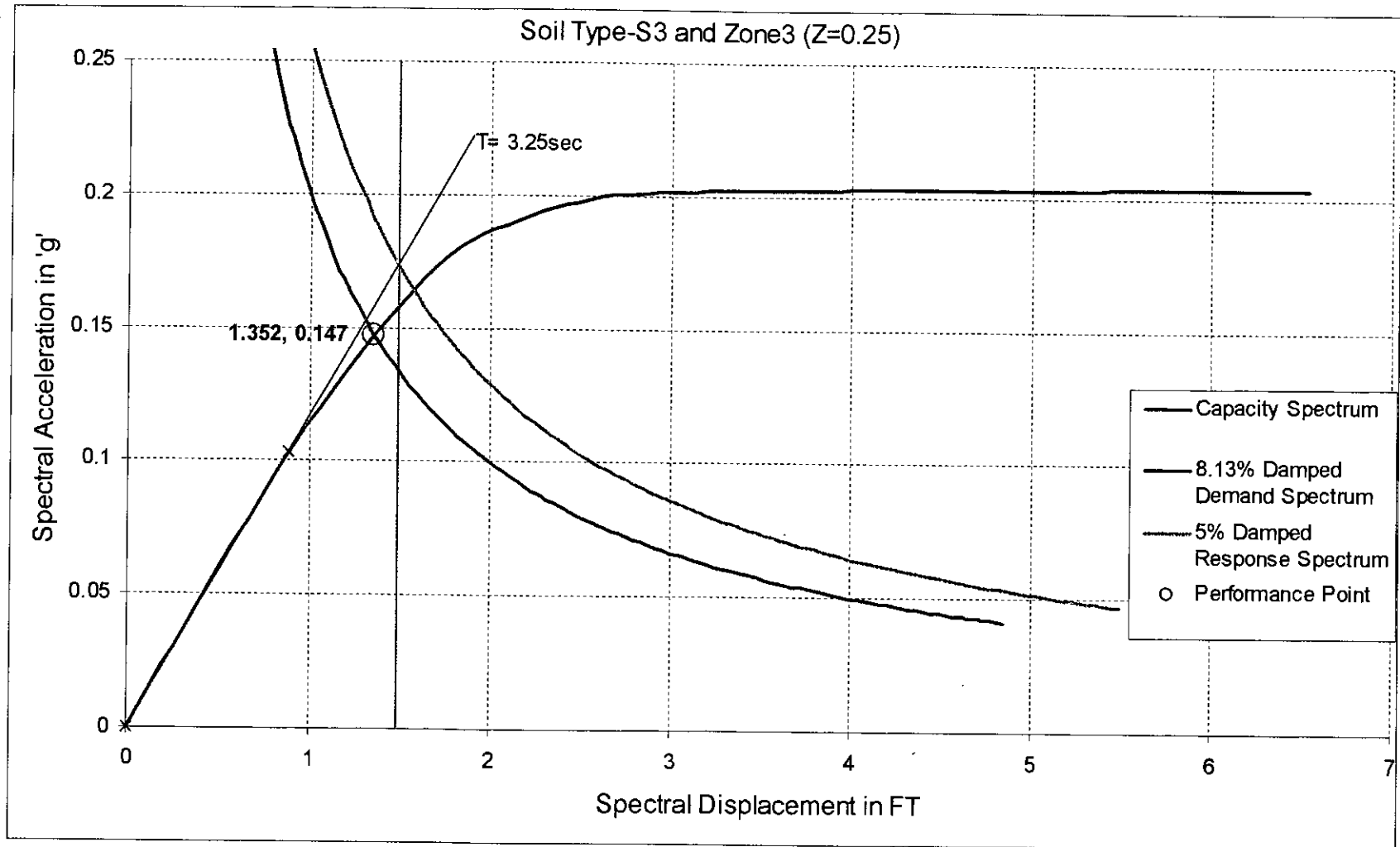
Figure 5.34 Performance Point of Ten Story Frame for Frame Type 'R60_SR40'

Figure 5.35 Structural Condition of Ten Story Frame at Performance Point for Frame Type 'R60_SR40'
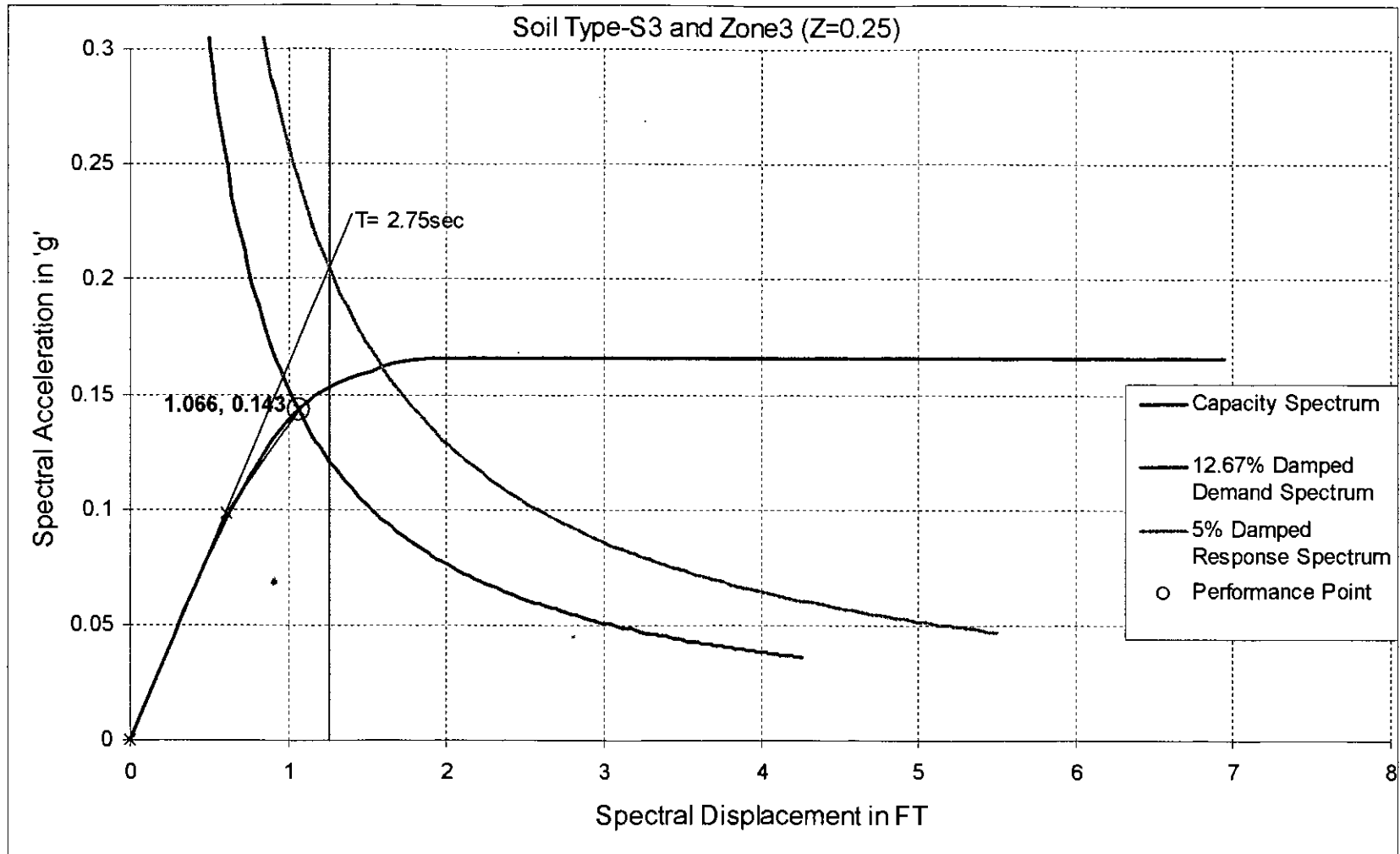
Figure 5.36 Performance Point of Ten Story Frame for Frame Type 'R80_SR20'

Figure 5.37 Structural Condition of Ten Story Frame at Performance Point for
Frame Type 'R80_SR20'

142

5.3 Study on Lateral Drift

To represent the sway behaviour of semi-rigid frames sway at different floors have been plotted against story level at their performance point (Figures 5.38 to 5.40). Figure 5.38 and Figure 5.40, where particular frame is assumed to possess same type of connection at all the joints, represent sway of the ten storied and six storied frame respectively is increasing due to increasing of connection semirigidity. Only few columns of the semirigid structures just have been started to yield but most of the columns of the rigid structure have reached beyond their elastic limit at their
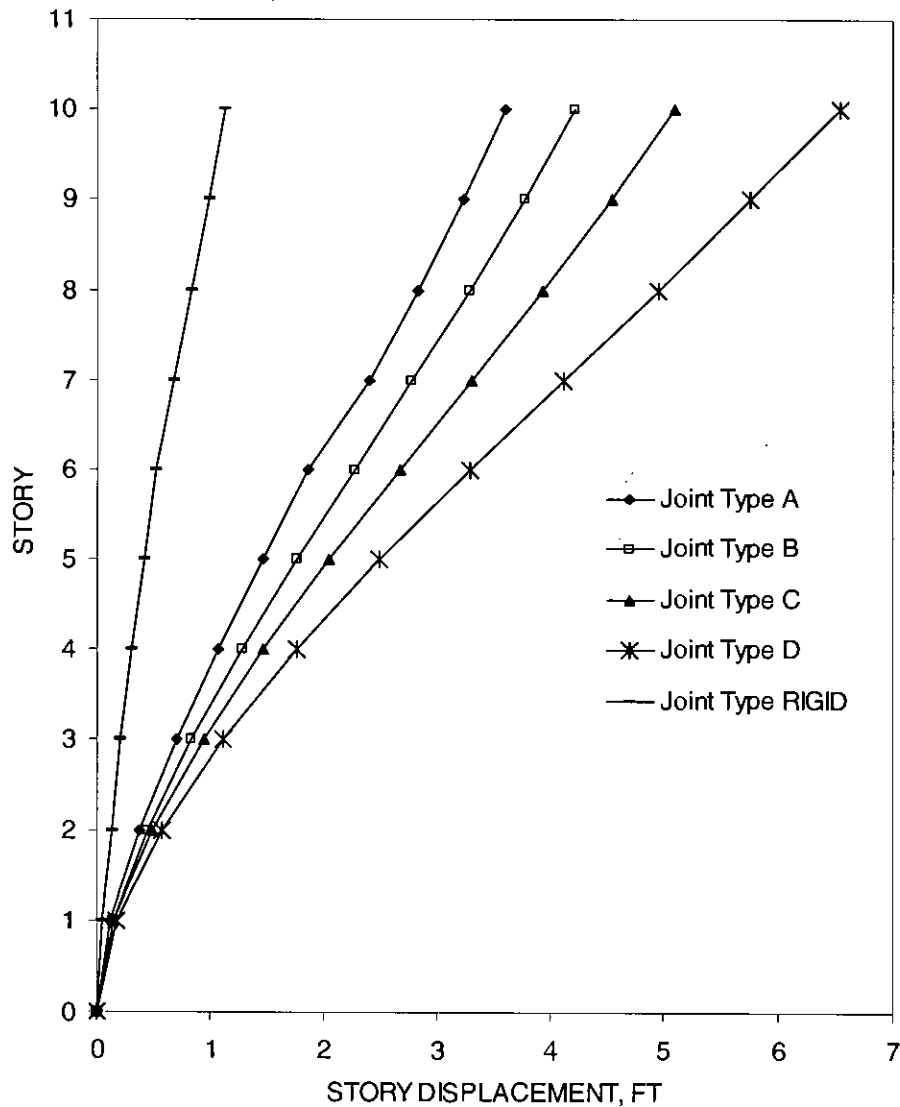
Figure 5.38 Sway of the Ten Story Frame with "RIGID" and Different Types of "Semi-Rigid" Connections at Their Performance Point

143

performance point, though the inter story drift of semi-rigid structures is higher than the rigid structure.
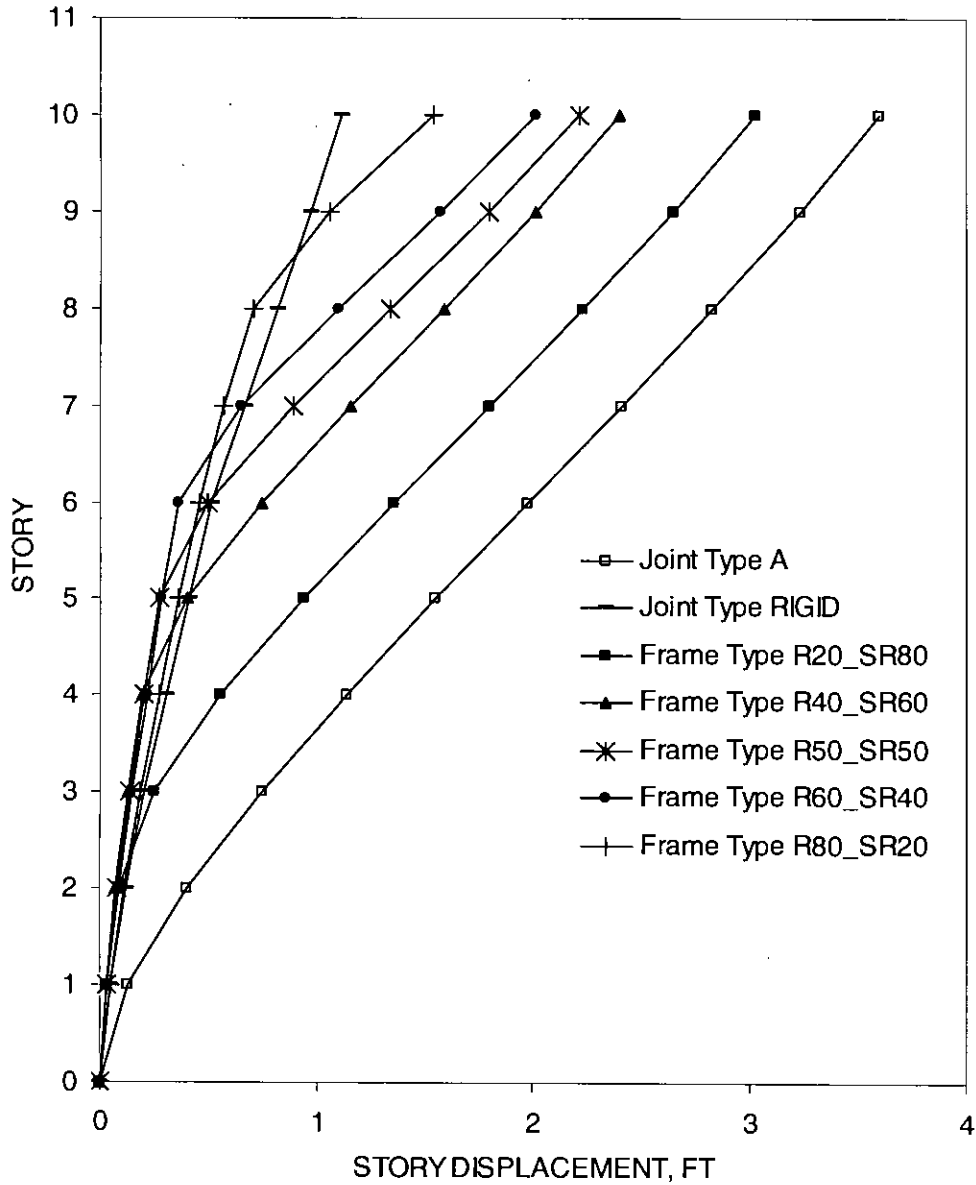
Figure 5.39 Sway of the Ten Story Frame for Combination of "RIGID" and "Semi-Rigid" Connections at Their Performance Point

Ten storied frames in combination of rigid and semirigid connection type 'A' are plotted on Figure 5.39 to get the shape of the structure at their performance point. Structure with semirigid connection type 'A' has higher seismic demand than any

other semirigid structures (Table 5-2). For this reason, connection type 'A' is used in combinations of rigid and semirigid connections. With increasing of rigid floors the sway of the structure is decreasing. On the other hand number of the plastic members is increasing due to the increase of rigid floors.
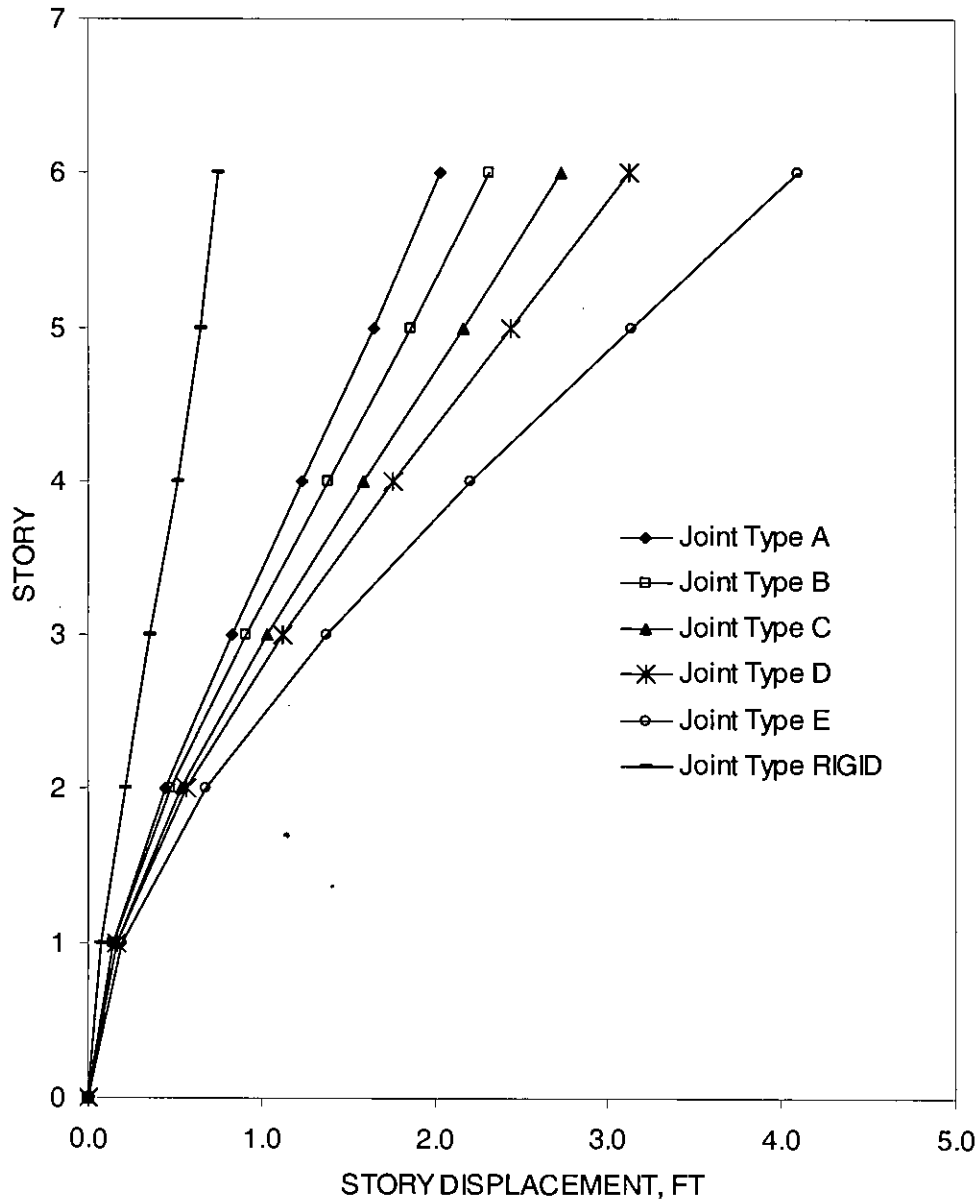
Figure 5.40 Sway of the Six Story Frame with "RIGID" and Different Types of "Semi-Rigid" Connections at Their Performance Point

5.4 Comparison of Equivalent Static Force Analysis with Nonlinear Static Analysis

Two dimensional four bays and ten storied steel building with special moment resisting system (Rigid beam-column connections) has been analyzed and designed on Section 4.2.1 of Chapter 4 by equivalent static force method (BNBC,1993). Again this
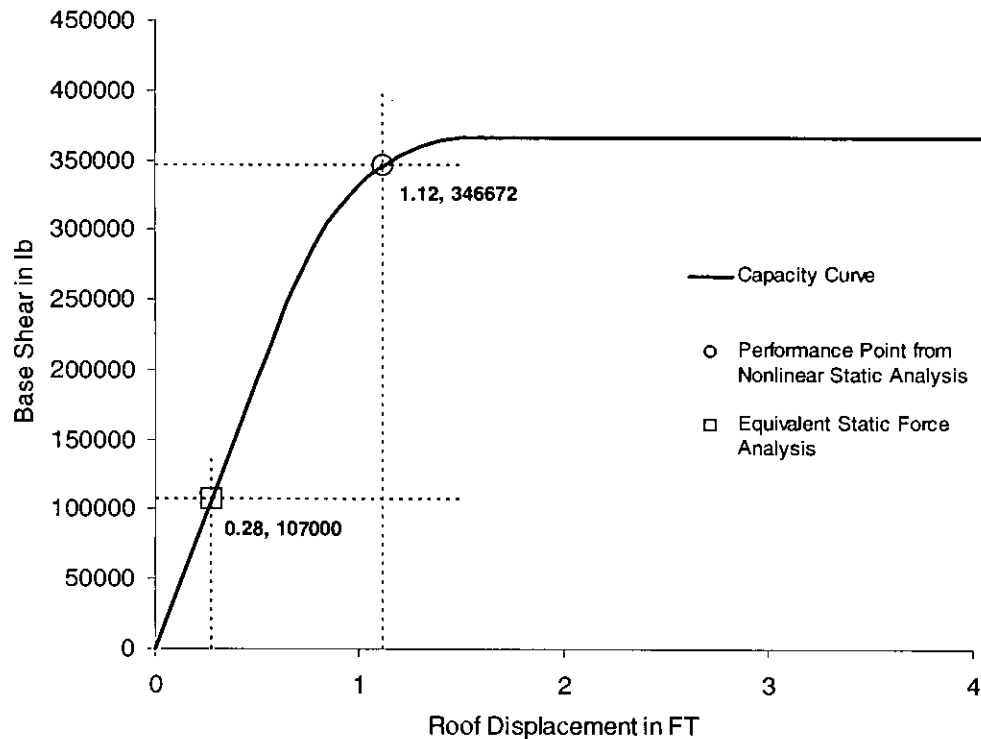
Figure 5.41 Comparison between Equivalent Static Analysis and Nonlinear Static Analysis for the Structure with Rigid Beam-Column Connection

structure has been analyzed by nonlinear static analysis to get the pushover curve (Figure 4.6) on Section 4.5 of Chapter 4. Figure 5.41 represents the results of base shear and roof displacement from two analyses. This figure shows that base shear and roof displacement from equivalent static force method is lower than those from nonlinear static analysis. Analysis and design by equivalent static force method may not be conservative.

5.5 Comparison of Demand Response Spectrum Using Site Coefficients of ATC-40 and BNBC, 1993

By considering Soil Profile Type S_E of ATC-40 (described in Chapter-4 of ATC-40) is equivalent with Soil Profile Type S_3 of BNBC, 1993 seismic coefficients C_A and C_V are 0.35 and 0.74 respectively by considering Z=0.25. Figure 5.42 represents the comparison between demand response spectrum of ATC-40 and BNBC, 1993. Response spectrum using site coefficients of ATC-40 is greater than that of BNBC, 1993.
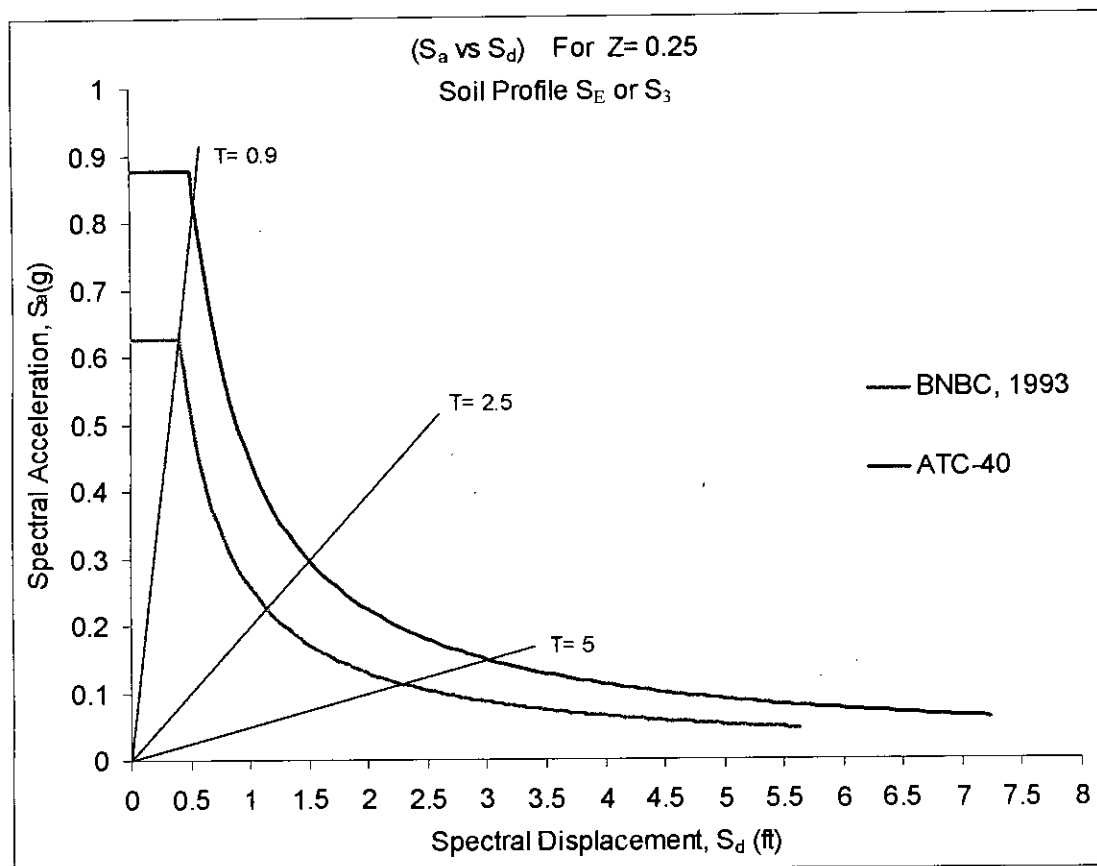
Figure 5.42 Comparison between Demand Response Spectrum of ATC-40 and BNBC, 1993

Capacity spectrum for Joint Type 'Rigid' (Fig 4.11) and 5% damped Response Spectrum using site coefficients of ATC-40 (Fig 5.42) are plotted on the same graph (Fig 5.43) to get the Performance Point (S_a = 0.1596g, S_d= 1.083ft) of the structure using the Procedure-A of ATC-40. Demand displacement using site coefficients of

ATC-40 is higher than demand displacement (S_d= 0.865ft) using response spectra of BNBC, 1993.
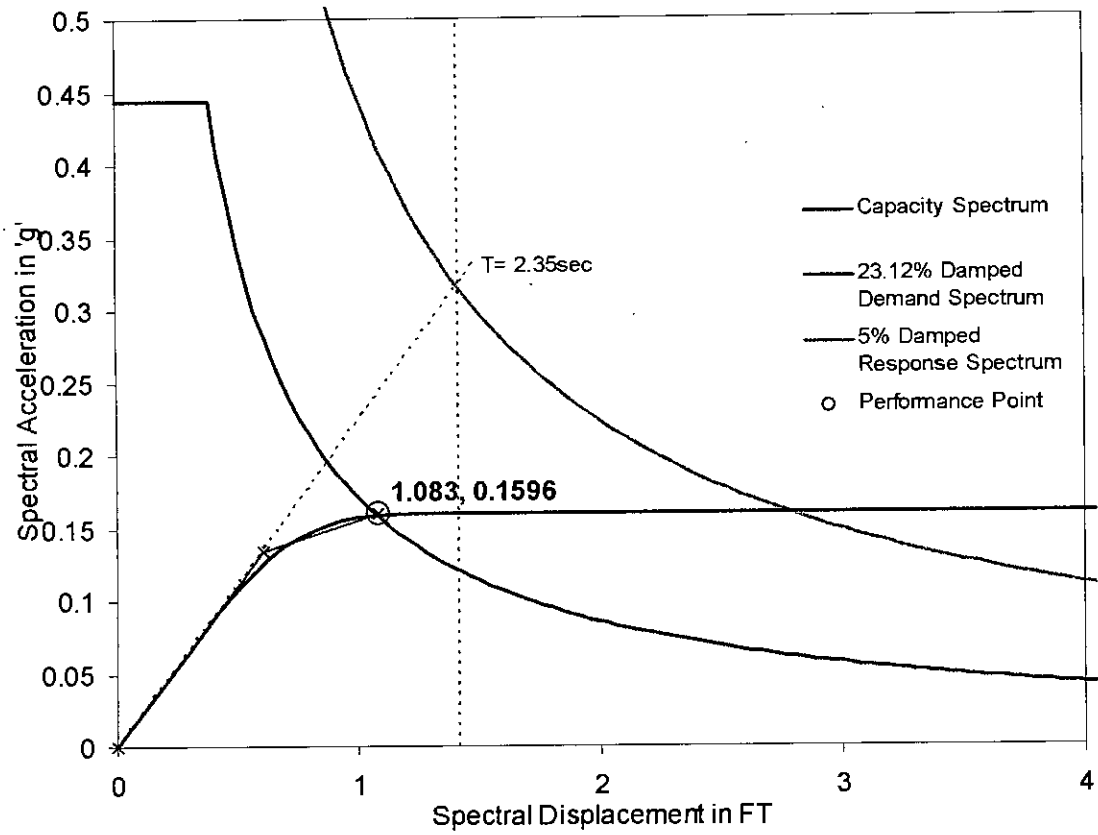
Figure 5.43 Performance Point for Connection Type 'Rigid' using Response
Spectrum of ATC-40

CHAPTER 6

Conclusions and Recommendations

6.1 Conclusions

It is clear that when subjected to major earthquake, buildings designed to meet the design requirements of typical building codes, such as the Bangladesh National Building Code (BNBC, 1993), Uniform Building Code, are expected to suffer damage in both structural and non-structural elements. The intent of the building code under this scenario is to avoid collapse and loss of life. Because of the economic impact, structural design to resist major earthquake ground motions with little or no damage has been limited to special buildings, such as post disaster critical structures (for example, hospitals, police, and fire stations) or structures that house potentially hazardous materials (for example, nuclear power plants).

The structural design for large seismic events must therefore explicitly consider the effects of response beyond the elastic range. A mechanism must be supplied within some elements of the structural system to accommodate the large displacement demand imposed by the earthquake ground motions. In typical applications, structural elements, such as walls, beams, braces, and to a lesser extent columns and connections, are designed to undergo local deformations well beyond the elastic limit of the material without significant loss of capacity. Provision of such large deformation capacity is a fundamental tenet of seismic design.

The relationship between base shear and roof displacement commonly known as the "pushover curve" which includes nonlinear connection response and plastification of beam-column elements has been developed. Conversion of the pushover curve to a capacity spectrum where the initial semi-rigidity of the connection is considered for the fundamental vibration mode has been done. This study investigated the phenomenon that the semirigid connections to absorb substantial energy and provide

149

major contributions to the displacement demand rather than rigid connections. A concise summary of the significant conclusion from the present study is given below:

- Response spectra of BNBC, 1993 have been converted to ADRS (Acceleration-Displacement Response Spectra) format. Construction of 5% damped elastic response spectrum has been developed by using seismic coefficients C_A and C_V as the seismic coefficients are not given in BNBC, 1993. Seismic coefficients are required to get the performance point of the structure by using capacity spectrum method. There should be some provisions for seismic coefficients in BNBC. Response spectrum using site coefficients of ATC-40 is greater than BNBC, 1993. For rigid structure, demand displacement (S_d= 1.083ft) using response spectrum of ATC-40 is higher than demand displacement (S_d= 0.865ft) using response spectrum of BNBC, 1993.

- Most of the members of the rigid structure are fully plastic at its performance point.

- Semirigid frames, where particular frame is assumed to posses same type of semirigid connection at all joints, it can be notified that they experience almost no plastic deformation at members at their performance point though the shear capacity is lower and the demand displacement is higher than those of rigid structures. For connection type "E", the ten storied steel frame structure is fail to withstand at the maximum considered earthquake but the six storied frame gives the performance. By selecting a proper semirigid frame one can make a structure which can give life safety.

- Different combinations of rigid and semirigid connections on frames have been studied. To get higher shear capacity for smaller roof displacement one can use combination of rigid and semirigid connections of frames but numbers of the plastic members increase due to the increase of rigid floors.

6.2 Recommendations for Future Work

The present study was mainly aimed at developing the relationship between base shear and roof displacement commonly known as the "pushover curve" which includes nonlinear connection response and plastification of beam-column elements and converting the pushover curve to a capacity spectrum where the initial semi-rigidity of the connection is considered for the fundamental vibration mode or first

natural mode. The effect of the post elastic semirigidity of the connections is needed to consider getting the dynamic characteristics of the structure by modal analysis. In conversion of pushover curve to capacity spectrum, nonlinear combination of higher modal characteristics is required.

In this study, a ten storied and a six storied frame have been studied with constant bay width and story height. Influence of these parameters on the seismic performance of the structure, may be taken into account.

To get the nonlinear moment rotation behaviour of the beam-column connection top and seat angle connection is considered only. Other type of connection detailing can be considered for moment rotation behaviour of connections.

Response spectrum using site coefficients; C_A and C_V, of ATC-40 is greater than BNBC, 1993. Further study is required on response spectrum of BNBC. Analysis and design by equivalent static force method in code should be reviewed further. Provision for connection flexibility should be made in building code according to the performance of the structure.

Two dimensional plane frames have been studied. Only major axis bending of members has been considered. The program may be modified to study the three dimensional building with nonlinear semirigid connections.

The other potential limitation of this study was that, P-Δ (second-order) effects were not considered in the analysis. The program also may be modified to study P-Δ effects with nonlinear semirigid connections.

151

REFERENCES

Abdalla, K. M. and Chen, W. F. (1995), "Expanded database of semi-rigid steel connections", Computers and Structures, Vol. 56(4), 553-564.

Ahmed, B. and Nethercot, D. A. (1996) "Effect of high shear on the moment capacity of composite cruciform endplate connections", Journal of Constructional Steel Research, UK, Vol. 40, No. 2, pp. 129-163.

Ahmed, I. (1992), "Manual for the semi-rigid analysis program", Department of Civil & Structural Engineering, The University of Sheffield.

Ahmed, I. (1992), "Semi-rigid action in steel frames", Ph.D. Thesis, Department of Civil and Structural Engineering, University of Sheffield.

Ahmad, S., 'Structural Analysis and Design HI', Chapter 4, pp. 51, 60.

Ahsan, R. (1997), "Semi-Rigid Joint Action in Sway Steel Frames," M.Sc. Thesis, Department of Civil Engineering, BUET.

Ahsan R., Das P. P., Rahman S. Z., (2005), "Time History Analysis of Semi-Rigid 2D Steel Frames Under Monotonic Loading" Proceedings, First Bangladesh Earthquake Symposium Dhaka, Dec.2005.

AISC, 1985, Specification for Structural Joints using ASTM A325 or A490 Bolts, American Institute of Steel Construction, Chicago, Illinois.

AISC, 1989, Manual of Steel Construction, ASD, Ninth Edition, American Institute of Steel Construction, Chicago, Illinois.

AISC, 1993, 1997, Load and Resistance Factor Design Specifications for Structural Steel Buildings, American Institute of Steel Construction, Chicago, Illinois.

AISC, 1994a, Proceedings of the AISC Special Task Committee on the Northridge Earthquake Meeting, American Institute of Steel Construction, Chicago, Illinois.

AISC, 1994b, Northridge Steel Update 1, American Institute of Steel Construction, Chicago, Illinois.

Akbas, B. and Shen, J.(2003), Seismic Behavior of Steel Buildings with Combined Rigid and Semi-Rigid Frames, Turkish J. Eng. Env. Sci.27 (2003), 253-264.

Anderson, D. and Benterkia, Z., (1991), "Analysis of semi-rigid steel frames and criteria for their design", J. of Constr. Steel Res., Vol. 18(3), 227-237.

Anderson, D., Bijlaard, F., Nethercot, D. A. and Zandonini, R. (1987), "Analysis and design of steel framesh with semi-rigid connections", IABSE Surveys S-39/87.

Anderson, D. and Lok, T. S. (1985), "Elastic analysis of semi-rigid steel frames", Research Report No. CE/17, University of Warwick.

ANSYS 5.6- A General Purpose Finite Element System by SAS IP Inc., November 1999.

Army (1986). "Seismic Design Guidelines for Essential Buildings", Departments of the Army (TM 5-809-10-1), Navy (NAVFAC P355.1), and the Air Force (AFM 88-3, Chapter 13, Section A), Washington, D.C., U.S.A.

ATC-40, Seismic Evaluation and Retrofit of Concrete Buildings (Volume1) by Applied Technology Council, 1996.

ATC (1982). "An Investigation of the Correlation between Earthquake Ground Motion and Building Performance", Report ATC-10, Applied Technology Council, Redwood City, California, U.S.A.

AWS, 1995, Presidential Task Group Report, AWS reports are published by the American Welding Society, Miami, Florida.

Bangladesh National Building Code (BNBC, 1993), Housing and Building Research Institute, 1st Edition, Dhaka.

Batho, C. (1931), "Investigations on beam and stanchion connections", 1st Report, Steel Structures Research Committee, Department of Scientific and Industrial Research, HMSO, London, Vol. 1(2), 61-137.

Batho, C., and Lash, S. D. (1936), "Further investigations on beam and stanchion connections encased in concrete together with laboratory investigation on a full scale steel frame', Final Report, Steel Structures Research Committee, Department of Scientific and Industrial Research, HMSO, London, 276-363.

Batho, C., and Rowan, H. C. (1931), "Investigations on beam and stanchion connections', 2nd Report, Steel Structures Research Committee, Department of Scientific and Industrial Research, HMSO, London, 92.

Bernuzzi C., R. Zandonini and P. Zanon, Experimental analysis and modelling of semi-rigid steel joints under cyclic reversal loading, Journal of Constructional Steel Research, Volume 38, Issue 2, June 1996, Pages 95-123

Bjorhovde R. and J. E. Christopher Response characteristics of frames with semi-rigid connections, Journal of Constructional Steel Research, Volume 46, Issues 1-3, April-June 1998, Pages 253-254.

Bjorhovde, R. (1984), "Effect of end restraint on column strength - practical applications", Engg. J., AISC, Vol. 21(1), 1-13

Bjorhovde, R. (1984), "Effect of end restraint on column strength - practical applications", Engg. J., AISC, Vol. 21(1), 1-13.

Chen, W. F. and Lui, E. M. (1985), "Effect of joint flexibility on the behaviour of steel frames", Report No. CE-STR-85-22, School of Civil Engineering, Purdue University, West Lafayette, IN.

Chopra, A. K., (2002), "Dynamics of Structure Theory and Applications of Earthquake Engineering", 2nd edition, Prentice-Hall of India private limited, New Delhi.

Chopra A.K. and Goel R.K., Capacity – Demand Diagram Methods for Estimating Seismic Deformation of Inelastic Structures: SDOF Systems, PEER Report 1999/02, Pacific Earthquake Engineering Research Center, University of California, Berkeley.

Corradi, L. and Poggi, C. (1985), "An analysis procedure for nonlinear elastic plastic frames accounting for the spread of local plasticity", Construzioni Metalliche, (1), 1-14.

Davison, J. B., Kirby, P. A. and Nethercot, D. A. (1987), "Rotational stiffness characteristics of steel beam-to-column connections", J. Constr. Steel Res., Vol. 8, 17-54.

Davison, J. B., Kirby, P. A. and Nethercot, D. A. (1987), "Semi-rigid connections in isolation and in frame", State-of-the Art Workshop on Connections, Strength and Design of Steel Structures, Cachan, France, 195-202.

Deierlein, G. G., and Hsieh, S-H. (1990). "Seismic response of steel frames with semi-rigid connections using the capacity spectrum method." Proceedings of 4th U.S. National Conference on Earthquake Engineering, Vol. 2, pp. 863-872.

Eurocode 3: Common Unified Code of Practice for Steel Structures (1984), commission of the European Communities, Rapport EUR 8849, Brussels.

Eurocode 3 (1993), Design of steel structures

FEMA 273, NEHRP Guidelines For The Seismic Rehabilitation Of Buildings by Federal Emergency Management Agency, October 1997

FEMA-267, 1995, Interim Guidelines, Inspection, Evaluation, Repair, Upgrade and Design of Welded Moment Resisting Steel Structures, prepared by the SAC Joint Venture for the Federal Emergency Management Agency, Washington, DC.

FEMA-350, 2000, Recommended Seismic Design Criteria for New Steel Moment-Frame Buildings, prepared by the SAC Joint Venture for the Federal Emergency Management Agency, Washington, DC.

Frye, M. J., and Moriss, G. A. (1975), "Analysis of flexibly connected steel frames', Canadian Journal of Civil Engineers, Vol. 2, 280-291.

Fajfar, P. (1998). Capacity spectrum method based on inelastic demand spectra. IKIPR Report EE 3/98, University of Ljubljana, Ljubljana, Slovenia, September.

FEMA (2000). Recommended Seismic Design Criteria for New Steel Moment-Frame Buildings, FEMA-350; and State of the Art Report on Connection Performance, FEMA -355D, June, Federal Emergency Management Agency, Washington, D.C.

Freeman, S. A., Nicoletti, J. P., and Tyrell, J. V. (1975). "Evaluations of existing buildings for seismic risk - A case study of Puget Sound Naval Shipyard, Bremerton, Washington." Proceedings of 1st U.S. National Conference on Earthquake Engineering, EERI, Berkeley, 113-122.

Freeman, S. A. (1978). "Prediction of response of concrete buildings to severe earthquake motion." Publication SP-55, American Concrete Institute, Detroit, MI, 1978, pp. 589-605.

Freeman, S.A., Nicoletti, J.P. and Matsumura, G. (1984). "Seismic Design Guidelines for Essential Buildings", Proceedings of 8th World Conference on Earthquake Engineering, San Francisco, California, U.S.A.

Freeman, S. A. (1989). "Equating Dynamic Analysis to Static Code Provisions, "Seismic engineering: Research and Practice, Edited by C.A. Kirchen and A. K. Chopra, ASCE, 1989, pp. 752-760.

Freeman, S.A. (1992). "On the Correlation of Code Forces to Earthquake Demands" in "Proceedings of 4th U.S.-Japan Workshop on the Improvement of Structural Design and Construction Practices", Report ATC 15-3, Applied Technology Council, Redwood City, California, U.S.A.

Freeman, S. A. (1998). "Development and use of capacity spectrum method." Proceedings of 6th U.S. National Conference on Earthquake Engineering, Seattle, CD-ROM, EERI, Oakland.

Freeman, S.A., Paret, T.F., Searer, G.R. and Irfanoglu, A. (2004). "Musings on Recent Developments in Performance-Based Seismic Engineering", Proceedings of ASCE Structures Congress 2004, Nashville, U.S.A.

Freeman(2004), Sigmund A., "Review of The Development Of The Capacity Spectrum Method", ISET Journal of Earthquake Technology, Paper No. 438, Vol. 41, No. 1, March 2004, pp. 1-13

Galambos, T. V., (1968), Structural Members and Frames, Prentice-Hall, New York.

Goverdhan, A. V. (1984), "A collection of experimental moment-rotation curves and evaluation of prediction equations for semi-rigid connections', Ph.D. Thesis, Vanderbilt University, Nashville, TN, USA.

ICBO, 1996, "Code Change Item 178- Committee Action and Challenge 1", Building Standards, Part III, pp. 148-172, International Conference of Building Officials, Whitter, California.

Johnston, B. and Mount, E. H. (1942), "Analysis of building frames with semi-rigid connections', Trans., ASCE, Vol. 107, 993-1019.

Jones, S. W., (1980), "Semi-rigid connections and their influence on steel column behaviour", Ph.D. Thesis, University of Sheffield.

Jones, S. W., Kirby, P. A. and Nethercot, D. A. (1980), "Effect of semi-rigid connections on steel column strength', J. Constr. Steel Res., Vol. 1, 38-46.

Jones, S. W., Kirby, P. A. and Nethercot, D. A. (1981), "Modelling of semi-rigid connection behaviour and its influence on steel column behaviour', joints in structural steelworks", edited by Howlett, J. H., Jenkins, W. M. and Stainsby, R., Pentech Press, London, 5.7-5.87.

Jones, S. W., Kirby, P. A. and Nethercot, D. A. (1982), "Columns with semi-rigid joints", J. Struc. Div., ASCE, Vol. 108(2), 361-372.

Judi, H.J., Davidson, B.J. and Fenwick, R.C. (2002). "Damping for the Nonlinear Static Procedure in ATC-40", Proceedings of 7th US National Conference on Earthquake Engineering, Boston, Massachusetts, U.S.A.

Kishi, N., and Chen, W. F. (1986), "Steel connection data bank program', Structural Engineering Report no. CE-STR-86-18, School of Civil Engineering, Purdue University, West Lafayette, IN, USA.

Kishi, N. and Chen, W.F. (1986), "Database of steel beam-to-column connections", Vols I and II, Structural Engineering Report no. CE-STR-86-26, School of Civil Engineering, Purdue University, West Lafayette, IN, USA.

Kishi, N. and Chen, W. F. (1990), "Moment-rotation relations of semi-rigid connections with angles", Journal of Structural Engineering, ASCE, Vol. 116, 1990, pp. 1813-1834.

Kishi, N., Chen, W. F., Goto, Y. and Hasan, R. (1996), "Behaviour of tall buildings with mixed use of rigid and semi-rigid connections", Computers & Structures, Vol. 61(6), 1193-1206.

Kishi, N., Chen, W. F., Goto, Y. and Matsuoka, K. G. (1991), "Applicability of three-parameter power model to structural analysis of flexibly jointed frames", Mechanics Computing in 1990's and Beyond Proc. / EM, Div / ASCE, Columbus, OH, 238-242.

Kishi, N., Chen, W. F., Goto, Y. and Matsuoka, K. G. (1993), "Design aid of semi-rigid connections for frame analysis", Engng. J. AISC, Vol. 30, 90-107.

Lee, S.L. (1987), "Large deformation elastic-plastic stability analysis of plane frames with partially restrained connections", M.S. Thesis, Vanderbilt University, Nashville, TN.

Leon T. Roberto, Semi-rigid composite construction, Journal of Constructional Steel Research, Volume 15, Issues 1-2, 1990, Pages 99-120

Lui, E.M. (1985), "Effect of Connection Flexibility and Panel Zone Deformation on the Behaviour of Plane Steel Frames", Ph.D. Thesis, School of Civil Engineering, Purdue University, West Lafayette, IN.

Lui and Chen Wai-Fah (1988) "Behavior of Braced and Unbraced Semi-Rigid Frames", International Journal of Solids and Structures, Volume 24, Issue 9, Pages 893-913

Mahaney, J. A., T. F. Paret, B. E. Kehoe, and S. A. Freeman, a 1993, "The Capacity Spectrum Method for Evaluating Structural Response During the Loma Prieta earthquake," National Earthquake Conference, Memphis.

Majid, K. I. and Anderson, D., (1968), "The computer analysis of large multi-storey framed structures", The Struc. Engr., Vol. 46, 357-365.

M. N. Nader and A. Astaneh, Dynamic behavior of flexible, semirigid and rigid steel frames, Journal of Constructional Steel Research, Volume 18, Issue 3, 1991, Pages 179-192.

Nethercot, D. A. (1974), "Residual stresses and their influences upon the lateral buckling of rolled steel beams", Struc. Engr., Vol. 52(3), 89-96.

Nethercot, D. A. (1985), "Steel beam to column connections - a reveiw of test data and their applications to the evaluation of joint behaviour on the performance of steel frames', CIRIA Project Study, London, 338.

Nethercot, D. A., Davison, J. B. and Kirby, P. A. (1988), "Connection flexibility and beam design in non-sway frames", Engg. J., AISC, Vol. 25(3), 99-108.

Newmark, N. M., and W. J. Hall, 1982, "Earthquake Spectra and Design", EERI Monograph Series, Earthquake Engineering Research Institure, Oakland, California.

Ohi, K. and Lin, X. (1997), "Hybrid simulation of seismic responses of semi-rigidly jointed steel frames," Belletin of Earthquake Resistant Structure Research Center, Institute of Industrial Science, University of Tokyo, No. 30, 19-26.

Poggi, C. and Zandonini, R. (1985), "Behaviour and strength of steel frames with semi-rigid connections", Session on Connection Flexibility and Steel Frames, ASCE Convention, Detroit.

Richard, R. M. and Abbott, B. J. (1975), "Versatile elastic-plastic stress-strain formula", J. Engng. Mech. ASCE, Vol. 101, 511-515.

Richard, R., Partridge, J.E., Allen, J., and Radau, S., 1995, "Finite Element Analysis and Tests of Beam-to-Column Connections," Modern Steel Construction, Vol. 35, No. 10, pp. 44-47, American Institute of Steel Construction, Chicago, Illinois.

Rifai, A. M., (1987), "Behaviour of columns in sub-frames with semi-rigid joints", Ph.D. Thesis, University of Sheffield.

SAC 94-01, 1994, Proceedings of the Invitational Workshop on Steel Seismic Issues, Los Angeles, September 1994, prepared by the SAC Joint Venture for the Federal Emergency Management Agency, Washington, DC.

SAC 94-01, 1994b, Proceedings of the International Workshop on Steel Moment Frames, Sacramento, December, 1994, prepared by the SAC Joint Venture for the Federal Emergency Management Agency, Washington, DC.

SAC 95-02, 1995, Interim Guidelines: Evaluation, Repair, Modification and Design of Welded Steel Moment Frame Structures, prepared by the SAC Joint Venture for the Federal Emergency Management Agency, Report No. FEMA-267, Washington, DC.

SAC 95-09, 1995, Background Reports: Metallurgy, Fracture Mechanics, Welding, Moment Connections and Frame Systems Behavior, prepared by the SAC Joint Venture for the Federal Emergency Management Agency, Report No. FEMA-288, Washington, DC.

Suarez, L.E., Singh, M.P. and Matheu, E.E. (1996), "Seismic response of structural frameworks with flexible connections," Computers & Structures, Vol. 58(1), 27-41.

Takanashi K., Zhengyu Fu, Kenichi Ohi, and Xiaoguang Lin, Seismic behavior of steel frames with semi-rigid connections and braces, Journal of Constructional Steel Research, Volume 46, Issues 1-3, April-June 1998, Pages 440-441

Uniform Building Code (UBC, 1994).

Wang, C. K., 'Statically Intermediate Structures', International Student Edition, Chapter 8, pp. 216-288

Wilson, W. M. and Moore, H. F. (1917), "Tests to determine the rigidity of riveted joints in steel structures', Bulletin no. 104, Engineering Experiment Station, University of Illinois, Urbana, USA.

WJE (1996). "Seismic Dynamic Analysis for Buildings", Report Prepared for U.S. Army Engineering Division, Wiss, Janney, Elstner Associates, Inc., Emeryville, California, U.S.A.

Young, C. R. and Dunbar, W. B. (1928), "Permissible stresses on rivets in tension', Bulletin no. 8, Section no. 16, School of Engineering Research, University of Toronto, Canada.

Appendix-A

Three Parameter Power Model

The three-parameter power model (kishi and chen, 1990) is used in this study to describe the non-linear M-θ_r curve of semi-rigid connections. This relationship was first proposed by Richard and Abbott, (Richard and Abbott, 1975). The model has three parameters: initial connection stiffness R_{ki} ; ultimate moment capacity M_u ; and shape parameter n. It has the following simple nondimensional form:

$$m = \frac{\theta}{(1+\theta^n)^{1/n}}$$ (Equation A-1)

in which M and θr are moment and relative rotation in connection respectively, $m = M / M_u$, $\theta = \theta_r / \theta_0$ and $\theta_0 = M_u / R_{ki}$. General shapes of moment-rotation curves of equation A.1 are shown in Fig. A.1. The two parameters of R_{ki} and M_u can be obtained by using simple structural mechanics and the third parameter n is obtained by curve fitting with the test data (Kishi et al, 1991).
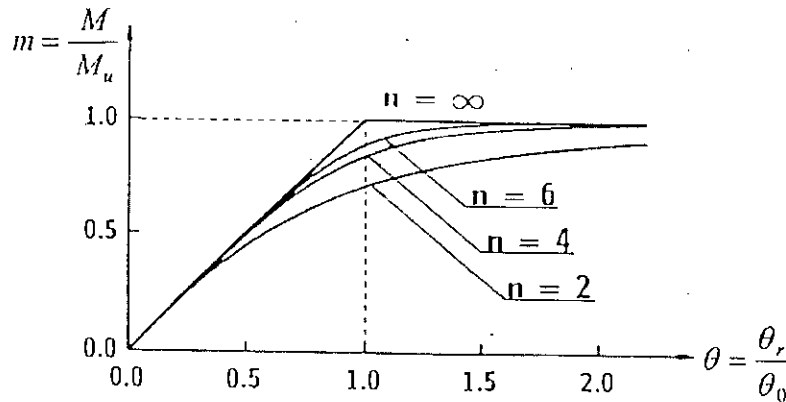
Figure A.1 General Curves of Non-Dimensional Three Parameter Power Model

A.1 Determination of Three Parameters

For given beam, column and angles, the initial connection stiffness R_{ki} and ultimate moment capacity M_u can be obtained by using nomographs provided in reference (kishi et al, 1996). Here is a brief review of the nomographs for top- and seat angle connections with/without double web angle (Figure A.2) will be made.
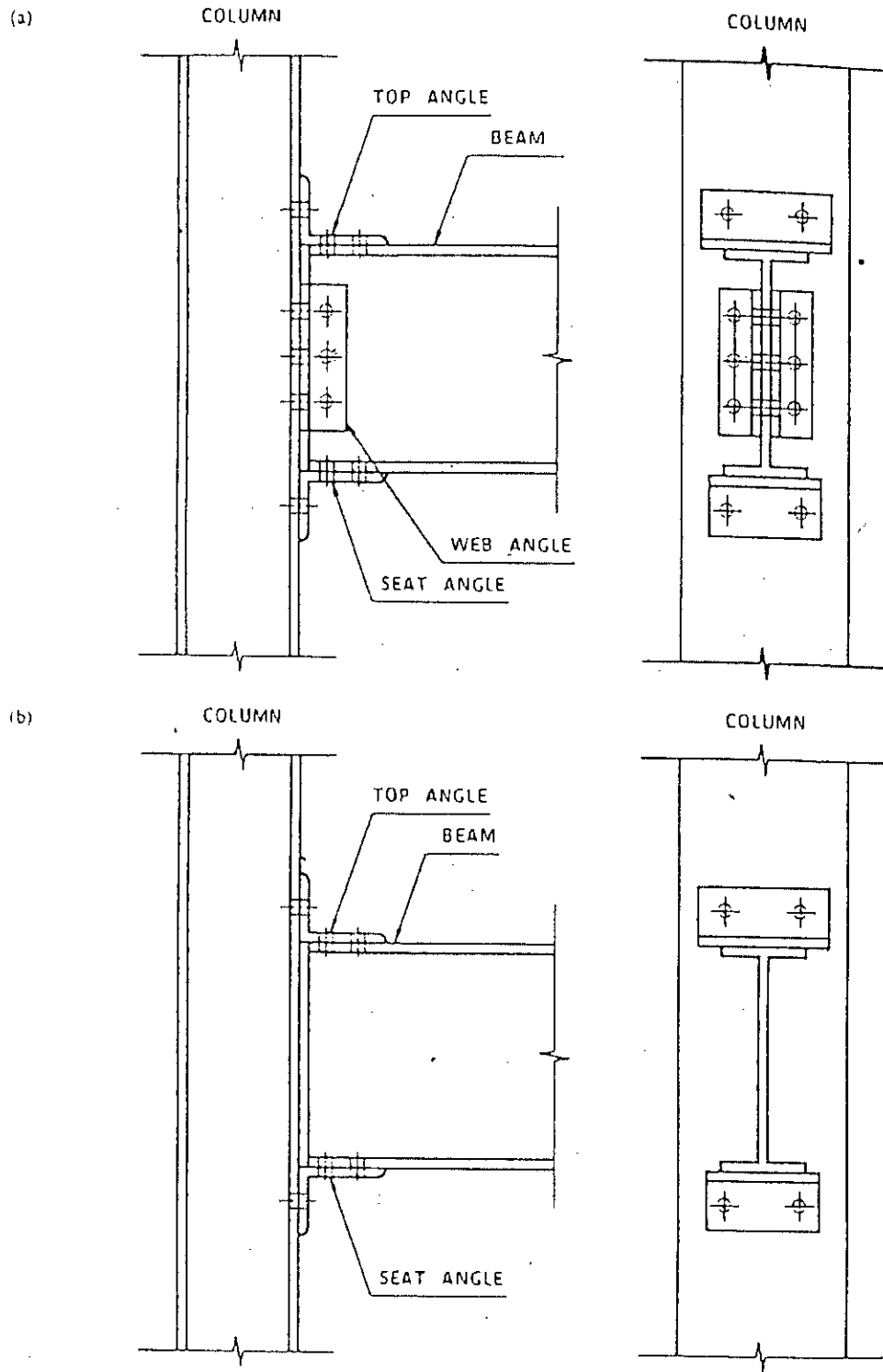
Figure A.2 Connections used as Semi-rigid Connections: Top and Seat-angle Connections (a) with and (b) without Double Web-angle

162

Defining the dimensions as shown in Figure A.3.

t = Angle thickness;

k = Gauge distance from heel to the top of fillet;

l = angle length;

g = distance between heel to the centre of fastener closest to web or flange of beam;

W = nut width;

$I_0 = t^3/12$ = geometrical moment of inertia per unit length of plate element of angle;

$M_0 = \sigma_y\, t^2/4$ = pure plastic bending moment per unit length of plate element of angle.

Here, σ_y is the yielding stress of steel and $\sigma_y = 25$ KN/cm² is used in this study. It is assumed that top and seat angles are of the same dimensions. All bolts used here are of nominal size of D = 20 mm and heavy hex nuts with nominal size of W = 30 mm.

The following non-dimensional parameters are used in the nomographs:

$$\beta = \frac{g}{l}, \ \ \gamma = \frac{l}{t}, \ \ \delta = \frac{d}{t}, \ \ \omega = \frac{W}{t}, \ \ \rho = \frac{t_w}{t_t}, \ \ \kappa = \frac{k}{t}.$$

in which d is the height of beam and subscripts "t" and "w" denote top angle and web angle, respectively.

Figures A.4 and A.5 are the nomogrpahs for the initial connection stiffness R_{ki} (R_{kits} in Fig A.4 and the ultimate moment capacity M_u (M_{uts} in Fig A.5) for top- and seat-angle connections without double web angle. In Fig A.4, β_t' is defined as follows:

$$\beta_t' = \beta_t - \frac{1}{2\gamma_t}(1 + \omega_t)$$ (Equation A-2)

and β_t^* in Fig A.5 is defined as

$$\beta_t^* = \beta_t'\gamma_t - k_t$$ (Equation A-3)

For top- and seat-angle connections with double web-angle, the initial connection stiffness R_{ki} and the ultimate moment capacity M_u can be evaluated by summing the contribution of top- and seat-angle part and double web-angle part as

$$\frac{R_{ki}}{EI_{ot}} = \frac{R_{kits}}{EI_{ot}} + \frac{R_{kiw}}{EI_{ot}} = (D_{ts} + D_w)(1 + \delta_t)^2 \ , \ \ \frac{M_u}{M_{ot}t_t} = \frac{M_{uts}}{M_{ot}t_t} + \frac{M_{uw}}{M_{ot}t_t}$$ (Equation A-4, A-5)
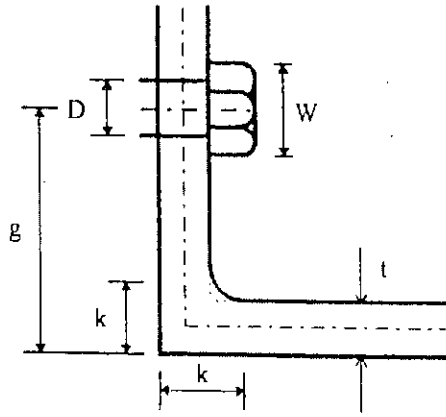
Figure A.3 Main Parameters for an Angle
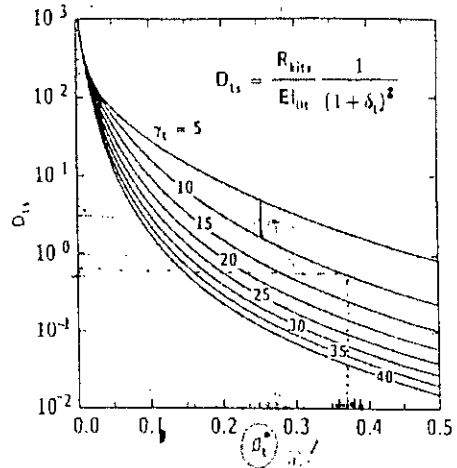
Figure A.4 Coefficients D_{ts} for R_{kits} of Connections without Double Web-angle
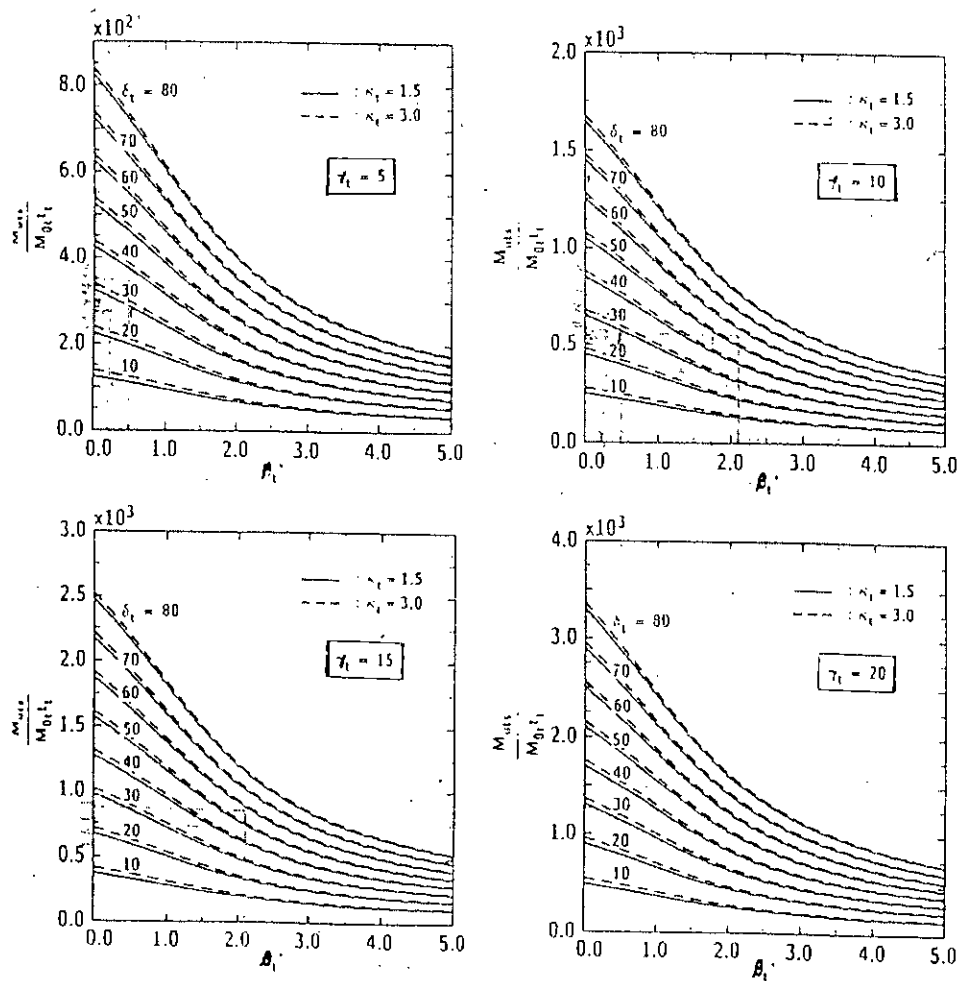
Figure A.5 Ultimate Moment Capacity for the Variation of δ_t for Connections without Double Web-angle

164

The values for top- and seat angle part can be obtained by the nomographs in Figures A.4 and A.5. The initial connection stiffness R_{kiw} on the double web angle connection part can be obtained from Fig. A.6. In this Figure, β_w' is defined as $\beta_w' = \beta_w - \dfrac{1}{2\gamma_w}(1+\omega_w)$ (A.6), that is, in the same way β_t' is defined in equation A.2. The nomograph of the ultimate moment moment capacity M_{uw} for web angle is shown in Fig. A.7.

The shape parameter n can be determined empirically and statistically as shown in figure A.8 by applying the least square technique. The equations for the top- and seat-angle connection with/without double web-angle are listed in Table A-1.

Table A-1 Empirical Equation for Shape Parameter n.

Connection Type	N	
Top and seat angle connections (with double web angle)	$1.398 \log_{10} \theta_0 + 4.631$ 0.827	if $\log_{10} \theta_0 > -2.721$ otherwise
Top and seat angle connections (without double web angle)	$2.003 \log_{10} \theta_0 + 6.070$ 0.302	$\log_{10} \theta_0 > -2.880$ otherwise

A.2 Example

Yield stress of steel, $\sigma_y = 36$ ksi $= 25$ KN/cm^2

Nominal Size of Bolts, $D = \,^7/_8$ inch $= 22.225$ mm

Nominal Size of Nuts, $W = 1\,\tfrac{1}{2}$ inch $= 38.1$ mm

Distance Between Heel of the web angle to the centre of fastener closest to web of beam, $g_w = 1\,\tfrac{3}{4}$ inch $= 45$mm

Distance Between Heel of the top or seat angle to the centre of fastener closest to flange of beam, $g_t = 3$ inch $= 75$ mm

$$D_w = \frac{R_{kiw}}{EI_{m}} \frac{t}{(1+\delta_t)^2}$$
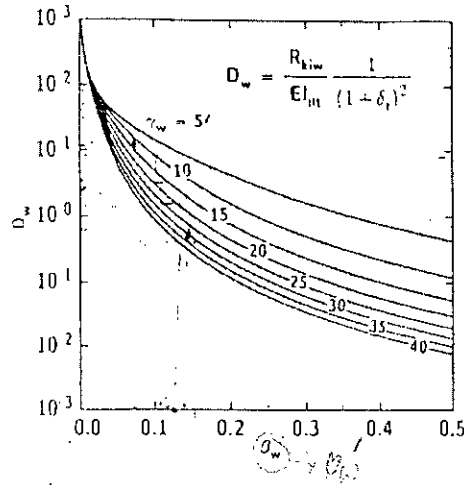
Figure A.6 Coefficient D_w for R_{kiw} of Double web-angle Part
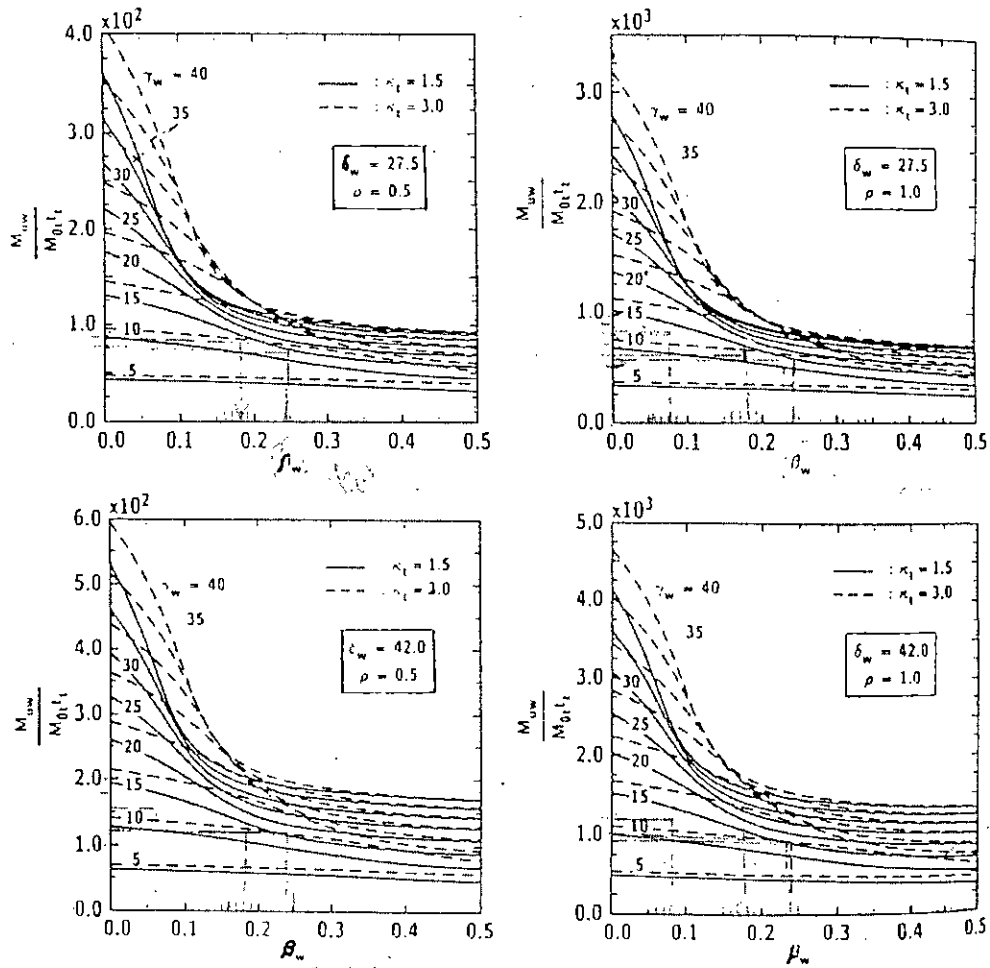
Figure A.7 Ultimate Moment Capacity for the Variation of γ_w for Double Web-angle part
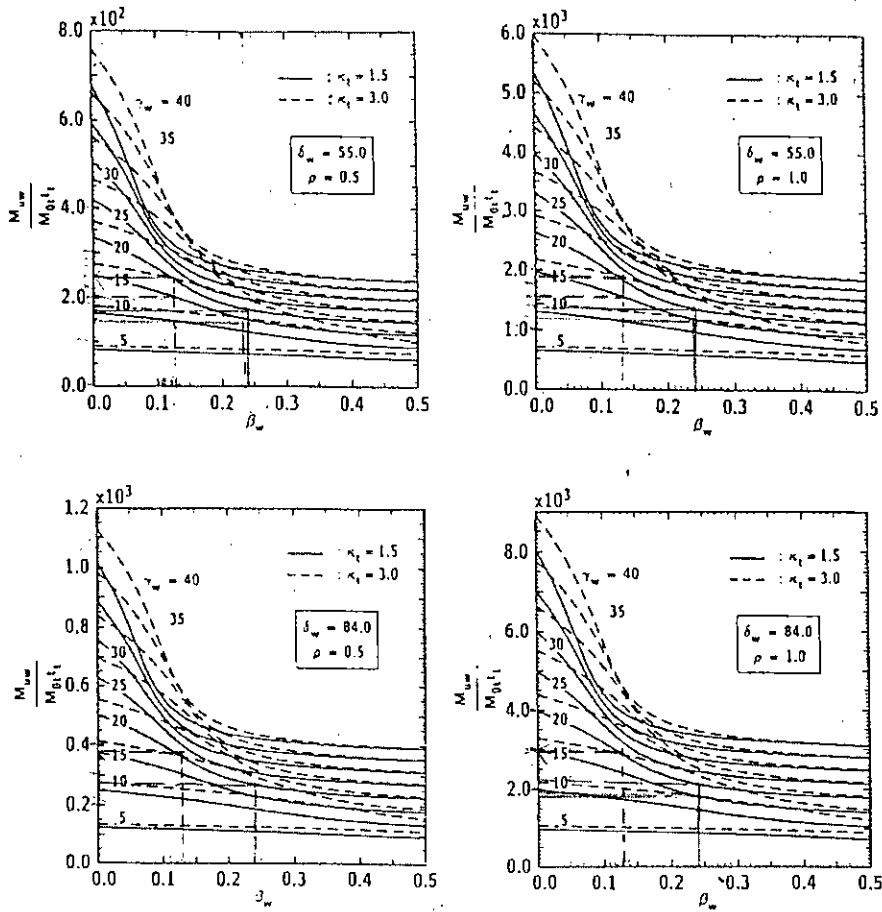
Figure A.7-continued
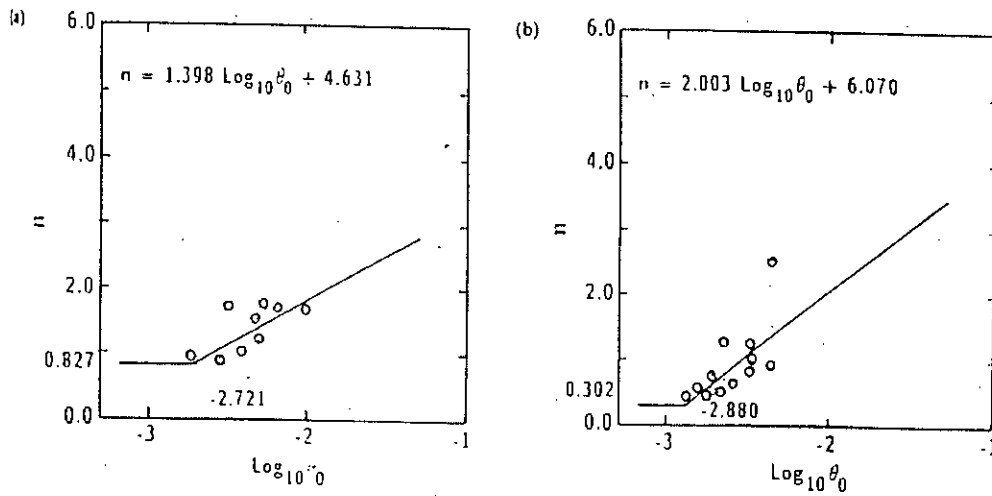
Figure A.8   Distribution of n: Top and Seat-angle Connections (a) with and (b) without Double Web-angle

Joint Type A

Top and Seat Angle: L 6 x 6 x 1

Web Angle: L 4 x 4 x 7/8

Beam depth: d = 24 inch = 609.6 mm

t_t = 25.4 mm; t_w = 22.225 mm

l_t = 25.4 cm; l_w = 25.4 cm

Calculation for Top and Seat Angles:

$$\beta_t = \frac{g_t}{l_t} = 0.295275591; \ \gamma_t = \frac{l_t}{t_t} = 10; \ w_t = \frac{W}{t_t} = 1.5$$

$$\beta_t^{\ \prime} = \beta_t - \frac{1}{2\gamma_t}(1+\omega_t) = 0.170275591$$

From Figure A.4 D_{ts} = 7

Let k = 38.1 mm; $k_t = \frac{k}{t} = 1.5$

$$\beta_t^{\ *} = \beta_t^{\ \prime}\gamma_t - k_t = 0.203$$

$$\delta_t = \frac{d}{t_t} = 24$$

From Figure A.5 $\frac{M_{uts}}{M_{ot}t_t} = 510$

Calculation for Web Angle:

$$\beta_w = \frac{g_w}{l_w} = 0.18 \ ; \ \gamma_w = \frac{l_w}{t_w} = 11.43 \ ; \ w_w = \frac{W}{t_w} = 1.72$$

$$\beta_w^{\ \prime} = \beta_w - \frac{1}{2\gamma_w}(1+\omega_w) = 0.0584$$

From Figure A.6 D_w = 25

$$\delta_w = \frac{d}{t_w} = 27.4286$$

$$\rho = \frac{t_w}{t_t} = 0.875$$

From Figure A.7 $\frac{M_{uw}}{M_{ot}t_t} = 440$

168

Computation of Three Parameters

$$\frac{R_{ki}}{EI_{ot}} = \frac{R_{kis}}{EI_{ot}} + \frac{R_{kiw}}{EI_{ot}} = (D_{ts} + D_w)(1 + \delta_t)^2 = 20000$$

$E = 210 \text{ KN/mm}^2$

$$I_{ot} = \frac{t_t^3}{12} = 1365.588667 \text{ mm}^3$$

Therefore, Initial connection stiffness $R_{ki} = 573547240$ KN-cm/rad

$$\frac{M_u}{M_{ot} t_t} = \frac{M_{uts}}{M_{ot} t_t} + \frac{M_{uw}}{M_{ot} t_t} = 950$$

$$M_{ot} = \frac{\delta_y t_t^2}{4} = 40.32 \text{ KN-cm/cm}$$

Therefore, Ultimate moment capacity $M_u = 97298.2$ KN-cm

$$\theta_0 = \frac{M_u}{R_{ki}} = 0.000169643; \quad \log_{10} \theta_0 = -3.770464422$$

Therefore $n = \qquad 0.827$

With the three parameters thus determined above the joint rotation at any value of moment can be determined by the following equation.

$$m = \frac{\theta}{(1 + \theta^n)^{\frac{1}{n}}} \quad \text{Where, } m = \frac{M}{M_u}; \ \theta = \frac{\theta_r}{\theta_0}; \ \theta_0 = \frac{M_u}{R_{ki}}$$

Therefore $M = \dfrac{\dfrac{\theta_r \times 0.001}{\theta_0}}{\left[(1 + (\dfrac{\theta_r \times 0.001}{\theta_0})^n \right]^{\frac{1}{n}}} \times M_u$ where θ_r is in milli-radian

Appendix B

Computation of Integration Points

B.1 Integration Points

The geometry, node locations, and the coordinate system for this element are shown in BEAM23 Figure B.1. Any one of four cross-sections may be selected with the appropriate value of KEYOPT(6). The element is defined by two nodes, the cross-sectional area, moment of inertia, the height for rectangular beams, the outer diameter (OD), and the wall thickness (TKWALL), for thin-walled pipes, the outer diameter for solid circular bars, and the isotropic material properties.
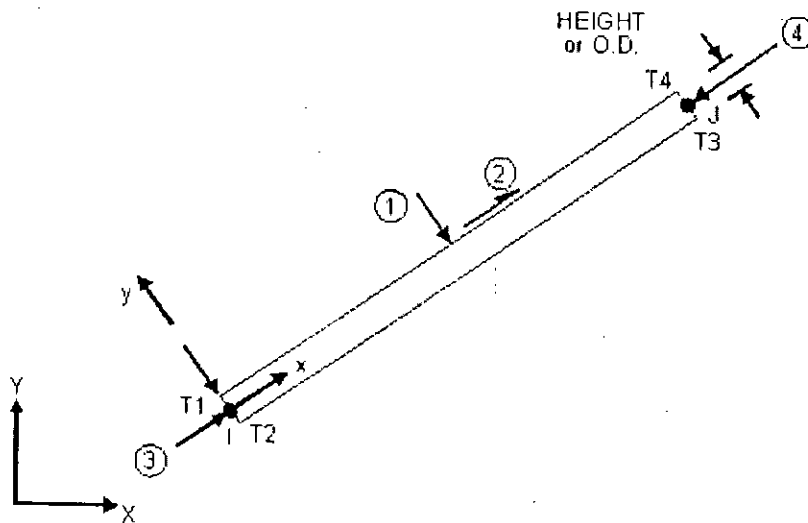
Figure B.1 Beam23

The general cross-section option (KEYOPT(6)=4) allows inputting a section height and a five-location area distribution. If the section is symmetric, only the first three of the five areas need be input since the fourth area defaults to the second and the fifth area defaults to the first. The areas input should be a weighted distribution at the -50% integration

point A(-50), the -30% integration point A(-30), the 0% integration point A(0), the 30% integration point A(30), and the 50% integration point A(50). Each area A(i) is as shown in *Characteristics*. The height is defined as the distance between the $\pm$ 50% integration points, and is not necessarily the distance between the outermost fibers of the section. Determination of the input areas is accomplished as follows. Estimate one of the input areas by the formula A(i) = L(i) x HEIGHT, where L(i) is the width of the section at integration point i (see *Characteristics* b). Substitute this area along with the section moment of inertia, I_{zz}, and total area, A, into the above equations and solve them simultaneously for the remaining two input areas. A(0) is usually the easiest to estimate; for instance, as a first guess A(0) for an I-beam would be the web thickness times the height. A trial and error procedure (by modifying the estimated input area) may be needed if the calculated input areas are inconsistent, such as a negative area. The input areas, A(i), are related to the true areas, $A_t(i)$, corresponding to each integration point, by:

a) Printout Locations

$(A(i) = L(i) \times HEIGHT)$

b) Weighting Functions for General Section (KEYOPT(6) = 4)
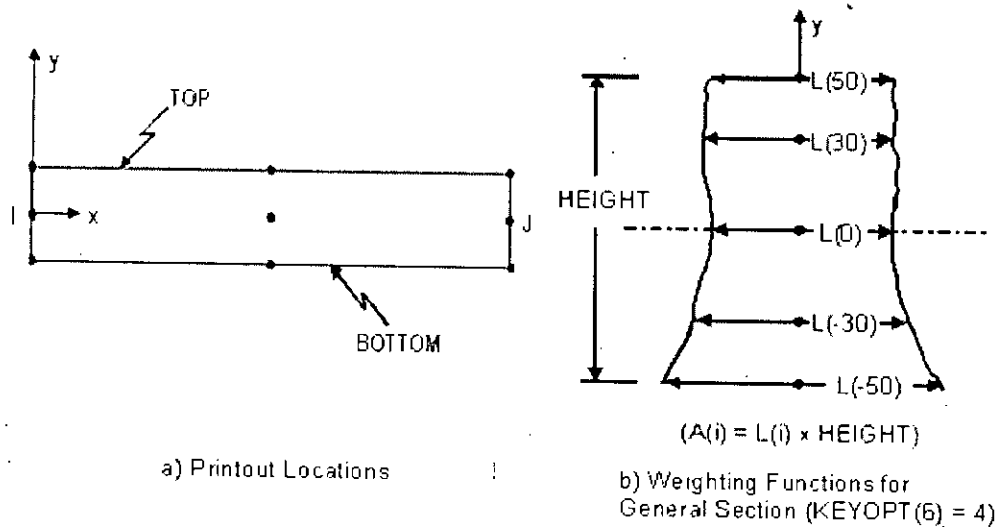
Figure B.2: BEAM23 Characteristics

B.2 Relation Between Input Areas and True Areas

$A_t(-50) = 0.0625\, A(-50)$ ... ... (Equation B.1)

$A_t(50) = 0.0625\, A(50)$ ...   . (Equation B.2)

$A_t(-30) = 0.28935\, A(-30)$ ... ... (Equation B.3)

$A_t(30) = 0.28935\, A(30)$ ...   . (Equation B.4)

$A_t(0) = 0.29630 \times A(0)$ ...   . (Equation B.5)

For WF sections the following formulae can be derived:

$A(0) = d \times t_w$ ...   . (Equation B.6)

$$A_t(0) + [A_t(30) + A_t(50)] \times 2 = A$$

$$\Rightarrow A_t(30) + A_t(50) = \frac{A - A_t(0)}{2}$$

$$\Rightarrow A_t(50) = \frac{A - A_t(0)}{2} - A_t(30) \quad ... \quad ... \quad ... \quad ... \text{(Equation B.7)}$$

172

$$[A_t(30) \times \{\frac{3}{5} \times \frac{d}{2}\}^2 + A_t(50) \times \{\frac{d}{2}\}^2] \times 2 = I$$

$$\Rightarrow [A_t(30) \times \frac{9}{100} d^2] + [\frac{A - A_t(0)}{2} - A_t(30)]\frac{d^2}{4} = I$$

$$\Rightarrow A_t(30) = \frac{25}{32} A - \frac{25}{8} \frac{I}{d^2} - \frac{25}{32} A_t(0) \dots \quad \dots \quad \dots \quad \dots \text{(Equation B.8)}$$

B.3 Sample Calculation

WF Section W27X84

d, in	b_f, in	t_f, in	t_w, in	I, in^4	A, in^2
24.06	12.75	0.75	0.500	3100.00	30.60

$$A(0) = 24.06 \times 0.50 = 12.03 in^2 \qquad \text{(Ref: Equation B.6)}$$

$$A_t(0) = 0.29630 \times 12.03 = 3.56 in^2 \qquad \text{(Ref: Equation B.5)}$$

$$A_{t(30)} = \frac{25}{32} \times 30.60 - \frac{25}{8} \times \frac{3100}{24.06^2} - \frac{25}{32} \times 3.56 = 4.40 in^2 \qquad \text{(Ref: Equation B.8)}$$

$$A_t(50) = \frac{30.60 - 3.56}{2} - 4.40 = 9.12 in^2 \qquad \text{(Ref: Equation B.7)}$$

$$A(30) = A(-30) = \frac{4.40}{0.28935} = 15.21 in^2 \qquad \text{(Ref: Equation B.3 or B.4)}$$

$$A(50) = A(-50) = \frac{9.12}{0.0625} = 145.92 in^2 \qquad \text{(Ref: Equation B.1 or B.2)}$$

173

Appendix-C

Background Information on Basic Principles of Structural Dynamics

C.1 Modal Quantities

C.1.1. Modal Participation Factor

The modal participation factor for each mode can be calculated for each mode using the following equation

$$PF_m = [\frac{\sum_{i=1}^{N}(w_i \phi_{im} / g)}{\sum_{i=1}^{N}(w_i \phi_{im}^2 / g)}]$$
(Equation C-1)

where:

PF_m = Modal participation factor for mode m

w_i / g = Mass assigned to level i.

ϕ_{im} = Amplitude of mode m at level i.

N= Level N, the level which is uppermost in the main portion of the structure.

The units of participation factor PF_m are dependent on the normalization procedure, in some references, ϕ is normalized to 1.0 at the uppermost mass level, other references will normalize the value of $\sum(w/g)\phi^2$ to 1.0. It should be noted that some references define a "modal story participation factor", PF_{im} as the quantity within the brackets in the above equation multiplied by the quantity ϕ_{im}, the amplitude of mode m at level i. the modal story participation factor, PF_{im}, is unitless.

$$PF_{im} = PF_m\phi_{im}$$

(Equation C-2)

C.1.2. Effective mass coefficient

The effective mass coefficient will be calculated for each mode using the following equation.

$$\alpha_m = \frac{[\sum_{i=1}^{N}(w_i\phi_{im})/g]^2}{[\sum_{i=1}^{N}(w_i/g)]\sum_{i=1}^{N}(w_i\phi_{im}^{2}/g)}$$

(Equation C-3)

The above quantity is unitless.

C.1.3. Modal story accelerations

The story accelerations for mode m are calculated using the following equation

$$a_{im} = PF_m\phi_{im}S_{am}$$

(Equation C-4)

175

where:

a_{im} = Story acceleration at level i for mode m (as a ratio of the acceleration of gravity, g).

S_{am} = Spectral acceleration for mode m from the response spectrum (as a ratio of the acceleration of gravity, g).

C.1.4. Modal Story Lateral Forces

The lateral forces (mass x acceleration) for mode m are calculated using the following equation

$$F_{im} = PF_m \phi_{im} S_{am} w_i$$
(Equation C-5)

where:

F_{im} = Story lateral force at level i for mode m.

w_i = Weight at or assigned to level i.

C.1.5. Modal Base Shear

The total lateral force corresponding to mode m is calculated using the following equation . Note that the sum of F_{im} from roof to base will equal to V_m.

$$V_m = \alpha_m S_{am} W$$
(Equation C-6)

where: W= Total deal load of the building and applicable portions of other loads.

176

C.1.6. Modal Displacements

modal lateral story displacements are related to modal spectral displacements by the following equation.

$$\delta_{im} = PF_m \phi_{im} S_{dm} = PF_{im} S_{dm}$$

where:

δ_{im} = Lateral displacement at level i for mode m.

S_{dm} = Spectral displacement for mode m calculated from the acceleration response spectrum (ie $S_{dm} = S_{am}(T/2\pi)^2 g$).

C.2. Explanation and Use of Modal Participation Factors and Effective Mass Coefficients

C.2.1. Single Degree of Freedom (SDOF) Systems.

The fundamental structural system is simple oscillator or SDOF system shown in Figure C.1a. This system is represented by a single lump of mass on the upper end of a vertically cantilevered pole or by a mass supported by two columns. This system is used in textbooks to illustrate fundamental principles of dynamics. It represents two kinds of real structures.: a single column structure with a relatively large mass at its top; and a single story frame structure with flexible columns and a rigid roof system. In the idealized system, the mass (M) represent the weight (W) of the system divided by the acceleration due to gravity (g). These quantities are related by the formula M=W/g. The pole or columns stiffness (K) of the system, which is equal to a horizontal force (F) applied to the mass divided by the displacement (δ) resulting from that force. These

177
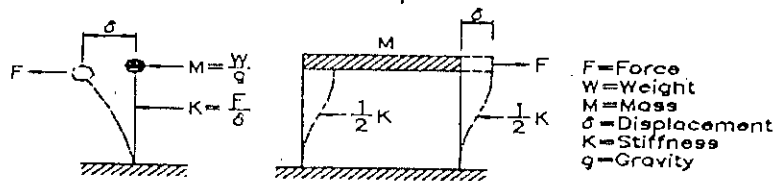
a. Idealized single lumped mass system
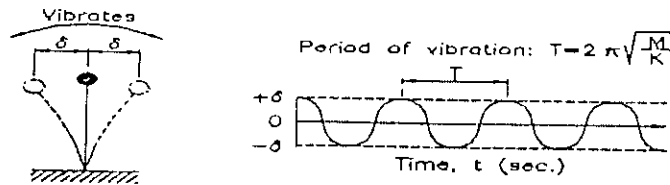
b. Free vibration (no damping)
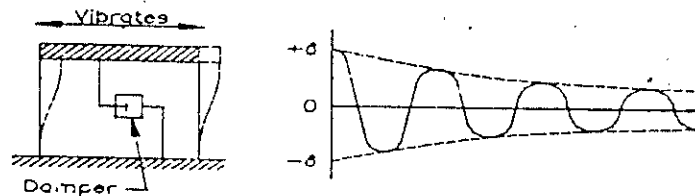
c. Damped free vibration

Figure c.1 Single Degree of Freedom Systems

quantities are related by the formula $K = F/\delta$. If the mass is deflected and then quickly released, it will freely vibrate at a certain frequency which is called its natural frequency of vibration. The period of vibration (T), which is the inverse of the frequency of vibration, is the time taken for the mass to move through one complete cycle (ie from one side to the other and back again (Figure C.1b). The period is equal to $2\pi(M/K)^{1/2}$.

The internal energy dissipation or friction within a structure causes the vibrational motion and to damp out as shown in Figure C.1c. The amount of damping is defined in terms of a ratio β, or percentage, of critical damping. In an ideal system having no damping ($\beta = 0$), a system, once displaced, would vibrate forever, ie, as in Figure C.1b. In a real system where there is some damping, the amplitude of motion will decrease for each cycle until the structure stops oscillating and comes to rest (Figure C.1c). The greater the

178

damping, the sooner the structure comes to rest. If the structure has damping equal to 100 percent of critical damping ($\beta=1$), the displaced structure will come to rest without crossing the initial point of zero displacement.
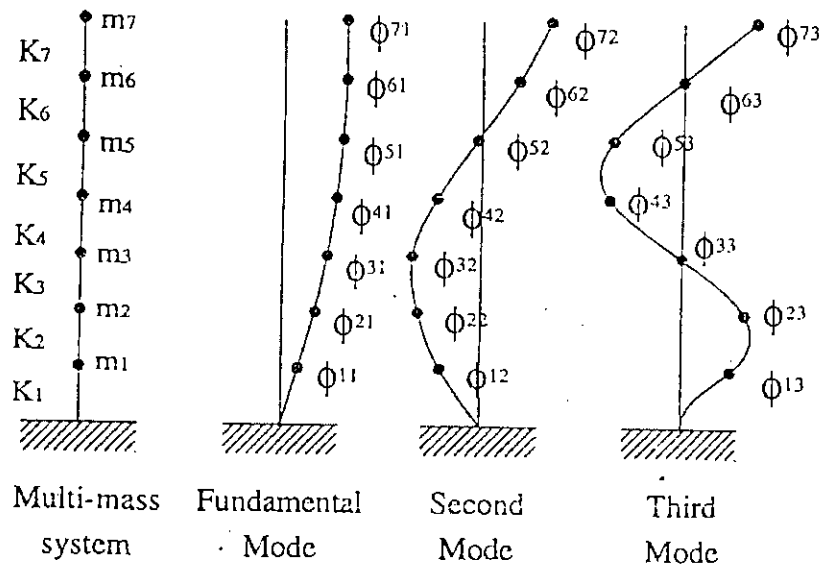
Figure c.2   Multi-Degree of Freedom System

C.2.2. Multi-Degree-of-Freedom (MDOF) Systems.

Multistory buildings are analyzed as MDOF systems. They can be represented by lumped masses attached at intervals along the length of a vertically cantilevered pole (Figure C.2). Each mass can be deflected in one direction or another; for example, all masses may simultaneously deflect in the same direction (the fundamental period of vibration), or some masses may go to the left while others are going to the right (higher modes of vibration). An idealized system, such as the one shown in Figure C.2 , has a number of mode equal to the number of masses. Each mode has its own natural modal period of vibration with a unique mode shape being formed by a line connecting the deflected masses (the first three mode shapes are shown in Figure C.2). When oscillating motion is applied to the base of the multi mass system, these masses move. The deflected shape is a

combination of all the mode shapes; but modes having periods that are near, or equal to, predominant periods of the base motion will be amplified more than the other modes.

Each mode of an MDOF system can be represented by an equivalent SDOF system having a normalized (M^*) and stiffness $(K)^*$ where the period equals to $2\pi(M^*/K^*)^{1/2}$. M^* and K^* are functions of mode shapes, mass and stiffness. This concept, as shown in Figure C.3, provides the computational basis for using site specific earthquake response spectra based on SDOF systems for analyzing multi storied buildings. With the period, mode shape, mass distribution, and response spectrum, one can compute the deflected shape, story accelerations, forces, and overturning moments.

a. Fundamental mode of a multi-mass system

b. Equivalent single mass system

M^* and K^* are effective values of mass and stiffness that represent the equivalent combined effects of the story masses (m) and the stiffnesses (k). W^* is the effective weight ($=M^*g$).
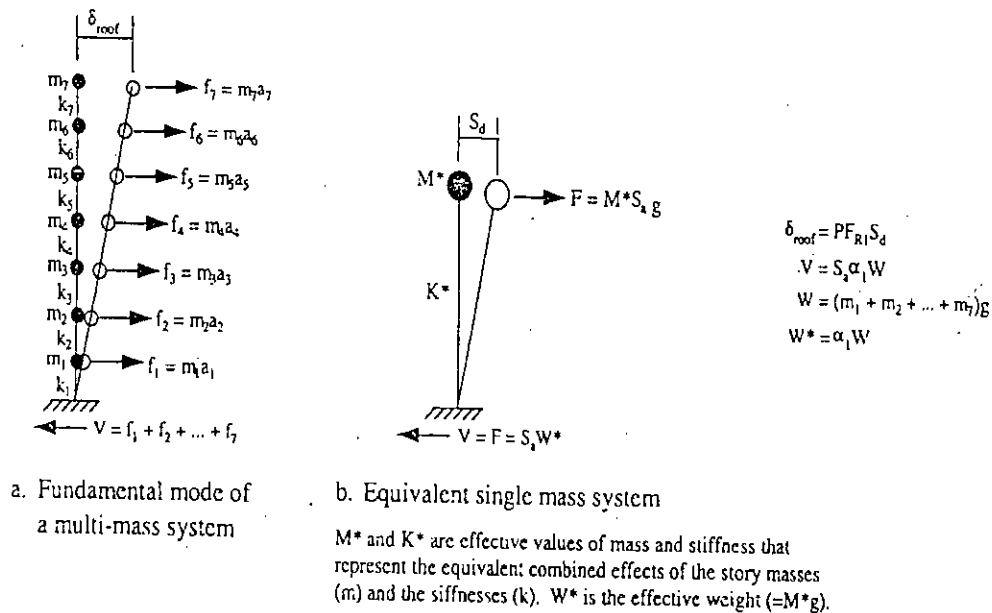
Figure C.3 . MDOF System Represented By a Single Mass System

C.2.3. Modal Participation Factors.

In Figure C.3 diagram b is equivalent to diagram a. In other words, if during an earthquake the mass M^* moves distance S_d, the roof of the building will move distance δ_{ROOF}. The ratio of δ_{ROOF} to S_d is, by definition, the modal participation for the fundamental mode at the roof level. This is the PF_{im} in Equation C.2, where i is the roof and m is mode 1. PF_m is calculated from Equation C.1 using the m-values and the

fundamental ϕ values in Figure C.2 (note mass m equals weight w divided by gravity), where m_7 is the mass at the roof and ϕ_{71} is the mode shape at roof (level 7) for mode 1.

Therefore, $PF_1 = (\dfrac{m_7\phi_{71} + m_6\phi_{61} + -------- + m_1\phi_{11}}{m_7\phi_{71}^2 + m_6\phi_{61}^2 + -------- + m_1\phi_{11}^2})\phi_{71}$ and

$$\delta_{ROOF} = PF_{R1}S_d \quad \text{(Figure C.3a)}$$

C.2.4. Effective Mass Coefficient.

In Figure C.3a the sum of f1 through f7 is the shear V, at the base of the structure for the fundamental mode. The f values are the same as the F_{im} values in Equation C.5 (eg f7= F_{71}, m_7= w_7/g, and a_7= $PF_1\phi_{71}S_{a1}g$ per Equation C.4). The sum of story forces, F_{im}, for mode 1 is equal to the base shear V_m for m=1. V_m= $\alpha_m S_{am}W$ (Equation C.6) is the base shear in diagram a in Figure C.3 for mode 1. $V=S_aW^*$ is the base shear in diagram b. W is the total weight (or mass x g) and W^* is the effective weight. $W^*=\alpha_m W$ where α_m is the effective mass coefficient for mode m. the formula for calculating α_m is given in Equation C.3. Thus for mode 1,

$$\alpha_1 = \dfrac{(m_7\phi_{71} + m_6\phi_{61} + ------- + m_1\phi_{11})^2}{(m_7 + m_6 + ---- +m_1)(m_7\phi_{71}^2 + m_6\phi_{61}^2 + -------- + m_1\phi_{11}^2)} \quad \text{and}$$

$V_1 = \alpha_1 WS_{a1}$ (Figure C.3a).

181

Appendix-D

Computer Program

D.1 Finite Element Model of the Structure with "RIGID" Beam-Column Connection.

```
/PREP7

!*********************
!OEFINING UNITS
!*********************

/UNITS,BFT                          !FORCE IN POUND; LENGTH IN FEET

NBAY= 4
NSTORY= 10

STORYHT= 12                         !TYPICAL STORY HEIGHT IS 12 FT
BAYSIZE= 30                         !FOUR BAY @30 FT

!******************************
!PLOTTING A COLUMN OF NODES
!******************************

/PNUM,NODE,0                        !/PNUM,LAB,KEY (0:OFF  1:ON)


N,1,0,0

        H=0
*DO,I,1,NSTORY
        H=H+STORYHT
        N,I+1,0,H
*ENDDO

!**********************
!*GET,PAR,NODE,0,...
!**********************

*GET,MAX_N,NODE,0,NUM,MAX

!**********************
!GENERATION OF NODES
!**********************

!NGEN,ITIME,INC,NODE1,NODE2,NINC,DX,DY,DZ,SPACE

        NODE1=1
        NODE2=MAX_N
        B=0
*DO,I,1,NBAY
        B=B+BAYSIZE
        NGEN,2,MAX_N,NODE1,NODE2,,B
        *GET,MAX_N,NODE,0,NUM,MAX

*ENDDO

!*********************************
!DEFINING MATERIAL PROPERTIES
!*********************************

MP,EX,1,43.24E8
MP,DENS,1,490.1
MP,DAMP,1,0.02

TB,BKIN,1,1                         ! BILINEAR KINEMATIC HARDENING
TBTEMP,70                           ! FARENHEIGHT
TBDATA,1,5.184E6,0                  ! YIELD POINT AND ZERO TANGENT MODULUS
```

```
!*****************
!DEFINING ELEMENT TYPES
!*****************

!ET,ITYPE,ENAME,KEYOPT1,KEYOPT2,KEYOPT3,.....

ET,1,BEAM23,,,,,,4
ET,3,MASS21,,,4

!*****************
!DEFINING REAL CONSTANTS
!*****************

!R,NSET,HEIGHT,A(-50),A(-30),A(0),A(30),A(50), AND SHEARZ IF KEYOPT (6) = 4

R,1,1.268,1.710,0.210,0.090,0.210,1.710              !COL  W14X176
R,2,2.005,1.01,0.11,0.08,0.11,1.010                  !BEAM W24X104


!*****************
!DEFINING COLUMN ATTRIBUTES
!*****************

TYPE,1
MAT,1
REAL,1

!*****************
!GENERATION OF COLUMNS
!*****************

!EN,IEL,I,J,K,L,M,N,O,P
!EGEN,ITIME,NINC,IEL1,IEL2......

        NSEL,S,LOC,X,0,0
        *GET,NINC,NODE,0,NUM,MAX
        NSEL,ALL

EN,1,1,2
EGEN,NSTORY,1,1
EGEN,NBAY+1,NINC,1,NSTORY

!*****************
!DEFINING BEAM ATTRIBUTES
!*****************

TYPE,1
MAT,1
REAL,2
!*****************
!GENERATION OF BEAMS
!*****************
!EN,IEL,I,J,K,L,M,N,O,P
!EGEN,ITIME,NINC,IEL1,IEL2......


        NSEL,S,LOC,X,0,0
        NSEL,R,LOC,Y,STORYHT,STORYHT
        *GET,PAR,NODE,N,CDUNT

        *GET,I,NODE,0,NUM,MAX
        NSEL,ALL

        NSEL,S,LOC,X,BAYSIZE,BAYSIZE
        NSEL,R,LOC,Y,STORYHT,STORYHT
        *GET,PAR,NODE,N,COUNT

        *GET,J,NODE,0,NUM,MAX
        NSEL,ALL

        NINC=NSTORY+1

            *GET,MAX_EN,ELEM,0,NUM,MAX
            IEL=MAX_EN+1
EN,IEL,I,J
EGEN,NBAY,NINC,IEL
        NINC=NODE(0,(STORYHT+STORYHT),0)-NODE(0,STORYHT,0)
EGEN,NSTORY,NINC,IEL,IEL+NBAY-1

!*************************************************************

/PNUM,NODE,1
/PNUM,ELEM,1
/PBC,ALL
GPLOT
```

```
!*****************************
!DELITING THE EXTRA NODES
!*****************************

        NSEL,S,LOC,Y,0,0

*DO,I,1,NBAY+1

        *GET,A,NODE,0,NUM,MIN
        NSEL,U,NODE,,A

*ENDDO

        NDELE,ALL

NSEL,ALL

!*****************************
!DEFINING SUPPORT CONDITIONS
!*****************************

/SOLU

!D,NODE,LAB,VALUE,VALUE2,NEND,NINC

NSEL,S,LOC,Y,0,0
D,ALL,ALL
D,ALL,ALL
NSEL,ALL

!!!!!!!!!!!!!!!!!!!!!!!!!!!!!!!!!!!!!!!!!!!!!!!!!!!!!!

*USE, MODIFY_COL.TXT    ! MODIFICATION OF COLUMN SECTIONS (Section D.4)


FINISH
```

D.2   Finite Element Model of the Structure with Nonlinear "SEMI-RIGID" Beam-Column Connection.

```
/PREP7

!*****************************
!DEFINING UNITS
!*****************************

/UNITS,BFT                    !FORCE IN POUND; LENGTH IN FEET

NBAY= 4
NSTORY= 10

STORYHT= 12                   !TYPICAL STORY HEIGHT IS 12 FT
BAYSIZE= 30                   !FOUR BAY @30 FT

!*****************************
!PLOTTING A COLUMN OF NODES
!*****************************

/PNUM,NODE,0            !/PNUM,LAB,KEY (0:OFF  1:ON)

N,1,0,0

        H=0
*DO,I,1,NSTORY
        H=H+STORYHT
        N,I+1,0,H
*ENDDO

!*****************************
!*GET,PAR,NODE,0,...
!*****************************

*GET,MAX_N,NODE,0,NUM,MAX

!*****************************
!GENERATION OF NODES
!*****************************
```

184

```
!NGEN,ITIME,INC,NODE1,NODE2,NINC,DX,DY,DZ,SPACE

        NODE1=1
        NODE2=MAX_N
        B=0
*DO,I,1,NBAY
        B=B+BAYSIZE
        NGEN,2,MAX_N,NODE1,NODE2,,B
        *GET,MAX_N,NODE,0,NUM,MAX

*ENDDO

!*************************
!DEFINING MATERIAL PROPERTIES
!*************************

MP,EX,1,43.24E8
MP,DENS,1,490.1
MP,DAMP,1,0.02

TB,BKIN,1,1                      ! BILINEAR KINEMATIC HARDENING
TBTEMP,70                        ! FARENHEIGHT
TBDATA,1,5.184E6,0               ! YIELD POINT AND ZERO TANGENT MODULUS


!*******************
!DEFINING ELEMENT TYPES
!*******************

!ET,ITYPE,ENAME,KEYOPT1,KEYOPT2,KEYOPT3,.....

ET,1,BEAM23,,,,,,4
ET,2,COMBIN39,,,6
!ET,2,COMBIN39,1,,6,,,1
!ET,2,COMBIN39,1,2,6,,,1
ET,3,MASS21,,,4
!*******************
!DEFINING REAL CONSTANTS
!*******************

!R,NSET,HEIGHT,A(-50),A(-30),A(0),A(30),A(50), AND SHEARZ IF KEYOPT(6) = 4

R,1,1.268,1.710,0.210,0.090,0.210,1.710          !COL  w14x176
R,2,2.005,1.01,0.11,0.08,0.11,1.010              !BEAM w24x104

!*******************
!DEFINING COLUMN ATTRIBUTES
!*******************

TYPE,1
MAT,1
REAL,1

!*******************
!GENERATION OF COLUMNS
!*******************

!EN,IEL,I,J,K,L,M,N,O,P
!EGEN,ITIME,NINC,IEL1,IEL2......

        NSEL,S,LOC,X,0,0
        *GET,NINC,NODE,0,NUM,MAX
        NSEL,ALL
EN,1,1,2
EGEN,NSTORY,1,1
EGEN,NBAY+1,NINC,1,NSTORY

!/PNUM,NODE,1
!/PNUM,ELEM,1
!GPLOT

        *GET,MAX_N,NODE,0,NUM,MAX
        NODE=MAX_N+1
N,NODE,0,0

        H=0
*DO,I,1,NSTORY
        H=H+STORYHT
        N,I+NODE,0,H
*ENDDO

!NGEN,ITIME,INC,NODE1,NODE2,NINC,DX,DY,DZ,SPACE

        *GET,MAX_N,NODE,0,NUM,MAX
        NODE1=NODE
        NODE2=MAX_N
```

185

```
                INC=(NODE2-NODE1)+1
                B=0

*IF,NBAY,GT,1,THEN
        *DO,I,1,NBAY-1
                B=BAYSIZE
                NGEN,2,INC,NODE1,NODE2,,B
                *GET,MAX_N,NDDE,0,NUM,MAX
                NODE1=NODE1+INC
                NODE2=MAX_N
                INC=(NODE2-NODE1)+1

        *ENDDD
*ENDIF

!******************************************************

        *GET,MAX_N,NODE,0,NUM,MAX
        NODE=MAX_N+1
N,NDDE,BAYSIZE,0

        H=0
*DO,I,1,NSTORY
        H=H+STORYHT
        N,I+NODE,BAYSIZE,H
*ENDDO

!NGEN,ITIME,INC,NODE1,NODE2,NINC,DX,DY,DZ,SPACE

        *GET,MAX_N,NODE,0,NUM,MAX
        NODE1=NODE
        NODE2=MAX_N
        INC=(NODE2-NODE1)+1
        B=0

*IF,NBAY,GT,1,THEN
        *DO,I,2,NBAY
                B=BAYSIZE
                NGEN,2,INC,NODE1,NODE2,,B
                *GET,MAX_N,NODE,0,NUM,MAX
                NODE1=NODE1+INC
                NODE2=MAX_N
                INC=(NODE2-NODE1)+1

        *ENDDO
*ENDIF

!*********************
!DEFINING BEAM ATTRIBUTES
!*********************

TYPE,1
MAT,1
REAL,2

!**********************
!GENERATION OF BEAMS
!**********************
!EN,IEL,I,J,K,L,M,N,O,P
!EGEN,ITIME,NINC,IEL1,IEL2......

        NSEL,S,LOC,X,0,0
        NSEL,R,LOC,Y,STORYHT,STORYHT
        *GET,PAR,NODE,N,COUNT

        *GET,I,NODE,0,NUM,MAX
        NSEL,ALL

        NSEL,S,LOC,X,BAYSIZE,BAYSIZE
        NSEL,R,LOC,Y,STORYHT,STORYHT
        *GET,PAR,NODE,N,COUNT

        *GET,J,NODE,0,NUM,MAX
        NSEL,ALL

        NINC=NSTORY+1

                *GET,MAX_EN,ELEM,0,NUM,MAX
                IEL=MAX_EN+1
EN,IEL,I,J
EGEN,NBAY,NINC,IEL
        NINC=NODE(0,(STORYHT+STORYHT),0)-NODE(0,STORYHT,0)
EGEN,NSTORY,NINC,IEL,IEL+NBAY-1

!*********************
!DEFINING SPRING ATTRIBUTES
!*********************
```

186

```
TYPE,2
REAL,3

!*******************************
!GENERATION OF SPRING ELEMENTS
!*******************************

        NSEL,S,LOC,X,0,0
        NSEL,R,LOC,Y,STORYHT,STORYHT
        *GET,PAR,NODE,N,COUNT

        *GET,I,NODE,0,NUM,MIN
        *GET,J,NODE,0,NUM,MAX
        NSEL,ALL

        NINC=NSTORY+1

                *GET,MAX_EN,ELEM,0,NUM,MAX
                IEL=MAX_EN+1
EN,IEL,I,J
EGEN,NBAY,NINC,IEL
        NINC=NOOE(0,(STORYHT+STORYHT),0)-NODE(0,STORYHT,0)
EGEN,NSTORY,NINC,IEL,IEL+NBAY-1

!*******************************************************************
!APPLYING DEAD LOAD
!*******************************************************************
!ACEL, ACELX, ACELY, ACELZ
!ACEL,0,1,0

!ESEL,S,REAL,,2
!SFBEAM,ALL,1,PRES,1000
ESEL,ALL

!*********************************
!APPLYING CONSTRAINT EQUATIONS
!*********************************
!CE,NEQN,CONST,NODE1,LAB1,C1,NODE2,LAB2,C2,NODE3,LAB3,C3
!CESGEN,ITIME,INC,NSET1,NSET2,NINC

CE,1,0,I,UX,1,J,UX,-1
CESGEN,NSTORY,1,1
CESGEN,NBAY,NSTORY+1,1,NSTORY

CE,NBAY*NSTORY+1,0,I,UY,1,J,UY,-1
CESGEN,NSTORY,1,NBAY*NSTORY+1
CESGEN,NBAY,NSTORY+1,NBAY*NSTORY+1,NSTORY+NBAY*NSTORY

!*******************************************************************

        NSEL,S,LOC,X,BAYSIZE,BAYSIZE
        NSEL,R,LOC,Y,STORYHT,STORYHT
        *GET,PAR,NODE,N,COUNT

        *GET,I,NODE,0,NUM,MAX
        *GET,J,NODE,0,NUM,MIN
        NSEL,ALL

        NINC=NSTORY+1

                *GET,MAX_EN,ELEM,0,NUM,MAX
                IEL=MAX_EN+1
EN,IEL,I,J
EGEN,NBAY,NINC,IEL
        NINC=NODE(0,(STORYHT+STORYHT),0)-NODE(0,STORYHT,0)
EGEN,NSTORY,NINC,IEL,IEL+NBAY-1

!*********************************
!APPLYING CONSTRAINT EQUATIONS
!*********************************

!CE,NEQN,CONST,NODE1,LAB1,C1,NODE2,LAB2,C2,NODE3,LAB3,C3
!CESGEN,ITIME,INC,NSET1,NSET2,NINC

CE,((NBAY*NSTORY)*2+1),0,I,UX,1,J,UX,-1
CESGEN,NSTORY,1,((NBAY*NSTORY)*2+1)
CESGEN,NBAY,NSTORY+1,((NBAY*NSTORY)*2+1),((NBAY*NSTORY)*2)+NSTORY

CE,((NBAY*NSTORY)*3+1),0,I,UY,1,J,UY,-1
CESGEN,NSTORY,1,((NBAY*NSTORY)*3+1)
CESGEN,NBAY,NSTORY+1,((NBAY*NSTORY)*3+1),((NBAY*NSTORY)*3)+NSTORY

!*******************************************************************

/PNUM,NODE,1
/PNUM,ELEM,1
```

```
/PBC,ALL
GPLOT

!********************************
!DELITING THE EXTRA NODES
!********************************

        NSEL,S,LOC,Y,0,0

*DO,I,1,NBAY+1

        *GET,A,NODE,0,NUM,MIN
        NSEL,U,NODE,,A

*ENDDO

        NDELE,ALL

NSEL,ALL

!********************************
!DEFINING SUPPORT CONDITIONS
!********************************

/SOLU

!D,NODE,LAB,VALUE,VALUE2,NEND,NINC

NSEL,S,LOC,Y,0,0
D,ALL,ALL
D,ALL,ALL
NSEL,ALL

!!!!!!!!!!!!!!!!!!!!!!!!!!!!!!!!!!!!!!!!!!!!!!!!!!!!!!!!!!

*USE, MODIFY_COL.TXT   ! MODIFICATION OF COLUMN SECTIONS (Section D.4)

!**************************************************
!WHICH SEMI RIGID CONNECTION I WILL USE?
!**************************************************

*USE,TYPEA_P.TXT      ! NONLINEAR BEAM-COLUMN CONNECTION TYPE-A (Section D.5)
!*USE,TYPEB_P.TXT     ! NONLINEAR BEAM-COLUMN CONNECTION TYPE-A (Section D.6)
!*USE,TYPEC_P.TXT     ! NONLINEAR BEAM-COLUMN CONNECTION TYPE-A (Section D.7)
!*USE,TYPED_P.TXT     ! NONLINEAR BEAM-COLUMN CONNECTION TYPE-A (Section D.8)
!*USE,TYPEE_P.TXT     ! NONLINEAR BEAM-COLUMN CONNECTION TYPE-A (Section D.9)

FINISH
```

D.3 Finite Element Model of the Structure in Combination of "RIGID" and "SEMI-RIGID" Beam-Column Connection.

```
/PREP7

!****************************
!DEFINING UNITS
!****************************

/UNITS,BFT                        !FORCE IN POUND; LENGTH IN FEET

NBAY= 4
NSTORY= 10
NSTORY_R= 4
NSTORY_S=NSTORY-NSTORY_R

STORYHT= 12            !TYPICAL STORY HEIGHT IS 12 FT
BAYSIZE= 30            !FOUR BAY @30 FT

!****************************
!PLOTTING A COLUMN OF NODES
```

188

```
!*************************

/PNUM,NODE,0              !/PNUM,LAB,KEY (0:OFF  1:ON)

N,1,0,0

        H=0
*DO,I,1,NSTORY
        H=H+STORYHT
        N,I+1,0,H
*ENDDO

!*******************
!*GET,PAR,NODE,0,....
!*********************

*GET,MAX_N,NODE,0,NUM,MAX

!*********************
!GENERATION OF NODES
!**********************

!NGEN,ITIME,INC,NODE1,NODE2,NINC,DX,DY,DZ,SPACE

        NODE1=1
        NODE2=MAX_N
        B=0
*DO,I,1,NBAY
        B=B+BAYSIZE
        NGEN,2,MAX_N,NODE1,NODE2,,B
        *GET,MAX_N,NODE,0,NUM,MAX

*ENDDO

!****************************
!DEFINING MATERIAL PROPERTIES
!*****************************

MP,EX,1,43.24E8
MP,DENS,1,490.1
MP,DAMP,1,0.02

TB,BKIN,1,1                     ! BILINEAR KINEMATIC HARDENING
TBTEMP,70                       ! FARENHEIGHT
TBDATA,1,5.184E6,0              ! YIELD POINT AND ZERO TANGENT MODULUS

!*********************
!DEFINING ELEMENT TYPES
!*********************

!ET,ITYPE,ENAME,KEYOPT1,KEYOPT2,KEYOPT3,.....

ET,1,BEAM23,,,,,,4
ET,2,COMBIN39,,,6
ET,3,MASS21,,,4
!*********************
!DEFINING REAL CONSTANTS
!*********************

!R,NSET,HEIGHT,A(-50),A(-30),A(0),A(30),A(50), AND SHEARZ IF KEYOPT (6) = 4

R,1,1.268,1.710,0.210,0.090,0.210,1.710          !COL  W14x176
R,2,2.005,1.01,0.11,0.08,0.11,1.010              !BEAM W24x104

!*********************
!DEFINING CDLUMN ATTRIBUTES
!*********************

TYPE,1
MAT,1
REAL,1

!*********************
!GENERATION OF COLUMNS
!*********************

!EN,IEL,I,J,K,L,M,N,O,P
!EGEN,ITIME,NINC,IEL1,IEL2......

        NSEL,S,LOC,X,0,0
        *GET,NINC,NODE,0,NUM,MAX
        NSEL,ALL
EN,1,1,2
EGEN,NSTORY,1,1
EGEN,NBAY+1,NINC,1,NSTDRY
```

189

```
!********************
!DEFINING BEAM ATTRIBUTES
!********************

TYPE,1
MAT,1
REAL,2
!********************
!GENERATION OF BEAMS
!********************
!EN,IEL,I,J,K,L,M,N,O,P
!EGEN,ITIME,NINC,IEL1,IEL2......


        NSEL,S,LOC,X,0,0
        NSEL,R,LOC,Y,STORYHT,STORYHT
        *GET,PAR,NODE,N,COUNT

        *GET,I,NODE,0,NUM,MAX
        NSEL,ALL

        NSEL,S,LOC,X,BAYSIZE,BAYSIZE
        NSEL,R,LOC,Y,STORYHT,STORYHT
        *GET,PAR,NODE,N,COUNT

        *GET,J,NODE,0,NUM,MAX
        NSEL,ALL

        NINC=NSTORY+1

                *GET,MAX_EN,ELEM,0,NUM,MAX
                IEL=MAX_EN+1
EN,IEL,I,J
EGEN,NBAY,NINC,IEL
        NINC=NODE(0,(STORYHT+STORYHT),0)-NODE(0,STORYHT,0)
EGEN,NSTORY_R,NINC,IEL,IEL+NBAY-1


!**********************************************************

/PNUM,NODE,1
/PNUM,ELEM,1
/PBC,ALL
GPLOT

!********************
!DELITING THE EXTRA NODES
!********************

        NSEL,S,LOC,Y,0,0

*DO,I,1,NBAY+1

        *GET,A,NODE,0,NUM,MIN
        NSEL,U,NODE,,A

*ENDDO

        NOELE,ALL

NSEL,ALL

!!!**********************************************************

        *GET,MAX_N,NODE,0,NUM,MAX
        NODE=MAX_N+1
N,NODE,0,((NSTORY_R+1)*STORYHT)

        H=(NSTORY_R+1)*STORYHT
*DO,I,1,(NSTORY_S-1)
        H=H+STORYHT
        N,I+NODE,0,H
*ENDDO

!NGEN,ITIME,INC,NODE1,NODE2,NINC,DX,DY,DZ,SPACE

        *GET,MAX_N,NODE,0,NUM,MAX
        NODE1=NODE
        NODE2=MAX_N
        INC=(NODE2-NODE1)+1
        B=0

*IF,NBAY,GT,1,THEN
        *DO,I,1,NBAY-1
                B=BAYSIZE
                NGEN,2,INC,NODE1,NODE2,,B
```

190

```
                    *GET,MAX_N,NODE,0,NUM,MAX
                    NODE1=NODE1+INC
                    NODE2=MAX_N
                    INC=(NODE2-NODE1)+1

            *ENDDO
     *ENDIF
     !!*************************************************

            *GET,MAX_N,NODE,0,NUM,MAX
            NODE=MAX_N+1
     N,NODE,BAYSIZE,((NSTORY_R+1)*STORYHT)

            H=(NSTORY_R+1)*STORYHT
     *DO,I,1,(NSTORY_S-1)
            H=H+STORYHT
            N,I+NODE,BAYSIZE,H
     *ENDDO

     !NGEN,ITIME,INC,NODE1,NODE2,NINC,DX,DY,DZ,SPACE

            *GET,MAX_N,NODE,0,NUM,MAX
            NODE1=NODE
            NODE2=MAX_N
            INC=(NODE2-NODE1)+1
            B=0

     *IF,NBAY,GT,1,THEN
            *DO,I,2,NBAY
                    B=BAYSIZE
                    NGEN,2,INC,NODE1,NODE2,,B
                    *GET,MAX_N,NODE,0,NUM,MAX
                    NODE1=NODE1+INC
                    NODE2=MAX_N
                    INC=(NODE2-NODE1)+1

            *ENDDO
     *ENDIF

     !!!!!!!!!!!!!!!!!!!!!!!!!!!!!!!!!!!!!!!!!!!!!!!!!!!!!!!!!!

     !********************
     !DEFINING BEAM ATTRIBUTES
     !********************

     TYPE,1
     MAT,1
     REAL,2

     !********************
     !GENERATION OF BEAMS
     !********************
     !EN,IEL,I,J,K,L,M,N,O,P
     !EGEN,ITIME,NINC,IEL1,IEL2......

            NSEL,S,LOC,X,0,0
            NSEL,R,LOC,Y,((NSTORY_R+1)*STORYHT),((NSTORY_R+1)*STORYHT)
            *GET,PAR,NODE,N,COUNT

            *GET,I,NODE,0,NUM,MAX
            NSEL,ALL

            NSEL,S,LOC,X,BAYSIZE,BAYSIZE
            NSEL,R,LOC,Y,((NSTORY_R+1)*STORYHT),((NSTORY_R+1)*STORYHT)
            *GET,PAR,NODE,N,COUNT

            *GET,J,NODE,0,NUM,MAX
            NSEL,ALL

            NINC=NSTORY_S

                    *GET,MAX_EN,ELEM,0,NUM,MAX
                    IEL=MAX_EN+1
     EN,IEL,I,J
     EGEN,NBAY,NINC,IEL
            NINC=NODE(0,(STORYHT+STORYHT),0)-NODE(0,STORYHT,0)
     EGEN,NSTORY_S,NINC,IEL,IEL+NBAY-1

     !!!!!!!!!!!!!!!!!!!!!!!!!!!!!!!!!!!!!!!!!!!!!!!!!!!!!!!!!!

     !********************
     !DEFINING SPRING ATTRIBUTES
     !********************

     TYPE,2
     REAL,3
```

O

191

```
!********************************************
!GENERATION OF SPRING ELEMENTS_RIGHT SIDE
!********************************************

        A=0
        B=0

        NSEL,S,LOC,X,0,0
        NSEL,R,LOC,Y,((NSTORY_R+1)*STDRYHT),((NSTORY_R+1)*STORYHT)
        *GET,PAR,NODE,N,COUNT

        *GET,A,NODE,0,NUM,MIN
        *GET,B,NODE,0,NUM,MAX
        NSEL,ALL

P=A
Q=B
                *GET,MAX_EN,ELEM,0,NUM,MAX
                IEL=MAX_EN


        *DO,I,1,NBAY

                EN,IEL+I,A,B
                A=A+NSTORY+1
                B=B+NSTORY_S

        *ENDDO


        NINC=NODE(0,(STORYHT+STORYHT),0)-NDDE(0,STORYHT,0)
EGEN,NSTORY_S,NINC,IEL+1,IEL+NBAY

!******************************
!APPLYING CONSTRAINT EQUATIONS
!******************************
!CE,NEQN,CONST,NODE1,LAB1,C1,NODE2,LAB2,C2,NODE3,LAB3,C3
!CESGEN,ITIME,INC,NSET1,NSET2,NINC

        CA=P
        CB=Q


        *DO,I,1,NBAY

                CE,I,0,CA,UX,1,CB,UX,-1
                CA=CA+NSTORY+1
                CB=CB+NSTORY_S

        *ENDDO

        NINC=NODE(0,(STORYHT+STORYHT),0)-NODE(0,STORYHT,0)
CESGEN,NSTORY_S,NINC,1,NBAY

        CA=P
        CB=Q

        *DO,I,1,NBAY

                CE,((NBAY*NSTDRY)+I),0,CA,UY,1,CB,UY,-1
                CA=CA+NSTORY+1
                CB=CB+NSTORY_S

        *ENDDO

        NINC=NODE(0,(STORYHT+STORYHT),0)-NODE(0,STDRYHT,0)
CESGEN,NSTORY_S,NINC,((NBAY*NSTORY)+1),((NBAY*NSTORY)+NBAY)

!********************************************
!GENERATION OF SPRING ELEMENTS_LEFT SIDE
!********************************************

        A=0
        B=0

        NSEL,S,LOC,X,BAYSIZE,BAYSIZE
        NSEL,R,LOC,Y,((NSTORY_R+1)*STORYHT),((NSTORY_R+1)*STORYHT)
        *GET,PAR,NODE,N,COUNT

        *GET,A,NODE,0,NUM,MIN
        *GET,B,NODE,0,NUM,MAX
        NSEL,ALL

P=A
Q=B
                *GET,MAX_EN,ELEM,0,NUM,MAX
```

```
                    IEL=MAX_EN

              *DO,I,1,NBAY

                        EN,IEL+I,A,B
                        A=A+NSTORY+1
                        B=B+NSTORY_S

              *ENDDO


          NINC=NODE(0,(STORYHT+STORYHT),0)-NODE(0,STORYHT,0)
     EGEN,NSTORY_S,NINC,IEL+1,IEL+NBAY



     !*****************************
     !APPLYING CONSTRAINT EQUATIONS
     !*****************************
     !CE,NEQN,CONST,NODE1,LAB1,C1,NODE2,LAB2,C2,NODE3,LAB3,C3
     !CESGEN,ITIME,INC,NSET1,NSET2,NINC

              CA=P
              CB=Q


              *DO,I,1,NBAY

                        CE,((NBAY*NSTORY)*2+I),0,CA,UX,1,CB,UX,-1
                        CA=CA+NSTORY+1
                        CB=CB+NSTORY_S

              *ENDDO

          NINC=NODE(0,(STORYHT+STORYHT),0)-NODE(0,STORYHT,0)
     CESGEN,NSTORY_S,NINC,((NBAY*NSTORY)*2+1),((NBAY*NSTORY)*2+NBAY)

              CA=P
              CB=Q

              *DO,I,1,NBAY

                        CE,((NBAY*NSTORY)*3+I),0,CA,UY,1,CB,UY,-1
                        CA=CA+NSTORY+1
                        CB=CB+NSTORY_S

              *ENDDO

          NINC=NODE(0,(STORYHT+STORYHT),0)-NODE(0,STORYHT,0)
     CESGEN,NSTORY_S,NINC,((NBAY*NSTORY)*3+1),((NBAY*NSTORY)*3+NBAY)

     !**************************
     !DEFINING SUPPORT CONDITIONS
     !**************************

     /SOLU

     !D,NODE,LAB,VALUE,VALUE2,NEND,NINC

     NSEL,S,LOC,Y,0,0
     D,ALL,ALL
     D,ALL,ALL
     NSEL,ALL

     !!!!!!!!!!!!!!!!!!!!!!!!!!!!!!!!!!!!!!!!!!!!!!!!!!!!

     *USE,MODIFY_COL.TXT    ! MODIFICATION OF COLUMN SECTIONS (Section D.4)

     !*************************************************
     !WHICH SEMI RIGIO CONNECTION I WILL USE?
     !*************************************************


     *USE,TYPEA_P.TXT        ! NONLINEAR BEAM-COLUMN CONNECTION TYPE-A (Section D.5)
     !*USE,TYPEB_P.TXT       ! NONLINEAR BEAM-COLUMN CONNECTION TYPE-A (Section D.6)
     !*USE,TYPEC_P.TXT       ! NDNLINEAR BEAM-COLUMN CONNECTION TYPE-A (Section D.7)
     !*USE,TYPED_P.TXT       ! NONLINEAR BEAM-COLUMN CONNECTION TYPE-A (Section D.8)
     !*USE,TYPEE_P.TXT       ! NONLINEAR BEAM-COLUMN CONNECTION TYPE-A (Section D.9)

     FINISH
```

193

D.4 Modification of Columns

```
/PREP7

/UNITS,BFT                          !FORCE IN POUND; LENGTH IN FEET

!R,NSET,HEIGHT,A(-50),A(-30),A(0),A(30),A(50), AND SHEARZ IF KEYOPT (6) = 4

R,6,1.193,1.170,0.100,0.050,0.100,1.170              !COL W14X109

R,7,1.193,0.810,0.090,0.050,0.090,0.810              !COL W14X82

R,8,1.268,1.710,0.210,0.090,0.210,1.710              !COL W14X176

R,9,1.193,1.170,0.100,0.050,0.100,1.170              !COL W14X109

R,10,1.168,0.990,0.080,0.040,0.080,0.990             !COL W14X90


!ESEL, TYPE, ITEM, COMP, VMIN, VMAX, VINC, KABS
ESEL,S,ELEM,,1,6,1
ESEL,A,ELEM,,41,46,1


!EMODIF, IEL, STLOC, I1, I2, I3, I4, I5, I6, I7, I8
.EMOOIF,ALL,REAL,6
ESEL,ALL

!!!!!!!!!!!!!!!!!!!!!!!!!!!!!!!!!!!!!!!!!!!!!!!!!!!!!!!!!
ESEL,S,ELEM,,7,10,1
ESEL,A,ELEM,,47,50,1

EMOOIF,ALL,REAL,7
ESEL,ALL

!!!!!!!!!!!!!!!!!!!!!!!!!!!!!!!!!!!!!!!!!!!!!!!!!!!!!!!!!
ESEL,S,ELEM,,11,13,1
ESEL,A,ELEM,,21,23,1
ESEL,A,ELEM,,31,33,1

EMODIF,ALL,REAL,8
ESEL,ALL

!!!!!!!!!!!!!!!!!!!!!!!!!!!!!!!!!!!!!!!!!!!!!!!!!!!!!!!!!
ESEL,S,ELEM,,14,16,1
ESEL,A,ELEM,,24,26,1
ESEL,A,ELEM,,34,36,1

EMODIF,ALL,REAL,9
ESEL,ALL

!!!!!!!!!!!!!!!!!!!!!!!!!!!!!!!!!!!!!!!!!!!!!!!!!!!!!!!!!
ESEL,S,ELEM,,17,20,1
ESEL,A,ELEM,,27,30,1
ESEL,A,ELEM,,37,40,1

EMODIF,ALL,REAL,10
ESEL,ALL


FINISH
```

D.5 Nonlinear Beam-Column Connection Type-A

```
/PREP7

R, 3,   0, 0, 0.064744231,628425, 0.504775818,693105

RMORE, 2.864788976, 707373.3095

FINISH
```

D.6   Nonlinear Beam-Column Connection Type-B

```
/PREP7
R, 3,   0, 0,   0.068754935,446880, 0.44690708,515235
RMORE, 2.911771515, 523603.0889
FINISH
```

D.7   Nonlinear Beam-Column Connection Type-C

```
/PREP7
R, 3,   0, 0,   0.080214091,323400, 0.528840045,385875
RMORE, 2.864788976, 395469.0956
FINISH
```

D.8   Nonlinear Beam-Column Connection Type-D

```
/PREP7
R, 3,   0, 0,   0.080214091, 174268.5, 0.566655259,220500
RMORE, 2.864788976, 226377.6167
FINISH
```

D.9   Nonlinear Beam-Column Connection Type-E

```
/PREP7
R, 3,   0, 0,   0.083651838, 22564.5, 0.610200052, 42556.5
RMORE, 2.864788976, 60049.5
FINISH
```

D.10   Modal Analysis_Extraction of Mode Shapes and Frequencies

```
/SOLU
ANTYPE, MOOAL              ! PERFORM MODAL ANALYSIS
MODOPT, SUBSP, 5           ! EXTRACT 5 MODES USING SUBSPACE ITERATION METHOD
MXPAND, 5                  ! EXPAND FIRST Five MODES
SOLVE
FINISH
```

195

D.11 Nonlinear Static Analysis_ Extraction of Pushover Curve

```
/CONFIG, NRES, 2000
/SOLU

!/CONFIG, LAB, VALUE

ANTYPE,STATIC
!NLGEOM,ON
!!!!!!!!!!!!!!!!!!!!!!!!!!!!!!
SOLCONTROL,0
NEQIT,100                       ! MAXIMUM 5 EQUILIBRIUM ITERATIONS PER STEP
NCNV,0                          ! OO NOT TERMINATE THE ANALYSIS IF THE SOLUTION FAILS
                                !   TO CONVERGE

OUTRES,ALL,ALL
CNVTOL,U                        ! CONVERGENCE CRITERION BASED UPON DISPLACEMENTS AND
CNVTOL,ROT                      ! ROTATIONS
CNVTOL,F,0.05                   ! FORCES
CNVTOL,M,0.05                   ! MOMENTS

!!!!!!!!!!
!D, NODE, LAB, VALUE, VALUE2, NEND, NINC, LAB2, LAB3, LAB4, LAB5, LAB6
!F, NODE, LAB, VALUE, VALUE2, NEND, NINC

NSEL,S,LOC,Y,H

*GET,LOAD_P,NODE,0,NUM,MIN

NSEL,ALL


!*************************************************************
!APPLYING DEAD LOAD
!*************************************************************
!ACEL, ACELX, ACELY, ACELZ
!*************************************************************

*DO,I,0,50

        D,LOAD_P,UX,I*0.20 ! APPLY DISPLACEMENT

        ACEL,0,1,0
        ESEL,S,REAL,,2
        SFBEAM,ALL,1,PRES,1660
        ESEL,ALL

        SOLVE
*ENDDO

!!!!!!!!!!!!!!!!!!!!!!!!!!!!!!!!!!!!!!!!!!!!!!!!!!!!!!!

FINISH

/POST26

!NUMVAR, NV

NUMVAR, 100

RFORCE,2,1,F,X,
RFORCE,3,12,F,X,
RFORCE,4,23,F,X,
RFORCE,5,34,F,X,
RFORCE,6,45,F,X,

ADD,7,2,3,4,BSHR1,,,-1, -1, -1
ADD,8,5,6,7,BSHR,,,-1,-1,1

!*
NSOL,9,11,U,X,RUF_DSP

!*
PLTIME,0,0
XVAR,9

PLVAR,8

/GRID,1


FINISH
```

196

Appendix E

Calculation of Performance Point

E.1 Calculating Performance Point Using Procedure-A of ATC-40

This appendix presents a sample calculation of the performance point using Procedure-A of ATC-40 of the ten storied 2D steel moment frame for "RIGID" beam-column connections. The step by step calculations are given below:

1. *Development of 5 percent damped (elastic) response spectrum:*

   As considered in this study, the building is situated on seismic Zone-3 and soil profile type of that location is S3. Development of 5 percent damped (elastic) response spectrum is described on Section 5.2.1 in Chapter 5. Bangladesh National Building Code (BNBC, 1993) is used for demand response spectrum.

2. *Conversion of capacity curve to capacity spectrum:*

   Figure 4.6 in Chapter 4 shows the capacity curve resulting from a pushover analysis of the ten storied 2D steel moment frame for "RIGID" beam-column connections. Conversion of capacity curve to capacity spectrum is discussed in Chapter 4 on Section 4.6. Figure 4.11 represents the capacity spectrum of the structure after transformation of capacity curve Figure 4.6.

3. *Development of bilinear representation of capacity spectrum:*

   The capacity spectrum has been plotted on the same chart as the 5% damped response spectra as shown in Figure E.1. A first choice of a_{pi} and d_{pi} is obtained using the equal displacement approximation. Bilinear representation using the procedure described in ATC-40 is shown in Figure E.1.

4. *Development of demand spectrum:*

   By using equations E-1 and E-2 spectral reduction factors are calculated to

$$SR_A = \frac{3.21 - 0.68\ln(\beta_{eff})}{2.12}$$
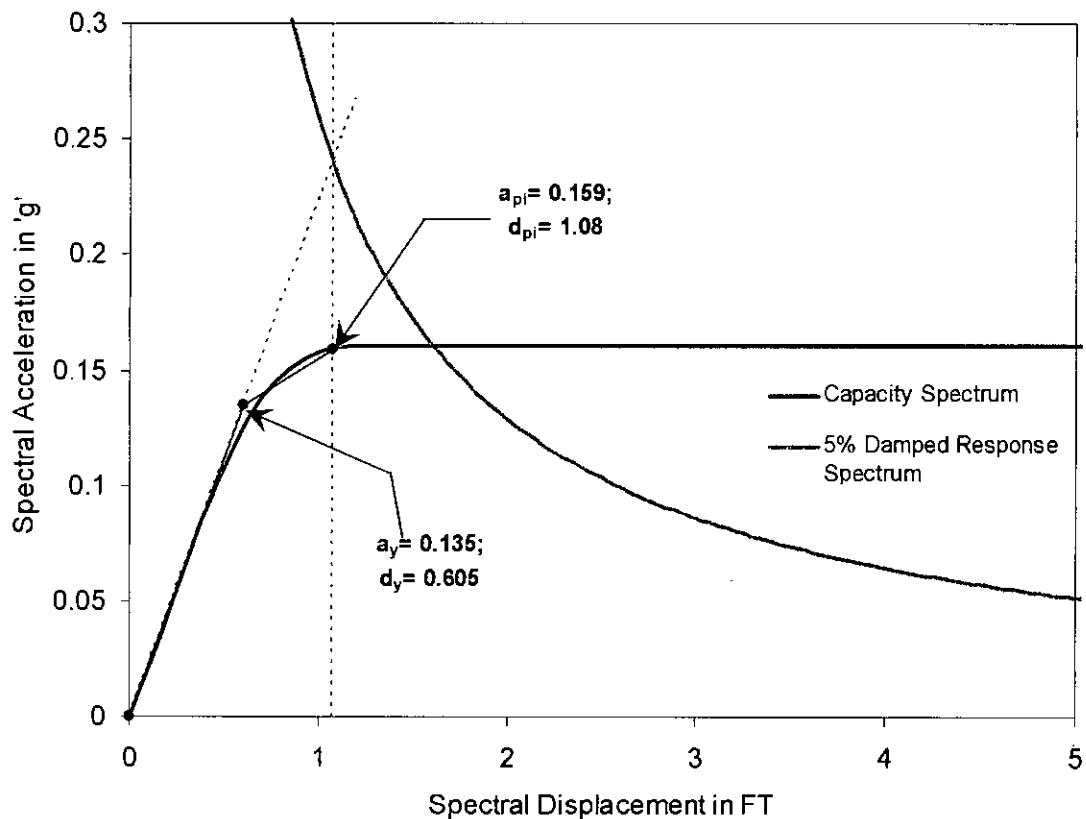(Equation E-1)

Figure E.1 Bilinear Representation of Capacity Spectrum

$$SR_V = \frac{2.31 - 0.41 \ln(\beta_{eff})}{1.65} \qquad \text{(Equation E-2)}$$

$$\beta_{eff} = \kappa\beta_o + 5 \qquad \text{(Equation E-3)}$$

$$\beta_o = \frac{63.7(a_y d_{pi} - d_y a_{pi})}{a_{pi} d_{pi}} \qquad \text{(Equation E-4)}$$

Where,

β_{eff} = Effective viscous damping.

. β_o = Hysteretic damping represented as equivalent viscous damping.

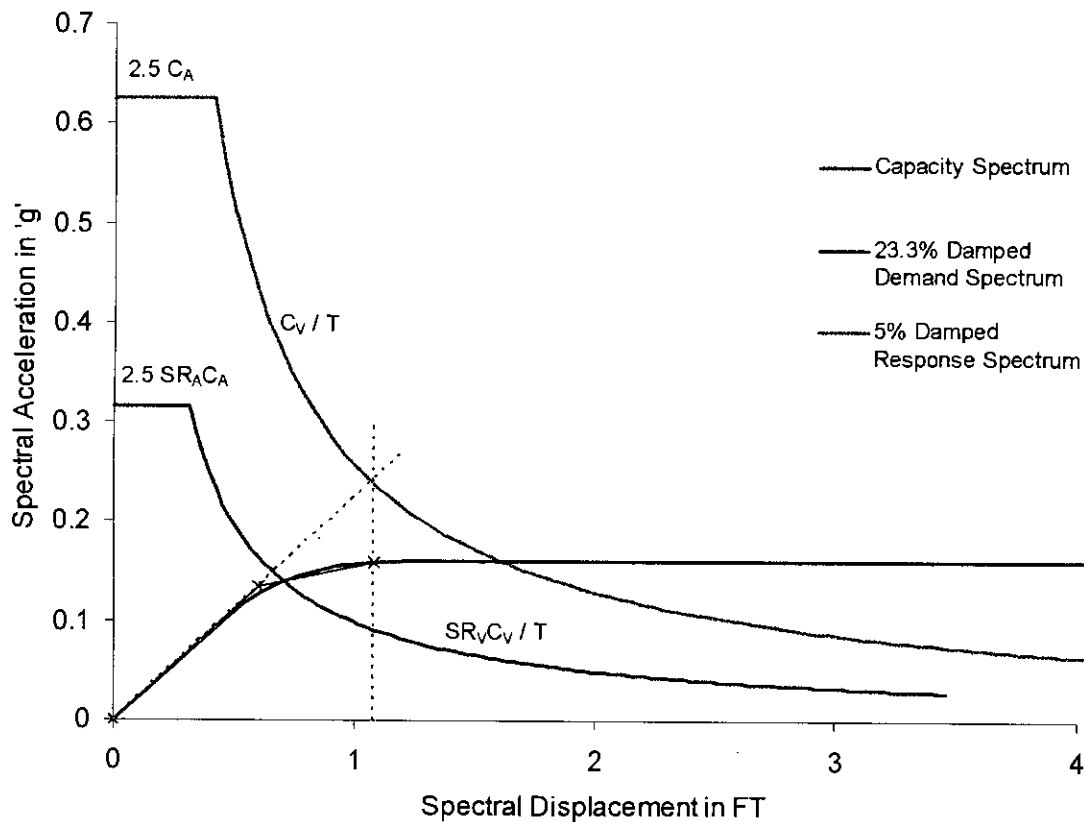5 = 5% viscous damping inherent the structure (assumed to be constant)

198

Figure E.2 Demand Spectrum

SR_A and SR_V = Spectral reduction factors.

κ = Damping modification factor.

develop demand spectrum using the process illustrated in Figure E.2. Calculations of the values needed to plot demand spectrum for the ten storied 2D steel moment frame with "RIGID" beam-column connections are below:

a_{p1} = 0.159g   (From Fig E.1)

d_{p1} = 1.08ft   (From Fig E.1)

a_y = 0.135g   (From Fig E.1)

d_y = 0.605ft   (From Fig E.1)

$$\beta_o = \frac{63.7(0.135x1.08 - 0.605x0.159)}{0.159x1.08} = 18.3$$

$$\kappa = 1$$

$$\beta_{eff} = 1x18.3 + 5 = 23.3\%$$

$$SR_A = \frac{3.21 - 0.68\ln(23.3)}{2.12} = 0.505$$

$$SR_V = \frac{2.31 - 0.41\ln(23.3)}{1.65} = 0.618$$

$C_A = 0.25$ (From Table 6-1 of Chapter 6)

$C_V = 0.563$ (From Table 6-1 of Chapter 6)

$$S_a = 2.5SR_A x\ C_A = 2.5 \times 0.505 \times 0.25 = 0.3155g$$

$$T_S = \frac{SR_V C_V}{2.5SR_A C_A} = \frac{0.618x0.563}{2.5x0.505x0.25} = 1.102 seconds$$

$$S_d \text{ at } T_S = S_a \left(\frac{T}{2\pi}\right)^2 = 0.315x32.14x\left(\frac{1.102}{2\pi}\right)^2 = 0.312$$

5. *Determination of performance point:*

The demand spectrum associated with point a_{p1}, d_{p1} is plotted as shown in Figure E.3. The demand spectrum does not intersect the capacity spectrum within $\pm 5\%$ of the trial point a_{p1}, d_{p1}. So iteration is required in this case.

The next trial point is $a_{p2} = 0.152g$; $d_{p2} = 0.865$ft. Calculations of the values needed to plot demand spectrum by this point are:
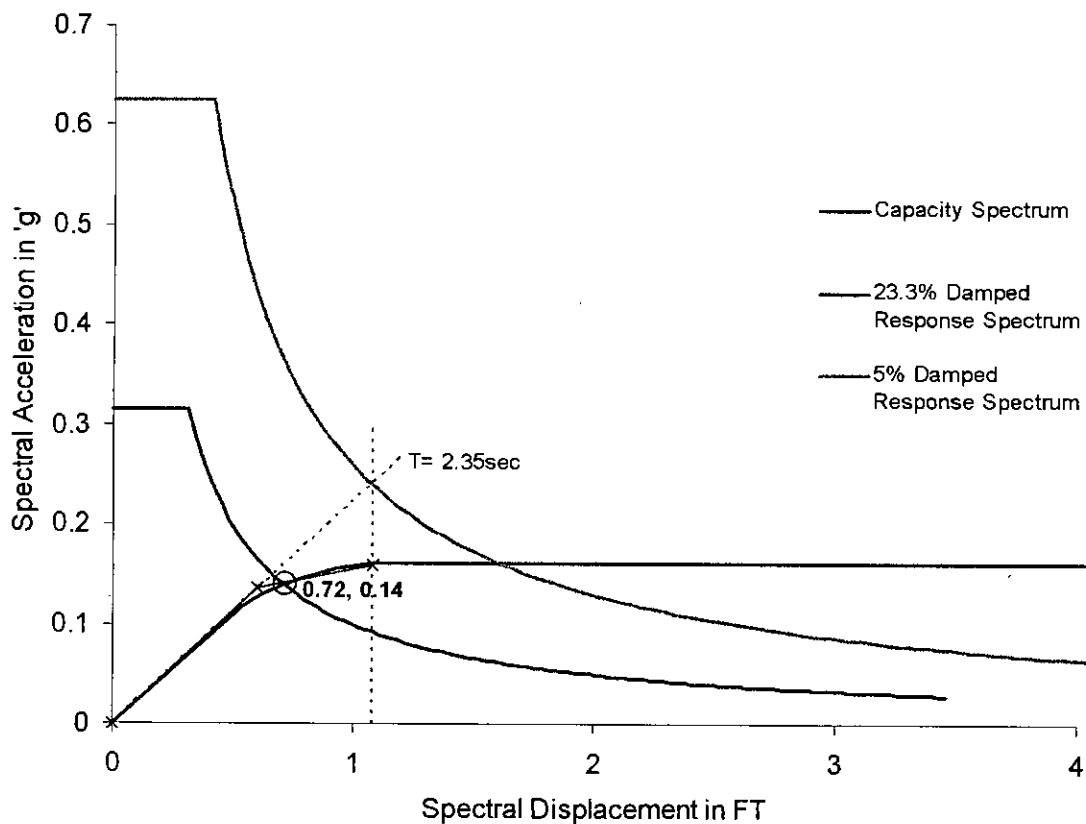
Figure E.3 Demand Response Spectrum by Using First Trial Point

$$a_{p2} = 0.152g$$

$$d_{p2} = 0.865ft$$

$$a_y = 0.123g$$

$$d_y = 0.55ft$$

$$\beta_o = \frac{63.7(0.123x0.865 - 0.55x0.152)}{0.152x0.865} = 11$$

$$\kappa = 1$$

$$\beta_{eff} = 1x11 + 5 = 16\%$$

$$SR_A = \frac{3.21 - 0.68\ln(16)}{2.12} = 0.625$$

$$SR_V = \frac{2.31 - 0.41\ln(16)}{1.65} = 0.711$$

$C_A = 0.25$ (From Table 6-1 of Chapter 6)

$C_V = 0.563$ (From Table 6-1 of Chapter 6)

$S_a = 2.5SR_A \times C_A = 2.5 \times 0.625 \times 0.25 = 0.391g$

$$T_S = \frac{SR_V C_V}{2.5SR_A C_A} = \frac{0.711x0.563}{2.5x0.625x0.25} = 1.025\sec onds$$

$$S_d \text{ at } T_S = S_a\left(\frac{T}{2\pi}\right)^2 = 0.391x32.14x\left(\frac{1.025}{2\pi}\right)^2 = 0.334$$
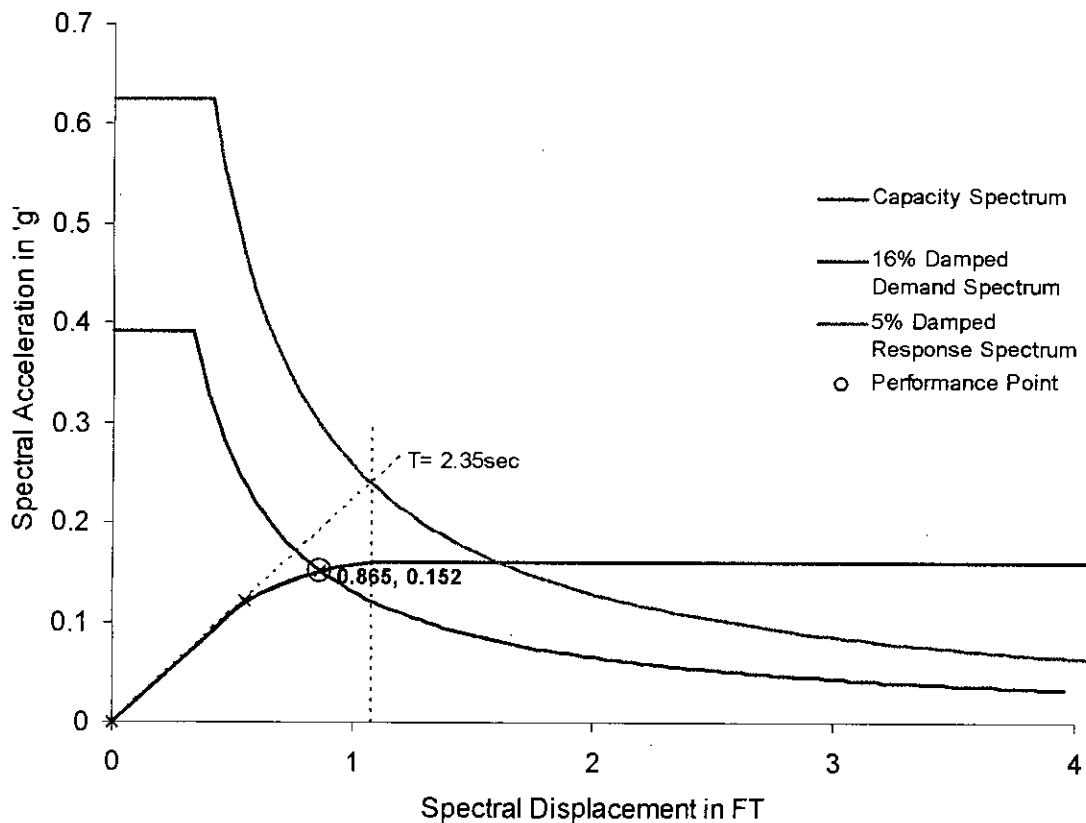

Figure E.4 Performance Point

The demand spectrum associated with point a_{p2}, d_{p2} is plotted as shown in Figure E.4. The demand spectrum intersects the capacity spectrum within $\pm 5\%$ of the trial point a_{p2}, d_{p2}, and thus that point is the performance point. Further iteration is not required.

Therefore, the demand displacement calculated for soil profile type S3 using Procedure-A of ATC-40 is 0.865 ft.